

Diffusion Mechanisms Between Heavy Oils and Light Hydrocarbons

by

Mojen Alizadehgiashi

A thesis submitted in partial fulfillment of the requirements for the degree of

Master of Science

in

Chemical Engineering

Department of Chemical and Materials Engineering

University of Alberta

## **Abstract**

Athabasca Bitumen and other heavy hydrocarbon resources are high-mean-molar-mass and structured organic materials with complex phase behaviors at the nano- and micro- meter length scales. Diffusion of light hydrocarbons, and non-hydrocarbons in these resources is of significant interest as new production and refining concepts that envision, for example, addition of light hydrocarbons and non-hydrocarbons to reservoirs to enhance production have begun to emerge. Composition-distance profiles arising during free diffusion scale as a function of the joint variable (distance/time<sup>n<sub>w</sub></sup>). Simple fluids are governed by Fickian diffusion, where n<sub>w</sub> = 0.5. For nanostructured fluids the value of n<sub>w</sub> can be as low as n<sub>w</sub> = 0.25, known as the single file limit but more typically the value for the exponent falls between these two limits and is composition dependent. In this work, five published data sets comprising free diffusion composition profiles for Athabasca bitumen fractions and for Cold Lake bitumen + light hydrocarbons obtained using diverse apparatus, are probed from this perspective. Additional experimental results are provided for Athabasca bitumen + toluene mixtures over the temperature range 273 to 313 K, and results from positive and negative control experiments for two well-defined mixtures: (0.25 mass fraction

carbon nanotubes + polybutene) + toluene, and polybutene + toluene, are also provided. The values of the exponent  $n_w$  are shown to be light hydrocarbon dependent. They increase from  $n_w \sim 0.25$  at low light hydrocarbon mass fraction up to  $n_w \sim 0.50$  at high light hydrocarbon mass fraction. An approximate solution to the composition profile arising during Single File diffusion is presented and used along with a standard composition profile for Fickian diffusion to simulate sets of free diffusion composition profiles in these complex mixtures. Three parameters: a Fickian mutual diffusion coefficient, a coefficient H fit to composition profile, and a composition dependent weighting function for the two diffusion mechanisms, are employed in the model. Outcomes, including Fickian mutual diffusion coefficients, order of magnitude estimates for Single File mobility coefficients and the roles of diluent type and asphaltene content on the controlling diffusion mechanism, and industrial implications are discussed.

## **Preface**

Chapter 2 of this thesis has been published in journal of Energy and Fuels with the title: “Fickian and Non-Fickian Diffusion in heavy oil + light hydrocarbon mixtures”.

## **Dedication**

This work is dedicated to my late sister,

Sepideh,

rest in peace.

*"Turn yourself not away from three best things: good deeds, good thoughts and good words. There is but one path in the world, the path of honesty"*

*Zoroaster*

## **Acknowledgements**

I would like to express my gratitude to Professor John M.Shaw for his insightful supervision, endless encouragement and support, great patience, and deep knowledge and mastery. Without his supervision such a great piece and novel idea would never have been possible I am forever in debt of such a great experience I have gained during the period I was working in his group.

I would like to thank all my colleagues in the Petroleum Thermodynamics Group especially, Amin Pourmohammadbagher, Robert Stewart, Dr. Marc Cassiede, Dr. Mohammad Javad Amani, Sajjad Pouralhosseini, our lab manager Mildred Becerra and our secretary Linda Kaert and all the support from other staff in the Department of Chemical and Materials Engineering.

I would like to thank Saman Jahani, Professor Lavasanifar, Nima Sammaknejad, Farzad Yazdanbakhsh, Hoda Soleymani, Dr. Kasra Nikouyeh and Dr. Shima Khatibisepehr for their insights on my projects and my friends Mahsa, Ammar H.K, Samaneh, Amir, Sarah Gh., Michelle Bendrich, Mahdie M., Sarah L., Rana R. and Sina Gh. for their kindness and heartfelt helps during this period.

Without my family, specially my parents, their patience and understanding during every stage of my life this work would never have been possible, I would like to wish them health and happiness in life. My beloved late sister who is not among us anymore but I always feel her love in my heart. Finally I would like to thank my dearest cousins Aida, Majid and Yashar for always being there for me.

# Table of Contents

<b>Chapter 1: Introduction.....</b>	<b>1</b>
<b>Chapter 2: Fickian and Non-Fickian Diffusion in heavy oil + light hydrocarbon mixtures.....</b>	<b>4</b>
<b>2.1. Introduction.....</b>	<b>4</b>
<b>2.2. Composition Profile Regression Algorithm to Determine Local Values of <math>n_w</math> and Their Uncertainty.....</b>	<b>9</b>
<b>2.3. Experimental.....</b>	<b>11</b>
2.3.1. Materials.....	11
2.3.2. Apparatus and Procedure.....	12
<b>2.4. Results and Discussion.....</b>	<b>17</b>
2.4.1. Local time invariant values of $n_w$ and their uncertainty derived from composition profiles of heavy oil + light hydrocarbon mixtures in the literature.....	17
2.4.2. Control Experiments .....	19
2.4.3. Local time invariant values of $n_w$ and their uncertainty derived from composition profiles of Athabasca Bitumen + Toluene Mixtures .....	22
2.4.4. Impact of asphaltene mass fraction and solvent choice on local time-invariant $n_w$ values.....	25
2.4.5. Temporal variation of $n_w$ values at high solvent mass fraction.....	27
<b>2.5 Conclusions.....</b>	<b>31</b>
<b>2.6 References.....</b>	<b>32</b>

<b>Chapter 3: On Fickian and Single File Mutual Diffusion Coefficients in Heavy Oil + Diluent Mixtures.....</b>	<b>37</b>
<b>4.1. Introduction.....</b>	<b>37</b>
<b>3.2. Experimental Section.....</b>	<b>43</b>
3.2.1. Acoustic Setup.....	43
3.2.2. Materials.....	47
3.2.3. Experimental Procedure.....	47
<b>3.3. Results and discussion.....</b>	<b>49</b>
3.3.1. Polybutene + Toluene and ( Polybutene + carbon nanotubes ) + Toluene.....	49
3.3.2. Joint Fickian + Single File Diffusion Model Fits to Literature Data.....	53
3.3.3. Athabasca bitumen + toluene data sets ( this work).....	60
3.3.4. Impact of asphaltene mass fraction and solvent choice on relative importance of the two diffusion mechanisms.....	60
<b>3.4. Conclusion.....</b>	<b>67</b>
<b>3.5. References.....</b>	<b>68</b>
<b>Chapter 4: Conclusion and Future works.....</b>	<b>74</b>
<b>4.1. General Conclusion.....</b>	<b>74</b>
<b>4.2. Future Works.....</b>	<b>77</b>
<b>4.3. References.....</b>	<b>78</b>
<b>Bibliography.....</b>	<b>79</b>
<b>Appendix .....</b>	<b>87</b>
<b>A. Single File Free Diffusion Equation Solution.....</b>	<b>87</b>
<b>A.1. Introduction.....</b>	<b>87</b>

<b>A.2.Theory.....</b>	<b>87</b>
<b>A.3.Conclusions.....</b>	<b>104</b>
<b>3.4 References.....</b>	<b>104</b>
<b>B. Matlab Codes.....</b>	<b>106</b>
B.1. Speed of Sound Data to Concentration.....	106
B.2. Calculating value of n.....	107
B.3. Smoothing the data.....	110
B.4. Calculating diffusion coefficient.....	111
B.5. Boltzman-Matano Method.....	112
B.6 fitting single file and Fickian diffusion and finding gamma.....	113
<b>C. Experimental and Literature Data.....</b>	<b>114</b>
C.1. 273K Experiment Smoothed Data.....	114
C.2. 298K Experiment Smoothed Data.....	118
C.3. 313K Experiment Smoothed Data.....	121
C.4. Calibration Curve 273K.....	124
C.5. Calibration Curve 298K.....	129
C.6. Calibration Curve 313K.....	131
C.7. Fadaei et al. raw data.....	134
C.8. Sadighian et al., Athabasca vacuum residue + pentane raw data.....	149
C.9. Sadighian et al., Athabasca atmospheric residue + pentane raw data.....	156
C.10. Wen et al., Cold Lake bitumen + heptane raw data. ....	164
C.11. Zhang et al., Athabasca bitumen + pentane raw data.....	165

## List of Tables

<b>Table 2.1.</b> Free diffusion composition profile data sets available in the literature.....	7
<b>Table 2.2.</b> Properties of Athabasca bitumen used in this study.....	12
<b>Table 3.1.</b> Values of mobility, F, for different examples of nanostructure from the literature.....	43
<b>Table 3.2.</b> Properties of Athabasca bitumen used in this study.....	47
<b>Table 3.3.</b> Composition range, G, H and D for different datasets.....	64

## List of Figures

<b>Figure 2.1.</b> Simplified schematic for mutual diffusion between a light hydrocarbon + a nano/micro structured hydrocarbon resource sample. (b) Single file diffusion and Fickian diffusion comparison.....	6
<b>Figure 2.2.</b> Schematic of the view cell and data acquisition system used for diffusion measurements showing the arrangement of the acoustic sensors as an inset.....	13
<b>Figure 2.3.</b> An illustration of the local composition calibration procedure: (a) acoustic path length determination at $\square$ , 273 K, $\bullet$ , 298 K and $\blacktriangle$ , 313 K; (b) speed of sound measurements for known mixtures of toluene + Athabasca bitumen at 313 K; (c) elevation specific composition calibration curve for toluene + Athabasca bitumen mixtures at 313 K for the 20.1 mm elevation sensor; (d) composition profiles for toluene + Athabasca bitumen at 313 K. ■ 6 hours, $\triangle$ 12 hours, $\nabla$ 24 hours, $\blacklozenge$ 36 hours, $\blacktriangleleft$ 48 hours, $\star$ 60 hours, $\ast$ 72 hours.....	14
<b>Figure 2.4.</b> Local values of the time scaling exponent $n_w$ and their uncertainty based on ■, minimizing $\sigma_w$ and $\diamond$ , least square regression of slopes for: (a) Athabasca bitumen + toluene system <sup>13</sup> ; (b) Cold Lake bitumen + heptane <sup>15</sup> ; (c) Athabasca bitumen + pentane <sup>11</sup> ; (d) Athabasca atmospheric residue + pentane <sup>14</sup> ; (e) Athabasca vacuum residue + pentane <sup>14</sup> ; at room temperature based on composition profiles obtained from the citations.....	18

**Figure 2.5.** Raw composition vs elevation profiles for: (a) polybutene + toluene, and (b) toluene + (polybutene + 0.25 mass fraction carbon nanotubes) at 298 K. ■ 6 hours, △ 12 hours, ▽ 24 hours, ◆ 36 hours, ▲ 48 hours, ☆ 60 hours, \* 72 hours.....21

**Figure 2.6.** Local values of the time scaling exponent  $n_w$  and their uncertainty based on ■, minimizing  $\sigma_w$  and ◇, least square regression of slopes for: (a) polybutene + toluene and (b) (polybutene + 0.25 mass fraction carbon nano tubes) + toluene mixtures at 298K.....21

**Figure 2.7.** Smoothed composition profiles for Athabasca bitumen + toluene at: (a) 273 K, (b) 298 K and (c) 313 K. ■ 6 hours, △ 12 hours, ▽ 24 hours, ◆ 36 hours, ▲ 48 hours, ☆ 60 hours, \* 72 hours.....23

**Figure 2.8.** The time scaling exponent ( $n_w$ ) for Athabasca bitumen + toluene mixtures at: (a) 273 K, (b) 298 K and (c) 313 K based on ■, minimizing  $\sigma_w$  and ◇, least square regression of slopes (d) Data set comparison for Athabasca bitumen + toluene mixtures based on minimizing □<sub>w</sub>: ☆, Fadaei et al<sup>13</sup>; ○, 273 K, △ 298 K and ◇ 313 K.....24

**Figure 2.9.** Values of  $n_w$  based on minimizing  $\sigma_w$  as a function of C5 asphaltene mass fraction in Athabasca bitumen derived samples: △ Athabasca bitumen + pentane<sup>11</sup>; ▽ Athabasca atmospheric residue + pentane<sup>14</sup>, ◇ Athabasca vacuum residue + pentane<sup>14</sup>; ■ Athabasca bitumen + toluene<sup>13</sup>; Athabasca bitumen + toluene (this work), ● 273 K, ► 298 K and ◀ 313 K.....26

**Figure 2.10.** Temporal variation of  $n_w$  for (a) Cold Lake bitumen + heptane<sup>15</sup>; (b) Athabasca bitumen + pentane<sup>11</sup>; (c) Athabasca atmospheric residue + pentane<sup>14</sup>; (d) Athabasca vacuum residue + pentane<sup>14</sup>.  $n_w$  values obtained by minimizing  $\sigma_w$ : □ 0.45

solvent mass fraction,  $\circ$  0.5 solvent mass fraction,  $\triangle$  0.55 solvent mass fraction,  $\nabla$  0.6  
 solvent mass fraction,  $\diamondsuit$  0.65 solvent mass fraction,  $\lhd$  0.7 solvent mass fraction,  $\circlearrowleft$  0.75  
 solvent mass fraction,  $\star$  0.8 solvent mass fraction,  $\lozenge$  0.85 solvent mass fraction,  $\lhd$  0.9  
 solvent mass fraction.  $n_w$  values obtained using least square regression of slopes: ■ 0.45  
 solvent mass fraction, ● 0.5 solvent mass fraction, ▲ 0.55 solvent mass fraction, ▼ 0.6  
 solvent mass fraction, ♦ 0.65 solvent mass fraction, ◀ 0.7 solvent mass fraction, ▶ 0.75  
 solvent mass fraction, ♦ 0.8 solvent mass fraction, ★ 0.85 solvent mass fraction.....29

**Figure 2.11.** Temporal variation of  $n_w$  values for Athabasca bitumen + toluene (a) 273K  
 (b) 298 K (c) 313 K.  $n_w$  values obtained by minimizing  $\sigma_w$ : □ 0.45 solvent mass fraction,  
 $\circ$  0.5 solvent mass fraction,  $\triangle$  0.55 solvent mass fraction,  $\nabla$  0.6 solvent mass fraction,  
 $\diamondsuit$  0.65 solvent mass fraction,  $\lhd$  0.7 solvent mass fraction,  $\circlearrowleft$  0.75 solvent mass fraction,  
 $\star$  0.8 solvent mass fraction.  $n_w$  values obtained from least square regression of slopes: ■  
 0.45 solvent mass fraction, ● 0.5 solvent mass fraction, ▲ 0.55 solvent mass fraction, ▼  
 0.6 solvent mass fraction, ♦ 0.65 solvent mass fraction, ◀ 0.7 solvent mass fraction, ▶  
 0.75 solvent mass fraction, ♦ 0.8 solvent mass fraction. ....30

**Figure 3.1.** Schematic of the view cell and data acquisition system used for diffusion  
 measurements showing the arrangement of the acoustic sensors as an inset.....45

**Figure 3.2.** An illustration of the local composition calibration procedure: (a) acoustic  
 path length determination at □, 273 K, ●, 298 K and ▲, 313 K; (b) speed of sound  
 measurements for known mixtures of toluene + Athabasca bitumen at 313 K; (c)  
 elevation specific composition calibration curve for toluene + Athabasca bitumen  
 mixtures at 313 K for the 20.1 mm elevation sensor; (d) composition profiles for toluene

+ Athabasca bitumen at 313 K. ■ 6 hours, △ 12 hours, ▼ 24 hours, ♦ 36 hours, ◀ 48 hours, ☆ 60 hours, * 72 hours.....	46
---	----

<b>Figure 3.3.</b> Example showing the impact of smoothing on composition profiles: (a) Raw toluene concentration profile calculated based on speed of sound data using concentration calibration curve at 313K and (b) Smoothed toluene concentration profile versus elevation using local regression method. ■ 6 hours, △ 12 hours, ▼, 24 hours, ◀ 36 hours, □, 48 hours, ☆, 60 hours. * 72 hours.....	46
--	----

<b>Figure 3.4.</b> Polybutene + toluene a) composition profiles after ● 12 hours, □ 48 hours; cross over point occurs at 0.37 mass fraction. b) Mass fraction versus joint variable in single file diffusion after ● 12 hours, □ 48 hours; cross over point occurs at 0.37 mass fraction. c) Fickian diffusion model fit: ○ 6 hours, Δ, 12 hours, ▼, 24 hours, ◀ 36 hours, □, 48 hours, ☆, 60 hours. d) Fickian diffusion model, $D = 2 \times 10^{-10} \text{ m}^2/\text{s}$ , $C_0 = 0.37$ for polybutene + toluene experimental data at 24 hours.....	51
---	----

<b>Figure 3.5.</b> (polybutene + CNT) + toluene a) Single file diffusion model fit with $H = 15$ and 30. ○ 6 hours, Δ, 12 hours, ▼, 24 hours, ◀ 36 hours, □, 48 hours, ☆, 60 hours. b) Fickian diffusion fit: ○ 6 hours, Δ, 12 hours, ▼, 24 hours, ◀ 36 hours, □, 48 hours, ☆, 60 hours. c) Single file and Fickian diffusion models, and equation (4.8) for 48 hours data. d) Fitted values for $\gamma$ , equation (4.8), as a function of toluene mass fraction where time is a parameter: ■ 6 hours, Δ, 12 hours, ▼, 24 hours, ◀ 36 hours, □, 48 hours and ☆, 60 hours.....	52
---	----

**Figure 3.6.** Athabasca bitumen + toluene at 296K<sup>27</sup> a) Fits for  $\lambda=0.5$  ○ 40 seconds, Δ, 90 seconds, ▼, 140 seconds, □, 200 seconds, ☆, 240 seconds for Athabasca bitumen+toluene<sup>27</sup>; cross over point occurs at 0.5 mass fraction. b) Fits for  $\lambda=0.25$  ○ 40 seconds, Δ, 90 seconds, ▼, 140 seconds, □, 200 seconds, ☆, 240 seconds. c) Single file and Fickian diffusion models, and equation (4.8) for 140 seconds data. d) Fitted values for  $\gamma$ , equation (4.8), as a function of toluene mass fraction where time is a parameter: ■ 40 seconds, Δ, 90 seconds, ▼, 140 seconds, □, 200 seconds and ☆, 240 seconds.....54

**Figure 3.7.** Athabasca atmospheric residue+pentane<sup>29</sup>a) Fits for  $\lambda=0.5$  ■, 3420 seconds, Δ, 6780 seconds, ▼, 14820 seconds, □, 25980 seconds for Athabasca atmospheric residue+pentane<sup>30</sup>; cross over point occurs at 0.67 mass fraction. B) Fits for  $\lambda=0.25$  ■, 3420 seconds, Δ, 6780 seconds, ▼, 14820 seconds, □, 25980 seconds for Athabasca atmospheric residue+pentane<sup>30</sup>. c) Single file and Fickian diffusion models, and equation (4.8) for 14820 seconds data. d) Fitted values for  $\gamma$ , equation (4.8), as a function of toluene mass fraction where time is a parameter: ■, 3420 seconds, Δ, 6780 seconds, ▼, 14820 seconds, □, 25980 seconds.....56

**Figure 3.8.** Athabasca vacuum residue+pentane<sup>30</sup>a) Fits for  $\lambda=0.5$  ■, 4860 seconds, Δ, 9120 seconds, ▼, 15780 seconds, □, 32040 seconds for Athabasca vacuum residue+pentane<sup>30</sup>; cross over point occurs at 0.65 mass fraction. b) Fits for  $\lambda=0.25$  ■, 4860 seconds, Δ, 9120 seconds, ▼, 15780 seconds, □, 32040 seconds for Athabasca vacuum residue+pentane. c) Single file and Fickian diffusion models, and equation (4.8) for 15780 seconds data. d) Fitted values for  $\gamma$ , equation (4.8), as a function of toluene

mass fraction where time is a parameter: ■, 4860 seconds, Δ, 9120 seconds, ▼, 15780 seconds, □, 32040 seconds.....57

**Figure 3.9.** Athabasca bitumen+pentane<sup>28,29</sup> a) Fits for  $\lambda=0.5$  ■ 630 minutes, Δ, 1470 minutes , ▼, 2910 minutes and □, 5790 minutes for Athabasca bitumen+pentane<sup>27,28</sup>; cross over point occurs at 0.3 mass fraction. b) Fits for  $\lambda=0.25$  ■ 630 minutes, Δ, 1470 minutes, ▼, 2910 minutes and □, 5790 minutes for Athabasca bitumen+pentane<sup>28,29</sup>. c) Single file and Fickian diffusion models, and equation (4.8) for 1470 minutes data. d) Fitted values for  $\gamma$ , equation (4.8), as a function of toluene mass fraction where time is a parameter: ■ 630 minutes, Δ, 1470 minutes, ▼, 2910 minutes and □, 5790 minutes.....58

**Figure 3.10.** Cold Lake bitumen+heptane<sup>26</sup> a) Fits for  $\lambda=0.5$  ■ 319 minutes, Δ, 606 minutes, ▼, 1398 minutes and □, 1753 minutes for Athabasca bitumen+pentane<sup>26</sup>; cross over point occurs at 0.3 mass fraction. b) Fits for  $\lambda=0.25$  ■ 319 minutes, Δ, 606 minutes, ▼, 1398 minutes and □, 1753 minutes for Athabasca bitumen+pentane<sup>26</sup>. c) Single file and Fickian diffusion models, and equation (4.8) for 1398 minutes data. d) Fitted values for  $\gamma$ , equation (4.8), as a function of toluene mass fraction where time is a parameter: ■ 319 minutes, Δ, 606 minutes, ▼, 1398 minutes and □, 1753 minutes.....60

**Figure 3.11.** Athabasca bitumen + toluene at 313 K a)  $\lambda=0.5$  ○ 6 hours, Δ, 12 hours, ▼, 24 hours, ◀ 36 hours, □, 48 hours, ☆, 60 hours for 313K; cross over point occurs at 0.5 mass fraction. b)  $\lambda=0.25$  ○ 6 hours, Δ, 12 hours, ▼, 24 hours, 36 hours, □, 48 hours, ☆, 60 hours for 313K; cross over point occurs at 0.5 mass fraction. c) Single file and Fickian diffusion models, and equation (4.8) for 48 hours data. d) Fitted values for  $\gamma$ ,

equation (4.8), as a function of toluene mass fraction where time is a parameter: ■ 6 hours, △, 12 hours, ▼, 24 hours, ▲ 36 hours, □, 48 hours and ★, 60 hours.....61

**Figure 3.12.** Athabasca bitumen + toluene at 298 K a) Fits for  $\lambda=0.5$  ○ 6 hours, △, 12 hours, ▼, 24 hours, ▲ 36 hours, □, 48 hours, ★, 60 hours for 298K; cross over point occurs at 0.43 mass fraction. B) Fits for  $\lambda=0.25$  ○ 6 hours, △, 12 hours, ▼, 24 hours, ▲ 36 hours, □, 48 hours, ★, 60 hours for 298K; cross over point occurs at 0.43 mass fraction. C) Single file and Fickian diffusion models, and equation (4.8) for 48 hours data. d) Fitted values for  $\gamma$ , equation (4.8), as a function of toluene mass fraction where time is a parameter: ■ 6 hours, △, 12 hours, ▼, 24 hours, ▲ 36 hours, □, 48 hours and ★, 60 hours.....62

**Figure 3.13.** Athabasca bitumen + toluene at 273 K a) Fits for  $n_w=0.5$  ○ 6 hours, △, 12 hours, ▼, 24 hours, ▲ 36 hours, □, 48 hours, ★, 60 hours for 273K; cross over point occurs at 0.43 mass fraction. B) Fits for  $n_w=0.25$  ○ 6 hours, △, 12 hours, ▼, 24 hours, ▲ 36 hours, □, 48 hours, ★, 60 hours for 273K; cross over point occurs at 0.41 mass fraction. C) Single file and Fickian diffusion models, and equation (4.8) for 48 hours data. d) Fitted values for  $\gamma$ , equation (4.8), as a function of toluene mass fraction where time is a parameter: ■ 6 hours, △, 12 hours, ▼, 24 hours, ▲ 36 hours, □, 48 hours and ★, 60 hours.....63

**Figure 3.14.** Asphaltene mass fraction versus the values of gamma for: ○ Athabasca atmospheric residue + pentane<sup>30</sup> ,△, Athabasca atmospheric residue + pentane<sup>30</sup> ,□,

Athabasca bitumen + pentane <sup>28,29</sup>	■	Athabasca bitumen + toluene at 273 K	▲	
Athabasca bitumen + toluene at 298 K	★	Athabasca bitumen + toluene at 313 K	●	
Athabasca bitumen + toluene <sup>27</sup>				66
<b>Figure 3.15.</b> Schematic representation of solvent effect on aggregation size				86
<b>Figure A.1.</b> Hypergeometric terms in the solution of equation 3.2-15: a) term 2, b) term 3 and c) term 4				93
<b>Figure A.2</b> Variation of value of calculated F versus solvent composition profile at different H values for: a) Athabasca bitumen + toluene at 273 K (G=1.5, H=16±4 $\frac{s^{0.25}}{m}$ ), b) Athabasca bitumen + toluene at 298 K (G=1.32, H=9±1 $\frac{s^{0.25}}{m}$ ), c) Athabasca bitumen + toluene at 313 K (G=1, H =5±0.5 $\frac{s^{0.25}}{m}$ ), d) Athabasca atmospheric residue + pentane <sup>7</sup> (G=0.53, H=6±3 $\frac{s^{0.25}}{m}$ ), e) Athabasca vacuum residue + pentane <sup>7</sup> (G=0.49, H=10±2 $\frac{s^{0.25}}{m}$ ), f) Athabasca bitumen + pentane <sup>8,9</sup> (G=2.33, H=6±2 $\frac{s^{0.25}}{m}$ ), g) Athabasca bitumen + toluene <sup>6</sup> (G=1, H=40±5 $\frac{s^{0.25}}{m}$ ), h) Polybutene + CNT + toluene (G=0.53, H=23±7 $\frac{s^{0.25}}{m}$ ), i) Cold Lake bitumen + heptane (G=0.95, H=8±4 $\frac{s^{0.25}}{m}$ )		104		

# Nomenclature

<b>D</b>	Diffusion Coefficient
<b>C</b>	Solvent Concentration
<b>C<sub>0</sub></b>	Mass fraction at the cross over point
<b>F</b>	Single File Mobility
<b>x</b>	Distance
<b>n<sub>w</sub></b>	Exponent of time
<b>t</b>	Time
<b>λ</b>	Joint variable
<b>w</b>	Solvent weight fraction
<b>λ<sub>w</sub></b>	Joint variable at a certain weight fraction
<b>σ<sub>w</sub></b>	Sum of absolute difference at certain weight fraction
<b>ρ</b>	Density of fluid
<b>γ</b>	Fickian diffusion mechanism effectiveness fraction.
<b>H</b>	Parameter defined in equation (3.2-31)
<b>G</b>	Parameter defined in equation (3.2-31)



# 1. Introduction

The worldwide use of hydrocarbon energy is increasing while the production of conventional oil and gas resources is decreasing. Unconventional resources of hydrocarbon energy such as oil sands bitumen are playing an increasingly important role in global production. Athabasca oil sands comprise 1.7 trillion barrels of bitumen, which is comparable to the world's total conventional petroleum. Athabasca Bitumen and other heavy hydrocarbon resources are high-mean-molar-mass and structured organic materials with complex phase behaviors at the nano- and micro- meter length scales. The reliability of current proposed production and processing techniques relies on the accuracy of our knowledge of thermophysical and transport properties of these materials on their own and in mixtures with hydrocarbon and non-hydrocarbon diluents.

For example, Steam assisted gravity drainage or SAGD is the standard technique for in situ production of Athabasca bitumen. In this process high-pressure steam is injected to the reservoir. This heats the reservoir to over 200°C, reducing the viscosity of the bitumen so that it flows under gravity to a producer well where it is pumped out to surface facilities. This process requires a huge amount of natural gas in order to produce the needed steam, leading to high greenhouse gas emissions. Application of organic diluents instead of or in addition to steam during in-situ extraction would reduce greenhouse gas emissions.

Diffusion of light hydrocarbons, and non-hydrocarbons in these resources is of significant interest as new production and refining concepts that envision, for

example, addition of light hydrocarbons and non-hydrocarbons to reservoirs to enhance production have begun to emerge. Production rates in a reservoir where hydrocarbons are injected mainly depend on how fast light hydrocarbons can penetrate into the heavy oil resources.

Diffusive mass transfer, the subject of this work, is expected to play a key role in the development of these new processes. Two aspects are considered here:

1. Identification of the active mechanism(s) for diffusive mass transfer.
2. Evaluation of mutual diffusion coefficients relevant to the modes of mass transfer identified, and the relative importance of modes of diffusion.

Understanding is developed from the well-established perspective of free diffusion concepts. Composition-distance profiles arising during free diffusion scale as a function of the joint variable (distance/time<sup>n<sub>w</sub></sup>). When scaled in this way composition profiles obtained at different times during the same free diffusion experiment superimpose on one another. Simple fluids are governed by Fickian diffusion, where  $n_w = 0.5$ . For nanostructured fluids the value of  $n_w$  can be as low as  $n_w = 0.25$ , known as the single file limit but more typically the value for the exponent falls between these two limits and is composition dependent. In this work, five published data sets comprising free diffusion composition profiles for Athabasca bitumen fractions and for Cold Lake bitumen + light hydrocarbons obtained using diverse apparatus, are probed from this perspective. Additional experimental results are provided for Athabasca bitumen + toluene mixtures over the temperature range 273 to 313 K, and results from positive and negative control

experiments for two well-defined mixtures: (0.25 mass fraction carbon nanotubes + polybutene) + toluene, and polybutene + toluene, are also provided. These latter measurements were used to demonstrate that the acoustic view-cell and the data analysis methods employed in this work discriminated the two mechanisms adequately. The value of  $n_w$  for the negative control experiment remains at  $0.50 \pm 0.05$  over the entire composition range and for the positive control experiment, the value drops to  $n_w = 0.30 \pm 0.02$  at low toluene mass fraction. While the quality of the diffusion profile data in the data sets analyzed is variable, the values of the exponent  $n_w$  are shown to be light hydrocarbon dependent and increase from  $n_w \sim 0.25$  at low light hydrocarbon mass fraction up to  $n_w \sim 0.50$  at high light hydrocarbon mass fraction. These mechanistic findings comprising chapter 2, were reported in “Fickian and Non-Fickian diffusion in heavy oil + light hydrocarbon mixtures” Energy and Fuels 29(4), 2177-2189.

While identification of active diffusion mechanisms was through direct application of known physics, assessment of mutual diffusion coefficient values for both mechanisms and identification of a composition dependent weighting function for the relative importance of the two diffusion mechanisms proved more challenging. First a simplified expression for the mutual diffusion coefficient according to the single file diffusion mechanism had to be derived. This work is reported in appendix A, and then sets free diffusion composition profiles were simulated using a three parameter joint Fickian-Single File diffusion model. This latter work, comprising Chapter 3, will be submitted for publication shortly with appendix A as an appendix. The over all conclusions and future work are presented in Chapter 4.

## 2.Fickian and non-Fickian diffusion in heavy oil + light hydrocarbon mixtures

### 2.1. Introduction

The solution of the well-known one-dimensional differential form of Fick's free diffusion equation<sup>1,2</sup>:

$$\frac{\partial c}{\partial t} = D \frac{\partial^2 c}{\partial x^2} \quad (2.1)$$

is normally expressed in dimensionless form as:

$$c(x, t) = \frac{x c_0}{\sqrt{4 \pi D t}} e^{\frac{-x^2}{4 D t}} \quad (2.2)$$

where  $c$  is the mass or mole fraction of one of the fluid components,  $t$  is time,  $D$  is the mutual diffusion coefficient and  $x$  is the spatial variable. According to equation 2.2, composition-distance profiles obtained at different times can be superimposed if composition is expressed in terms of the joint variable:

$$\lambda = x / \sqrt{t} \quad (2.3)$$

This general and well-known result facilitates the evaluation of diffusion coefficients and is typically an excellent check on composition profile data quality where, for example, impacts of convection on results are readily detected. In structured fluids the concept of space-time similarity still holds but the exponent is variable and equation 2.3 becomes:

$$\lambda_w = x / t^{n_w} \quad (2.4)$$

where the exponent  $n_w$  is a function of composition and fluid structure. In this work, the weight fraction of the penetrant,  $w$  is the composition variable. The minimum value for  $n_w$  was identified by Hodgkin and Keynes<sup>3</sup> who introduced the concept of the single file diffusion limit in 1955. At the single file limit,  $n_w = 0.25$ . This limit arises in highly structured fluids where molecules or particles cannot pass one another freely but must move through a medium or a constriction sequentially. This theoretical limit has been observed experimentally in diverse contexts over time.<sup>4-7</sup> In micro channels, Kamholz<sup>8</sup> and later Kamholz and Yager<sup>9</sup> showed that near the walls of a 10  $\mu\text{m}$  wide microfluidic channel,  $n_w = 1/3$  for pressure driven flow, on the basis of both theoretical calculations and experimental measurements. Ismagilov et al.<sup>10</sup> also demonstrated experimentally that at steady state near the wall of pressure driven two phase laminar flow in a channel, transverse diffusion across the fluid-fluid interface scales with  $n_w = 1/3$  as well. From a theoretical perspective, it is easily shown that for integer values  $i = 1, 2, 3, 4$ , that the general solution to the family of differential equations of the form:

$$\frac{\partial C}{\partial t} = D_i \frac{\partial^i C}{\partial x^i} \quad (2.5)$$

is expressed in terms of the joint variable:

$$\lambda = x/t^{1/i} \quad (2.6)$$

While the subject of a future work, from equations 2.5 and 2.6, the values of  $n_w = 1/2, 1/3$  and  $1/4$  have clear roots both in mathematics and in observed physical phenomena. It is therefore possible to envision interpreting mixed mode diffusion in structured media as a sum of Fickian and non-Fickian diffusive contributions.

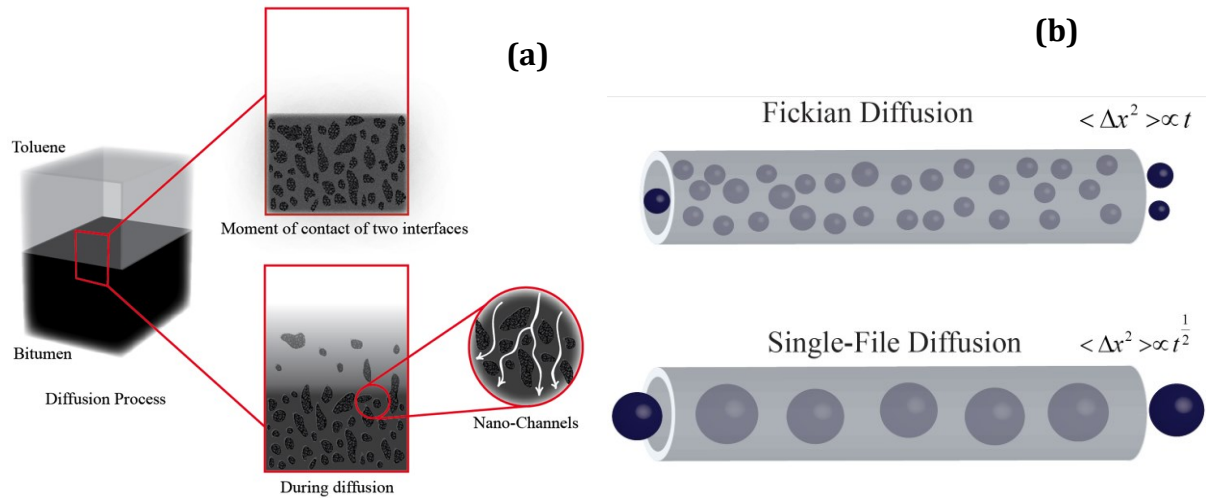


**Figure 2.1.** (a) Simplified schematic for mutual diffusion between a light hydrocarbon + a nano/micro structured hydrocarbon resource sample. (b) Single file diffusion and Fickian diffusion comparison.

To date, only Equation 2.2 has been used to interpret free diffusion data for hydrocarbon resource + light hydrocarbon mixtures. Pertinent examples are noted in Table 2.1. In these published works<sup>11-15</sup>, a lower density species diffuses and composition profiles are obtained as a function of time in viscous and hence quiescent media. Mutual diffusion coefficients were obtained in all of these examples by regressing composition vs distance profiles assuming  $n_w = 0.5$ . It is worth noting that temperature was not controlled precisely for these measurements and that the Athabasca bitumen referred to in references 11-13 are subsamples of the same master sample.

**Table 2.1.** Free diffusion composition profile data sets available in the literature.

Mixture (number of composition profiles)	T (K)	experimental method	composition resolution (wt %)	C5 asphaltene (wt %)	reference	
Athabasca bitumen + pentane	9	293	Vial + X-ray video imaging	0.3	18.6	11,12
Athabasca bitumen + toluene	5	~293	Microfluidic apparatus + visible light transmission imaging	0.15	18.6	13
Athabasca vacuum residue + pentane	5	293	Vial + X-ray video imaging	0.3	32	14
Athabasca atmospheric residue + pentane	5	293	Vial + X-ray video imaging	0.3	24 <sup>a</sup>	14
Cold Lake bitumen + heptane	5	~293	Vial placed in a CAT scanner	1	17.5 <sup>b</sup>	15

<sup>a</sup> This is an estimated value.

<sup>b</sup> C7 asphaltene is 12 wt%<sup>15</sup>

The assumption that  $n_w = 0.5$  for heavy hydrocarbon resource + light hydrocarbon mixtures is revisited in the present work. These resources exhibit complex phase behaviors on their own<sup>16-19</sup> and in mixtures with light hydrocarbons<sup>20</sup> and non-hydrocarbons.<sup>21,22</sup> For example, phase diagrams for Athabasca Bitumen, Maya crude oil, and Safaniya vacuum residue have been prepared<sup>16-19</sup>. These fluids comprise well-dispersed nano-scale asphaltene-rich phase domains, and maltene-rich phase domains that undergo phase transitions in a largely independent manner<sup>16-19</sup>. The asphaltene-rich phase domains comprise approximately 20 wt % of these fluids and are multiphase. Further, at temperatures below approximately 310 K a fraction of the maltene-rich phase domains can also be multiphase - including solids. The presence of additional microscopic-length-scale liquid-crystal-rich domains further complicates the phase

space<sup>23,24</sup>. Finally, addition of light hydrocarbons to resource samples impacts their phase behavior both in time<sup>24,25</sup> and with respect to the number and nature of phases<sup>26-28</sup>. While the exact structure and spatial distribution of phase domains in hydrocarbon resources such as Maya crude oil, Safaniya vacuum residue and Athabasca bitumen are unknown, free diffusion between a light hydrocarbon and structured resource samples may be viewed from the perspective of a simple molecular fluid penetrating into a structured fluid comprising a broad range of nanoscopic and microscopic fluid-filled channels, as illustrated in Figure 2.1. In such complex fluids, Fickian and non-Fickian diffusive effects are expected to arise both with respect to composition, irrespective of time, and with respect to time at fixed composition as local phase behavior evolves.

The motivation to test this hypothesis arises from known aspects of the phase behavior of heavy oils, noted above, but it is also driven by industrial need. New processes for producing these resources are under development, which rely principally on diffusion for their successful application. Driven by joint desires to reduce the viscosity of the produced fluid, and hence to increase the rate of production, and to reduce the carbon dioxide emissions linked to current practice, interest in the development of new processes where light-hydrocarbons or non-hydrocarbons are injected into heavy oil and bitumen reservoirs<sup>29,30</sup> has grown rapidly. If these processes are to be successful, detailed understanding of diffusion mechanisms and accurate diffusion rates for such mixtures are required. Consequently, this contribution comprises three parts. Composition profiles for the examples noted in Table 2.1 are evaluated to determine whether there is a detectable composition dependence for  $n_w$  as anticipated for structured fluids. Further, as the nature and extent of the nano and micro structures present is expected to be temperature

dependent, additional composition profiles are obtained for Athabasca bitumen + toluene mixtures over a range of temperatures. Supporting measurements comprising positive and negative controls related to the determination of the exponent  $n_w$ , based on the free diffusion method and equipment employed in the present study are also performed and outcomes are discussed.

## **2.2. Composition Profile Regression Algorithm to Determine Local Values of $n_w$ and Their Uncertainty**

This algorithm comprises three parts. First, local regression<sup>31</sup> is used to smooth composition profile data so that comparisons at fixed composition can be made consistently. Following the local regression procedure, smoothing of weight fraction data,  $w_i$ , at a fixed elevation,  $x_i$ , is performed using a polynomial fit to  $(w_j, x_j)$  pairs in the neighborhood of the elevation of interest. The data point to be smoothed has the most influence on the fit and data points outside the neighborhood have no influence on the fit. In this work, the neighborhood is defined as an interval of 0.05 mass fraction solvent centered on the point of interest.

For free diffusion experiments there is one elevation for which the composition is time invariant. This elevation is the origin of the coordinate system underlying equations 2.1-2.6. All composition profiles pass through this point, colloquially referred to as the cross-over point. The elevation corresponding to the origin of the coordinate system is identified on the basis of smoothed composition profile data.

In the second step of the algorithm, sets of smoothed composition profiles are regressed to identify local values for  $n_w$ . Values and uncertainties related to two different regression

approaches are presented. The local derivatives of the composition profiles, over a 0.05 mass fraction composition range, were fit by adjusting the value of  $n_w$  in equation 4, using least squares regression to minimize the variation of the slope of the composition profiles within the composition interval of interest. Local integral fits to the composition profile data were also performed on the smoothed data. In this approach, local  $n_w$  values were obtained by minimizing the sum of absolute differences,  $\sigma_w$ , between individual  $\lambda_w$  values, defined in equation 4, that possess a common composition,  $w$ , obtained at 0.01 mass fraction increments and mean values,  $\overline{\lambda_w}$ , obtained over 0.05 mass fraction intervals:

$$\sigma_w = \frac{1}{j} \sum_{i=1}^j \left| 1 - \frac{\lambda_{w,i}}{\overline{\lambda_w}} \right| \quad (2.7)$$

For these fits the search limits for  $n_w$  were set as  $0.15 < n_w < 0.75$  at a resolution of 0.025. Best-fit values were identified as the mid point between adjacent values with the least error. These two regression approaches are complimentary, even if they yield comparable values for  $n_w$  locally because of the composition dependence of their sensitivity to uncertainty in composition profile data. For example, at the cross over point where composition is time invariant, regression of the slopes of the composition profiles can in principle provide good estimates for  $n_w$ , whereas irrespective of the value of  $n_w$  identified by minimizing the value of  $\sigma_w$  in equation 2.7, any value of  $n_w$  from negative to positive infinity is equally valid and the best-fit value merely reflects experimental uncertainties related to composition, or distance. At compositions approaching  $w = 0$  or 1, large uncertainties are anticipated for both approaches but the values of  $n_w$  determined from derivative fits to the composition data are expected to be greater.

The third step of the algorithm comprises an assessment of the uncertainties of local  $n_w$  values. The range of uncertainty of  $n_w$  values for a given composition and for a specific data sets were established by determining the range of  $n_w$  values that allowed the composition profiles at all time steps to overlap within the composition measurement uncertainty. As a key objective of this study is to identify values for  $n_w$ , and it is not clear whether individual data sets are sufficiently accurate to do so, composition intervals where it was not possible to identify a range of  $n_w$  values that meet this criterion, are treated separately. Local values of  $n_w$  with an uncertainty that exceed 0.1 are excluded from the  $n_w$  determination irrespective of the mean. These criteria restrict the composition ranges for individual data sets from which  $n_w$  values can be extracted but provide reliable and objective criteria for their assessment.

## **2.3. Experimental**

### **2.3.1. Materials**

Toluene (99%) was obtained from Fischer Scientific. Polybutene, supplied by Cannon Instruments as a Newtonian viscosity standard, has a viscosity of 1600 Pa.S, and a density of 907 kg/m<sup>3</sup> at 298 K. Carbon nanotubes, possessing an internal diameter of 5.5 nm, outer diameter of 6 to 9 nm and a length of 5μm were obtained from Aldrich. Athabasca Bitumen was provided from Syncrude Canada. Relevant properties of the Athabasca Bitumen sample are summarized in Table 2.2.

**Table 2.2.** Properties of Athabasca bitumen used in this study.

Property	Value	Reference
Density (kg/m <sup>3</sup> ) @ 293 K	1026	16
Complex Viscosity (Pa.s) $\omega=63\text{ s}^{-1}$ and 0.3% shear strain @ 273 K @ 298 K @ 313 K	~90000 ~2000 ~300	34
SARA fractions (wt. %)		
Saturates	16.1	
Aromatics	48.5	
Resins	16.8	
Asphaltenes (C5)	18.6	

### 2.3.2. Apparatus and Procedure

In this work, composition profiles were determined by calibrating speed of sound values with composition and making use of an acoustic array data acquisition system attached to a thermostatted cell. Local compositions were determined in a 4 cm tall cell using sealed sets of probes with elevation spacings of 600  $\mu\text{m}$ . Measurements are averaged over a local length of 600  $\mu\text{m}$ . Typical composition profiles comprise 50-70 composition-elevation pairs. The accuracy of the composition measurements is dictated by the reproducibility of local speed of sound values, better than +/- 3 m/s, and the difference in the speed of sound between the hydrocarbon resource sample and the light

hydrocarbon, frequently more than 400 m/s. Thus composition reproducibility uncertainties for composition are less than 0.01 (mass fraction basis).

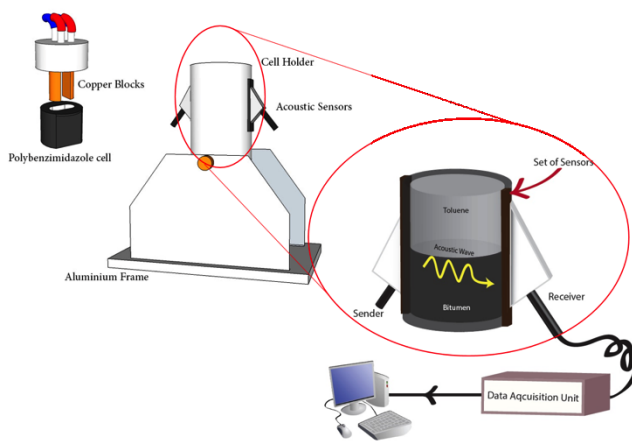


**Figure 2.2.** Schematic of the view cell and data acquisition system used for diffusion measurements showing the arrangement of the acoustic sensors as an inset.

A detailed description of the principles of measurement, the apparatus, the operating procedures, the data acquisition and data interpretation procedures are provided elsewhere<sup>32</sup>. Only a brief overview and case specific details are presented here with reference to an apparatus schematic shown in Figure 2.2. Fluid samples were placed in a polybenzimidazole cell within an aluminum frame. The cell was then sealed with an end cap. The temperature was monitored and controlled using a thermistor probe, with an effective tolerance of  $\pm 0.1$  K. An ethylene glycol + water mixture from a thermostatted reservoir (Fisher Scientific Isotemp 3006D) was circulated through the two copper blocks that are attached to the end cap and which fit within the cell cavity. The acoustic array sensors were screwed into place and coupled to the external walls of the cell using an

acoustic coupling gel. The data acquisition hardware comprises a TomoScan Focus LT and the data acquisition software comprises TomoView Software, both from Olympus NDT.

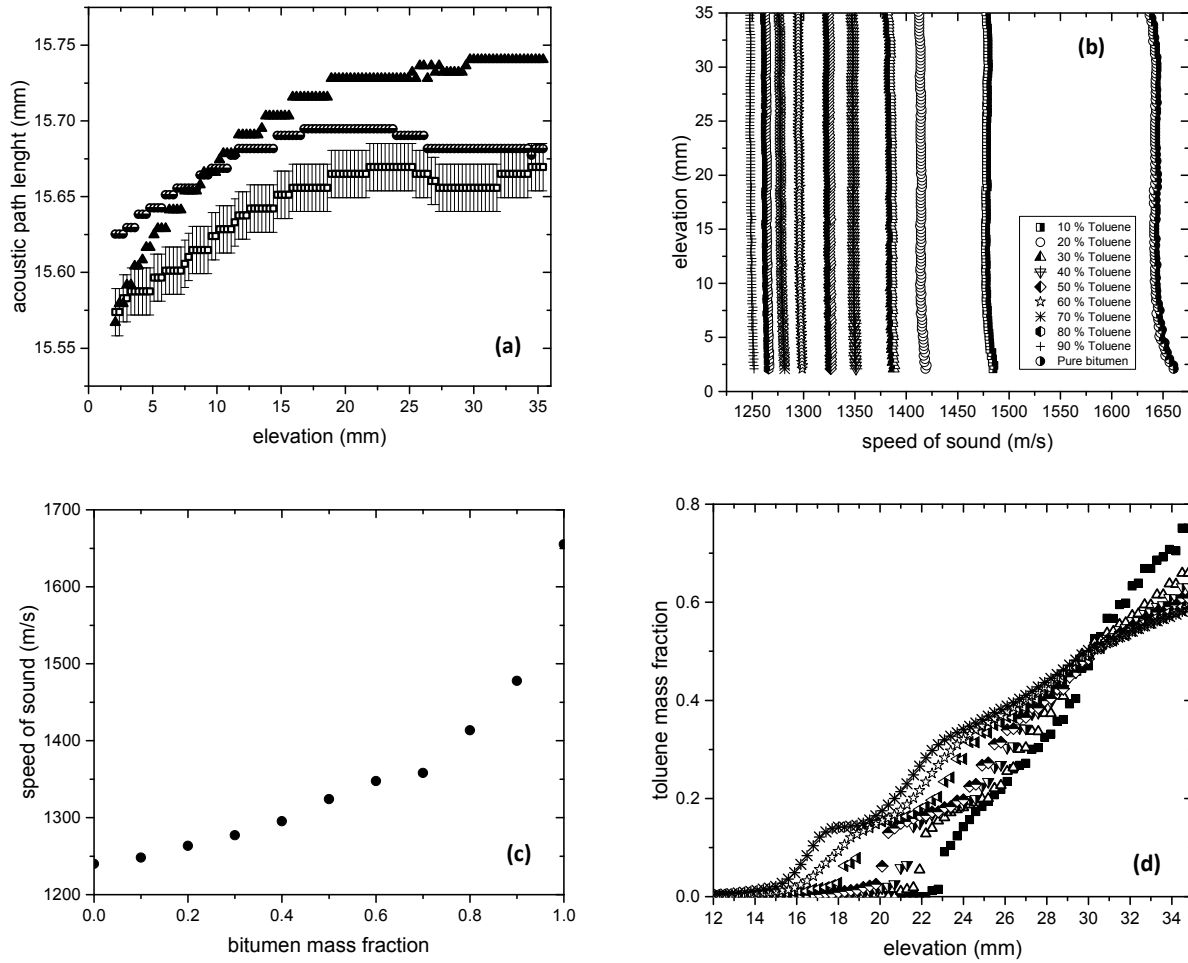


**Figure 2.3.** An illustration of the local composition calibration procedure: (a) acoustic path length determination at  $\square$ , 273 K,  $\bullet$ , 298 K and  $\blacktriangle$ , 313 K; (b) speed of sound measurements for known mixtures of toluene + Athabasca bitumen at 313 K; (c) elevation specific composition calibration curve for toluene + Athabasca bitumen mixtures at 313 K for the 20.1 mm elevation sensor; (d) composition profiles for toluene

+ Athabasca bitumen at 313 K. ■ 6 hours, △ 12 hours, ▼ 24 hours, ♦ 36 hours, ▲ 48 hours,  
☆ 60 hours, \* 72 hours.

Speed of sound vs composition calibrations were assessed at each elevation for each pseudo binary mixture and at each temperature. The procedure is illustrated in Figure 2.3. First, path lengths as a function of elevation were determined based on time of flight measurements for toluene, which possesses a well-known speed of sound value as a function of temperature at atmospheric pressure [NIST]<sup>33</sup> (Figure 2.3-a). Speeds of sound for mixtures of known composition, Athabasca bitumen + toluene in this example, Figure 2.3-b, were then used to prepare composition calibration curves (Figure 2.3-c) for each elevation so that mixtures of unknown composition could be interpolated. For this example, mixtures of known composition were prepared by combining Athabasca bitumen with toluene. At higher mass fractions of toluene, a homogenizer (Fischer Scientific Analog Vortex Mixer) was used to homogenize mixtures. At lower toluene mass fractions a bath sonicator operated at temperatures ranging 60°C to 70°C for at least 1 hour was used to homogenize sealed vials containing mixtures. As, composition profiles for Athabasca bitumen + toluene mixtures were obtained at 273 K, 298 K and 313 K, local calibrations were obtained for each elevation at each of these temperatures. Calibrations for polybutene + toluene and polybutene + carbon nanotubes + toluene, at 298K were performed in a similar manner.

Athabasca bitumen is semi solid at room temperature, as noted in the introduction, and sub-samples were heated to 353 K for 10 minutes so that they could be poured into the cell. The cell was then sealed and placed in an oven with air atmosphere at 353 K for 1

hour before it was equilibrated in the frame at 323 K over night to ensure the sample was uniformly distributed and free of gas bubbles. The bath temperature was then set to the desired temperature and after thermal equilibrium was reached, toluene was injected into the upper portion of the cell using a syringe. As the cell and the copper blocks have a large thermal mass, and the temperature difference between the toluene and the set temperature of the cell is small, the duration of the thermal transient, at less than ten seconds, is orders of magnitude smaller than the time scale of the diffusion measurements – hours. Composition profile evolution was assumed to begin at the time of injection.

Control experiments were performed at 298 K. Polybutene + toluene provided a negative control because polybutene + toluene mixtures comprise a single liquid phase.  $n_w$  is expected to be 0.5 over the entire composition range. To ensure that the high-viscosity polybutene was free of bubbles, it was placed in the polybenzimidazole cell and left in the oven at 353 K for 12 hours. 25% carbon nanotubes + polybutene comprise a model structured fluid and for toluene + (carbon nanotubes + polybutene) pseudo binary mixtures values of  $n_w$  less than 0.5 are expected, particularly at low toluene mass fractions. The carbon nanotubes were combined with the polybutene at 353 K using a turbine impeller, described in detail elsewhere<sup>14</sup>, and then treated in the same manner as the negative control sample. For these control experiments care was also taken to ensure the absence of gas bubbles and well defined horizontal interfaces at time zero. Polybutene was selected for control experiments because the viscosity of polybutene is comparable to the zero shear viscosity of Athabasca bitumen.

## **2.4. Results and Discussion**

### **2.4.1. Local time invariant values of $n_w$ and their uncertainty derived from composition profiles of heavy oil + light hydrocarbon mixtures in the literature**

Local values of  $n_w$ , based on the criteria set out above, are presented in Figure 2.4 a-e for the mixtures listed in Table 2.1. In all cases the exponent values are much less than 0.5 at low mass fractions of the light hydrocarbon. Convective or other effects, especially at longer times and at high light hydrocarbon mass fractions where the viscosity is orders of magnitude lower than the heavy hydrocarbon<sup>35,36</sup>, impact the certainty of the exponent value determinations. The data obtained using the microfluidic free-diffusion apparatus, shown in Figure 2.4-a, appear to be least impacted by this limitation due to the short time scale of the measurements. Composition profiles were obtained over a few minutes<sup>13</sup> as opposed to multiple days for the other measurements. For the other data sets, Figure 2.4b-e, the composition ranges shown are restricted because it was not possible to fit all of the composition profiles to within experimental composition error simultaneously at higher light hydrocarbon mass fractions. All of the data sets deviate from Fickian behavior ( $n_w = 1/2$ ). The mixtures reported in Figures 2.4a, 2.4b, 2.4d and 2.4e appear to be trending toward the single file limit ( $n_w = 1/4$ ) at low light hydrocarbon mass fraction. These same mixtures trend toward Fickian behavior at high light hydrocarbon mass fraction. The mixture reported in Figure 2.4 c, possesses an intermediate and constant value,  $n_w \sim 0.4$ , for the composition range  $0 < w < 0.5$ . The hypothesized non-Fickian behavior, particularly as the hydrocarbon resource axis is approached is clearly evident and this preliminary analysis sets the stage for careful experiments explicitly targeting the

evaluation of  $n_w$  as a function of temperature and composition for heavy oil or bitumen + solvent mixtures.

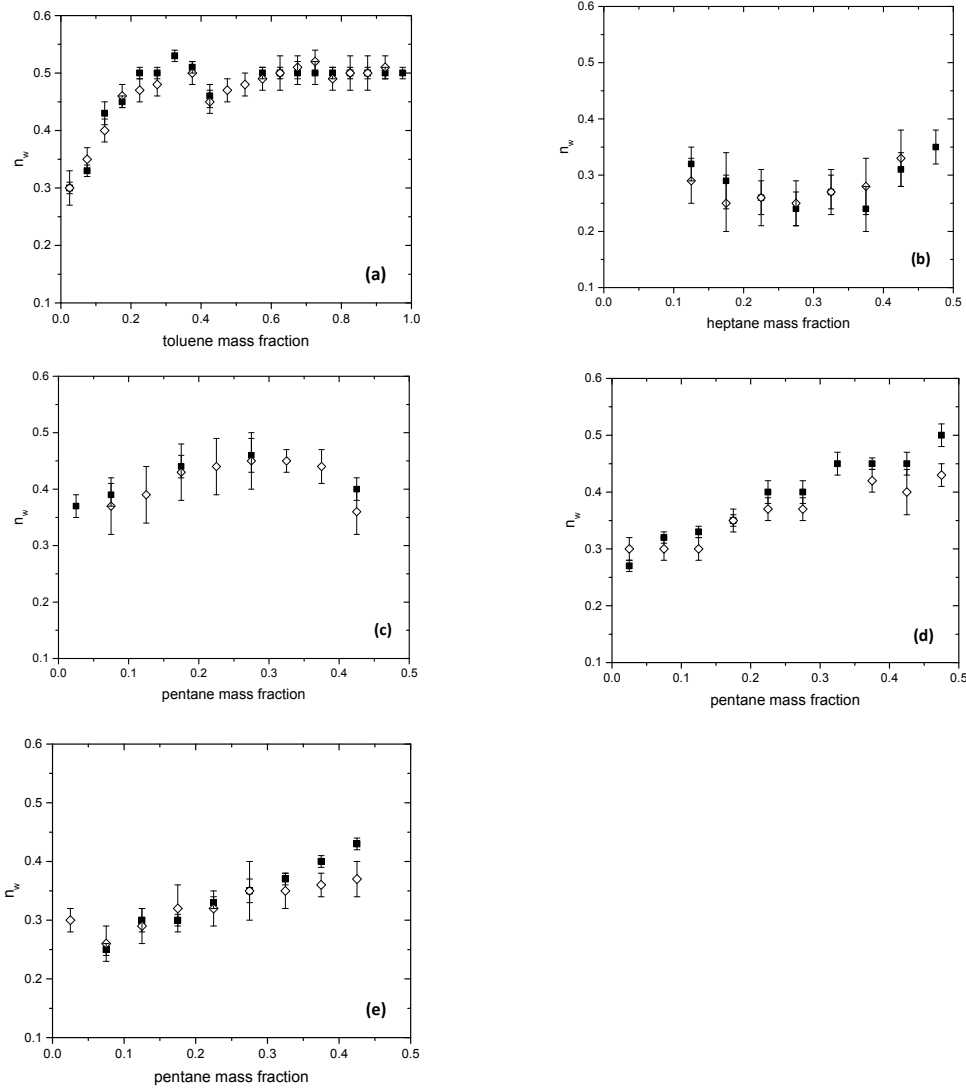


**Figure 2.4.** Local values of the time scaling exponent  $n_w$  and their uncertainty based on ■, minimizing  $\sigma_w$  and ◇, least square regression of slopes for: (a) Athabasca bitumen + toluene system<sup>13</sup>; (b) Cold Lake bitumen + heptane<sup>15</sup>; (c) Athabasca bitumen + pentane<sup>11</sup>; (d) Athabasca atmospheric residue + pentane<sup>14</sup>; (e) Athabasca vacuum residue

+ pentane<sup>14</sup>; at room temperature based on composition profiles obtained from the citations.

#### **2.4.2. Control Experiments**

Toluene + polybutene mixtures should exhibit Fickian diffusion behavior irrespective of composition because both components are single phase and are fully miscible. Toluene + (0.25 mass fraction carbon nanotubes + polybutene) mixtures should exhibit non-Fickian diffusion behavior, especially at low toluene mass fraction. For these experiments, sets of composition calibration curves were prepared and used to interpret local speed of sound profiles, and to obtain raw composition vs elevation profiles, Figures 2.5-a and 2.5-b respectively, following the procedure illustrated in Figure 2.3. These composition profiles were then processed in the same manner as the profiles obtained from the literature to derive local  $n_w$  values and their uncertainty. As is clear from Figure 2.6, toluene + polystyrene exhibit Fickian diffusion behavior and  $n_w$  is well approximated as a composition invariant constant possessing a value of  $0.50 \pm 0.05$ . For toluene + (0.25 mass fraction carbon nanotubes + polybutene),  $n_w$  possesses a marked composition dependence.  $n_w$  trends from  $\sim 0.3$  at low toluene mass fraction toward  $n_w = 0.5$  as the pure toluene axis is approached. While  $n_w$  values determined by minimizing  $\sigma_w$  possess lower uncertainty than those obtained using least square regression of composition profile slopes, it is evident that the impact of the carbon nanotubes on diffusion persists up toluene mass fractions exceeding 0.90 based on either set of  $n_w$  values. The persistence of nanostucture is readily illustrated. If the density differences among constituents are ignored, then in the absence of toluene the mean distance between

adjacent carbon nanotubes at a mass fraction of 0.25 is approximately equal to the diameter of the nanotubes (5-7 nm). At a toluene mass fraction of 0.5, this mean distance becomes approximately 1.5 nanotube diameters (9-14 nm) and at a toluene mass fraction of 0.9, the mean distance is approximately 5 nanotube diameters (30-40 nm) and remains nanoscopic. It is only at toluene mass fractions approaching unity that the mean distances between nanoparticles become microscopic, much less macroscopic.

These control experiment data sets also serve two more general purposes. They illustrate that free diffusion measurements, made with the acoustic cell, provide reliable values for  $n_w$  with a resolution better than +/- 0.05 for viscous fluid + light hydrocarbon mixtures over the entire composition range, even though the measurements take two or more days to complete. Convection even at high light hydrocarbon mass fractions has a minor impact on fluid transport over this long time interval. Consequently, variations in  $n_w$  values with time are interpretable. These results also illustrate that nanoparticles introduced into a fluid that exhibits Fickian diffusion behavior leads to non-Fickian diffusion behaviors that even for closely related fluids, are observable, and interpretable on the basis of free diffusion experiments.

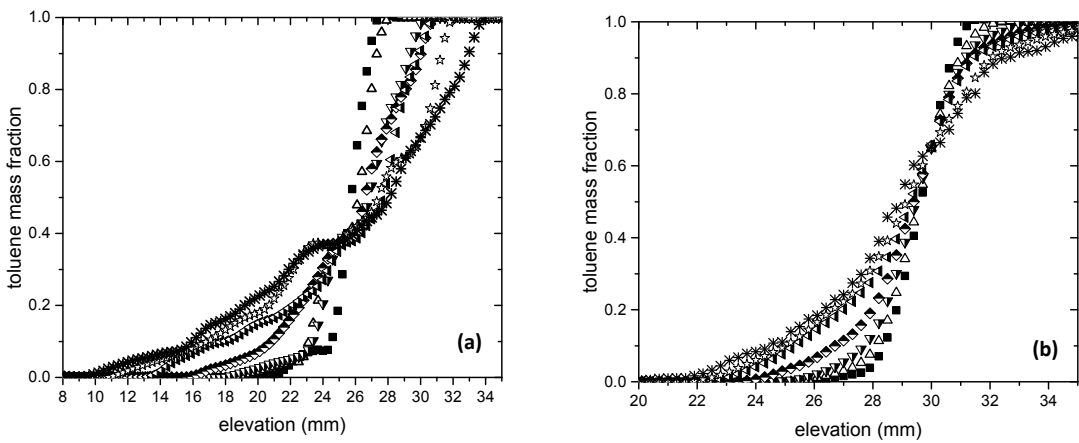


**Figure 2.5.** Raw composition vs elevation profiles for: (a) polybutene + toluene, and (b) toluene + (polybutene + 0.25 mass fraction carbon nanotubes) at 298 K. ■ 6 hours, △ 12 hours, ▽ 24 hours, ◆ 36 hours, ▲ 48 hours, ☆ 60 hours, \* 72 hours.

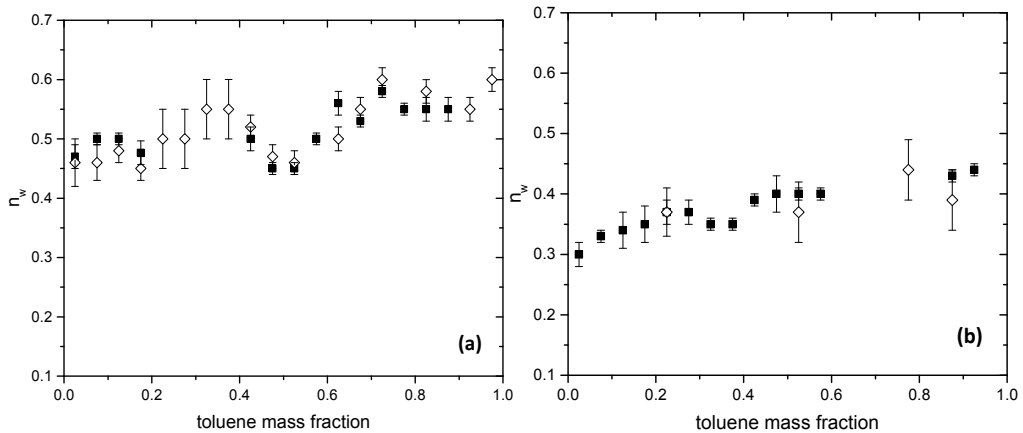


**Figure 2.6.** Local values of the time scaling exponent  $n_w$  and their uncertainty based on ■, minimizing  $\sigma_w$  and ◇, least square regression of slopes for: (a) polybutene + toluene and (b) (polybutene + 0.25 mass fraction carbon nano tubes) + toluene mixtures at 298 K.

### **2.4.3. Local time invariant values of $n_w$ and their uncertainty derived from composition profiles of Athabasca Bitumen + Toluene Mixtures**

Raw composition profiles for Athabasca bitumen + toluene mixtures were obtained as illustrated in Figure 2.3 and are shown in Figure 2.7 a-c for 273, 298 and 313 K. These profiles were then smoothed and processed as noted above. Local best-fit time-invariant values for  $n_w$  are shown for 273, 298 and 313 K in Figures 2.8 a-c respectively over the composition interval 0 – 0.4 mass fraction toluene. The  $n_w$  values approach the single file limit ( $n_w = 0.25$ ) at low toluene mass fraction and possess a marked composition dependence, at all three temperatures, with a transition at  $\sim 0.25$  mass fraction toluene. The temperature invariance of the composition dependence is readily seen in the comparison graphic, Figure 2.8-d. While the Athabasca bitumen sample was not expected to be at equilibrium due to the metastability of liquid maltenes arising during the thermal treatment prior to experiments<sup>16</sup>, temperature variation had been anticipated to play a more prominent role in the nature of the dominant diffusion mechanism(s). The absence of a temperature effect suggests that the nanostructure present in heated and then cooled Athabasca bitumen is essentially invariant over the temperature interval investigated. Regrettably, the nano-structure cannot be attributed to the maltene-rich or the asphaltene-rich phases on the basis of these experimental results because neither phase undergoes a significant phase transition on reheating through the temperature range 273 to 313 K<sup>16</sup>.

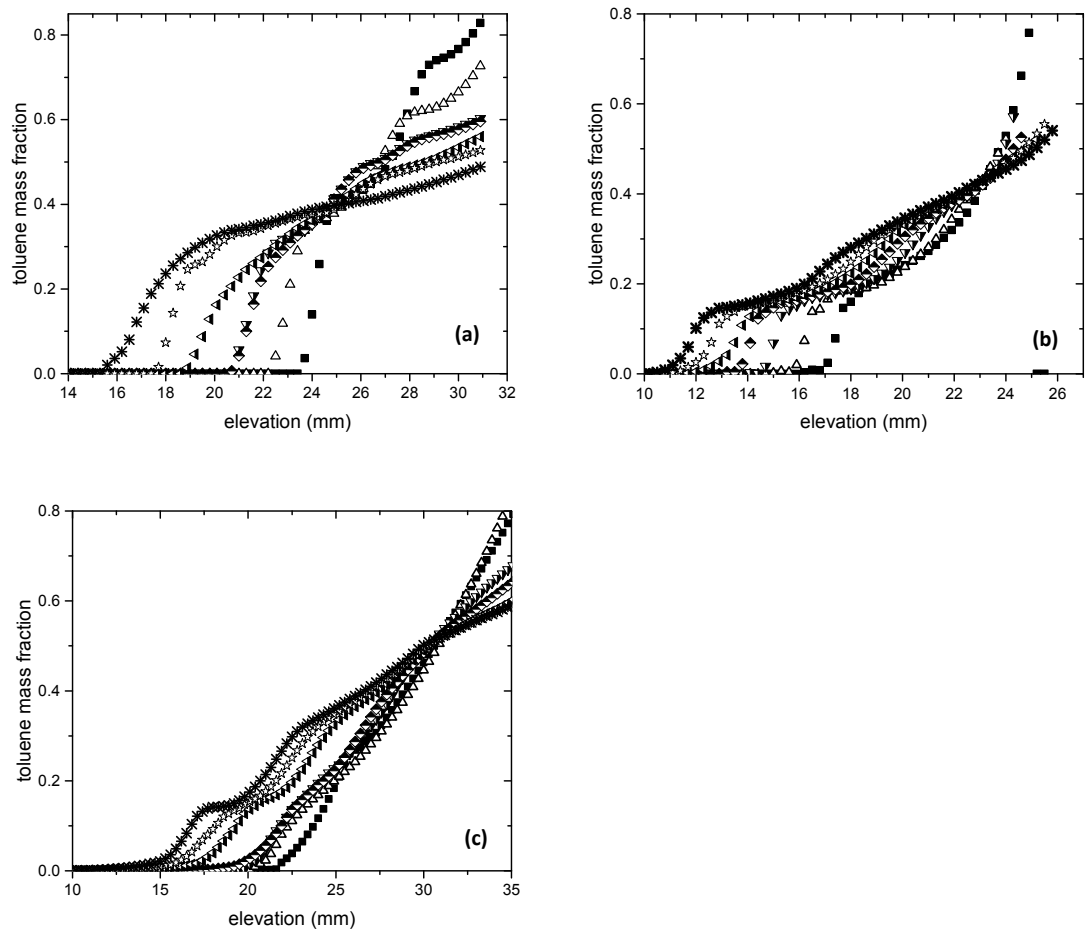


**Figure 2.7.** Smoothed composition profiles for Athabasca bitumen + toluene at: (a) 273 K, (b) 298 K and (c) 313 K. ■ 6 hours, △ 12 hours, ▼ 24 hours, ♦ 36 hours, ◁ 48 hours, ☆ 60 hours, \* 72 hours.

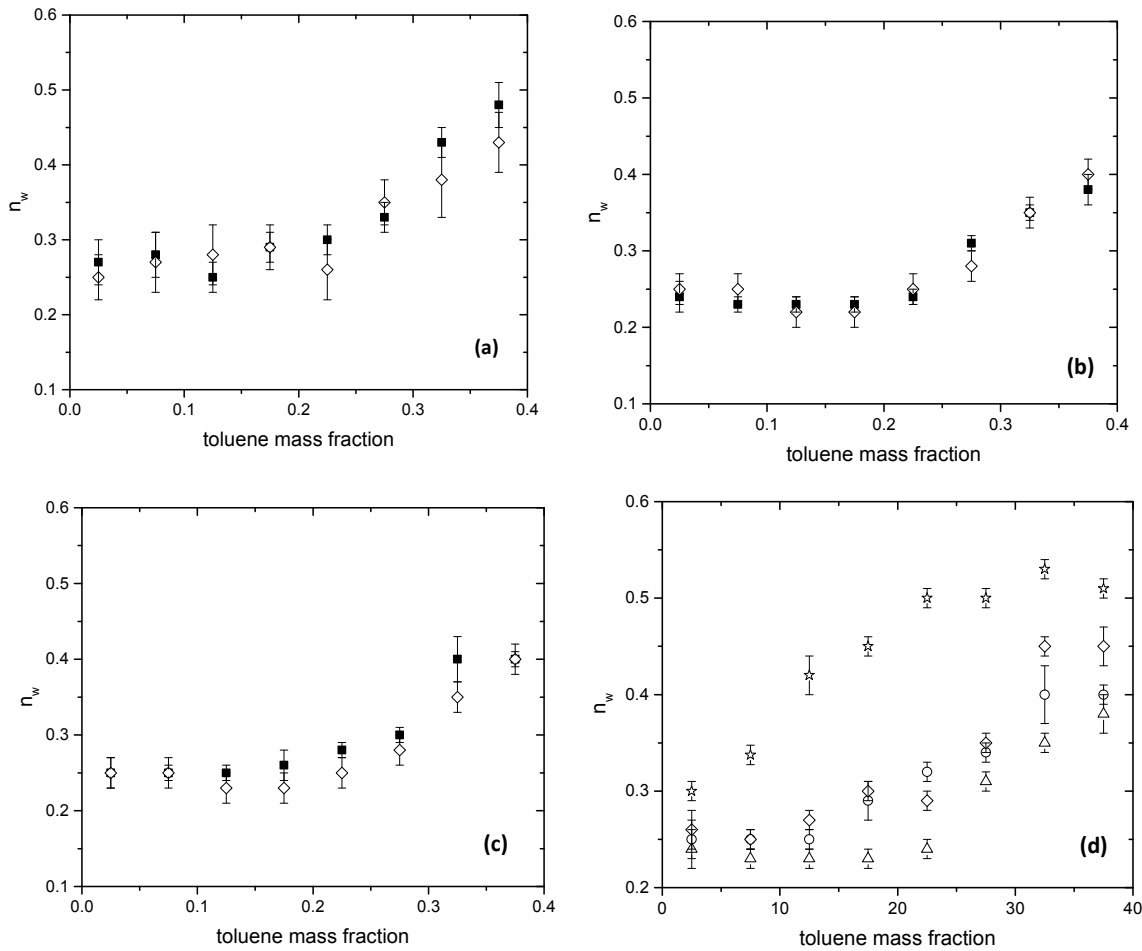


**Figure 2.8.** The time scaling exponent ( $n_w$ ) for Athabasca bitumen + toluene mixtures at:

(a) 273 K, (b) 298 K and (c) 313 K based on ■, minimizing  $\sigma_w$  and ◊, least square regression of slopes (d) Data set comparison for Athabasca bitumen + toluene mixtures based on minimizing  $\sigma_w$ : ☆, Fadaei et al<sup>13</sup>; ○, 273 K, △ 298 K and ◊ 313 K.

Figure 2.8-d also provides a comparison between  $n_w$  outcomes from the current work and the work of Fadaei et al.<sup>13</sup> for the same mixture. The two groups used subsamples from the same master sample, but variations in subsequent storage, handling, and sample pretreatment affect the details of the phase behavior<sup>16</sup> of Athabasca bitumen, and the duration of the experiments differ by orders of magnitude. The two sets of  $n_w$  values are

qualitatively similar and share common limits but possess quantitatively dissimilar composition dependencies over the composition interval 0-0.40 mass fraction toluene. A second point of contrast between the two sets of results arises at higher toluene mass fraction. It was not possible to identify low-uncertainty values for  $n_w$ , in the current work, while from Fadaei et al.<sup>13</sup>, a value of  $n_w = 0.50$  obtains from 0.40 to 1.00 mass fraction toluene. In the absence of the negative control experiment, one would be tempted to attribute this to convection arising in the toluene rich fluid over time. However, the negative control experiment clearly illustrates that this is an inappropriate attribution. Further, the long-duration bitumen + solvent diffusion experiments from the literature share this same feature and it would appear interpretable. Thus kinetic effects linked to variation of nanostructure and microstructure with time at fixed composition require probing.

#### **2.4.4. Impact of asphaltene mass fraction and solvent choice on local time-invariant $n_w$ values**

With the large number of data points for Athabasca bitumen related samples, it is possible to prepare a master plot showing values of  $n_w$  as a function of asphaltene mass fraction across the available studies. Sample pretreatments, storage and handling differences remain uncontrolled variables in Figure 2.9 but it is possible to observe trends in the nature of the mutual diffusion behavior for Athabasca bitumen related samples + n-alkanes (open symbols) and toluene (closed symbols). As expected, Fickian diffusion is observed at low asphaltene mass fractions, and the single file limit is approached at high asphaltene mass fraction. That the single file limit is approached at a lower asphaltene

mass fraction in toluene, a good solvent for asphaltenes, than in n-alkanes, poor solvents for asphaltenes, is superficially counter intuitive but readily explained. When aromatic solvents are added to heavy oils in general and to Athabasca bitumen fractions in particular, the size of nano aggregates is largely unaffected, while addition of n-alkanes causes significant aggregate growth<sup>37</sup>, leading to precipitation.<sup>38</sup> By definition, asphaltenes in crude oils become microscopic and macroscopic on addition of n-alkanes. Thus the spacing among structural elements also becomes microscopic and macroscopic. With toluene addition, asphaltenes remain nanoscopic and the spacing among structural elements increases in a more limited manner with dilution and dissolution as more toluene is added (Figure 2.10). The positive control experiment, with carbon nanotubes, illustrates the significance of the impact of even small volume fractions of nanostructured elements on diffusive mass transfer. Thus, n-alkanes, or other poor solvents for asphaltenes, appear to be preferred penetrants for heavy oils and bitumen from a diffusion perspective as suggested by the results in Figure 2.9. Larger  $n_w$  values imply faster penetration.

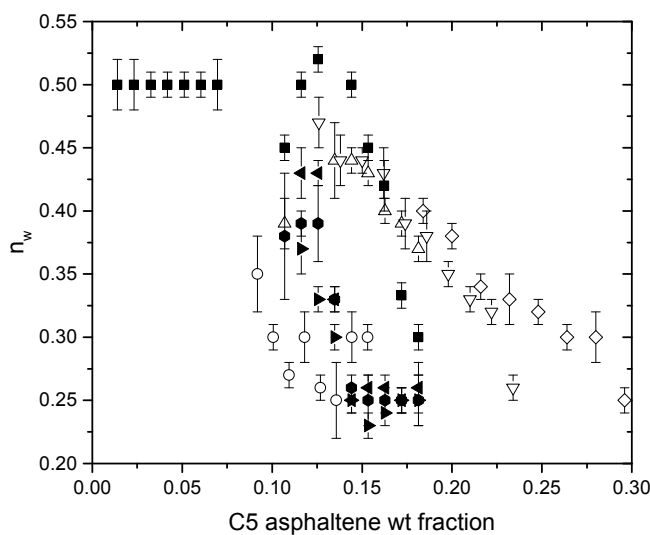
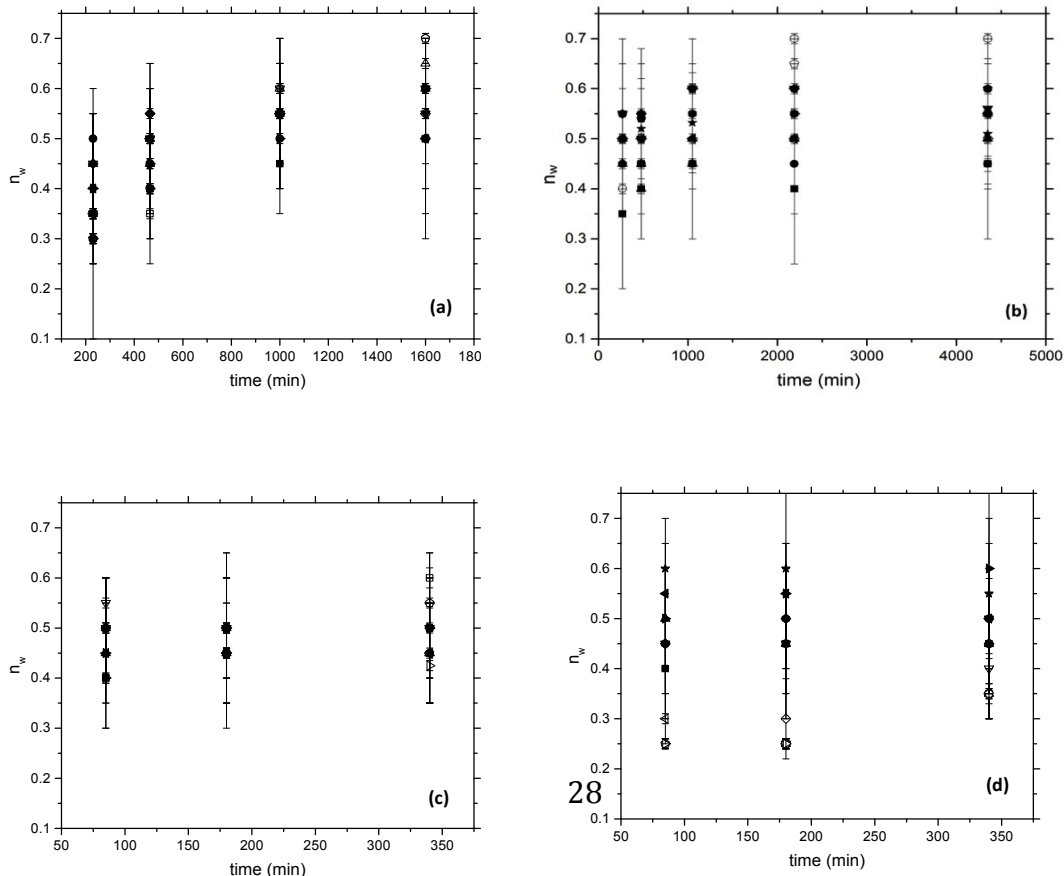


**Figure 2.9.** Values of  $n_w$  based on minimizing  $\sigma_w$  as a function of C5 asphaltene mass fraction in Athabasca bitumen derived samples:  $\triangle$  Athabasca bitumen + pentane<sup>11</sup>;  $\nabla$  Athabasca atmospheric residue + pentane<sup>14</sup>,  $\diamond$  Athabasca vacuum residue + pentane<sup>14</sup>;  $\blacksquare$  Athabasca bitumen + toluene<sup>13</sup>; Athabasca bitumen + toluene (this work),  $\bullet$  273 K,  $\blacktriangleright$  298 K and  $\blacktriangleleft$  313 K.

#### 2.4.5. Temporal variation of $n_w$ values at high solvent mass fraction

Temporal variation of  $n_w$  values arising at high solvent mass fraction in heavy oil + light hydrocarbon mutual diffusion experiments, may arise from temporal changes in fluid physics and chemistry or as a consequence of convective and other fluid mechanic effects in systems with flow. This issue is explored in Figure 2.11, for data sets from the literature, and in Figure 2.12, for Athabasca bitumen + toluene mixtures studied in this work. For these evaluations, two consecutive composition profiles in the composition profile time series were fit at 0.05 mass fraction intervals, outside the composition range where low-uncertainty time-invariant values were obtained. The  $n_w$  values at fixed composition reported in Figures 2.11 and 2.12 possess high uncertainties and do not vary significantly with time. The best-fit value data sets as a whole clearly do drift to higher values with time for Cold Lake bitumen + heptane (Figure 2.11 a) and for Athabasca bitumen + pentane (Figure 2.11 b). Beyond 1500 minutes there is evidence for convection at high pentane/heptane mass fraction as  $n_w$  values as large as 0.7 are derived from the data. Changes in those parts of the composition profiles cannot be interpreted as reflecting diffusive mass transfer alone, and should be excluded from mutual diffusion coefficient evaluation calculations. For Athabasca atmospheric and vacuum residue +

pentane (Figure 2.11 c and d), that cover a narrower range of compositions, there is no apparent systematic variation with time within the uncertainty of the data. Possible impacts of convection cannot be detected. For the measurements reported in this work, Figure 2.12 a-c, the outcome is comparable. The individual values for  $n_w$  possess significant uncertainty. The best-fit  $n_w$  values drift higher as a collective but remain largely within the  $0.45 < n_w < 0.55$  range. Consequently, the possible impact of convection is approaching the detection limit. Over all, there is no evidence for a composition linked temporal dependence for  $n_w$  across all of the data sets, and from the perspective of minimizing the impact of convective effects at high penetrant mass fraction, the microfluidics method is clearly preferred.



28

**Figure 2.10.** Temporal variation of  $n_w$  for (a) Cold Lake bitumen + heptane<sup>15</sup>; (b) Athabasca bitumen + pentane<sup>11</sup>; (c) Athabasca atmospheric residue + pentane<sup>14</sup>; (d) Athabasca vacuum residue + pentane<sup>14</sup>.  $n_w$  values obtained by minimizing  $\sigma_w$ : □ 0.45 solvent mass fraction, ○ 0.5 solvent mass fraction, △ 0.55 solvent mass fraction, ▽ 0.6 solvent mass fraction, ◇ 0.65 solvent mass fraction, ◁ 0.7 solvent mass fraction, ○ 0.75 solvent mass fraction, ☆ 0.8 solvent mass fraction, □ 0.85 solvent mass fraction, ▲ 0.9 solvent mass fraction.  $n_w$  values obtained using least square regression of slopes: ■ 0.45 solvent mass fraction, ● 0.5 solvent mass fraction, ▲ 0.55 solvent mass fraction, ▼ 0.6 solvent mass fraction, ◆ 0.65 solvent mass fraction, ◁ 0.7 solvent mass fraction, ▶ 0.75 solvent mass fraction, ◉ 0.8 solvent mass fraction, ★ 0.85 solvent mass fraction.

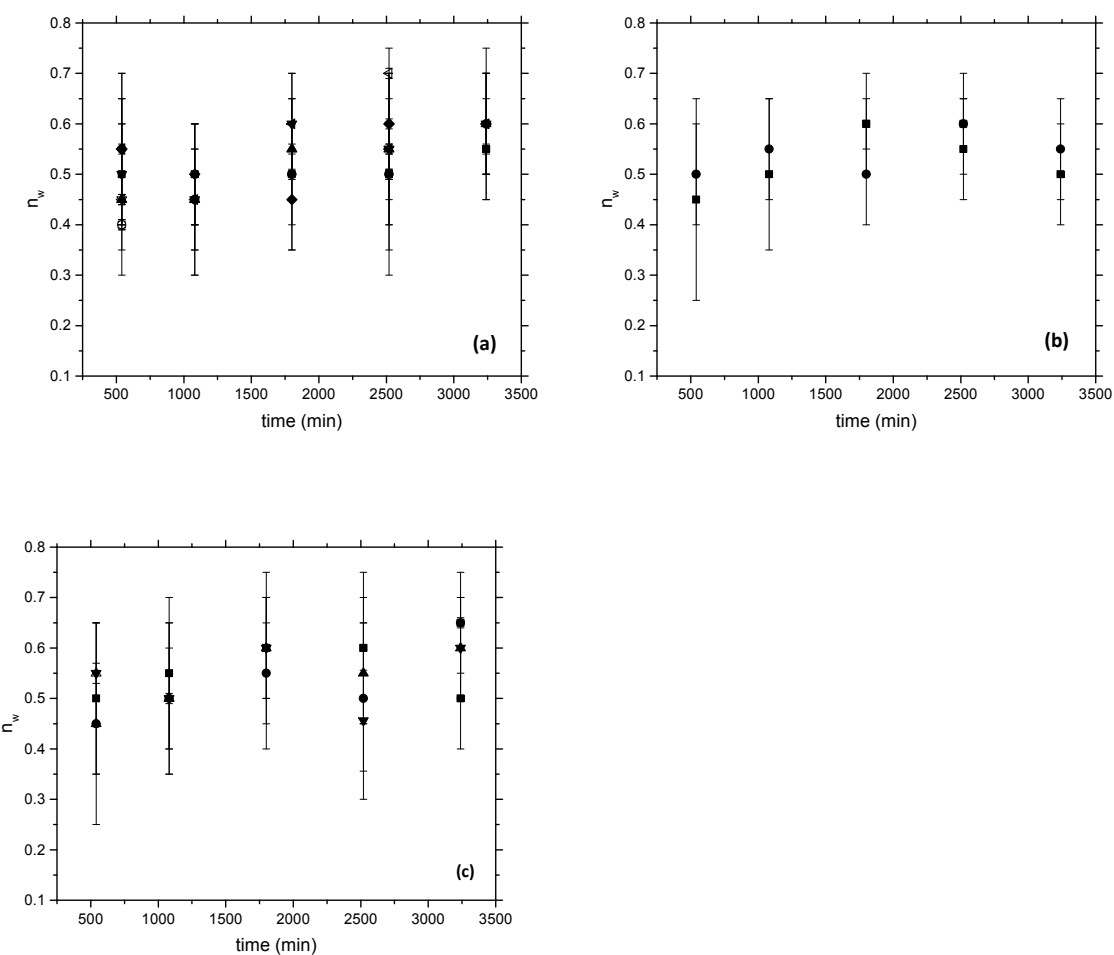


**Figure 2.11.** Temporal variation of  $n_w$  values for Athabasca bitumen + toluene (a) 273K  
 (b) 298 K (c) 313 K.  $n_w$  values obtained by minimizing  $\sigma_w$ : □ 0.45 solvent mass fraction,  
 ○ 0.5 solvent mass fraction, △ 0.55 solvent mass fraction, ▽ 0.6 solvent mass fraction,  
 ◇ 0.65 solvent mass fraction, ▲ 0.7 solvent mass fraction, ○ 0.75 solvent mass fraction,  
 ★ 0.8 solvent mass fraction.  $n_w$  values obtained from least square regression of slopes: ■  
 0.45 solvent mass fraction, ● 0.5 solvent mass fraction, ▲ 0.55 solvent mass fraction, ▼  
 0.6 solvent mass fraction, ◆ 0.65 solvent mass fraction, ▲ 0.7 solvent mass fraction, ▶  
 0.75 solvent mass fraction, ◉ 0.8 solvent mass fraction.

## 2.5. Conclusions

Unambiguous identification of Fickian and non-Fickian diffusion mechanisms in sets of free diffusion composition profile data imposes significant constraints on the quality of time, distance and composition measurements, and careful data processing. Control experiments and two composition profile fitting techniques applied to polybutene + toluene and polybutene + toluene + carbon nanotube showed that free diffusion is in principle an appropriate basis for discriminating diffusion behaviors of closely related mixtures and that convective effects play a secondary role even in mixtures with low viscosity. Convective effects do not interfere with the identification of the principal diffusion mechanisms from composition profiles in the literature or obtained in this work. Diffusion at low penetrant mass fractions in nano- and micro -structured hydrocarbon resources, such as Athabasca and Cold Lake bitumen, is shown to be governed by the

single file limit, a non-Fickian diffusion mechanism, while at high penetrant mass fraction, diffusion is shown to be governed by Fickian diffusion. The transition from non-Fickian to Fickian diffusion as penetrant is added is shown to be penetrant dependent. The difference in the behavior of n-alkanes and toluene as penetrants is attributed to their respective impacts on asphaltene nano-structure. N-alkanes cause the asphaltene fraction to aggregate and to form micro or macro scale objects. In toluene, the asphaltenes remain nanodispersed. The mixture remains nanostructured at higher penetrant mass fractions in toluene than in n-alkanes and this delays the gradual transition from non-Fickian to Fickian diffusion. Mixed Fickian and single file diffusion modes of diffusion co-exist at intermediate compositions. The impacts of these findings on mutual diffusion coefficient evaluation and on industrial applications are currently being explored. However, it is clear that the time for light hydrocarbons to penetrate a fixed distance into nano- and micro- structured hydrocarbon resources is significantly greater than anticipated based on Fickian diffusion.

## 2.6. References

- (1) R.B. Bird, W.E. Stewart, E.N. Lightfoot, *Transport Phenomena*, John Wiley & Sons, 2007.
- (2) J. Crank, *The mathematics of diffusion*, Clarendon Press, 1975.
- (3) A.L. Hodgkin, R.D. Keynes, The potassium permeability of a giant nerve fibre, *J. Physiol.* 128 (1955) 61–88.
- (4) Q.-H. Wei, C. Bechinger, P. Leiderer, Single-File Diffusion of Colloids in One-Dimensional Channels, *Science*. 287 (2000) 625–627. doi:10.1126/science.287.5453.625.

- (5) B. Lin, M. Meron, B. Cui, S.A. Rice, H. Diamant, From Random Walk to Single-File Diffusion, *Phys. Rev. Lett.* 94 (2005) 216001. doi:10.1103/PhysRevLett.94.216001.
- (6) T.G. Mason, Osmotically driven shape-dependent colloidal separations, *Phys. Rev. E*. 66 (2002) 060402. doi:10.1103/PhysRevE.66.060402.
- (7) T. Meersmann, J.W. Logan, R. Simonutti, S. Caldarelli, A. Comotti, P. Sozzani, et al., Exploring Single-File Diffusion in One-Dimensional Nanochannels by Laser-Polarized  $^{129}\text{Xe}$  NMR Spectroscopy, *J. Phys. Chem. A*. 104 (2000) 11665–11670. doi:10.1021/jp002322v.
- (8) A.E. Kamholz, B.H. Weigl, B.A. Finlayson, P. Yager, Quantitative Analysis of Molecular Interaction in a Microfluidic Channel: The T-Sensor, *Anal. Chem.* 71 (1999) 5340–5347. doi:10.1021/ac990504j.
- (9) A.E. Kamholz, P. Yager, Molecular diffusive scaling laws in pressure-driven microfluidic channels: deviation from one-dimensional Einstein approximations, *Sens. Actuators B Chem.* 82 (2002) 117–121. doi:10.1016/S0925-4005(01)00990-X.
- (10) R.F. Ismagilov, A.D. Stroock, P.J.A. Kenis, G. Whitesides, H.A. Stone, Experimental and theoretical scaling laws for transverse diffusive broadening in two-phase laminar flows in microchannels, *Appl. Phys. Lett.* 76 (2000) 2376–2378. doi:10.1063/1.126351.
- (11) X. Zhang, M. Fulem, J.M. Shaw, Liquid-Phase Mutual Diffusion Coefficients for Athabasca Bitumen + Pentane Mixtures, *J. Chem. Eng. Data.* 52 (2007) 691–694. doi:10.1021/je060234j.

- (12) X. Zhang, J.M. Shaw, Liquid-phase Mutual Diffusion Coefficients for Heavy Oil + Light Hydrocarbon Mixtures, *Pet. Sci. Technol.* 25 (2007) 773–790. doi:10.1080/10916460500411796.
- (13) H. Fadaei, J.M. Shaw, D. Sinton, Bitumen–Toluene Mutual Diffusion Coefficients Using Microfluidics, *Energy Fuels.* 27 (2013) 2042–2048. doi:10.1021/ef400027t.
- (14) A. Sadighian, M. Becerra, A. Bazyleva, J.M. Shaw, Forced and Diffusive Mass Transfer between Pentane and Athabasca Bitumen Fractions, *Energy Fuels.* 25 (2011) 782–790. doi:10.1021/ef101435r.
- (15) Y.W. Wen, A. Kantzas, Monitoring Bitumen–Solvent Interactions with Low-Field Nuclear Magnetic Resonance and X-ray Computer-Assisted Tomography†, *Energy Fuels.* 19 (2005) 1319–1326. doi:10.1021/ef049764g.
- (16) A. Bazyleva, M. Fulem, M. Becerra, B. Zhao, J.M. Shaw, Phase Behavior of Athabasca Bitumen, *J. Chem. Eng. Data.* 56 (2011) 3242–3253. doi:10.1021/je200355f.
- (17) M. Fulem, M. Becerra, M.D.A. Hasan, B. Zhao, J.M. Shaw, Phase behaviour of Maya crude oil based on calorimetry and rheometry, *Fluid Phase Equilibria.* 272 (2008) 32–41. doi:10.1016/j.fluid.2008.06.005.
- (18) B. Zhao, J.M. Shaw, Composition and Size Distribution of Coherent Nanostructures in Athabasca Bitumen and Maya Crude Oil, *Energy Fuels.* 21 (2007) 2795–2804. doi:10.1021/ef070119u.
- (19) A. Bazyleva, M. Becerra, D. Stratichuk-Dear, J.M. Shaw, Phase behavior of Safaniya vacuum residue, *Fluid Phase Equilibria.* 380 (2014) 28–38. doi:10.1016/j.fluid.2014.07.037.

- (20) O.C. Díaz, J. Modaresghazani, M.A. Satyro, H.W. Yarranton, Modeling the phase behavior of heavy oil and solvent mixtures, *Fluid Phase Equilibria*. 304 (2011) 74–85. doi:10.1016/j.fluid.2011.02.011.
- (21) M.J. Amani, M.R. Gray, J.M. Shaw, The phase behavior of Athabasca bitumen + toluene + water ternary mixtures, *Fluid Phase Equilibria*. 370 (2014) 75–84. doi:10.1016/j.fluid.2014.02.028.
- (22) M.J. Amani, M.R. Gray, J.M. Shaw, Phase behavior of Athabasca bitumen + water mixtures at high temperature and pressure, *J. Supercrit. Fluids*. 77 (2013) 142–152. doi:10.1016/j.supflu.2013.03.007.
- (23) S.R. Bagheri, A. Bazyleva, M.R. Gray, W.C. McCaffrey, J.M. Shaw, Observation of Liquid Crystals in Heavy Petroleum Fractions, *Energy Fuels*. 24 (2010) 4327–4332. doi:10.1021/ef100376t.
- (24) S.R. Bagheri, B. Masik, P. Arboleda, Q. Wen, K.H. Michaelian, J.M. Shaw, Physical Properties of Liquid Crystals in Athabasca Bitumen Fractions, *Energy Fuels*. 26 (2012) 4978–4987. doi:10.1021/ef300339v.
- (25) K. Nikooyeh, S.R. Bagheri, J.M. Shaw, Interactions Between Athabasca Pentane Asphaltenes and n-Alkanes at Low Concentrations, *Energy Fuels*. 26 (2012) 1756–1766. doi:10.1021/ef201845a.
- (26) N. Saber, X. Zhang, X.-Y. Zou, J.M. Shaw, Simulation of the phase behaviour of Athabasca vacuum residue + n-alkane mixtures, *Fluid Phase Equilibria*. 313 (2012) 25–31. doi:10.1016/j.fluid.2011.09.038.
- (27) N. Saber, J.M. Shaw, On the phase behaviour of Athabasca vacuum residue + n-decane, *Fluid Phase Equilibria*. 302 (2011) 254–259. doi:10.1016/j.fluid.2010.09.038.

- (28) N. Saber, J.M. Shaw, Toward multiphase equilibrium prediction for ill-defined asymmetric hydrocarbon mixtures, *Fluid Phase Equilibria.* 285 (2009) 73–82. doi:10.1016/j.fluid.2009.07.014.
- (29) R. Stewart, C.V. Wood, S.J. Murowchuk, J.M. Shaw, Phase Order Inversion During Heavy Oil and Bitumen Production with Solvent Addition, *Energy Fuels.* (2014). doi:10.1021/ef500723e.
- (30) A. Shah, R. Fishwick, J. Wood, G. Leeke, S. Rigby, M. Greaves, A review of novel techniques for heavy oil and bitumen extraction and upgrading, *Energy Environ. Sci.* 3 (2010) 700–714. doi:10.1039/B918960B.
- (31) W.S. Cleveland, Robust Locally Weighted Regression and Smoothing Scatterplots, *J. Am. Stat. Assoc.* 74 (1979) 829–836. doi:10.1080/01621459.1979.10481038.
- (32) M. Khammar, J.M. Shaw, Phase behaviour and phase separation kinetics measurement using acoustic arrays, *Rev. Sci. Instrum.* 82 (2011) 104902. doi:10.1063/1.3650767.
- (33) NIST Chemistry WebBook. <http://webbook.nist.gov/chemistry/>, (n.d.).
- (34) A.B. Bazyleva, M.A. Hasan, M. Fulem, M. Becerra, J.M. Shaw, Bitumen and Heavy Oil Rheological Properties: Reconciliation with Viscosity Measurements, *J. Chem. Eng. Data.* 55 (2010) 1389–1397. doi:10.1021/je900562u.
- (35) J.G. Guan, M. Kariznovi, H. Nourozieh, J. Abedi, Density and Viscosity for Mixtures of Athabasca Bitumen and Aromatic Solvents, *J. Chem. Eng. Data.* 58 (2013) 611–624. doi:10.1021/je3010722.

- (36) G. Centeno, G. Sánchez-Reyna, J. Ancheyta, J.A.D. Muñoz, N. Cardona, Testing various mixing rules for calculation of viscosity of petroleum blends, *Fuel*. 90 (2011) 3561–3570. doi:10.1016/j.fuel.2011.02.028.
- (37) Amundarain, Jesus, Chadakowski, Martin, Long, Bingwen, Shaw, J.M., Characterization of Physically and Chemically Separated Athabasca Asphaltenes Using Small-Angle Scattering, *Energy & Fuels* 2011, 25(11) 5100-5122.
- (38) Long B., Chadakowski M., Shaw J., "Impact of Liquid-Vapor to Liquid-Liquid-Vapor Phase Transitions on Asphaltene-Rich Nanoaggregate Behavior in Athabasca Vacuum Residue + Pentane Mixtures", *Energy & Fuels* 2013, 27(4) 1779-1790.

### **3. On Fickian and Single File Mutual Diffusion Coefficients in Heavy Oil + Diluent Mixtures**

#### **3.1. Introduction**

Non-thermal bitumen viscosity reduction during in-situ production is a research and development priority for the oilsands industry. Solvent injection<sup>1</sup> offers the potential to lower production costs relative to thermal production and to reduce environmental impacts associated with production. Solvent assisted extraction processes have begun to emerge for in-situ oilsands production<sup>2</sup>. Understanding diffusion mechanisms and diffusion rates for solvents in bitumen, and the interaction of solvents with the reservoir rock<sup>3</sup> are key to the success of environmentally and economically sustainable processes for solvent assisted bitumen production.

Petroleum consists of wide variety of components with different molecular weights, elemental compositions and structures. From a mass transfer perspective there are two categories of constituents of particular importance, because they impart structure to the oil leading to inhomogeneous mass transfer. Bagheri and Nikooyeh<sup>4-6</sup> identified discotic amphotropic liquid-crystalline domains in Athabasca bitumen, with micron scale dimensions, that become anisotropic with changes in temperature and on solvent addition. The mass fraction of these constituents remains a topic of ongoing investigation. The more well-known asphaltene fraction isolated from oils using *n*-pentane or *n*-heptane (ASTM D4055) comprise nanoscale domains with leading dimensions ranging in size from 1- 5 nm<sup>3</sup>. Fulem et al.<sup>7</sup> applied a combination of calorimetry and rheometry methods

to show that heavy oil and bitumen undergo complex transitions from solid-like to liquid-like behavior over a temperature range of 150-520 K. Well-dispersed nano-scale asphaltene-rich phase domains, and maltene-rich phase domains undergo phase transitions in a largely independent manner. The asphaltene-rich phase domains comprise more than 20 wt % of Athabasca bitumen and are multiphase over a broad range of temperatures<sup>8</sup>. On organic solvent addition to heavy oils, asphaltenes flocculate, aggregate and sediment,<sup>9-11</sup> and asphaltenes also aggregate even in aromatic solvents such as toluene at low concentrations.<sup>12</sup> The aggregation of asphaltenes in solvents has been surveyed using diverse techniques<sup>13-15</sup>. Nanodispersed asphaltene rich domains present in the hydrocarbon resource, remain nanodispersed or become micro dispersed with solvent addition. There is conflicting evidence regarding the shapes and structures of these domains. The hard sphere assumption appears to apply to rheological measurements for Athabasca bitumen along with its permeate and retentate fractions obtained by nanofiltration<sup>16</sup>. Bouhadda<sup>17</sup> et al. showed that aggregated asphaltene particles appear to be nearly spherical up to 15 vol% in toluene. Lorenz<sup>18</sup> et al. found that asphaltenes have almost spherical shape for less than 2% concentration in light fractions of crude oil. Gawrys and Kilpatrick<sup>19</sup> have used SANS to show asphaltenes in solutions of methanol+toluene or heptane+toluene form cylindrical aggregates. Other works suggest that asphaltene domains are less coherent, with Sirota<sup>20</sup> suggesting that asphaltene structures are temporal. Irrespective of the nature of these dispersed domains, their presence creates tortuous paths within the hydrocarbon resources with nano and micro length scales that vary with composition and that impact the relative importance of mass transport mechanisms and rates.

Diffusion measurements of small molecules and mutual diffusion measurement in structured fluids such as polymer melts have been performed for some time. Examples include the desorption rate method<sup>21</sup>, the quartz-spring sorption method<sup>22</sup>, thermogravimetric analysis (TGA)<sup>23</sup>, magnetic suspension balance<sup>21</sup> and Dynamic Pendant Drop Volume Analysis<sup>24</sup>. Application of the TGA method to cyclohexane + thin asphaltene films showed that the apparent diffusion coefficient is two to three orders of magnitude smaller than for cyclohexane + Athabasca bitumen films.<sup>25</sup> This result illustrates the importance of understanding the impact of structure on diffusion in hydrocarbon resources.

Free diffusion measurements have also been applied to hydrocarbon resource and resource fractions + diluent mixtures. In these experiments diluents, such as toluene and n-alkanes, penetrate from above and mutual diffusion coefficients for these pseudo binary mixtures are derived from the composition profiles that develop over time. To date, these profiles have only been used to obtain single values or composition dependent values that presume Fickian diffusion behavior based on diverse data acquisition and data interpretation procedures. For example, Wen and Kantzas<sup>26</sup> used NMR and X-ray CAT to investigate mutual diffusion of heptane + Cold Lake bitumen and identified composition dependent mutual diffusion coefficients for this mixture. Fadaei et al.<sup>27</sup> measured the diffusion coefficient of toluene in Athabasca bitumen using a microfluidic device coupled with visible light transmission imaging. They found a mass fraction independent mutual diffusion coefficient value of  $1.5 \times 10^{-10} \frac{m^2}{s}$  valid from 0.2 to 1 mass fraction toluene. X-ray tomography has also been used to measure composition independent mutual diffusion coefficient values over broad composition ranges<sup>28-30</sup>. All

of these measurements were preformed at ambient conditions. Thus, the temperature dependence of mutual diffusion coefficient values is unknown. Further, care must be taken to avoid artifacts leading to time dependent mutual diffusion coefficient values at fixed composition and to avoid over interpretation of data<sup>27-30</sup>.

In Chapter 2<sup>31</sup>, it was hypothesized that given the complexity and structure of the heavy oils on their own<sup>32</sup> and in mixtures with light hydrocarbons<sup>33</sup> and non-hydrocarbons<sup>34,35</sup> that both Fickian and Single file diffusion mechanisms are active in these mixtures. This outcome was expected because it is well known that Single File diffusion arises in structured fluids for both molecules and colloidal particles, i.e.: in fluids with micro and nano channels<sup>36-40</sup>. Data from several sets of measurements were found to be consistent with this hypothesis. Single File diffusion was shown to dominate at low diluent mass fraction and Fickian diffusion was shown to dominate at high diluent mass fraction.

In Appendix A, an approximate solution for the Single File diffusion equation is derived. It is applied to the interpretation of free diffusion composition profiles. Here the solutions for both Fickian and Single file diffusion are applied jointly to the interpretation of composition profiles discussed in detail in Chapter 2. Given the uncertainty of the composition profile data and the desire to avoid regressing data uncertainty, the Fickian mutual diffusion coefficient and the Single File mobility coefficient are both assumed to be composition independent. Mutual diffusion in the mixtures is further assumed to be a weighted sum of contributions from the two mechanisms.

For Fickian diffusion, composition profiles at different times align when expressed as a function of the joint variable:

$$\lambda_w = x / t^{n_w} \quad (3.1)$$

where  $n_w = 0.5$

The general solution for the Fickian diffusion equation:

$$\frac{\partial C}{\partial t} = D \frac{\partial^2 C}{\partial x^2} \quad (3.2)$$

in terms of  $\lambda_w$  and assuming a fixed value for the diffusion coefficient and the boundary conditions for C at (+) infinity and (-) infinity is:

$$C = C_0 \operatorname{erf} \left( \frac{x}{\sqrt{4Dt}} \right) \quad (4.3)$$

where Fickian mutual diffusion coefficient is obtained by fitting composition profiles directly.

For single file diffusion, an approximate solution for the differential expression:

$$\frac{\partial C}{\partial t} = F \frac{\partial^4 C}{\partial x^4} \quad (3.4)$$

in terms of  $\lambda_w$  with  $n_w = 0.25$  is derived in Appendix A :

$$C = \frac{1}{1 + \left( \frac{1}{C_0} - 1 \right) \exp(-H \cdot U)} \quad (3.5)$$

where:

$$U = \frac{x^n}{t^{n/4}} \quad (3.6a) \quad G = \left( \frac{1}{C_0} - 1 \right) \quad (3.6b)$$

Values of H are fit to the composition profiles and the mobility coefficient F is obtained indirectly from equation 3.4:

*F*

$$= - \frac{[H.G.\exp(-H.U) + 3HG^2.\exp(-2H.U) + 3HG^3.\exp(-3H.U) + HG^4.\exp(-4H.U)]}{U.[-4H^4.G.\exp(-H.U) + 44H^4.G^2.\exp(-2H.U) - 44H^4.G^3.\exp(-3H.U) + 4H^4.G^4\exp(-4H.U)]}$$

Order of magnitude estimates for the Single File mobility coefficients are obtained using equation 3.7 as illustrated in Appendix A.

For mixed mode diffusion, the contributions from both mechanisms are summed:

$$C(x, t) = \gamma C_0 \operatorname{erf} \left( \frac{x}{\sqrt{4Dt}} \right) + \frac{(1 - \gamma)}{1 + (\frac{1}{C_0} - 1)\exp(-H.U)} \quad (3.8)$$

Equation (3.8) has three unknowns: the Fickian diffusion coefficient (*D*) *H*, and the fractional contributions from each mechanism  $\gamma$ .  $C_0$  is known from the experiments. This simple model is one way to interpret the composition profiles. It assumes that the fluid structure permits both mechanisms to operate in parallel. Other modeling approaches, leading to a larger number of unknowns, but are not precluded by known fluid physics.

Best fit mutual diffusion and mobility coefficient values, and the importance of each mechanism over ranges of composition are presented for heavy oil + light hydrocarbon liquid data sets in literature<sup>26-30</sup> in addition to the data obtained from this work for Athabasca bitumen + toluene and for polybutene + toluene and (polybutene + carbon nanotubes 25 wt %) + toluene mixtures are presented. Mutual diffusion coefficient values obtained are validated using values in the literature, and values for the mobility coefficients are validated by analogy based on experimental values for mobility coefficients also available in the literature<sup>37-39,41</sup>. These values, shown in Table 3.1, range

from  $1 \times 10^{-10} \frac{m^2}{s^2}$  for the diffusion of CF<sub>4</sub> gas molecules with a diameter of 0.47 nm

through AlPO<sub>4</sub>-5 with 0.73 nm pores to  $1 \times 10^{-13} \frac{m^2}{\frac{1}{s^2}}$  for an aqueous suspension of paramagnetic polystyrene colloidal particles with the diameter of 3.6 μm in a confined one dimensional channel with a width of 7 μm. N-alkane and toluene transport among the nanodispersed domains in heavy oils is expected to resemble colloid transport in confined channels, more closely than gas transport in channels, consequently values on low end of this range are anticipated.

**Table 3.1.** Values of mobility coefficients, F, for example nanostructured materials.

Sample	Single file Mobility, F ( $\frac{m^2}{\frac{1}{s^2}}$ )	Size of penetrant	Pore/channel size	Ratio	Reference
CF <sub>4</sub> gas molecules in AlPO <sub>4</sub> -5 at 180K.	$7 \times 10^{-13} - 1 \times 10^{-10}$	4.7 Å	7.3 Å	0.64	36
paramagnetic colloidal spheres circular trenches.	$1 \times 10^{-13} - 2.5 \times 10^{-13}$	3.6 μm	7 μm	0.51	37
Colloidal particles confined to one dimensional channels.	$2.5 \times 10^{-13} - 12.5 \times 10^{-13}$	2.9 μm	<5.8 μm	-	38
Ethane gas molecules passing through AlPO <sub>4</sub> -5.	$8.74 \times 10^{-10}$	4.4 Å	7.3 Å	0.6	39
Methane in ZSM-48	$2 \times 10^{-12}$	3.8 Å	5.3 Å	0.71	41

## 3.2. Experimental Section

### 3.2.1. Acoustic Setup

In this work, composition profiles were determined by calibrating speed of sound values with composition and making use of an acoustic array data acquisition system attached to a thermostatted cell. Local compositions were determined in a 4 cm tall cell using sealed sets of probes with elevation spacings of 600 μm. Measurements are

averaged over a local length of 600  $\mu\text{m}$ . Typical composition profiles comprise 50-70 composition-elevation pairs. The accuracy of the composition measurements is dictated by the reproducibility of local speed of sound values, better than +/- 3 m/s, and the difference in the speed of sound between the hydrocarbon resource sample and the light hydrocarbon, frequently more than 400 m/s. Thus composition reproducibility uncertainties for composition are less than 0.01 (mass fraction basis).

A detailed description of the principles of measurement, the apparatus, the operating procedures, the data acquisition and data interpretation procedures are provided elsewhere<sup>42,43</sup>. Only a brief overview and case specific details are presented here with reference to an apparatus schematic shown in Figure 3.1. The apparatus consists of two acoustic probes, which are attached to a polybenzimidazole vertical cell. Each probe comprises an array of 64 individual piezoelectric elements in 35 mm elevations. Sets of calibration curves have been used at each elevation and temperature (Mixtures of toluene bitumen solutions at different concentrations) to convert speed of sound data to weight percent at each elevation. The sample is put in the polybenzimidazole cell, which is held in place using a cylindrical aluminum frame. The cell was then sealed with an end cap. The temperature is controlled using online monitoring with  $\pm 0.1^\circ\text{C}$  tolerance. Ethylene Glycol / Water bath is circulated (Fisher Scientific Isotemp 3006D) through two copper blocks which fits in the polybenzimidazole cavity as shown in fig 3.1. The acoustic array sensors were screwed into place and coupled to the external walls of the cell using an acoustic coupling gel. The data acquisition hardware comprises a TomoScan Focus LT and the data acquisition software comprises TomoView Software, both from Olympus NDT.

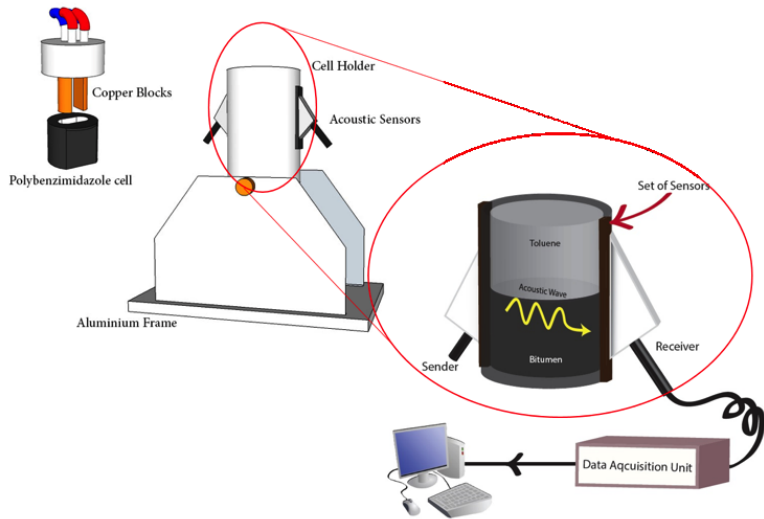


**Figure 3.1.** Schematic of the view cell and data acquisition system used for diffusion measurements showing the arrangement of the acoustic sensors as an inset.

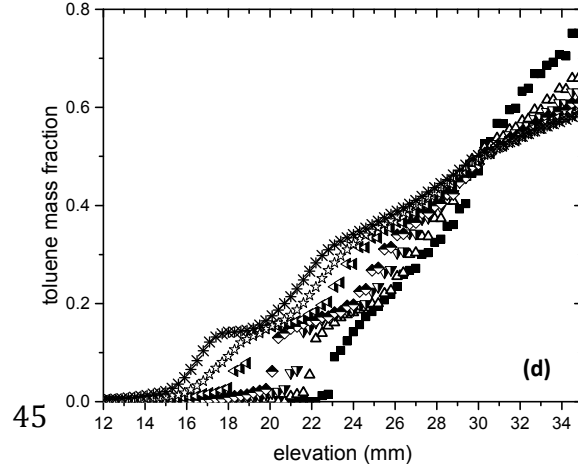
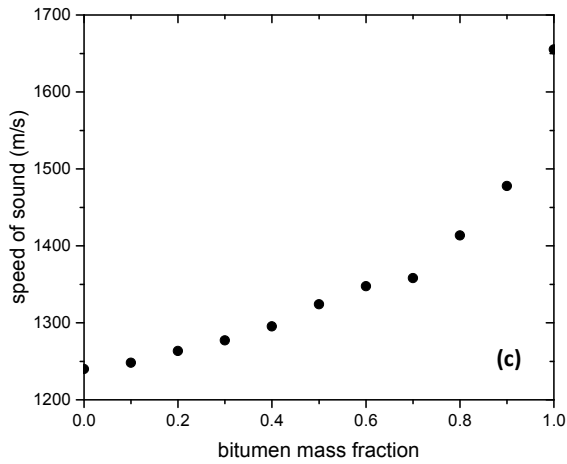
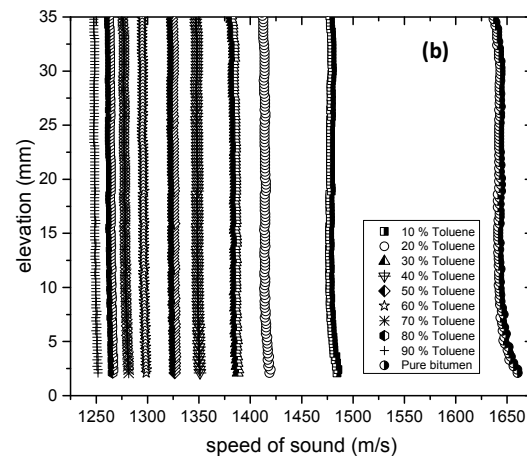
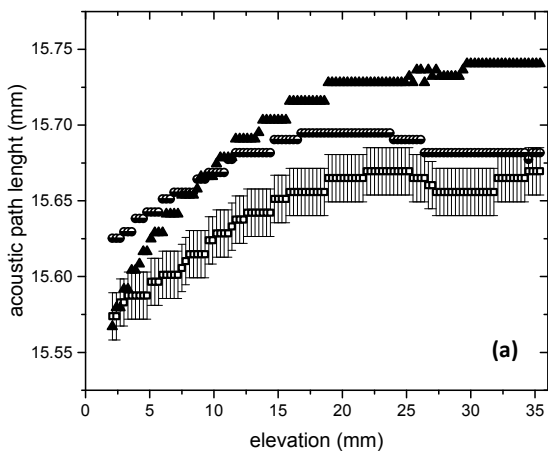


**Figure 3.2.** An illustration of the local composition calibration procedure: (a) acoustic path length determination at  $\square$ , 273 K,  $\bullet$ , 298 K and  $\blacktriangle$ , 313 K; (b) speed of sound measurements for known mixtures of toluene + Athabasca bitumen at 313 K; (c) elevation specific composition calibration curve for toluene + Athabasca bitumen mixtures at 313 K for the 20.1 mm elevation sensor; (d) composition profiles for toluene + Athabasca bitumen at 313 K. ■ 6 hours,  $\triangle$  12 hours,  $\nabla$  24 hours,  $\blacktriangleright$  36 hours,  $\blacktriangleleft$  48 hours,  $\star$  60 hours,  $\ast$  72 hours.

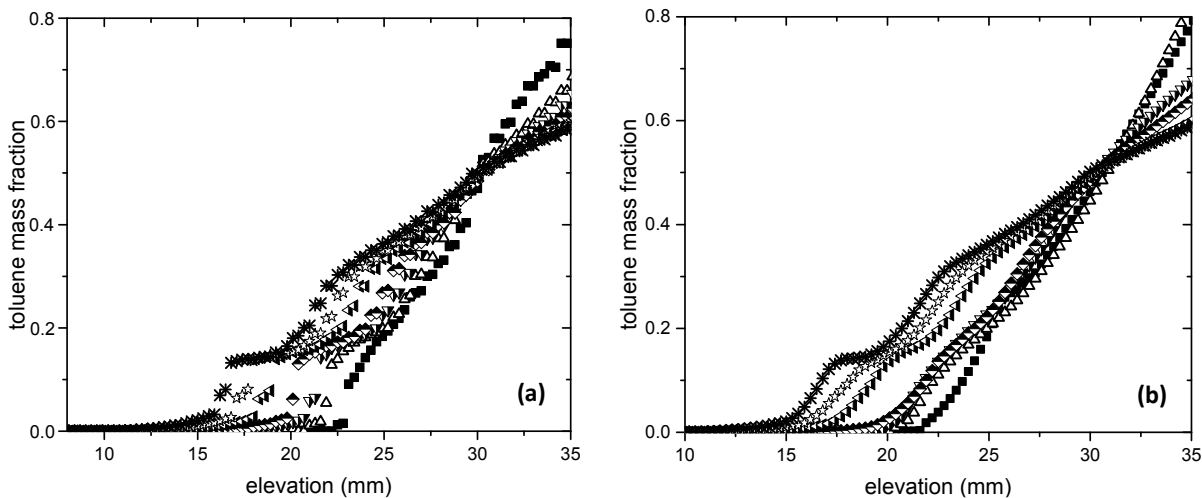


**Figure 3.3.** Example showing the impact of smoothing on composition profiles: (a) Raw toluene concentration profile calculated based on speed of sound data using concentration calibration curve at 313K and (b) Smoothed toluene concentration profile versus elevation using local regression method. ■ 6 hours,  $\triangle$  12 hours,  $\nabla$ , 24 hours,  $\blacktriangleright$  36 hours,  $\square$ , 48 hours,  $\star$ , 60 hours,  $\ast$  72 hours.

### 3.2.2. Materials

Toluene with a purity better than 99% was acquired from Fischer Scientific and Athabasca Bitumen was provided from Suncor.

Polybutene which is a viscosity standard Newtonian fluid with viscosity of 1600 Pa.s and a density of 907 kg/m<sup>3</sup> at 298 K was supplied by Cannon instrument. Carbon nanotubes having internal diameter of 5.5 nm, outer diameter of 6-9 nm and a length of 5μm were obtained from Aldrich. Table 3.2. shows the characterizations of the bitumen that has been used in this study at different temperatures.

**Table 3.2.** Properties of Athabasca bitumen used in this study

Temperature	273 K	298 K	313 K
Density (kg/m <sup>3</sup> ) <sup>1</sup>	1038.6	1023.24	1013.903
Complex Viscosity (Pa·s) <sup>32</sup>  ω=63 s <sup>-1</sup> and 0.3% shear strain	9000	2000	~300
SARA fractions (wt. %)			
Saturate	16.1		
Aromatic	48.5		
Resin	16.8		
Asphaltenes (C5)	18.6		

### 3.2.3. Experimental Procedure

Speed of sound vs composition calibrations were assessed at each elevation for each pseudo binary mixture and at each temperature. The procedure is illustrated in Figure 3.2.

First, path lengths as a function of elevation were determined based on time of flight measurements for toluene, which possesses a well-known speed of sound value as a function of temperature at atmospheric pressure [NIST]<sup>44</sup> (Figure 3.2-a). Speeds of sound for mixtures of known composition, Athabasca bitumen + toluene in this example, Figure 3.2b, were then used to prepare composition calibration curves (Figure 3.2-c) for each elevation so that mixtures of unknown composition could be interpolated. For this example, mixtures of known composition were prepared by combining Athabasca bitumen with toluene. At higher mass fractions of toluene, a homogenizer (Fischer Scientific Analog Vortex Mixer) was used to homogenize mixtures. At lower toluene mass fractions a bath sonicator operated at temperatures ranging 60°C to 70°C for at least 1 hour was used to homogenize sealed vials containing mixtures. As, composition profiles for Athabasca bitumen + toluene mixtures were obtained at 273 K, 298 K and 313 K, local calibrations were obtained for each elevation at each of these temperatures. Calibrations for polybutene + toluene and polybutene + carbon nanotubes + toluene, at 298K were performed in a similar manner.

Athabasca bitumen is semi solid at room temperature, as noted in the introduction, and sub-samples were heated to 353 K for 10 minutes so that they could be poured into the cell. The cell was then sealed and placed in an oven with air atmosphere at 353 K for 1 hour before it was equilibrated in the frame at 323 K over night to ensure the sample was uniformly distributed and free of gas bubbles. The bath temperature was then set to the desired temperature and after thermal equilibrium was reached, toluene was injected into the upper portion of the cell using a syringe. As the cell and the copper blocks have a large thermal mass, and the temperature difference between the toluene and the set

temperature of the cell is small, the duration of the thermal transient, at less than ten seconds, is orders of magnitude smaller than the time scale of the diffusion measurements – hours. Composition profile evolution was assumed to begin at the time of injection.

Control experiments were performed at 298 K. Polybutene + toluene provided a negative control because polybutene + toluene mixtures comprise a single liquid phase.  $n_w$  is expected to be 0.5 over the entire composition range. To ensure that the high-viscosity polybutene was free of bubbles, it was placed in the polybenzimidazole cell and left in the oven at 353 K for 12 hours. 25% carbon nanotubes + polybutene comprise a model structured fluid and for toluene + (carbon nanotubes + polybutene) pseudo binary mixtures values of  $n_w$  less than 0.5 are expected, particularly at low toluene mass fractions. The carbon nanotubes were combined with the polybutene at 353 K using a turbine impeller, described in detail elsewhere<sup>30</sup>, and then treated in the same manner as the negative control sample. For these control experiments care was also taken to ensure the absence of gas bubbles and well defined horizontal interfaces at time zero. Polybutene was selected for control experiments because the viscosity of polybutene is comparable to the zero shear viscosity of Athabasca bitumen.

### **3.3. Results and Discussion**

#### **3.3.1. Polybutene + Toluene and (Polybutene + carbon nanotubes) + Toluene**

Data for these two clearly defined model cases provide key tests for the modeling approach and limits on data quality. The model outcomes are illustrated in Figures 3.4 and 3.5 for Polybutene + Toluene and (Polybutene + carbon nanotubes) + Toluene mixtures respectively. Model coefficients are presented in Table 3.3. Figure 3.4a shows two concentration profiles for the polybutene + toluene mixture and illustrates how the

crossover point, defining  $C_0$  and  $x=0$  for the coordinate system are determined from experimental data. Figure 3.4b illustrates the dispersion arising from the application of the Fickian diffusion model, the only pertinent model in this case. Ideally, the curves superimpose. Figure 3.4c illustrates that all of the composition profiles obtained over a two-day period fall within a range of mutual diffusion coefficients from  $0.5$  and  $3 \times 10^{-10} \frac{m^2}{s}$ . Figure 3.4d illustrates the quality of the fit at 24 hrs based on  $C_0 = 0.37$  and  $D = 1.8 \times 10^{-10} \frac{m^2}{s}$ . Composition profiles for the (polybutene + carbon nanotubes) + toluene case, Figure 3.5, were fit independently. For this and subsequent cases, determination of the crossover point is not presented. Values for  $C_0$  used to determine  $G$  (equation 3.7b) are presented in Table 3.3. Figure 3.5a illustrates the appropriateness of the Fickian diffusion assumption. At high toluene mass fraction the composition profiles superimpose, indicating that Fickian diffusion is important, and at low toluene mass fraction, the composition profiles obtained at different times diverge. However, the range of diffusion coefficients that bound all of the data is only marginally broader than the range for polybutene + toluene, Figure 3.4c. From Figure 3.5b, it is clear that Single File diffusion plays a role over the entire composition range. All of the composition profiles fall within a narrow range of  $H$  values. Thus, both models fit the data within experimental uncertainty, and caution must be applied in the interpretation of this outcome and other outcomes with comparable ambiguity. If one assigns the mean values for  $D$  and  $H$ , shown in Table 3.3, then for this example one observes that by fitting individual composition profiles, as illustrated in Figure 3.5c,  $\gamma$  approaches 0 at low toluene mass fraction and 1 at high toluene mass fraction for all (polybutene + carbon nanotubes) + toluene cases, Figure 3.5d. However, there is significant scatter in the fitted  $\gamma$  values at any given

composition. From Figure 2.6, the values of  $n_w$  for (polybutene + carbon nanotubes) + toluene mixtures are intermediate between 0.25 and 0.5 over the entire composition range. Perhaps this outcome, which pushes the limits on data quality, is not surprising.

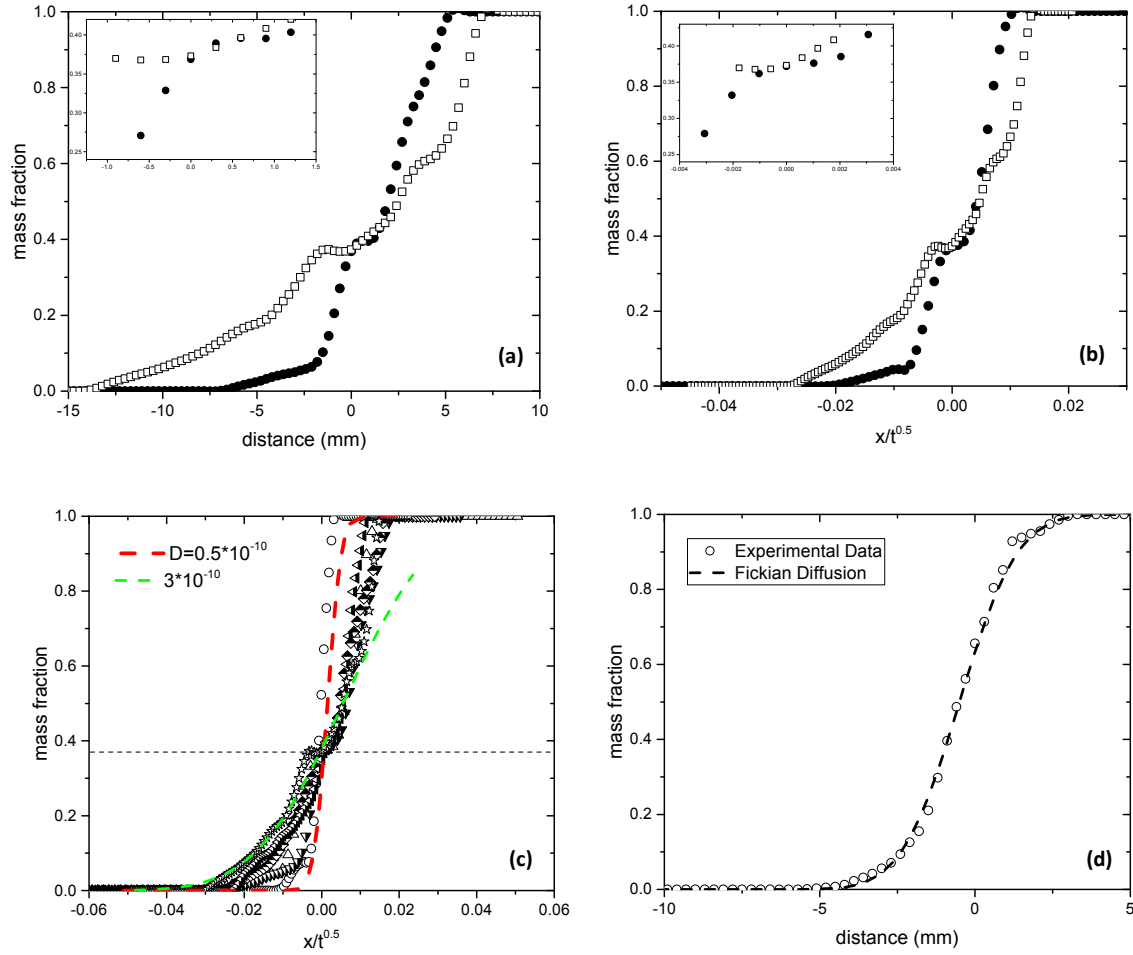


**Figure 3.4.** Polybutene + toluene a) composition profiles after ● 12 hours, □ 48 hours; cross over point occurs at 0.37 mass fraction. b) Mass fraction versus joint variable in single file diffusion after ● 12 hours, □ 48 hours; cross over point occurs at 0.37 mass fraction. c) Fickian diffusion model fit: ○ 6 hours, Δ, 12 hours, ▽, 24 hours, ▲ 36 hours,

$\square$ , 48 hours,  $\star$ , 60 hours. d) Fickian diffusion model,  $D = 2 \times 10^{-10} \text{ m}^2/\text{s}$ ,  $C_0 = 0.37$  for polybutene + toluene experimental data at 24 hours.

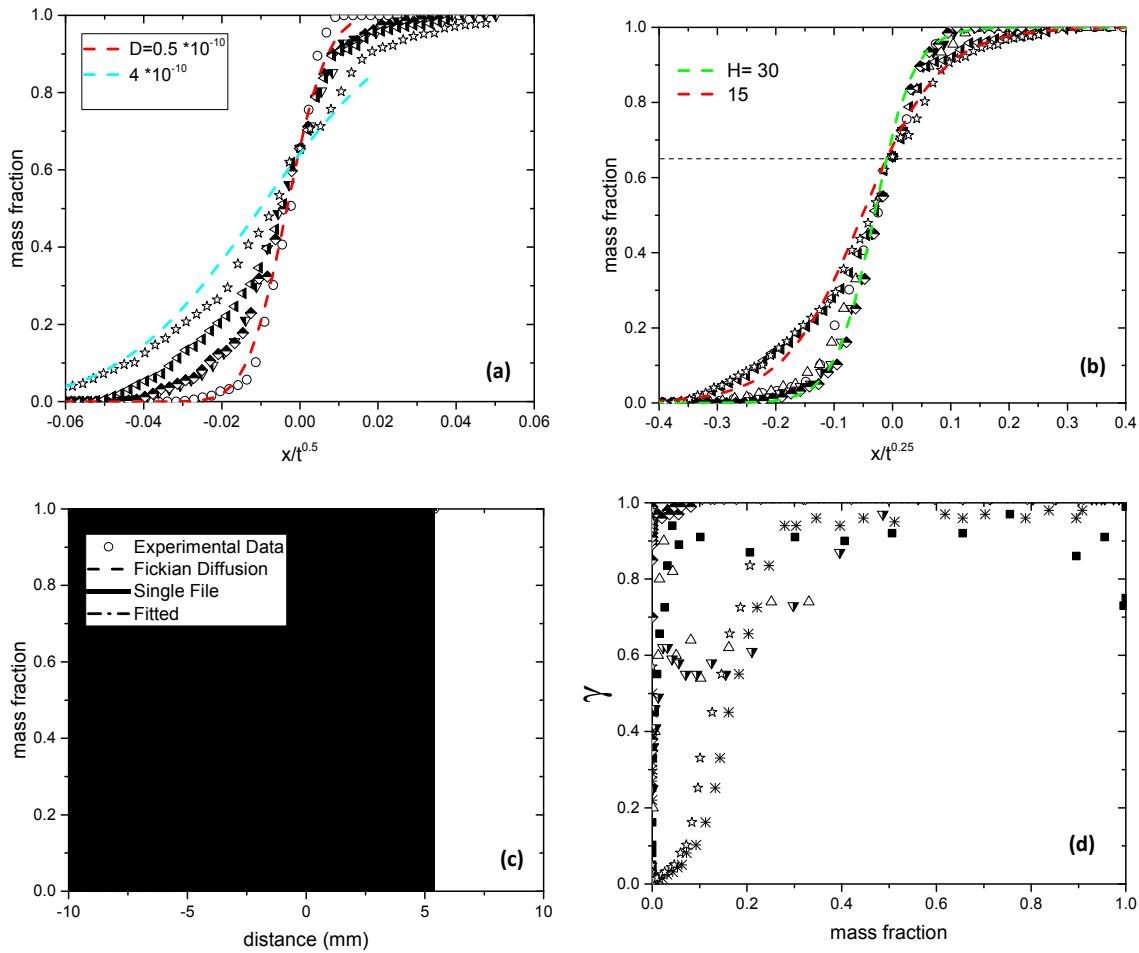


**Figure 3.5.** (polybutene + CNT) + toluene a) Single file diffusion model fit with  $H = 15$  and 30.  $\bigcirc$  6 hours,  $\Delta$ , 12 hours,  $\nabla$ , 24 hours,  $\blacktriangleleft$  36 hours,  $\square$ , 48 hours,  $\star$ , 60 hours. b) Fickian diffusion fit:  $\bigcirc$  6 hours,  $\Delta$ , 12 hours,  $\nabla$ , 24 hours,  $\blacktriangleleft$  36 hours,  $\square$ , 48 hours,  $\star$ , 60 hours. c) Single file and Fickian diffusion models, and equation (3.8) for 48 hours data. d) Fitted values for  $\gamma$ , equation (3.8), as a function of toluene mass fraction where

time is a parameter: ■ 6 hours, △, 12 hours, ▽, 24 hours, ▲ 36 hours, □, 48 hours and ★, 60 hours.

### 3.3.2 Joint Fickian + Single File Diffusion Model Fits to Literature Data

Composition profile data sets from the literature, ranging from Athabasca bitumen fractions to Athabasca atmospheric residue and Athabasca vacuum residue + different light hydrocarbons that were obtained using diverse apparatus are used to test the joint Fickian + Single File diffusion model. Figure 3.6 shows the model fits for Athabasca bitumen + toluene composition profiles at 296K<sup>27</sup>. For the Fickian diffusion model, Figure 3.6a, the composition profiles superimpose at high toluene mass fraction. At low toluene mass fraction, the composition profiles obtained at different times diverge. From Figure 3.6b, it is clear that Single File diffusion plays a role over the entire composition range. The composition profiles fall within the predicted range for H values between 35-45  $\frac{s^{0.25}}{m}$ , yielding a value for the mobility coefficient of  $8\pm3\times10^{-13}\frac{m^2}{s^{0.5}}$ . As noted in appendix A, this is the only data set that provides mobility coefficient values with a small uncertainty. Assigning the mean values for D and H, shown in Table 3.3, one observes that by fitting individual composition profiles, as illustrated in Figure 3.6c, the value for  $\gamma$  approaches 0 at low toluene mass fraction and 1 at high toluene mass fraction as shown in Figure 3.6d. As expected, there is significant scatter in the fitted  $\gamma$  values at any given composition.

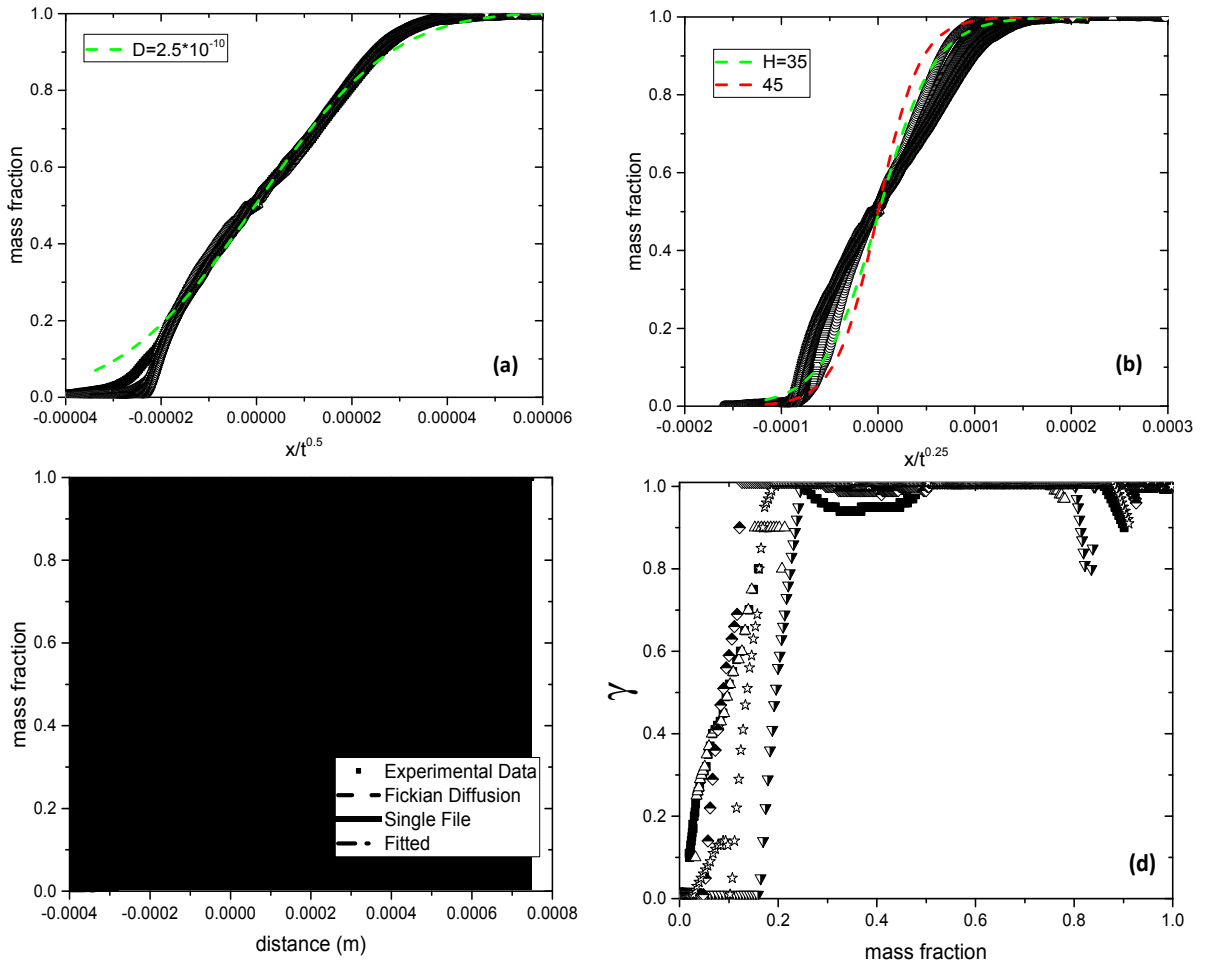


**Figure 3.6.** Athabasca bitumen + toluene at 296K<sup>27</sup> a) Fits for  $\lambda=0.5$  ○ 40 seconds, Δ, 90 seconds, ▼, 140 seconds, □, 200 seconds, ☆, 240 seconds for Athabasca bitumen+toluene<sup>27</sup>; cross over point occurs at 0.5 mass fraction. b) Fits for  $\lambda=0.25$  ○ 40 seconds, Δ, 90 seconds, ▼, 140 seconds, □, 200 seconds, ☆, 240 seconds. c) Single file and Fickian diffusion models, and equation (3.8) for 140 seconds data. d) Fitted values for  $\gamma$ , equation (3.8), as a function of toluene mass fraction where time is a parameter: ■ 40 seconds, Δ, 90 seconds, ▼, 140 seconds, □, 200 seconds and ☆, 240 seconds.

Joint Fickian + Single File diffusion model fits for Athabasca atmospheric residue + pentane<sup>30</sup>, Athabasca vacuum residue + pentane<sup>30</sup>, and Athabasca bitumen + pentane<sup>27,28</sup> data sets are presented in Figures 3.7 a-c and 3.8 a-c, and 3.9 a-c respectively. While the details vary, the outcomes for these mixtures are qualitatively similar to the outcomes for Athabasca bitumen + toluene shown in Figure 3.6. Mean values and ranges for the mutual diffusion coefficient, D, and the parameter H are reported in Table 3.3. along with their ranges of uncertainty. The values for D are consistent with values regressed by the authors. As noted in appendix A, for these data sets only order of magnitude estimates for F are obtained. Upper and lower limit values are reported in Table 3.3.

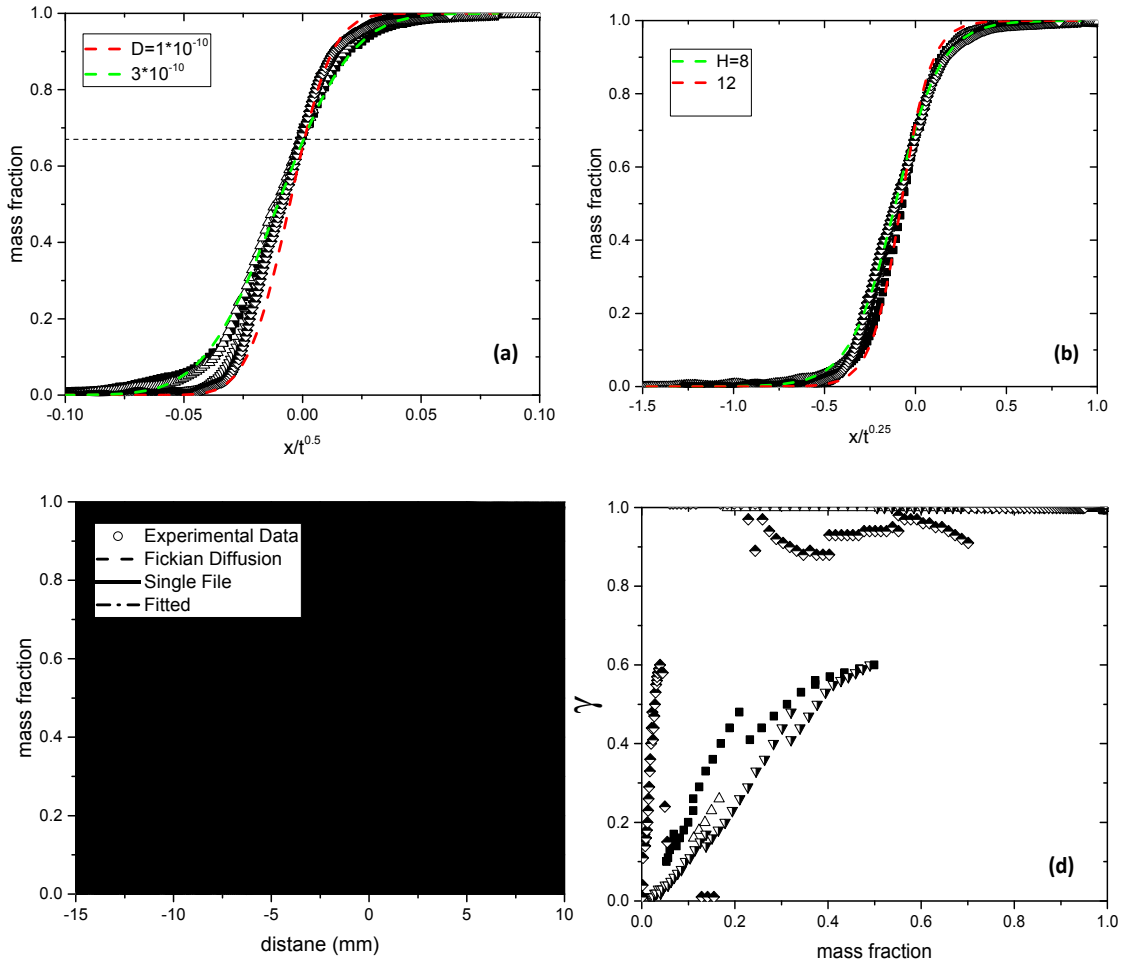


**Figure 3.7.** Athabasca atmospheric residue+pentane<sup>30</sup> a) Fits for  $\lambda=0.5$  ■, 3420 seconds,  $\Delta$ , 6780 seconds,  $\nabla$ , 14820 seconds,  $\square$ , 25980 seconds for Athabasca atmospheric residue+pentane<sup>30</sup>; cross over point occurs at 0.67 mass fraction. B) Fits for  $\lambda=0.25$  ■, 3420 seconds,  $\Delta$ , 6780 seconds,  $\nabla$ , 14820 seconds,  $\square$ , 25980 seconds for Athabasca atmospheric residue+pentane. c) Single file and Fickian diffusion models, and equation (3.8) for 14820 seconds data. d) Fitted values for  $\gamma$ , equation (3.8), as a function of toluene mass fraction where time is a parameter: ■, 3420 seconds,  $\Delta$ , 6780 seconds,  $\nabla$ , 14820 seconds,  $\square$ , 25980 seconds.

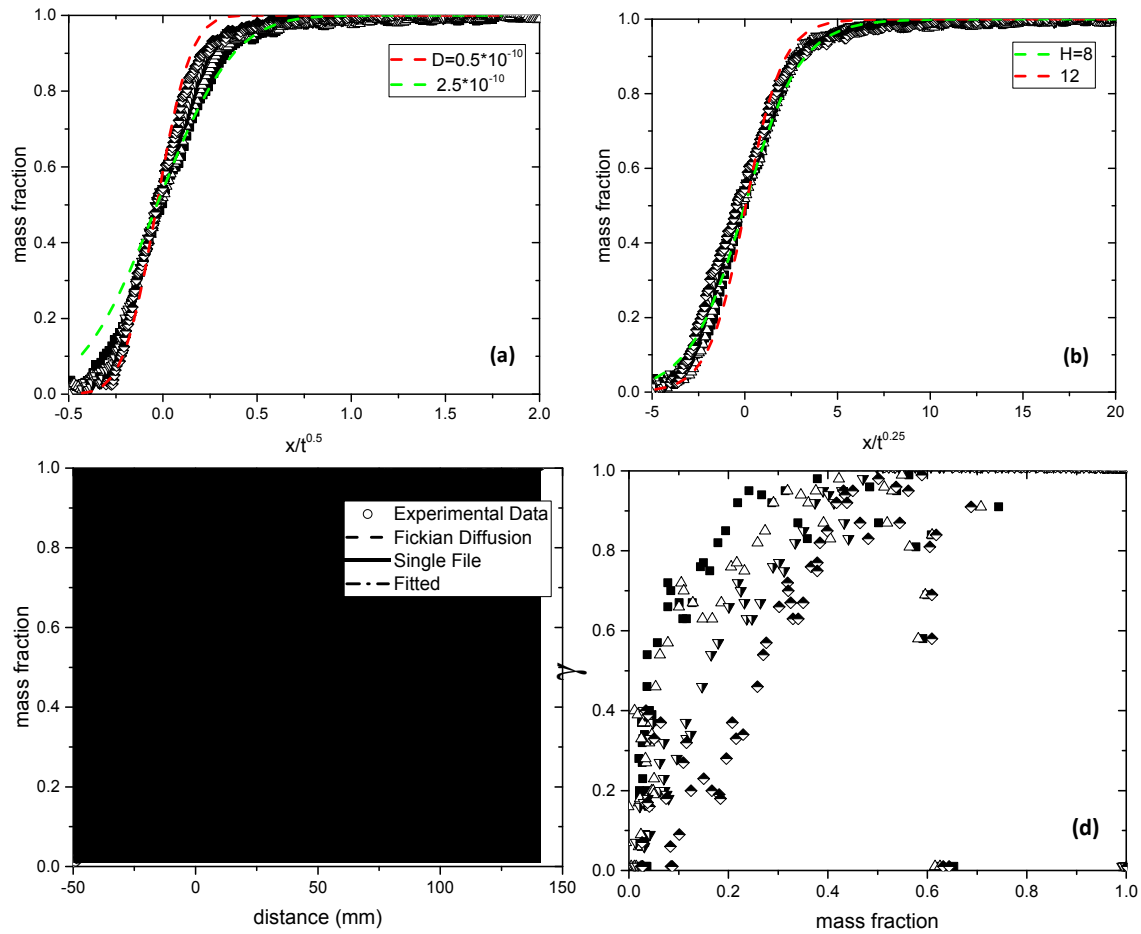


**Figure 3.8.** Athabasca vacuum residue+pentane<sup>30</sup>a) Fits for  $\lambda=0.5$  ■, 4860 seconds, Δ, 9120 seconds, ▼, 15780 seconds, □, 32040 seconds for Athabasca vacuum residue+pentane<sup>30</sup>; cross over point occurs at 0.65 mass fraction. b) Fits for  $\lambda=0.25$  ■, 4860 seconds, Δ, 9120 seconds, ▼, 15780 seconds, □, 32040 seconds for Athabasca vacuum residue+pentane. c) Single file and Fickian diffusion models, and equation (3.8) for 15780 seconds data. d) Fitted values for  $\gamma$ , equation (3.8), as a function of toluene mass fraction where time is a parameter: ■, 4860 seconds, Δ, 9120 seconds, ▼, 15780 seconds, □, 32040 seconds.

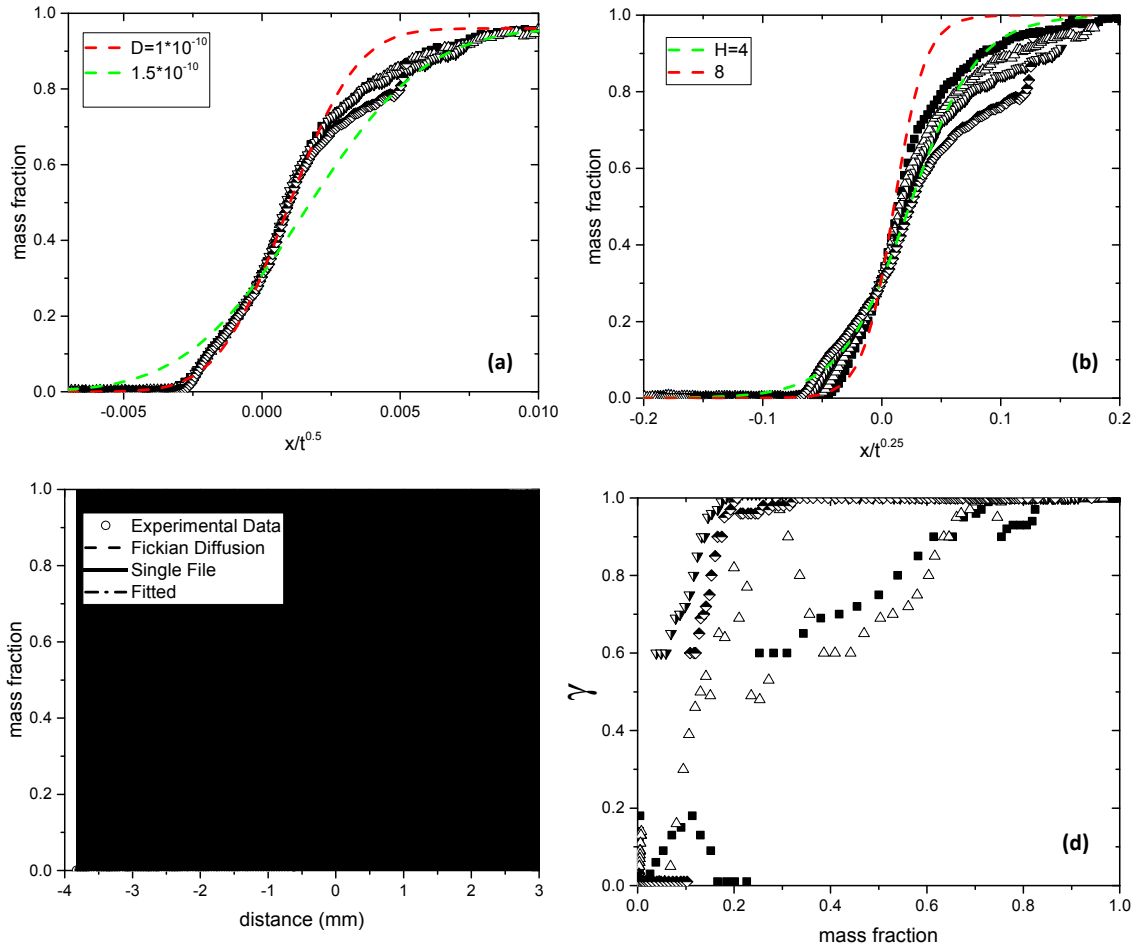


**Figure 3.9.** Athabasca bitumen+pentane<sup>28,29</sup> a) Fits for  $\lambda=0.5$  ■ 630 minutes,  $\Delta$ , 1470 minutes,  $\nabla$ , 2910 minutes and □, 5790 minutes for Athabasca bitumen+pentane<sup>28,29</sup>; cross over point occurs at 0.3 mass fraction. b) Fits for  $\lambda=0.25$  ■ 630 minutes,  $\Delta$ , 1470 minutes,  $\nabla$ , 2910 minutes and □, 5790 minutes for Athabasca bitumen+pentane<sup>27,28</sup>. c) Single file and Fickian diffusion models, and equation (3.8) for 1470 minutes data. d) Fitted values for  $\gamma$ , equation (3.8), as a function of toluene mass fraction where time is a parameter: ■ 630 minutes,  $\Delta$ , 1470 minutes,  $\nabla$ , 2910 minutes and □, 5790 minutes.

Figure 3.10 shows the joint Fickian + Single File diffusion model fit to the Cold lake bitumen + heptane<sup>26</sup> composition profile data. Figures 3.10a and 3.10b show the composition profile fitting using the Fickian and single file models separately. In Table 3.3. mean values and ranges for the mutual diffusion coefficient, D, and the parameter H are reported with their ranges of uncertainty. The values for Fickian diffusion coefficient are consistent with values reported by the authors. Fitting the set on the mix model (Figure 3.10c) and calculating the value of gamma as shown in Figure 3.10d however does not show a good agreement with the expected range of values as previous data sets which we can attribute to the poor quality of composition data. As noted previously, for these data sets only order of magnitude estimates for F are obtained.

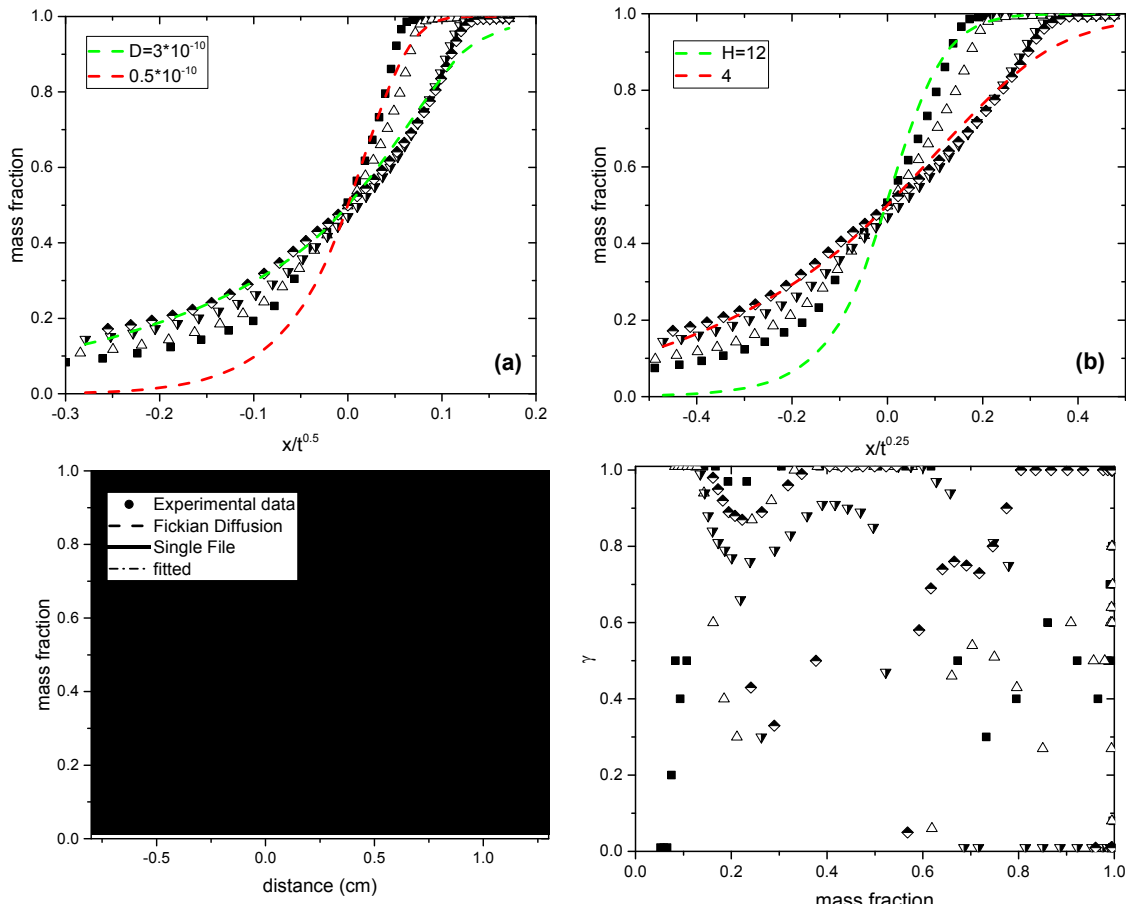


**Figure 3.10.** Cold Lake bitumen+heptane<sup>26</sup> a) Fits for  $\lambda=0.5$  ■ 319 minutes,  $\Delta$ , 606 minutes,  $\nabla$ , 1398 minutes and □, 1753 minutes for Athabasca bitumen+pentane<sup>26</sup>; cross over point occurs at 0.3 mass fraction. b) Fits for  $\lambda=0.25$  ■ 319 minutes,  $\Delta$ , 606 minutes,  $\nabla$ , 1398 minutes and □, 1753 minutes for Athabasca bitumen+pentane<sup>26</sup>. c) Single file and Fickian diffusion models, and equation (3.8) for 1398 minutes data. d) Fitted values for  $\gamma$ , equation (3.8), as a function of toluene mass fraction where time is a parameter: ■ 319 minutes,  $\Delta$ , 606 minutes,  $\nabla$ , 1398 minutes and □, 1753 minutes.

### 3.3.3. Athabasca bitumen + toluene data sets (this work).

Composition profile data sets for Athabasca bitumen + toluene at 273, 293 and 313 K (this work), were also fit using the joint Fickian + Single File diffusion model. The outcomes are reported in Figures 3.11-3.13 and coefficient values are reported in Table 3.3. The mutual diffusion coefficient values,  $3\pm1\times10^{-10}\left(\frac{m^2}{s}\right)$  at 273K,  $3.5\pm1.5\times10^{-10}\left(\frac{m^2}{s}\right)$  at 298K and  $10\pm2\times10^{-10}\left(\frac{m^2}{s}\right)$  at 313K, are less than the self diffusion coefficients for toluene ( $2.4\times10^{-9}\left(\frac{m^2}{s}\right)$  at 273K, 298K  $3.1\times10^{-9}$  at 298 K and  $9\times10^{-9}$  at 313K<sup>45</sup>) and are consistent with the value (Athabasca bitumen+toluene at 296 K) obtained by Fadaei et al.<sup>27</sup> for the same mixture.

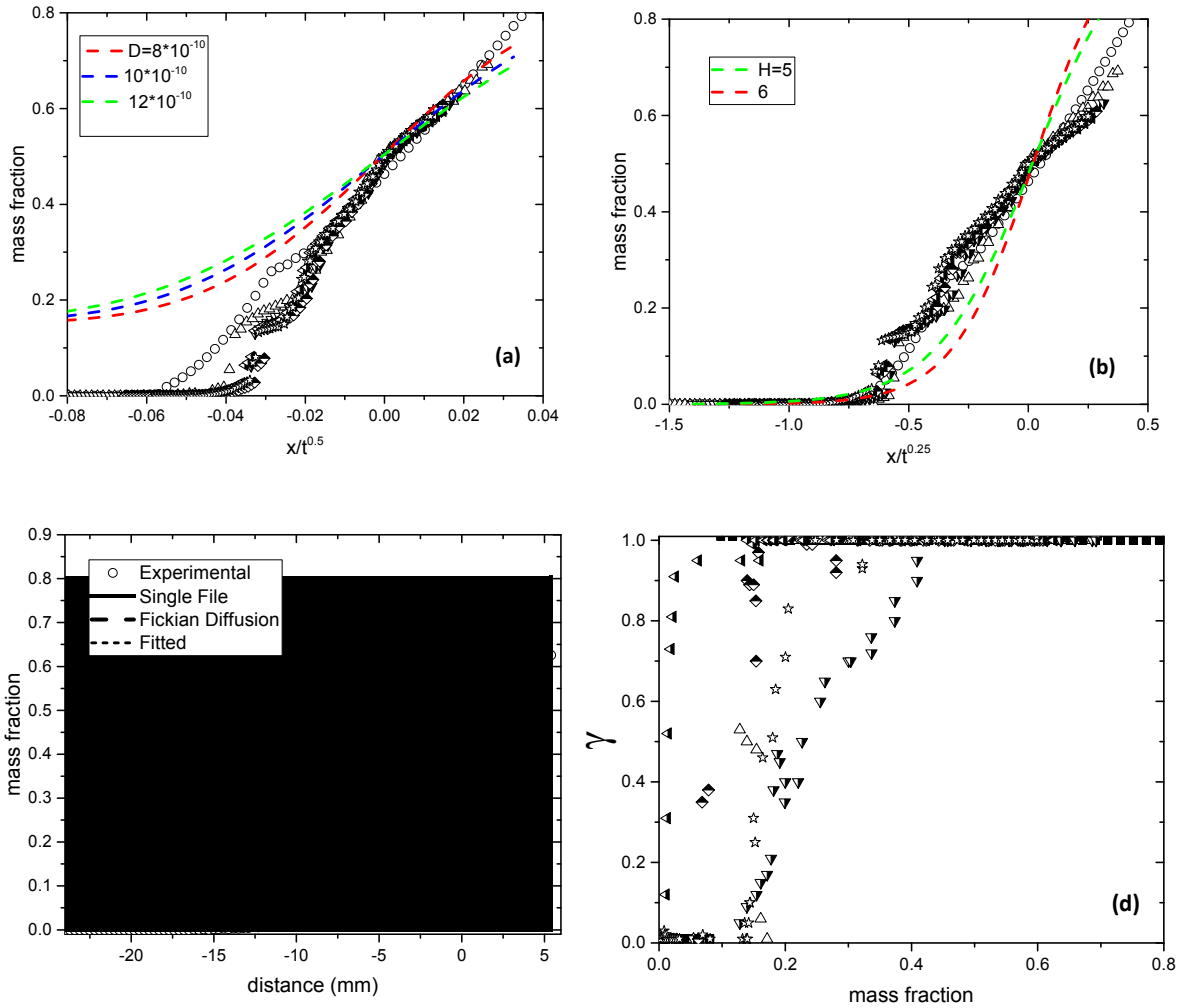


**Figure 3.11.** Athabasca bitumen + toluene at 313 K a)  $\lambda=0.5$   $\circ$ , 6 hours,  $\Delta$ , 12 hours,  $\nabla$ , 24 hours,  $\blacktriangleleft$ , 36 hours,  $\square$ , 48 hours,  $\star$ , 60 hours for 313K; cross over point occurs at 0.5 mass fraction. b)  $\lambda=0.25$   $\circ$ , 6 hours,  $\Delta$ , 12 hours,  $\nabla$ , 24 hours, 36 hours,  $\square$ , 48 hours,  $\star$ , 60 hours for 313K; cross over point occurs at 0.5 mass fraction. c) Single file and Fickian diffusion models, and equation (3.8) for 48 hours data. d) Fitted values for  $\gamma$ , equation (3.8), as a function of toluene mass fraction where time is a parameter: ■ 6 hours,  $\Delta$ , 12 hours,  $\nabla$ , 24 hours,  $\blacktriangleleft$ , 36 hours,  $\square$ , 48 hours and  $\star$ , 60 hours.

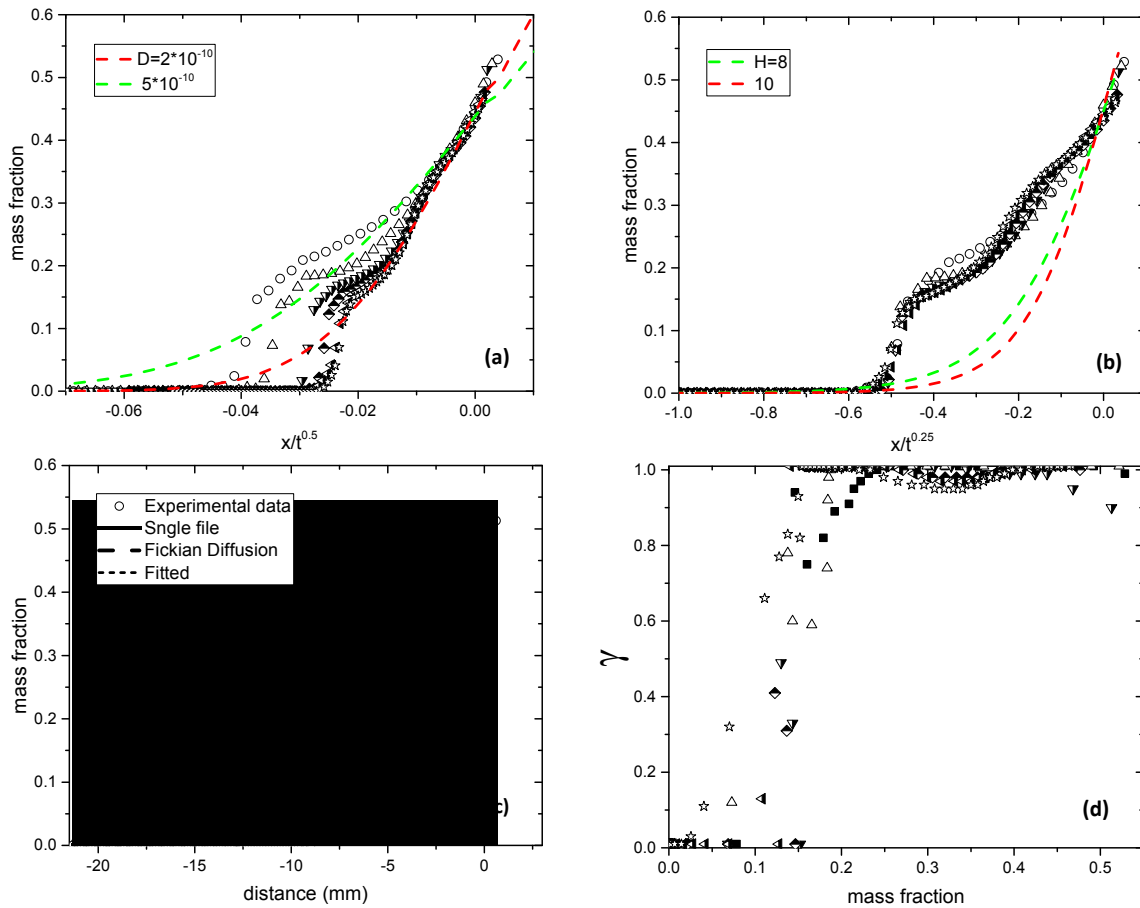


**Figure 3.12.** Athabasca bitumen + toluene at 298 K a) Fits for  $\lambda=0.5$   $\bigcirc$  6 hours,  $\Delta$ , 12 hours,  $\nabla$ , 24 hours,  $\blacktriangleleft$  36 hours,  $\square$ , 48 hours,  $\star$ , 60 hours for 298K; cross over point occurs at 0.43 mass fraction. B) Fits for  $\lambda=0.25$   $\bigcirc$  6 hours,  $\Delta$ , 12 hours,  $\nabla$ , 24 hours,  $\blacktriangleleft$  36 hours,  $\square$ , 48 hours,  $\star$ , 60 hours for 298K; cross over point occurs at 0.43 mass fraction. c) Single file and Fickian diffusion models, and equation (3.8) for 48 hours data. d) Fitted values for  $\gamma$ , equation (3.8), as a function of toluene mass fraction where time is a parameter: ■ 6 hours,  $\Delta$ , 12 hours,  $\nabla$ , 24 hours,  $\blacktriangleleft$  36 hours,  $\square$ , 48 hours and  $\star$ , 60 hours.

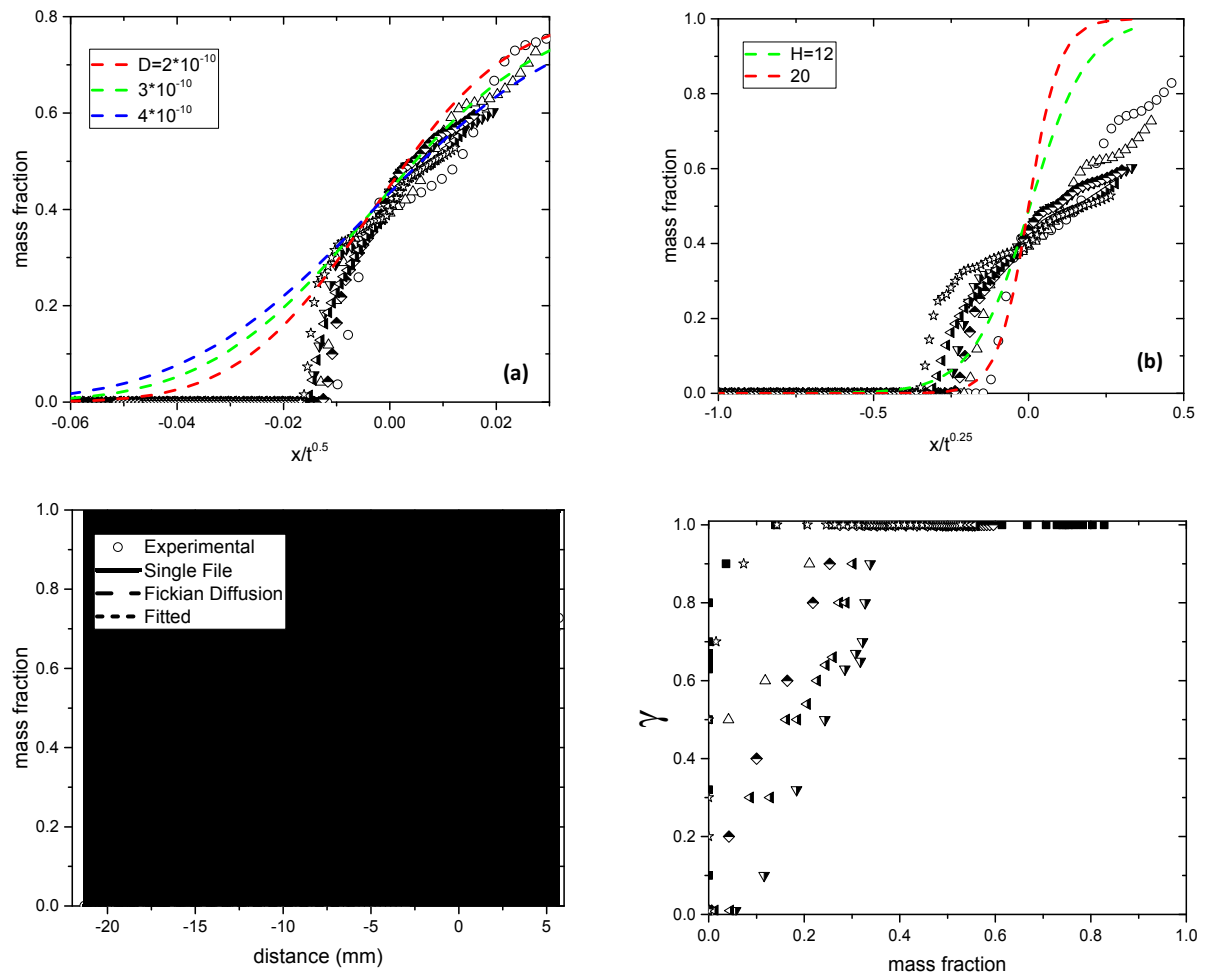


**Figure 3.13.** Athabasca bitumen + toluene at 273 K a) Fits for  $n_w=0.5$   $\circ$  6 hours,  $\Delta$ , 12 hours,  $\nabla$ , 24 hours,  $\blacktriangleleft$  36 hours,  $\square$ , 48 hours,  $\star$ , 60 hours for 273K; cross over point occurs at 0.43 mass fraction. B) Fits for  $n_w=0.25$   $\circ$  6 hours,  $\Delta$ , 12 hours,  $\nabla$ , 24 hours,  $\blacktriangleleft$  36 hours,  $\square$ , 48 hours,  $\star$ , 60 hours for 273K; cross over point occurs at 0.41 mass fraction. c) Single file and Fickian diffusion models, and equation (3.8) for 48 hours data. d) Fitted values for  $\gamma$ , equation (3.8), as a function of toluene mass fraction where time is a parameter: ■ 6 hours,  $\Delta$ , 12 hours,  $\nabla$ , 24 hours,  $\blacktriangleleft$  36 hours,  $\square$ , 48 hours and  $\star$ , 60 hours.

**Table 3.3.:** Composition range, G and H for different data sets.

Data set	Single file diffusion fit, wt. frac.	G	H	$F \left( \frac{m^2}{s^{\frac{1}{2}}} \right)$	$D \left( \frac{m^2}{s} \right)$	
					this work	reported in the source citation
Polybutene + toluene 298 K	-	1.7	-	-	$1.8 \pm 1.2 \times 10^{-10}$	N/A
(Polybutene + CNT)+ toluene 298 K	0-1	0.53	$23 \pm 7$	$\sim 10^{-12}$	$2.3 \pm 1.8 \times 10^{-10}$	N/A
Athabasca bitumen + toluene at 313 K	0-0.05	1	$5 \pm 0.5$	$\sim 10^{-12}$	$10 \pm 2 \times 10^{-10}$	N/A
Athabasca bitumen + toluene at 298 K	0-0.05	1.32	$9 \pm 1$	$\sim 10^{-14}$	$3.5 \pm 1.5 \times 10^{-10}$	N/A
Athabasca bitumen + toluene at 273 K	0-0.05	1.5	$14 \pm 6$	$\sim 10^{-13}$	$3 \pm 1 \times 10^{-10}$	N/A
Athabasca bitumen	0-0.05	1	$40 \pm 5$	$8 \pm 3 \times 10^{-13}$	$2.5 \pm$	$1.5 \pm$

+ toluene <sup>27</sup> at 296 K					$1.5 \times 10^{-10}$	$1 \times 10^{-10}$
Athabasca atmospheric residue + pentane <sup>30</sup> at 297 K	0-0.20	0.49	8±5	$\sim 10^{-13}$	$2 \pm 1 \times 10^{-10}$	$0.5 \pm 0.1 \times 10^{-10}$
Athabasca vacuum residue +pentane <sup>30</sup> at 297 K	0-0.20	0.53	10±2	$\sim 10^{-12}$	$1.5 \pm 1 \times 10^{-10}$	N/A
Athabasca bitumen + pentane <sup>28,29</sup> at 295 K	0-0.20	2.33	6±2	$\sim 10^{-12}$	$1.3 \pm 0.3 \times 10^{-10}$	$1.7 \pm 0.4 \times 10^{-10}$
Cold Lake bitumen +heptane <sup>26</sup>	0-0.20	0.95	8±4	$\sim 10^{-13}$	$2 \pm 1.5 \times 10^{-10}$	$5 \pm 3 \times 10^{-10}$

### 3.3.4. Impact of asphaltene mass fraction and solvent choice on the relative importance of the two diffusion mechanisms

A master plot illustrating the impact of asphaltene mass fraction and solvent choice on  $\gamma$  for Athabasca bitumen at  $\sim 295$  K is shown in Figure 3.14. Sample pretreatment, storage and handling differences are uncontrolled. However, a clear trend is observed in the nature of the dominant mutual diffusion mechanism whether with n-alkanes (open

symbols) or with toluene (closed symbols). Similar trends were shown for values of  $n_w$  in Chapter 2. At higher asphaltene mass fraction Single File diffusion dominates. At low asphaltene mass fraction, Fickian diffusion dominates. The explanation for the difference between the impact of addition of aromatic versus n-alkane diluents is also the same. Aromatics do not affect the size of asphaltene nanoaggregates significantly. The length scale of the channels among aggregates increases by dilution only. With the addition of n-alkanes, asphaltene aggregates grow<sup>46</sup>. This increases the scale of the channels among aggregates (Figure 3.15) and drives the mixture to conditions where Fickian diffusion dominates at lower extents of dilution. Thus, n-alkanes appear to penetrate bitumen faster and appear to be better candidates for enhanced SAGD production process for heavy oils and bitumen than aromatic compounds.

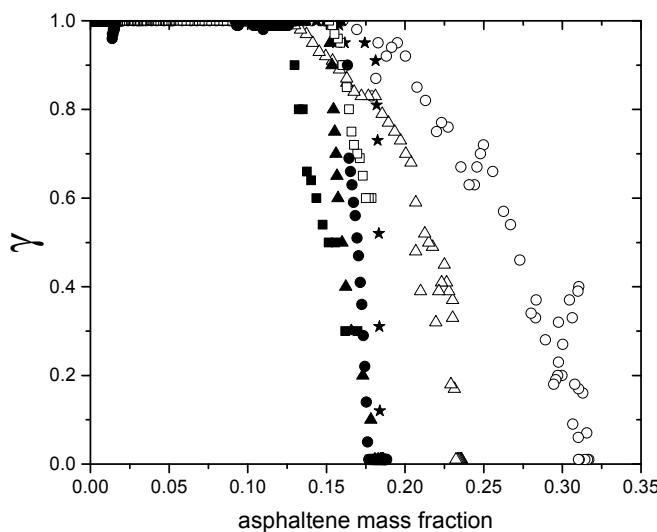


**Figure 3.14.** Asphaltene mass fraction versus the values of  $\gamma$  for:  $\circ$ , Athabasca atmospheric residue + pentane<sup>30</sup>,  $\Delta$ , Athabasca atmospheric residue + pentane<sup>30</sup>,  $\square$ , Athabasca bitumen + pentane<sup>28,29</sup> ■, Athabasca bitumen + toluene at 273 K ,  $\blacktriangle$ ,

Athabasca bitumen + toluene at 298 K,  $\star$ , Athabasca bitumen + toluene at 313 K,  $\bullet$ ,  
Athabasca bitumen + toluene<sup>27</sup>.

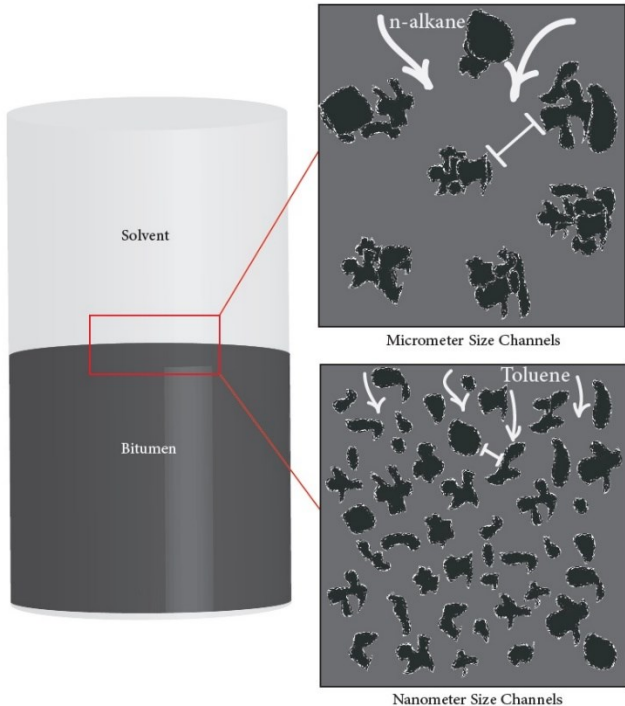


**Figure 3.15.** Schematic representation of solvent impacts on the importance of the Single File diffusion mechanism.

### 3.4. Conclusions

Sets of composition profiles arising from free diffusion experiments performed as part of this work and composition profiles extracted from the literature were analyzed using a three parameter joint Fickian + Single File mutual diffusion model. The parameters included a heavily constrained Fickian mutual diffusion coefficient value,  $D$ , a composition and mixture dependent weighting factor for the diffusion mechanisms,  $0 < \gamma$

< 1, and a coefficient H fit to the composition profiles. With these three parameters it was possible to fit all of the sets of composition profiles within the uncertainty of their respective spatial, time, and composition measurements, and to identify composition ranges where the Single File and Fickian mutual diffusion mechanisms dominate. The composition ranges and transition zones identified, and the roles played by asphaltenes and diluents that were identified, enrich the understanding obtained in Chapter 2 and provide a basis for quantitative prediction for mutual diffusion processes in heavy oil and bitumen + diluent mixtures. From the perspective of engineering data, new Fickian mutual diffusion coefficient values showing the impact of temperature were identified for Athabasca bitumen + toluene, and Fickian diffusion coefficients for bitumen and bitumen fraction + diluent mixtures reported in the literature were confirmed. With the exception of one data set, only order of magnitude estimates for single file mobility coefficients in the literature were obtained. It is not clear if this last outcome is an inherent limitation of the experimental and data analysis technique or if short duration free diffusion experiments, such as those realized in micro fluidics apparatus, can be used as a basis for deriving Single File mobility coefficients.<sup>47</sup>

### **3.5. References:**

- (1) Stewart, R.; Wood, C. V.; Murowchuk, S. J.; Shaw, J. M. Phase Order Inversion During Heavy Oil and Bitumen Production with Solvent Addition, *Energy Fuels* **2014**.
- (2) Shah, A.; Fishwick, R.; Wood, J.; Leeke, G.; Rigby, S.; Greaves, M. A review of novel techniques for heavy oil and bitumen extraction and upgrading, *Energy Environ. Sci.* **2010**, 3, 700–714.

- (3) Pourmohammadbagher, A; Shaw, J.M. On probing contaminant transport to and from clay surfaces in organic solvents and water using solution calorimetry *Env Sci Tech*, in press 2015.
- (4) Bagheri, S. R.; Bazyleva, A.; Gray, M. R.; McCaffrey, W. C.; Shaw, J. M. Observation of Liquid Crystals in Heavy Petroleum Fractions, *Energy Fuels* **2010**, *24*, 4327–4332.
- (5) Bagheri, S. R.; Masik, B.; Arboleda, P.; Wen, Q.; Michaelian, K. H.; Shaw, J. M. Physical Properties of Liquid Crystals in Athabasca Bitumen Fractions, *Energy Fuels* **2012**, *26*, 4978–4987.
- (6) Nikooyeh, K.; Bagheri, S. R.; Shaw, J. M. Interactions Between Athabasca Pentane Asphaltenes and n-Alkanes at Low Concentrations, *Energy Fuels* **2012**, *26*, 1756–1766.
- (7) Fulem, M.; Becerra, M.; Hasan, M. D. A.; Zhao, B.; Shaw, J. M. Phase behaviour of Maya crude oil based on calorimetry and rheometry, *Fluid Phase Equilibria* **2008**, *272*, 32–41.
- (8) Bazyleva, A. B.; Hasan, M. A.; Fulem, M.; Becerra, M.; Shaw, J. M. Bitumen and Heavy Oil Rheological Properties: Reconciliation with Viscosity Measurements, *J. Chem. Eng. Data* **2010**, *55*, 1389–1397.
- (9) Branco, V. A. M.; Mansoori, G. A.; De Almeida Xavier, L. C.; Park, S. J.; Manafi, H. Asphaltene flocculation and collapse from petroleum fluids, *J.Pet. Sci. Eng.* **2001**, *32*, 217–230.
- (10) Murgich, J.; Strausz, O. P. Molecular mechanics of aggregates of asphaltenes and resins of the Athabasca oil, *Pet. Sci. Technol.* **2001**, *19*, 231–243.

- (11) Yarranton, H. W. Asphaltene Self- Association, *J.Dispers. Sci. Technol.* **2005**, *26*, 5–8.
- (12) Andreatta, G.; Bostrom, N.; Mullins, O. C. High-*Q* Ultrasonic Determination of the Critical Nanoaggregate Concentration of Asphaltenes and the Critical Micelle Concentration of Standard Surfactants, *Langmuir* **2005**, *21*, 2728–2736.
- (13) Mostowfi, F.; Indo, K.; Mullins, O. C.; McFarlane, R. Asphaltene Nanoaggregates Studied by Centrifugation, *Energy Fuels* **2009**, *23*, 1194–1200.
- (14) Takeshige, W. Hydrodynamic Shape and Size of Khafji Asphaltene in Benzene, *J.Colloid Interface Sci.* **2001**, *234*, 261–268.
- (15) Sheu, E. Y. Petroleum Asphaltene-Properties, Characterization, and Issues, *Energy Fuels* **2002**, *16*, 74–82.
- (16) Hasan, M. A.; Fulem, M.; Bazyleva, A.; Shaw, J. M. Rheological Properties of Nanofiltered Athabasca Bitumen and Maya Crude Oil, *Energy Fuels* **2009**, *23*, 5012–5021.
- (17) Bouhadda, Y.; Bendedouch, D.; Sheu, E.; Krallafa, A. Some Preliminary Results on a Physico-Chemical Characterization of a Hassi Messaoud Petroleum Asphaltene, *Energy Fuels* **2000**, *14*, 845–853.
- (18) Lorenz, P. B.; Bolen, R. J.; Dunning, H. N.; Eldib, I. A. Ultracentrifugation and viscosities of crude oils, *J. Colloid Sci.* **1961**, *16*, 493–496.
- (19) Gawrys, K. L.; Kilpatrick, P. K. Asphaltenic aggregates are polydisperse oblate cylinders, *J.Colloid Interface Sci.* **2005**, *288*, 325–334.
- (20) Sirota, Eric B. Physical structure of asphaltenes. *Energy fuels* **2005** *19*, 1290-1296.
- (21) Areerat, S.; Funami, E.; Hayata, Y.; Nakagawa, D.; Ohshima, M. Measurement

and prediction of diffusion coefficients of supercritical CO<sub>2</sub> in molten polymers, *Polym. Eng. Sci.* **2004**, *44*, 1915–1924.

- (22) Duda, J. L.; Kimmerly, G. K.; Sigelko, W. L.; Vrentas, J. S. Sorption Apparatus for Diffusion Studies with Molten Polymers, *Ind. Eng. Chem. Fundam.* **1973**, *12*, 133–136.
- (23) Hung, G. W.; Autian, J. Use of thermal gravimetric analysis in sorption studies. II. Evaluation of diffusivity and solubility of a series of aliphatic alcohols in polyurethane, *J. Pharm. Sci.* **1972**, *61*, 1094–1098.
- (24) Yang, C.; Gu, Y. A New Experimental Method for Measuring Gas Diffusivity in Heavy Oil by the Dynamic Pendant Drop Volume Analysis (DPDVA), *Ind. Eng. Chem. Res.* **2005**, *44*, 4474–4483.
- (25) Noorjahan, A.; Tan, X.; Liu, Q.; Gray, M. R.; Choi, P. Study of Cyclohexane Diffusion in Athabasca Asphaltenes, *Energy Fuels* **2014**, *28*, 1004–1011.
- (26) Wen, Y. W.; Kantzas, A. Monitoring Bitumen–Solvent Interactions with Low-Field Nuclear Magnetic Resonance and X-ray Computer-Assisted Tomography, *Energy Fuels* **2005**, *19*, 1319–1326.
- (27) Fadaei, H.; Shaw, J. M.; Sinton, D. Bitumen–Toluene Mutual Diffusion Coefficients Using Microfluidics, *Energy Fuels* **2013**, *27*, 2042–2048.
- (28) Zhang, X.; Fulem, M.; Shaw, J.M. Liquid-Phase Mutual Diffusion Coefficients for Athabasca Bitumen + Pentane Mixtures, *J. Chem. Eng. Data.* **52** (2007) 691–694.
- (29) Zhang, X.; Shaw, J.M. Liquid-phase Mutual Diffusion Coefficients for Heavy Oil + Light Hydrocarbon Mixtures, *Pet. Sci. Technol.* **25** (2007) 773–790.
- (30) Sadighian, A.; Becerra, M.; Bazyleva, A.; Shaw, J. M. Forced and Diffusive Mass

Transfer between Pentane and Athabasca Bitumen Fractions, *Energy Fuels* **2011**, *25*, 782–790.

- (31) Alizadehgiashi, M.; Shaw, J. M. Fickian and non-Fickian diffusion in heavy oil + light hydrocarbon mixtures. *Energy Fuels* **2015**, *29* (4), 2177–2189.
- (32) Bazyleva, A.; Fulem, M.; Becerra, M.; Zhao, B.; Shaw, J. M. *J. Phase Behavior of Athabasca Bitumen*, *Chem. Eng. Data* **2011**, *56*, 3242–3253.
- (33) O.C. Díaz, J. Modaresghazani, M.A. Satyro, H.W. Yarranton, Modeling the phase behavior of heavy oil and solvent mixtures, *Fluid Phase Equilibria*. 304 (2011) 74–85.  
doi:10.1016/j.fluid.2011.02.011.
- (34) M.J. Amani, M.R. Gray, J.M. Shaw, The phase behavior of Athabasca bitumen + toluene + water ternary mixtures, *Fluid Phase Equilibria*. 370 (2014) 75–84.  
doi:10.1016/j.fluid.2014.02.028.
- (35) M.J. Amani, M.R. Gray, J.M. Shaw, Phase behavior of Athabasca bitumen + water mixtures at high temperature and pressure, *J. Supercrit. Fluids*. 77 (2013) 142–152. doi:10.1016/j.supflu.2013.03.007.
- (36) Hahn, K.; Kärger, J.; Kukla, V. Single-File Diffusion Observation, *Phys. Rev. Lett.* **1996**, *76* (15), 2762–2765.
- (37) Wei, Q.-H.; Bechinger, C.; Leiderer, P. Single-File Diffusion of Colloids in One-Dimensional Channels, *Science* **2000**, *287* (5453), 625–627.
- (38) Lutz, C.; Kollmann, M.; Bechinger, C. Single-File Diffusion of Colloids in One-Dimensional Channels, *Phys. Rev. Lett.* **2004**, *93* (2), 026001.

- (39) Keffer, D.; McCormick, A. V.; Davis, H. T. Unidirectional and single-file diffusion in AlPO<sub>4</sub>-5: molecular dynamics investigations, *Mol. Phys.* **1996**, *87* (2), 367–387.
- (40) Kollmann, M. Single-file diffusion of atomic and colloidal systems: Asymptotic laws, *Phys. Rev. Lett.* **2003** *90* (18), 180602.
- (41) Jobic, H.; Hahn, K.; Kärger, J.; Bée, M.; Tuel, A.; Noack, M.; Kearley, G. J. Unidirectional and single-file diffusion of molecules in one-dimensional channel systems. A quasi-elastic neutron scattering study, *J. Phy. Chem. B.* **1997** *101*(30), 5834-5841.
- (42) Khammar, M.; Shaw, J. M. Phase behaviour and phase separation kinetics measurement using acoustic arrays, *Rev. Sci. Instrum.* **2011**, *82*, 104902.
- (43) Pouralhosseini, S.; Alizadehgiashi, M.; Shaw, J.M. On the Phase Behavior of Athabasca Asphaltene + Polystyrene + Toluene Mixtures at 298 K, *Energy Fuels* **2015**.
- (44) NIST Chemistry WebBook. <http://webbook.nist.gov/chemistry/>, (n.d.).
- (45) O'Reilly, D. E.; Peterson, E. M. Self- Diffusion Coefficients and Rotational Correlation Times in Polar Liquids. III. Toluene, *J. Chem. Phys.* 1972, *56*, 2262–2266.
- (46) Long B., Chadakowski M., Shaw J., "Impact of Liquid-Vapor to Liquid-Liquid-Vapor Phase Transitions on Asphaltene-Rich Nanoaggregate Behavior in Athabasca Vacuum Residue + Pentane Mixtures", *Energy & Fuels* 2013, *27*(4) 1779-1790.
- (47) Alizadehgiashi, M.; Shaw, J. M On Fickian and Single File Mutual Diffusion Coefficients in Heavy Oil + Diluent Mixtures (In preparation)



## **4. Concluding Remarks and Future Work**

### **4.1. General Conclusions**

From Chapter 2 one learns that unambiguous identification of Fickian and non-Fickian diffusion mechanisms, and related mutual diffusion/mobility coefficients in sets of free diffusion composition profile data imposes significant constraints on the quality of time, distance and composition measurements, and careful data processing. Control experiments and two composition profile fitting techniques applied to polybutene + toluene and polybutene + toluene + carbon nanotube showed that free diffusion is in principle an appropriate basis for discriminating diffusion behaviors of closely related mixtures and that convective effects play a secondary role even in mixtures with low viscosity. Convective effects do not interfere with the identification of the principal diffusion mechanisms from composition profiles in the literature or obtained in this work. Diffusion at low penetrant mass fractions in nano- and micro -structured hydrocarbon resources, such as Athabasca and Cold Lake bitumen, is shown to be governed by the single file limit, a non-Fickian diffusion mechanism, while at high penetrant mass fraction, diffusion is shown to be governed by Fickian diffusion. The transition from non-Fickian to Fickian diffusion as penetrant is added is shown to be penetrant dependent. The difference in the behavior of n-alkanes and toluene as penetrants is attributed to their respective impacts on asphaltene nano-structure. N-alkanes cause the asphaltene fraction to aggregate and to form micro or macro scale objects. In toluene, the asphaltenes remain nanodispersed. The mixture remains nanostructured at higher penetrant mass fractions in toluene than in n-alkanes and this delays the gradual transition from non-Fickian to

Fickian diffusion. Mixed Fickian and single file diffusion modes of diffusion co-exist at intermediate compositions.

In Chapter 3, sets of composition profiles arising from free diffusion experiments performed as part of this work and composition profiles extracted from the literature were analyzed using a three parameter joint Fickian + Single File mutual diffusion model, based on the approximate solution to the Single File Diffusion equation obtained in appendix A. The parameters included a heavily constrained Fickian mutual diffusion coefficient value, D, a composition and mixture dependent weighting factor for the diffusion mechanisms,  $0 < \gamma < 1$ , and a coefficient H fit to the composition profiles. With these three parameters it was possible to fit all of the sets of composition profiles within the uncertainty of their respective spatial, time, and composition measurements, and to identify composition ranges where the Single File and Fickian mutual diffusion mechanisms dominate. The composition ranges and transition zones identified, and the roles played by asphaltenes and diluents that were identified, enrich the understanding obtained in Chapter 2 and provide a basis for quantitative prediction for mutual diffusion processes in heavy oil and bitumen + diluent mixtures. From the perspective of engineering data, new Fickian mutual diffusion coefficient values showing the impact of temperature were identified for Athabasca bitumen + toluene, and Fickian diffusion coefficients for bitumen and bitumen fraction + diluent mixtures reported in the literature were confirmed. With the exception of one data set, only order of magnitude estimates for single file mobility coefficients in the literature were obtained. Again, it is not clear if this last outcome is an inherent limitation of the experimental and data analysis technique

or if short duration free diffusion experiments, such as those realized in micro fluidics apparatus, can be used as a basis for deriving Single File mobility coefficients.

From appendix A one learns that to go from identification of diffusion mechanisms to evaluation of their relative importance, a solution for the Single File Diffusion equation is needed. Direct analytical solution of the single file diffusion equation to obtain composition profiles and values for the mobility coefficient is shown to be an impractical. An approximate analytical solution based on the known sigmoidal behavior of the normalized composition profile function, and including only one unknown parameter,  $H$ , was introduced. Further, it is shown how mobility coefficient values,  $F$ , are obtained from the derivatives of this composition profile function. The simplest relationship between the fitted parameter  $H$  and the mobility coefficient  $F$  is complex and provides only order of estimates for mobility coefficient values with the possible exception of the very short duration microfluidics measurements. This outcome would appear to be a limitation of the measurement and data analysis method and suggests that new or alternative measurement and data analysis techniques are needed to identify Single File mobility coefficients in this application area more precisely unless the results obtained using the high speed microfluidics approach prove robust.

Current industrial and academic practice is to assume a constant mutual diffusion coefficient values in reservoir applications. These are either imposed in reservoir models or fit to production data. This work suggests that a more fundamental approach would be both inherently predictive robust.

The impacts of these findings on mutual diffusion coefficient evaluation and on industrial applications require additional exploration because it is clear that the time for light hydrocarbons to penetrate a fixed distance into nano- and micro- structured hydrocarbon resources is significantly greater than anticipated based on Fickian diffusion alone.

## **4.2. Future Work**

Future work comprises practical and theoretical elements and possibly the development of new experimental techniques. Clearly identified projects include:

### **1. Investigating mutual diffusion processes at higher temperatures**

The upper temperature, with the acoustic cell, is limited by the thermal stability of the acoustic probes. High temperature measurements would lead to better understanding of the effect of temperature on the relative importance of the two diffusion mechanisms and provide a better link between the phase behaviors of the heavy oil and bitumen + diluent mixtures and diffusion rates.

### **2. The effect of water saturation of solvent on diffusion**

Understanding the effect of water on mutual diffusion processes in heavy oil and bitumen + diluent mixtures, either on mechanisms or rates. This is an open question.

### **3. Diffusion mechanisms in porous media**

Recently Cassiede and Shaw<sup>1</sup>, introduced a 2-dimensional imaging techniques that provides high resolution images of multiphase materials. This new method can be applied to better understand diffusion mechanisms in porous media that, for example, resemble reservoir rock.

**4. Evaluation of the impact of measurement time scale and bulk composition on the stability and quality of Single File mobility value estimates.**

This study arises directly from observations in appendix A.

**5. Development of more robust methods for identifying Single File mobility value estimates.**

This study also arises directly from observations in appendix A.

**6. Development of a practical and predictive joint Fickian-Single File diffusion equation for industrial application**

**4.3. References**

- (1) Cassiède, M., and J. M. Shaw. Non-intrusive, high-resolution, real-time, two-dimensional imaging of multiphase materials using acoustic array sensors. *Review of Scientific Instruments* 86.4 (2015): 044902.

# Bibliography

- (1) R.B. Bird, W.E. Stewart, E.N. Lightfoot, *Transport Phenomena*, John Wiley & Sons, 2007.
- (2) J. Crank, *The mathematics of diffusion*, Clarendon Press, 1975.
- (3) A.L. Hodgkin, R.D. Keynes, The potassium permeability of a giant nerve fibre, *J. Physiol.* 128 (1955) 61–88.
- (4) Q.-H. Wei, C. Bechinger, P. Leiderer, Single-File Diffusion of Colloids in One-Dimensional Channels, *Science*. 287 (2000) 625–627. doi:10.1126/science.287.5453.625.
- (5) B. Lin, M. Meron, B. Cui, S.A. Rice, H. Diamant, From Random Walk to Single-File Diffusion, *Phys. Rev. Lett.* 94 (2005) 216001. doi:10.1103/PhysRevLett.94.216001.
- (6) T.G. Mason, Osmotically driven shape-dependent colloidal separations, *Phys. Rev. E*. 66 (2002) 060402. doi:10.1103/PhysRevE.66.060402.
- (7) T. Meersmann, J.W. Logan, R. Simonutti, S. Caldarelli, A. Comotti, P. Sozzani, et al., Exploring Single-File Diffusion in One-Dimensional Nanochannels by Laser-Polarized  $^{129}\text{Xe}$  NMR Spectroscopy, *J. Phys. Chem. A*. 104 (2000) 11665–11670. doi:10.1021/jp002322v.
- (8) A.E. Kamholz, B.H. Weigl, B.A. Finlayson, P. Yager, Quantitative Analysis of Molecular Interaction in a Microfluidic Channel: The T-Sensor, *Anal. Chem.* 71 (1999) 5340–5347. doi:10.1021/ac990504j.
- (9) A.E. Kamholz, P. Yager, Molecular diffusive scaling laws in pressure-driven microfluidic channels: deviation from one-dimensional Einstein approximations, *Sens. Actuators B Chem.* 82 (2002) 117–121. doi:10.1016/S0925-4005(01)00990-X.

- (10) R.F. Ismagilov, A.D. Stroock, P.J.A. Kenis, G. Whitesides, H.A. Stone, Experimental and theoretical scaling laws for transverse diffusive broadening in two-phase laminar flows in microchannels, *Appl. Phys. Lett.* 76 (2000) 2376–2378. doi:10.1063/1.126351.
- (11) X. Zhang, M. Fulem, J.M. Shaw, Liquid-Phase Mutual Diffusion Coefficients for Athabasca Bitumen + Pentane Mixtures, *J. Chem. Eng. Data.* 52 (2007) 691–694. doi:10.1021/je060234j.
- (12) X. Zhang, J.M. Shaw, Liquid-phase Mutual Diffusion Coefficients for Heavy Oil + Light Hydrocarbon Mixtures, *Pet. Sci. Technol.* 25 (2007) 773–790. doi:10.1080/10916460500411796.
- (13) H. Fadaei, J.M. Shaw, D. Sinton, Bitumen–Toluene Mutual Diffusion Coefficients Using Microfluidics, *Energy Fuels.* 27 (2013) 2042–2048. doi:10.1021/ef400027t.
- (14) A. Sadighian, M. Becerra, A. Bazyleva, J.M. Shaw, Forced and Diffusive Mass Transfer between Pentane and Athabasca Bitumen Fractions, *Energy Fuels.* 25 (2011) 782–790. doi:10.1021/ef101435r.
- (15) Y.W. Wen, A. Kantzas, Monitoring Bitumen–Solvent Interactions with Low-Field Nuclear Magnetic Resonance and X-ray Computer-Assisted Tomography†, *Energy Fuels.* 19 (2005) 1319–1326. doi:10.1021/ef049764g.
- (16) A. Bazyleva, M. Fulem, M. Becerra, B. Zhao, J.M. Shaw, Phase Behavior of Athabasca Bitumen, *J. Chem. Eng. Data.* 56 (2011) 3242–3253. doi:10.1021/je200355f.

- (17) M. Fulem, M. Becerra, M.D.A. Hasan, B. Zhao, J.M. Shaw, Phase behaviour of Maya crude oil based on calorimetry and rheometry, *Fluid Phase Equilibria.* 272 (2008) 32–41. doi:10.1016/j.fluid.2008.06.005.
- (18) B. Zhao, J.M. Shaw, Composition and Size Distribution of Coherent Nanostructures in Athabasca Bitumen and Maya Crude Oil, *Energy Fuels.* 21 (2007) 2795–2804. doi:10.1021/ef070119u.
- (19) A. Bazyleva, M. Becerra, D. Stratiychuk-Dear, J.M. Shaw, Phase behavior of Safaniya vacuum residue, *Fluid Phase Equilibria.* 380 (2014) 28–38. doi:10.1016/j.fluid.2014.07.037.
- (20) O.C. Díaz, J. Modaresghazani, M.A. Satyro, H.W. Yarranton, Modeling the phase behavior of heavy oil and solvent mixtures, *Fluid Phase Equilibria.* 304 (2011) 74–85. doi:10.1016/j.fluid.2011.02.011.
- (21) M.J. Amani, M.R. Gray, J.M. Shaw, The phase behavior of Athabasca bitumen + toluene + water ternary mixtures, *Fluid Phase Equilibria.* 370 (2014) 75–84. doi:10.1016/j.fluid.2014.02.028.
- (22) M.J. Amani, M.R. Gray, J.M. Shaw, Phase behavior of Athabasca bitumen + water mixtures at high temperature and pressure, *J. Supercrit. Fluids.* 77 (2013) 142–152. doi:10.1016/j.supflu.2013.03.007.
- (23) S.R. Bagheri, A. Bazyleva, M.R. Gray, W.C. McCaffrey, J.M. Shaw, Observation of Liquid Crystals in Heavy Petroleum Fractions, *Energy Fuels.* 24 (2010) 4327–4332. doi:10.1021/ef100376t.

- (24) S.R. Bagheri, B. Masik, P. Arboleda, Q. Wen, K.H. Michaelian, J.M. Shaw, Physical Properties of Liquid Crystals in Athabasca Bitumen Fractions, *Energy Fuels.* 26 (2012) 4978–4987. doi:10.1021/ef300339v.
- (25) K. Nikooyeh, S.R. Bagheri, J.M. Shaw, Interactions Between Athabasca Pentane Asphaltenes and n-Alkanes at Low Concentrations, *Energy Fuels.* 26 (2012) 1756–1766. doi:10.1021/ef201845a.
- (26) N. Saber, X. Zhang, X.-Y. Zou, J.M. Shaw, Simulation of the phase behaviour of Athabasca vacuum residue + n-alkane mixtures, *Fluid Phase Equilibria.* 313 (2012) 25–31. doi:10.1016/j.fluid.2011.09.038.
- (27) N. Saber, J.M. Shaw, On the phase behaviour of Athabasca vacuum residue + n-decane, *Fluid Phase Equilibria.* 302 (2011) 254–259. doi:10.1016/j.fluid.2010.09.038.
- (28) N. Saber, J.M. Shaw, Toward multiphase equilibrium prediction for ill-defined asymmetric hydrocarbon mixtures, *Fluid Phase Equilibria.* 285 (2009) 73–82. doi:10.1016/j.fluid.2009.07.014.
- (29) R. Stewart, C.V. Wood, S.J. Murowchuk, J.M. Shaw, Phase Order Inversion During Heavy Oil and Bitumen Production with Solvent Addition, *Energy Fuels.* (2014). doi:10.1021/ef500723e.
- (30) A. Shah, R. Fishwick, J. Wood, G. Leeke, S. Rigby, M. Greaves, A review of novel techniques for heavy oil and bitumen extraction and upgrading, *Energy Environ. Sci.* 3 (2010) 700–714. doi:10.1039/B918960B.
- (31) W.S. Cleveland, Robust Locally Weighted Regression and Smoothing Scatterplots, *J. Am. Stat. Assoc.* 74 (1979) 829–836. doi:10.1080/01621459.1979.10481038.

- (32) M. Khammar, J.M. Shaw, Phase behaviour and phase separation kinetics measurement using acoustic arrays, *Rev. Sci. Instrum.* 82 (2011) 104902. doi:10.1063/1.3650767.
- (33) NIST Chemistry WebBook. <http://webbook.nist.gov/chemistry/>, (n.d.).
- (34) A.B. Bazyleva, M.A. Hasan, M. Fulem, M. Becerra, J.M. Shaw, Bitumen and Heavy Oil Rheological Properties: Reconciliation with Viscosity Measurements, *J. Chem. Eng. Data.* 55 (2010) 1389–1397. doi:10.1021/je900562u.
- (35) J.G. Guan, M. Kariznovi, H. Nourozieh, J. Abedi, Density and Viscosity for Mixtures of Athabasca Bitumen and Aromatic Solvents, *J. Chem. Eng. Data.* 58 (2013) 611–624. doi:10.1021/je3010722.
- (36) G. Centeno, G. Sánchez-Reyna, J. Ancheyta, J.A.D. Muñoz, N. Cardona, Testing various mixing rules for calculation of viscosity of petroleum blends, *Fuel.* 90 (2011) 3561–3570. doi:10.1016/j.fuel.2011.02.028.
- (37) Amundarain, Jesus, Chadakowski, Martin, Long, Bingwen, Shaw, J.M., Characterization of Physically and Chemically Separated Athabasca Asphaltenes Using Small-Angle Scattering, *Energy & Fuels* 2011, 25(11) 5100-5122.
- (38) Long B., Chadakowski M., Shaw J., "Impact of Liquid-Vapor to Liquid-Liquid-Vapor Phase Transitions on Asphaltene-Rich Nanoaggregate Behavior in Athabasca Vacuum Residue + Pentane Mixtures", *Energy & Fuels* 2013, 27(4) 1779-1790.  
*Sci.* **2010**, 3, 700–714.
- (39) Pourmohammadbagher, A; Shaw, J.M. On probing contaminant transport to and from clay surfaces in organic solvents and water using solution calorimetry *Env Sci Tech*, in press 2015.

- (40) Branco, V. A. M.; Mansoori, G. A.; De Almeida Xavier, L. C.; Park, S. J.; Manafi, H. Asphaltene flocculation and collapse from petroleum fluids, *J.Pet. Sci. Eng.* **2001**, *32*, 217–230.
- (41) Murgich, J.; Strausz, O. P. Molecular mechanics of aggregates of asphaltenes and resins of the Athabasca oil, *Pet. Sci. Technol.* **2001**, *19*, 231–243.
- (42) Yarranton, H. W. Asphaltene Self- Association, *J.Dispers. Sci. Technol.* **2005**, *26*, 5–8.
- (43) Andreatta, G.; Bostrom, N.; Mullins, O. C. High-*Q* Ultrasonic Determination of the Critical Nanoaggregate Concentration of Asphaltenes and the Critical Micelle Concentration of Standard Surfactants, *Langmuir* **2005**, *21*, 2728–2736.
- (44) Mostowfi, F.; Indo, K.; Mullins, O. C.; McFarlane, R. Asphaltene Nanoaggregates Studied by Centrifugation, *Energy Fuels* **2009**, *23*, 1194–1200.
- (45) Takeshige, W. Hydrodynamic Shape and Size of Khafji Asphaltene in Benzene, *J.Colloid Interface Sci.* **2001**, *234*, 261–268.
- (46) Sheu, E. Y. Petroleum Asphaltene-Properties, Characterization, and Issues, *Energy Fuels* **2002**, *16*, 74–82.
- (47) Hasan, M. A.; Fulem, M.; Bazyleva, A.; Shaw, J. M. Rheological Properties of Nanofiltered Athabasca Bitumen and Maya Crude Oil, *Energy Fuels* **2009**, *23*, 5012–5021.
- (48) Bouhadda, Y.; Bendedouch, D.; Sheu, E.; Krallafa, A. Some Preliminary Results on a Physico-Chemical Characterization of a Hassi Messaoud Petroleum Asphaltene, *Energy Fuels* **2000**, *14*, 845–853.
- (49) Lorenz, P. B.; Bolen, R. J.; Dunning, H. N.; Eldib, I. A. Ultracentrifugation and

- viscosities of crude oils, *J. Colloid Sci.* **1961**, *16*, 493–496.
- (50) Gawrys, K. L.; Kilpatrick, P. K. Asphaltenic aggregates are polydisperse oblate cylinders, *J. Colloid Interface Sci.* **2005**, *288*, 325–334.
- (51) Sirota, Eric B. Physical structure of asphaltenes. *Energy fuels* **2005**, *19*, 1290–1296.
- (52) Areerat, S.; Funami, E.; Hayata, Y.; Nakagawa, D.; Ohshima, M. Measurement and prediction of diffusion coefficients of supercritical CO<sub>2</sub> in molten polymers, *Polym. Eng. Sci.* **2004**, *44*, 1915–1924.
- (53) Duda, J. L.; Kimmerly, G. K.; Sigelko, W. L.; Vrentas, J. S. Sorption Apparatus for Diffusion Studies with Molten Polymers, *Ind. Eng. Chem. Fundam.* **1973**, *12*, 133–136.
- (54) Hung, G. W.; Autian, J. Use of thermal gravimetric analysis in sorption studies. II. Evaluation of diffusivity and solubility of a series of aliphatic alcohols in polyurethane, *J. Pharm. Sci.* **1972**, *61*, 1094–1098.
- (55) Yang, C.; Gu, Y. A New Experimental Method for Measuring Gas Diffusivity in Heavy Oil by the Dynamic Pendant Drop Volume Analysis (DPDVA), *Ind. Eng. Chem. Res.* **2005**, *44*, 4474–4483.
- (56) Noorjahan, A.; Tan, X.; Liu, Q.; Gray, M. R.; Choi, P. Study of Cyclohexane Diffusion in Athabasca Asphaltenes, *Energy Fuels* **2014**, *28*, 1004–1011.
- (57) Alizadehgiashi, M.; Shaw, J. M. Fickian and non-Fickian diffusion in heavy oil + light hydrocarbon mixtures. *Energy Fuels* **2015**, *29* (4), 2177–2189.
- (58) Hahn, K.; Kärger, J.; Kukla, V. Single-File Diffusion Observation, *Phys. Rev. Lett.* **1996**, *76* (15), 2762–2765.

- (59) Lutz, C.; Kollmann, M.; Bechinger, C. Single-File Diffusion of Colloids in One-Dimensional Channels, *Phys. Rev. Lett.* **2004**, *93* (2), 026001.
- (60) Keffer, D.; McCormick, A. V.; Davis, H. T. Unidirectional and single-file diffusion in AlPO<sub>4</sub>-5: molecular dynamics investigations, *Mol. Phys.* **1996**, *87* (2), 367–387.
- (61) Kollmann, M. Single-file diffusion of atomic and colloidal systems: Asymptotic laws, *Phys. Rev. Lett.* **2003** *90* (18), 180602.
- (62) Jobic, H.; Hahn, K.; Kärger, J.; Bée, M.; Tuel, A.; Noack, M.; Kearley, G. J. Unidirectional and single-file diffusion of molecules in one-dimensional channel systems. A quasi-elastic neutron scattering study, *J. Phy. Chem. B.* **1997** *101*(30), 5834-5841.
- (63) Pouralhosseini, S.; Alizadehgiashi, M.; Shaw, J.M. On the Phase Behavior of Athabasca Asphaltene + Polystyrene + Toluene Mixtures at 298 K, *Energy Fuels* **2015**.
- (64) O'Reilly, D. E.; Peterson, E. M. Self- Diffusion Coefficients and Rotational Correlation Times in Polar Liquids. III. Toluene, *J. Chem. Phys.* **1972**, *56*, 2262–2266.
- (65) Alizadehgiashi, M.; Shaw, J. M On Fickian and Single File Mutual Diffusion Coefficients in Heavy Oil + Diluent Mixtures (In preparation)
- (66) Cassiède, M., and J. M. Shaw. Non-intrusive, high-resolution, real-time, two-dimensional imaging of multiphase materials using acoustic array sensors. Review of Scientific Instruments **86**.4 (2015): 044902.

# Appendix

## A. Single File Diffusion Equation Solution

### A.1. Introduction

Complex numerical solutions for the Single File Diffusion equation permitting derivation of mobility coefficients from data where only this mechanism arises are available<sup>1-5</sup>.

These solutions are not viable in this work because Fickian and Single File diffusion are expected to arise concurrently. An approximate analytical solution is needed to facilitate interpretation of composition profiles. In this chapter approaches are evaluated and a method is proposed.

### A.2. Theory

The general equation for single file diffusion:

$$\frac{\partial C}{\partial t} = F \frac{\partial^4 C}{\partial x^4} \quad (A.2 - 1)$$

can be solved using joint variables of the form:

$$U = \frac{x^n}{t^{n/4}} \quad (A.2 - 2)$$

where  $n$  is an integer.

From the perspective of the mechanism for diffusion, only the power ratio is “known” and the solution to the single file diffusion equation (A.2-1) is dependent on the value of  $n$  chosen as this affects the degree of the partial derivatives of (A.2-1) with respect to  $x$

that are non-zero. If  $n = 1$ , the second derivative values are zero, if  $n = 2$  then the third derivative is zero and so on.

The general solution to (A.2-1) using a joint variable of the form (A.2-2) follows:

The left side of (A.2-1) can be expanded using the chain rule:

$$\frac{\partial C}{\partial t} = \frac{dC}{dU} \times \frac{\partial U}{\partial t} \quad (A. 2 - 3)$$

Expansion of the right side of (A.2-1) requires more attention and multiple applications of the chain rule. Application of the Fa  di Bruno formula yields:

$$\frac{\partial C}{\partial x} = \frac{dC}{dU} \times \frac{\partial U}{\partial x} \quad (A. 2 - 4)$$

$$\frac{\partial^2 C}{\partial x^2} = \frac{\partial}{\partial x} \left( \left( \frac{dC}{dU} \right) \left( \frac{\partial U}{\partial x} \right) \right) \quad (A. 2 - 5)$$

$$\frac{\partial^2 C}{\partial x^2} = \left( \frac{\partial}{\partial x} \left( \frac{dC}{dU} \right) \left( \frac{\partial U}{\partial x} \right) \right) + \left( \left( \frac{dC}{dU} \right) \left( \frac{\partial}{\partial x} \left( \frac{\partial U}{\partial x} \right) \right) \right) \quad (A. 2 - 6)$$

$$\frac{\partial^2 C}{\partial x^2} = \left( \left( \frac{\partial^2 C}{\partial x \partial U} \right) \left( \frac{\partial U}{\partial x} \right) \right) + \left( \left( \frac{dC}{dU} \right) \left( \frac{\partial^2 U}{\partial x^2} \right) \right) \quad (A. 2 - 7)$$

$$\frac{\partial^2 C}{\partial x^2} = \left( \frac{\partial^2 C}{\partial U^2} \right) \left( \frac{\partial U}{\partial x} \right)^2 + \left( \frac{dC}{dU} \right) \left( \frac{\partial^2 U}{\partial x^2} \right) \quad (A.2)$$

- 8)

$$\frac{\partial^3 C}{\partial x^3} = \left( \frac{d^3 C}{dU^3} \right) \left( \frac{\partial U}{\partial x} \right)^3 + 3 \left( \frac{d^2 C}{dU^2} \right) \left( \frac{\partial U}{\partial x} \right) \left( \frac{\partial^2 U}{\partial x^2} \right) + \left( \frac{dC}{dU} \right) \left( \frac{\partial^3 U}{\partial x^3} \right) \quad (A.2)$$

- 9)

and finally one obtains:

$$\begin{aligned} \frac{\partial^4 C}{\partial x^4} &= \left( \frac{d^4 C}{dU^4} \right) \left( \frac{\partial U}{\partial x} \right)^4 + 6 \left( \frac{d^3 C}{dU^3} \right) \left( \frac{\partial U}{\partial x} \right)^2 \left( \frac{\partial^2 U}{\partial x^2} \right) \\ &+ \left( \frac{d^2 C}{dU^2} \right) \left[ 4 \left( \frac{\partial U}{\partial x} \right) \left( \frac{\partial^3 U}{\partial x^3} \right) + 3 \left( \frac{\partial^2 U}{\partial x^2} \right)^2 \right] + \left( \frac{dC}{dU} \right) \left( \frac{\partial^4 U}{\partial x^4} \right) \end{aligned} \quad (A.2)$$

- 10)

Substituting (A.2-3) and (A.2-10) into (A.2-1):

$$\begin{aligned} \frac{dC}{dU} \times \frac{\partial U}{\partial t} &= F \left\{ \left( \frac{d^4 C}{dU^4} \right) \left( \frac{\partial U}{\partial x} \right)^4 + 6 \left( \frac{d^3 C}{dU^3} \right) \left( \frac{\partial U}{\partial x} \right)^2 \left( \frac{\partial^2 U}{\partial x^2} \right) \right. \\ &\left. + \left( \frac{d^2 C}{dU^2} \right) \left[ 4 \left( \frac{\partial U}{\partial x} \right) \left( \frac{\partial^3 U}{\partial x^3} \right) + 3 \left( \frac{\partial^2 U}{\partial x^2} \right)^2 \right] + \left( \frac{dC}{dU} \right) \left( \frac{\partial^4 U}{\partial x^4} \right) \right\} \end{aligned} \quad (A.2)$$

- 11)

The impact of the selection of the power of  $n$  in (A.2-2) becomes apparent. For values of  $n \geq 4$  all terms in (A.2-11) are active. For  $n = 3$ ,  $n = 2$  and  $n = 1$ , fourth, third and second partial derivatives of  $U$  with respect to distance,  $x$ , are zero and (A.2-11) simplifies.

### For $n = 1$

$$\frac{dU}{dx} = \frac{1}{t^{\frac{1}{4}}} \text{ and } \frac{dU}{dt} = -\frac{1}{4} \frac{x}{t^{\frac{5}{4}}} \quad (A.2-12)$$

$$\frac{\partial C}{\partial U} \times \left( -\frac{1}{4} \frac{x}{t^{\frac{5}{4}}} \right) = F \left\{ \frac{\partial^4 C}{\partial U^4} \left( \frac{1}{t^{\frac{1}{4}}} \right)^4 \right\} \quad (A.2-13)$$

One obtains a much simpler equation

$$0 = F \left\{ \left( \frac{4}{U} \right) \frac{\partial^4 C}{\partial U^4} \right\} + \frac{dC}{dU} \quad (A.2-14)$$

Equation (A.2-14) possesses a somewhat different functional form than (A.2-11).

Comparable differences arise for solutions based on other values of  $n$ , and the solutions

are not subsets of one another and the general solution of (A.2-1) includes the sum of the infinite series of solutions obtained for all positive integer values of  $n$ .

Given the geometry and boundary conditions of the one dimensional free diffusion equation where the coordinate system possesses positive and negative values of  $x$  with differing values of composition, odd values of  $n$  are preferred because the boundary conditions associated with (A.2-1) can then be expressed as:

$$\begin{cases} U = +\infty \rightarrow C(U) = 1 \\ U = -\infty \rightarrow C(U) = 0 \\ U = +\infty \rightarrow \frac{\partial C}{\partial U} = 0 \\ U = -\infty \rightarrow \frac{\partial C}{\partial U} = 0 \end{cases}$$

The simplest joint variable expression equivalent to (A.2-1) is (A.2-14). Solution of (A.2-14) using Maple<sup>6</sup> and Mathematica<sup>7</sup> with these boundary conditions, and the composition at  $x=0$  (the cross over point), yields:

$$\begin{aligned} C(U) &= A_1 + A_2 \cdot U \cdot \text{hypergeom}\left(\left[\frac{1}{4}\right], \left[\frac{1}{2}, \frac{3}{4}, \frac{4}{5}\right], -\frac{1}{256} \frac{U^4}{F}\right) \\ &\quad + A_3 \cdot U^2 \cdot \text{hypergeom}\left(\left[\frac{1}{2}\right], \left[\frac{3}{4}, \frac{5}{4}, \frac{3}{2}\right], -\frac{1}{256} \frac{U^4}{F}\right) \\ &\quad + A_4 \cdot U^3 \cdot \text{hypergeom}\left(\left[\frac{3}{4}\right], \left[\frac{5}{4}, \frac{3}{2}, \frac{7}{4}\right], -\frac{1}{256} \frac{U^4}{F}\right) \quad (A.2 \\ &\quad - 15) \end{aligned}$$

Hypergeometric functions have the forms shown in Figure A.1.

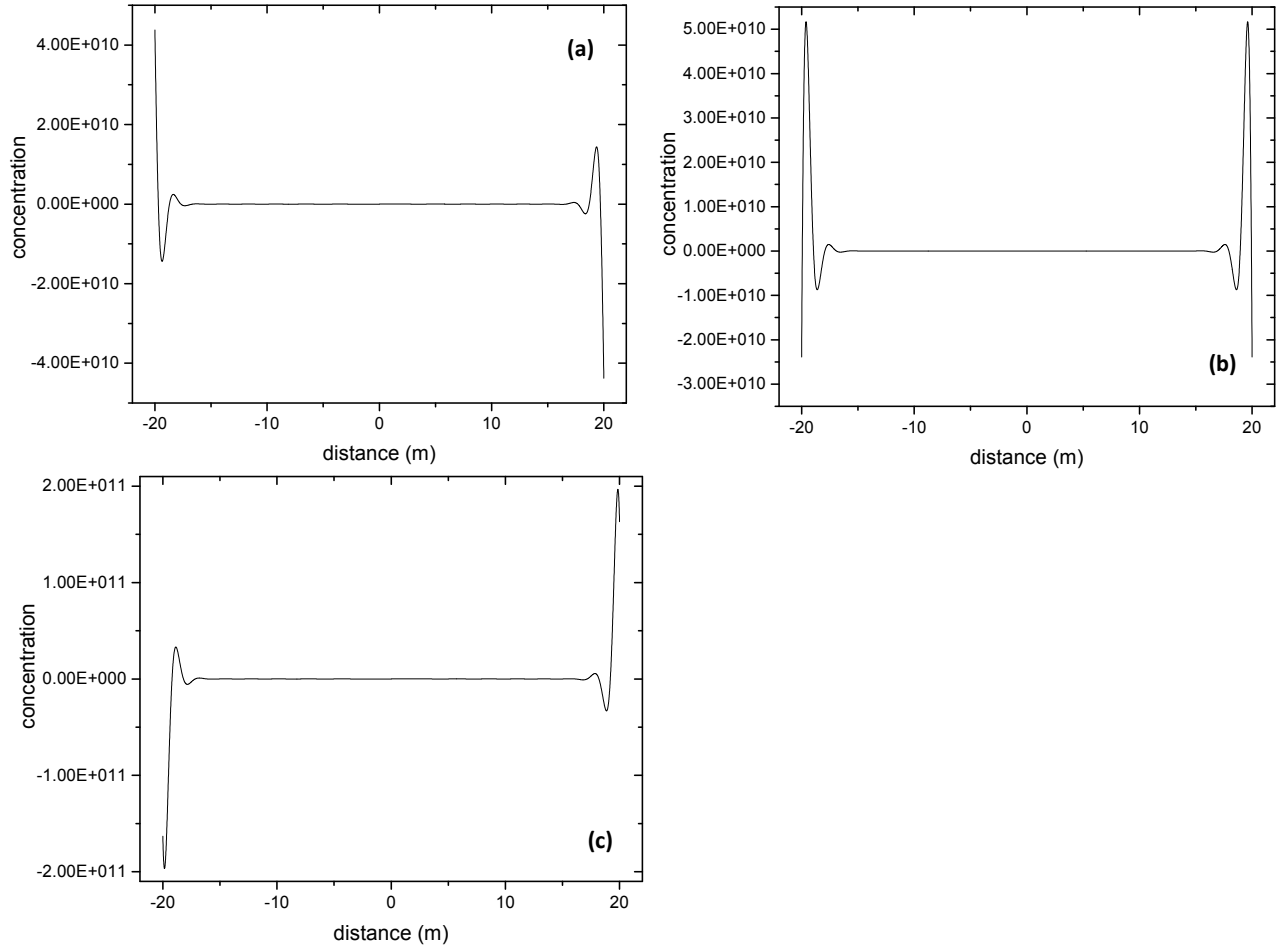


**Figure A.1.** Hypergeometric terms in the solution of equation A.2-15: a) term 2, b) term 3 and c) term 4.

**For  $n = 2$ :**

$$\frac{dU}{dx} = 2 \frac{x}{t^{\frac{1}{2}}}, \frac{d^2U}{dx^2} = \frac{2}{t^{\frac{1}{2}}} \text{ and } \frac{dU}{dt} = -\frac{1}{2} \frac{x^2}{t^{\frac{3}{2}}} \quad (A.2-16)$$

On substitution into (A.2-11):

$$\begin{aligned} \frac{dC}{dU} &\times \left( -\frac{1}{2} \frac{x^2}{t^{\frac{3}{2}}} \right) \\ &= F \left\{ \left( \frac{d^4C}{dU^4} \right) \left( 2 \frac{x}{t^{\frac{1}{2}}} \right)^4 + 6 \left( \frac{d^3C}{dU^3} \right) \left( 2 \frac{x}{t^{\frac{1}{2}}} \right)^2 \left( \frac{2}{t^{\frac{1}{2}}} \right) \right. \\ &\quad \left. + \left( \frac{d^2C}{dU^2} \right) \left[ \frac{12}{t} \right] \right\} \end{aligned} \quad (A.2-17)$$

$$\frac{dC}{dU} = F \left\{ \frac{d^4C}{dU^4} (-32U) + (-96) \frac{d^3C}{dU^3} + \left( \frac{d^2C}{dU^2} \right) \left[ \frac{-24t^{\frac{1}{2}}}{x^2} \right] \right\} \quad (A.2-18)$$

$$\frac{dC}{dU} = F \left\{ (-32U) \frac{d^4C}{dU^4} + (-96) \frac{d^3C}{dU^3} + \frac{d^2C}{dU^2} \left( -\frac{24}{U} \right) \right\} \quad (A.2-19)$$

One obtains:

$$0 = F \left\{ (32U) \frac{d^4C}{dU^4} + (96) \frac{d^3C}{dU^3} + \frac{d^2C}{dU^2} \left( \frac{24}{U} \right) \right\} + \frac{dC}{dU} \quad (A.2-20)$$

Using Maple and Mathematica:

$$\begin{aligned}
C(U) = & A_1 + A_2 \cdot U \cdot \text{hypergeom} \left( \left[ \frac{1}{2} \right], \left[ \frac{3}{4}, \frac{5}{4}, \frac{3}{2} \right], -\frac{1}{256} \frac{U^2}{F} \right) \\
& + A_3 \cdot U^{\frac{1}{2}} \text{hypergeom} \left( \left[ \frac{1}{4} \right], \left[ \frac{1}{2}, \frac{3}{4}, \frac{5}{4} \right], -\frac{1}{256} \frac{U^2}{F} \right) \\
& + A_4 \cdot U^{\frac{3}{2}} \cdot \text{hypergeom} \left( \left[ \frac{3}{4} \right], \left[ \frac{5}{4}, \frac{3}{2}, \frac{7}{4} \right], -\frac{1}{256} \frac{U^2}{F} \right)
\end{aligned} \tag{A.2 - 21}$$

For  $n = 3$

$$\frac{dU}{dx} = 3 \frac{x^2}{t^{\frac{3}{4}}} \text{ and } \frac{d^2U}{dx^2} = 6 \frac{x}{t^{\frac{3}{4}}} \text{ and } \frac{d^3U}{dx^3} = 6 \frac{1}{t^{\frac{3}{4}}} \text{ and } \frac{dU}{dt} = -\frac{3}{4} \frac{x^3}{t^{\frac{7}{4}}} \tag{A.2 - 22}$$

$$\begin{aligned}
\frac{dC}{dU} \times & \left( -\frac{3}{4} \frac{x^3}{t^{\frac{7}{4}}} \right) \\
= & F \left\{ \left( \frac{d^4C}{dU^4} \right) \left( 3 \frac{x^2}{t^{\frac{3}{4}}} \right)^4 + 6 \left( \frac{d^3C}{dU^3} \right) \left( 3 \frac{x^2}{t^{\frac{3}{4}}} \right)^2 \left( 6 \frac{x}{t^{\frac{3}{4}}} \right) \right. \\
& \left. + \left( \frac{d^2C}{dU^2} \right) \left[ 4 \left( 3 \frac{x^2}{t^{\frac{3}{4}}} \right) \left( 6 \frac{1}{t^{\frac{3}{4}}} \right) + 3 \left( 6 \frac{x}{t^{\frac{3}{4}}} \right)^2 \right] \right\}
\end{aligned} \tag{A.2 - 23}$$

$$\begin{aligned}
\frac{dC}{dU} + F \left\{ \left( \frac{d^4C}{dU^4} \right) (108 U^{\frac{5}{3}}) + 432 \left( \frac{d^3C}{dU^3} \right) \left( U^{\frac{3}{2}} \right) + 240 \left( \frac{d^2C}{dU^2} \right) \left( \frac{1}{U^{\frac{1}{3}}} \right) \right\} \\
= 0
\end{aligned} \tag{A.2 - 24}$$

Using the Maple and Mathematica:

$$\begin{aligned}
C(U) = & A_1 + A_2 \cdot U \cdot {}_{hypergeom} \left( \left[ \frac{1}{2} \right], \left[ \frac{3}{4}, \frac{5}{4}, \frac{3}{2} \right], -\frac{1}{256} \frac{U^2}{F} \right) \\
& + A_3 \cdot U^{\frac{1}{2}} \cdot {}_{hypergeom} \left( \left[ \frac{1}{4} \right], \left[ \frac{1}{2}, \frac{3}{4}, \frac{5}{4} \right], -\frac{1}{256} \frac{U^2}{F} \right) \\
& + A_4 \cdot U^{\frac{3}{2}} \cdot {}_{hypergeom} \left( \left[ \frac{3}{4} \right], \left[ \frac{5}{4}, \frac{3}{2}, \frac{7}{4} \right], -\frac{1}{256} \frac{U^2}{F} \right) \quad (A.2) \\
& - 25)
\end{aligned}$$

For  **$n = 4$**

$$\begin{aligned}
\frac{dU}{dx} = & 4 \frac{x^3}{t} \text{ and } \frac{d^2U}{dx^2} = 12 \frac{x^2}{t} \text{ and } \frac{d^3U}{dx^3} = 24 \frac{x}{t} \text{ and } \frac{d^4U}{dx^4} = 24 \frac{1}{t} \text{ and } \frac{dU}{dt} \\
= & -\frac{x^4}{t^2} \quad (A.2 - 26)
\end{aligned}$$

$$\begin{aligned}
\frac{dC}{dU} \times \left( -\frac{x^4}{t^2} \right) = & F \left\{ \left( \frac{d^4C}{dU^4} \right) \left( 4 \frac{x^3}{t} \right)^4 + 6 \left( \frac{d^3C}{dU^3} \right) \left( 4 \frac{x^3}{t} \right)^2 \left( 12 \frac{x^2}{t} \right) \right. \\
& \left. + \left( \frac{d^2C}{dU^2} \right) \left[ 4 \left( 4 \frac{x^3}{t} \right) \left( 24 \frac{x}{t} \right) + 3 \left( 12 \frac{x^2}{t} \right)^2 \right] + \frac{dC}{dU} \left( 24 \frac{1}{t} \right) \right\} \quad (A.2) \\
& - 27)
\end{aligned}$$

$$\begin{aligned}
\frac{dC}{dU} = & F \left\{ -256 \left( \frac{d^4C}{dU^4} \right) \left( \frac{x^8}{t^2} \right) - 1152 \left( \frac{d^3C}{dU^3} \right) \left( \frac{x^4}{t} \right) - \left( \frac{d^2C}{dU^2} \right) [816] \right. \\
& \left. - \frac{dC}{dU} \left( 24 \frac{t}{x^4} \right) \right\} \quad (A.2 - 28)
\end{aligned}$$

$$\frac{dC}{dU} + F \left\{ (256 \times U^2) \left( \frac{d^4 C}{dU^4} \right) + (1152 \times U) \left( \frac{d^3 C}{dU^3} \right) + 816 \left( \frac{d^2 C}{dU^2} \right) + \left( \frac{24}{U} \right) \frac{dC}{dU} \right\} = 0 \quad (A.2 - 29)$$

Using Maple and Mathematica:

$$\begin{aligned} C(U) &= A_1 + A_2 \cdot U^{\frac{1}{2}} \cdot \text{hypergeom} \left( \left[ \frac{1}{2} \right], \left[ \frac{3}{4}, \frac{5}{4}, \frac{3}{2} \right], -\frac{1}{256} \frac{U}{F} \right) \\ &\quad + A_3 \cdot U^{\frac{1}{4}} \cdot \text{hypergeom} \left( \left[ \frac{1}{4} \right], \left[ \frac{1}{2}, \frac{3}{4}, \frac{5}{4} \right], -\frac{1}{256} \frac{U}{F} \right) \\ &\quad + A_4 \cdot U^{\frac{3}{4}} \cdot \text{hypergeom} \left( \left[ \frac{3}{4} \right], \left[ \frac{5}{4}, \frac{3}{2}, \frac{7}{4} \right], -\frac{1}{256} \frac{U}{F} \right) \end{aligned} \quad (A.2 - 30)$$

All of the solutions above for  $n = 1,2,3,4$  comprise discontinuous hypogeometric functions. Thus, an infinite series with potentially innumerable counterbalancing coefficients may be needed to model composition profiles. This approach while preferred theoretically was abandoned. An approximate solution based on the fact that the composition profiles are known to be sigmoidal, that also meets the boundary conditions is presented below.

Using a standard sigmoidal form:

$$C(U) = \frac{A}{B + G \cdot \exp(-H U)} + E \quad (A.2 - 31)$$

$$U = 0 \rightarrow C = C_0 \Rightarrow \left( \frac{A}{B + G} \right) + E = C_0$$

$$U \rightarrow +\infty \rightarrow C = 1 \Rightarrow \frac{A}{B} + E = 1$$

$$U \rightarrow -\infty \rightarrow C = 0 \Rightarrow E = 0$$

Even though the choice of A is arbitrary, A must equal B (from the boundary conditions) and G is proportional to A. Thus A cancels from the numerator and the denominator of the first term on the right hand side of equation A.2-31 and all solutions of are equivalent to:

$$A = B = 1; G = \left( \frac{1}{C_0} - 1 \right)$$

$C_0$  is the time invariant composition at the origin of the coordinate system obtained from each set of free diffusion experiments.

In this approximation, compositions follow C (U) where

$$U = \frac{x}{t^{1/4}}$$

and

$$\frac{dC(U)}{dU} = \frac{H \cdot G \cdot \exp(-H \cdot U)}{[1 + G \cdot \exp(-H \cdot U)]^2} \quad (A.2 - 32)$$

The only unknown, H, is fit to a set of composition profiles simultaneously. As the experimental composition and time measurements possess uncertainty, it is expected that a range of H values will be required to bound the composition profiles in the composition region where the Single File diffusion mechanism dominates. To link values of H to the mobility coefficient, F, equation A.2-32 is substituted into the simplest relationship

described above - equation A.2-14. The terms corresponding to the second, third and fourth derivatives on the right hand side of this equation are expanded as:

$$\begin{aligned}
 & \frac{d^2C}{dU^2} \\
 &= \frac{-H^2 \cdot G \cdot \exp(-H \cdot U) \times [1 + G \cdot \exp(-H \cdot U)]^2}{[1 + G \cdot \exp(-H \cdot U)]^4} \\
 & - \frac{2[1 + G \cdot \exp(-H \cdot U)][-H \cdot G \cdot \exp(-H \cdot U)][H \cdot G \cdot \exp(-H \cdot U)]}{[1 + G \cdot \exp(-H \cdot U)]^4} \quad (A.2 - 33)
 \end{aligned}$$

$$\frac{d^2C}{dU^2} = \frac{H^2 \cdot G^2 \cdot \exp(-2H \cdot U) - H^2 \cdot G \cdot \exp(-H \cdot U)}{[1 + G \cdot \exp(-H \cdot U)]^3} \quad (A.2 - 34)$$

$$\begin{aligned}
 & \frac{d^3C}{dU^3} \\
 &= \frac{[-2H^3 \cdot G^2 \cdot \exp(-H \cdot U) + H^3 \cdot G \cdot \exp(-H \cdot U)] \times [1 + G \cdot \exp(-H \cdot U)]^3}{[1 + G \cdot \exp(-H \cdot U)]^6} \\
 & - \frac{3[1 + G \cdot \exp(-H \cdot U)]^2 [-H \cdot G \cdot \exp(-H \cdot U)][H^2 \cdot G^2 \cdot \exp(-2H \cdot U) - H^2 \cdot G \cdot \exp(-H \cdot U)]}{[1 + G \cdot \exp(-H \cdot U)]^6} \quad (A.2 \\
 & - 35)
 \end{aligned}$$

$$\begin{aligned}
& \frac{d^3 C}{dU^3} \\
&= \frac{[-2H^3 \cdot G^2 \cdot \exp(-H \cdot U) + H^3 \cdot G \cdot \exp(-H \cdot U) - 2H^3 \cdot G^2 \cdot \exp(-3H \cdot U) + H^3 \cdot G^2 \cdot \exp(-2H \cdot U)]}{[1 + G \cdot \exp(-H \cdot U)]^4} \\
&- \frac{[-3H^3 \cdot G^3 \cdot \exp(-3H \cdot U) + 3H^3 \cdot G^2 \cdot \exp(-2H \cdot U)]}{[1 + G \cdot \exp(-H \cdot U)]^4} \\
&- 36) \tag{A.2}
\end{aligned}$$

$$\begin{aligned}
& \frac{d^3 C}{dU^3} = \frac{[H^3 \cdot G \cdot \exp(-H \cdot U) - 4H^3 \cdot G^2 \cdot \exp(-2H \cdot U) + H^3 \cdot G^3 \cdot \exp(-3H \cdot U)]}{[1 + G \cdot \exp(-H \cdot U)]^4} \\
&- 37) \tag{A.2}
\end{aligned}$$

$$\begin{aligned}
& \frac{d^4 C}{dU^4} \\
&= \frac{[-H^4 \cdot G \cdot \exp(-H \cdot U) + 8H^4 \cdot G^2 \cdot \exp(-2H \cdot U) - 3H^4 \cdot G^3 \cdot \exp(-3H \cdot U)][1 + G \cdot \exp(-H \cdot U)]^4}{[1 + G \cdot \exp(-H \cdot U)]^8} \\
&- \frac{4[1 + G \cdot \exp(-H \cdot U)]^3[-H \cdot G \cdot \exp(-H \cdot U)]}{[1 + G \cdot \exp(-H \cdot U)]^8} \\
&\times \frac{[H^3 \cdot G \cdot \exp(-H \cdot U) - 4H^3 \cdot G^2 \cdot \exp(-2H \cdot U) + H^3 \cdot G^3 \cdot \exp(-3H \cdot U)]}{[1 + G \cdot \exp(-H \cdot U)]^8} \\
&- 38) \tag{A.2}
\end{aligned}$$

$$\begin{aligned}
& \frac{d^4 C}{dU^4} \\
&= \frac{[-H^4 \cdot G \cdot \exp(-H \cdot U) + 7H^4 \cdot G^2 \cdot \exp(-2H \cdot U) + 5H^4 \cdot G^3 \cdot \exp(-3H \cdot U) - 3H^4 \cdot G^4 \cdot \exp(-4H \cdot U)]}{[1 + G \cdot \exp(-H \cdot U)]^5} \\
&- \frac{[-4H^4 \cdot G^2 \cdot \exp(-2H \cdot U) + 16H^4 \cdot G^3 \cdot \exp(-3H \cdot U) + H^4 \cdot G^4 \cdot \exp(-4H \cdot U)]}{[1 + G \cdot \exp(-H \cdot U)]^5} \\
&- 39) \tag{A.2}
\end{aligned}$$

$$\frac{d^4 C}{dU^4} = \frac{[-H^4 \cdot G \cdot \exp(-H \cdot U) + 11H^4 \cdot G^2 \cdot \exp(-2H \cdot U) - 11H^4 \cdot G^3 \cdot \exp(-3H \cdot U) + H^4 \cdot G^4 \exp(-H \cdot U)]}{[1 + G \cdot \exp(-H \cdot U)]^5}$$

– 40)

$$\begin{aligned} & \frac{H \cdot G \cdot \exp(-H \cdot U)}{[1 + G \cdot \exp(-H \cdot U)]^2} + 4F \\ & \times \frac{[-H^4 \cdot G \cdot \exp(-H \cdot U) + 11H^4 \cdot G^2 \cdot \exp(-2H \cdot U) - 11H^4 \cdot G^3 \cdot \exp(-3H \cdot U) + H^4 \cdot G^4 \exp(-H \cdot U)]}{U \cdot [1 + G \cdot \exp(-H \cdot U)]^5} \\ & = 0 \quad (A.2 - 41) \end{aligned}$$

Gathering and simplifying terms one obtains:

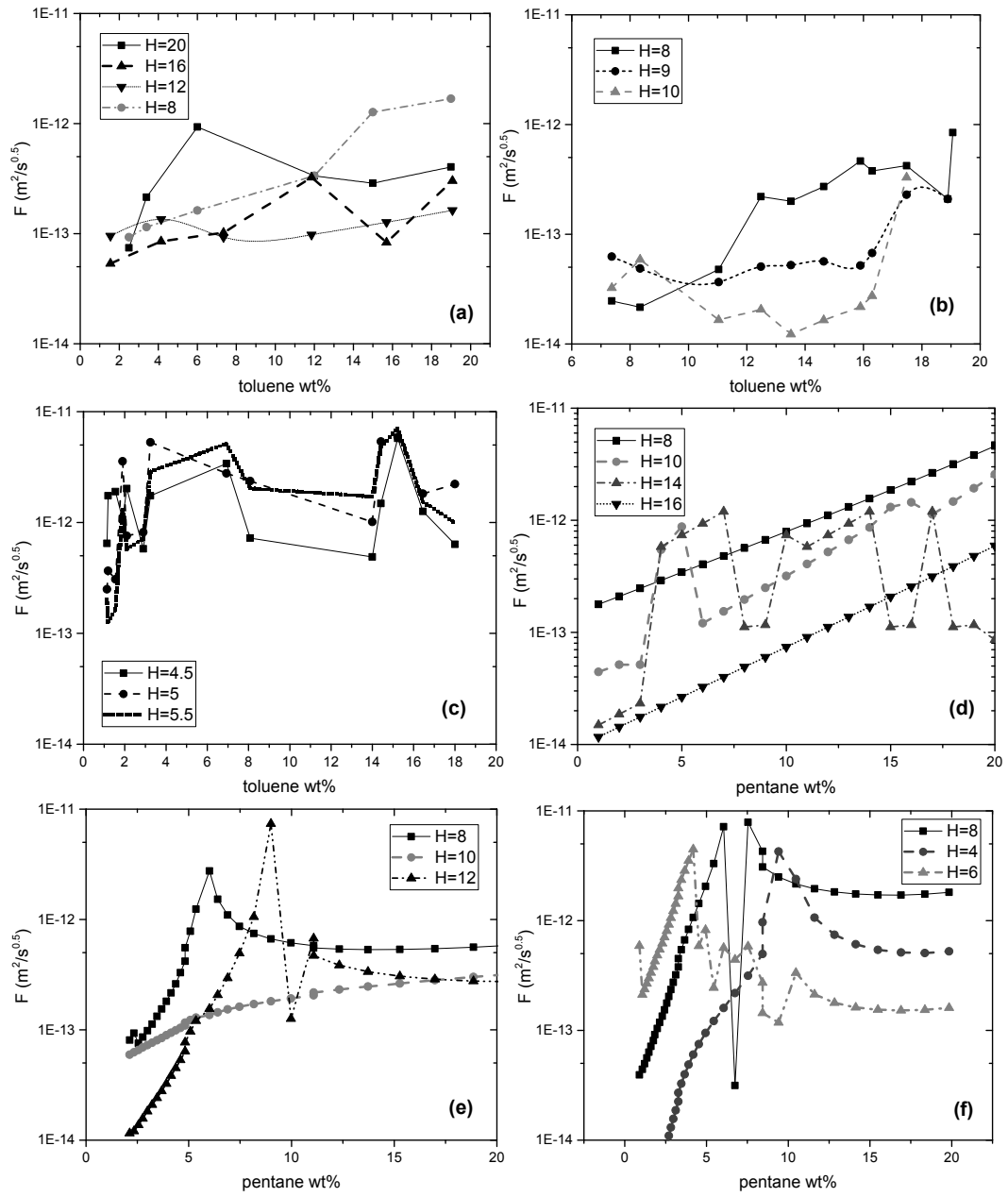
$$\begin{aligned} & H \cdot G \cdot \exp(-H \cdot U) [1 + G \cdot \exp(-H \cdot U)]^3 + 4F \\ & \times [-H^4 \cdot G \cdot \exp(-H \cdot U) \\ & + 11H^4 \cdot G^2 \cdot \exp(-2H \cdot U) - 11H^4 \cdot G^3 \cdot \exp(-3H \cdot U) \\ & + H^4 \cdot G^4 \exp(-H \cdot U)] = 0 \quad (A.2 - 4.2) \end{aligned}$$

The simplest expression linking H and F becomes:

$$\begin{aligned} & F \\ & = -\frac{[H \cdot G \cdot \exp(-H \cdot U) + 3HG^2 \cdot \exp(-2H \cdot U) + 3HG^3 \cdot \exp(-3H \cdot U) + HG^4 \cdot \exp(-4H \cdot U)]}{U \cdot [-4H^4 \cdot G \cdot \exp(-H \cdot U) + 44H^4 \cdot G^2 \cdot \exp(-2H \cdot U) - 44H^4 \cdot G^3 \cdot \exp(-3H \cdot U) + 4H^4 \cdot G^4 \exp(-4H \cdot U)]} \\ & - 43) \end{aligned}$$

Given the complexity of equation A.2-43, variation of F values with composition can be expected, especially because the value of H is uncertain. It is also important to recognize that Fickian Diffusion coefficients, arising from direct fits to composition profiles, and dependent only on first and second derivatives of normalized composition profiles, possess uncertainties of  $\pm 40\%$ <sup>8</sup>. Thus, F values, derived from a coefficients fit to experimental composition profiles, and dependent on first through fourth derivatives of normalized composition profiles are expected to possess significant uncertainty.

Figure A.2 a-h shows the sensitivity of the mobility coefficient values obtained from equation A.2-43 to the values of H that bound the composition profile data sets presented in Chapter 2. At any given composition, values of H with their uncertainty, generate bounded ranges for the mobility coefficient values. In general, only order of magnitude estimates for mobility coefficients are obtained. Only one data set, Figure A.2 g, yields a consistent and stable value with significant precision over a broad composition range,  $F \sim 8 \times 10^{-13}$  ( $m^2/s^{0.5}$ ). For the other data sets, a cloud of mobility coefficient values is obtained that is only loosely correlated with the H value. However, this approach does provide reliable order of magnitude estimates for the mobility coefficient values.



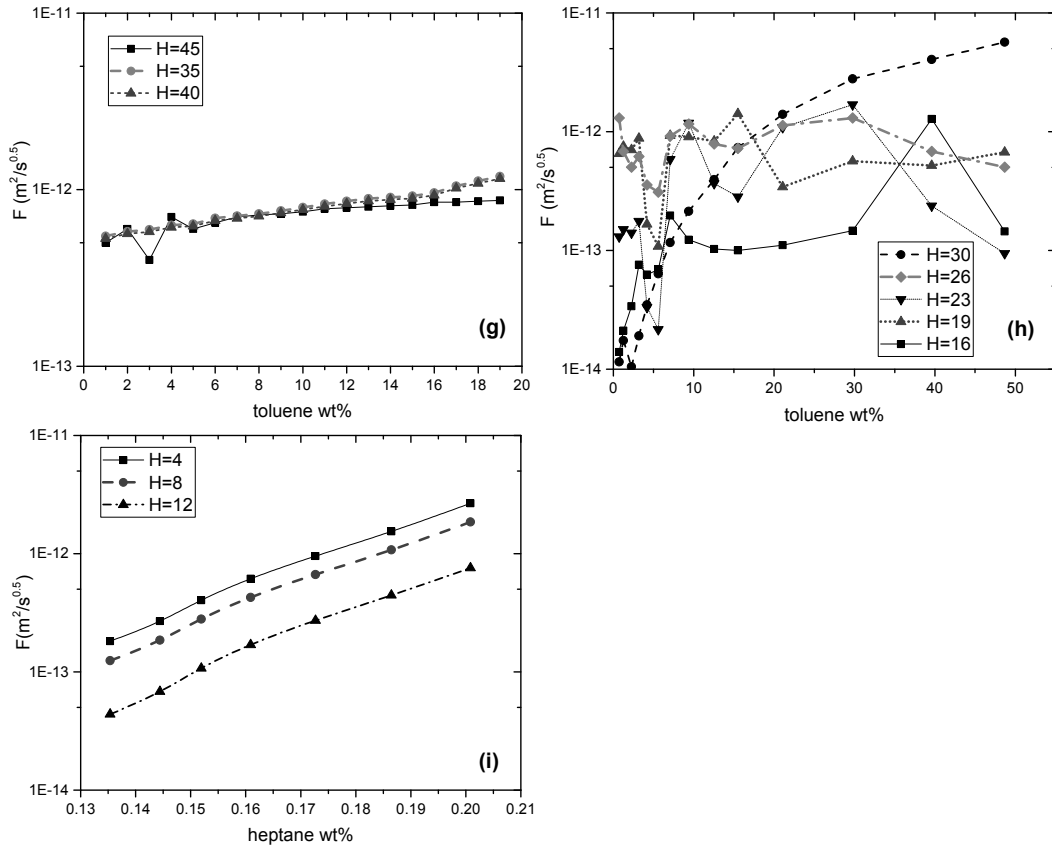


**Figure A.2** Variation of value of calculated  $F$  versus solvent composition profile at different  $H$  values for: a) Athabasca bitumen + toluene at 273 K ( $G=1.5$ ,  $H=16\pm 4 \frac{\text{s}^{0.25}}{\text{m}}$ ), b) Athabasca bitumen + toluene at 298 K ( $G=1.32$ ,  $H=9\pm 1 \frac{\text{s}^{0.25}}{\text{m}}$ ), c) Athabasca bitumen + toluene at 313 K ( $G=1$ ,  $H=5\pm 0.5 \frac{\text{s}^{0.25}}{\text{m}}$ ), d) Athabasca atmospheric residue + pentane<sup>9</sup> ( $G=0.53$ ,  $H=6\pm 3 \frac{\text{s}^{0.25}}{\text{m}}$ ), e) Athabasca vacuum residue + pentane<sup>9</sup> ( $G=0.49$ ,  $H=10\pm 2 \frac{\text{s}^{0.25}}{\text{m}}$ ), f) Athabasca bitumen + pentane<sup>10,11</sup> ( $G=2.33$ ,  $H=6\pm 2 \frac{\text{s}^{0.25}}{\text{m}}$ ), g) Athabasca bitumen + toluene<sup>8</sup> ( $G=1$ ,  $H=40\pm 5 \frac{\text{s}^{0.25}}{\text{m}}$ ), h) Polybutene + CNT + toluene ( $G=0.53$ ,  $H=23\pm 7 \frac{\text{s}^{0.25}}{\text{m}}$ ), i) Cold Lake bitumen + heptane<sup>12</sup> ( $G=0.95$ ,  $H=8\pm 4 \frac{\text{s}^{0.25}}{\text{m}}$ ).

### A.3. Conclusion

Analytical solution of the single file diffusion equation to obtain composition profiles and values for the mobility coefficient is shown to be an impractical. An approximate analytical solution based on the known sigmoidal behavior of the normalized composition profile function, and including only one unknown parameter,  $H$ , is introduced. Further it is shown how mobility coefficient values,  $F$ , are obtained from the derivatives of this composition profile function. The simplest relationship between the fitted parameter  $H$  and the mobility coefficient  $F$  is complex and provides only order of estimates for mobility coefficient values with the exception of the very short duration microfluidics measurements. This outcome would appear to be a limitation of the measurement and data analysis method and suggests that new or alternative measurement and data analysis techniques are needed to identify Single File mobility coefficients in this application area more precisely unless the results obtained using the high speed microfluidics approach prove robust.

### A.4. Reference

- (1) Hahn, K.; Kärger, J.; Kukla, V. Single-File Diffusion Observation, *Phys. Rev. Lett.* **1996**, *76* (15), 2762–2765.
- (2) Wei, Q.-H.; Bechinger, C.; Leiderer, P. Single-File Diffusion of Colloids in One-Dimensional Channels, *Science* **2000**, *287* (5453), 625–627.
- (3) Lutz, C.; Kollmann, M.; Bechinger, C. Single-File Diffusion of Colloids in One-Dimensional Channels, *Phys. Rev. Lett.* **2004**, *93* (2), 026001.

- (4) Keffer, D.; McCormick, A. V.; Davis, H. T. Unidirectional and single-file diffusion in AlPO<sub>4</sub>-5: molecular dynamics investigations, *Mol. Phys.* **1996**, *87* (2), 367–387.
- (5) Jobic, H.; Hahn, K.; Kärger, J.; Bée, M.; Tuel, A.; Noack, M.; Kearley, G. J. Unidirectional and single-file diffusion of molecules in one-dimensional channel systems. A quasi-elastic neutron scattering study, *J. Phys. Chem. B.* **1997** *101*(30), 5834-5841.
- (6) Maple 2014. Maplesoft, a division of Waterloo Maple Inc., Waterloo, Ontario.
- (7) Wolfram Research, Inc., Mathematica, Version 10.0, Champaign, IL (2014).
- (8) Fadaei, H.; Shaw, J. M.; Sinton, D. Bitumen–Toluene Mutual Diffusion Coefficients Using Microfluidics, *Energy Fuels* **2013**, *27*, 2042–2048.
- (9) Sadighian, A.; Becerra, M.; Bazyleva, A.; Shaw, J. M. Forced and Diffusive Mass Transfer between Pentane and Athabasca Bitumen Fractions, *Energy Fuels* **2011**, *25*, 782–790.
- (10) Zhang, X.; Fulem, M.; Shaw, J.M. Liquid-Phase Mutual Diffusion Coefficients for Athabasca Bitumen + Pentane Mixtures, *J. Chem. Eng. Data.* **52** (2007) 691–694.
- (11) Zhang, X.; Shaw, J.M. Liquid-phase Mutual Diffusion Coefficients for Heavy Oil + Light Hydrocarbon Mixtures, *Pet. Sci. Technol.* **25** (2007) 773–790.
- (12) Wen, Y. W.; Kantzas, A. Monitoring Bitumen–Solvent Interactions with Low-Field Nuclear Magnetic Resonance and X-ray Computer-Assisted Tomography, *Energy Fuels* **2005**, *19*, 1319–1326.

## B. MatLab Codes

### B.1. Speed of Sound Data to Concentration

```
clear all
close all
A=xlsread('Experiment 40c.xlsx','72 hour(or any other data set)','G15:G115');
B=xlsread('Cal.xlsx');
[m,n]=size(A);
C=zeros(m,n);
for i=1:11
c(i,1)=(i-1)*10;
end
for i=1:11

if i<11
for j=1:99
if A(j,1)<=B(j,i) && A(j,1)>=B(j,i+1)
m=j;
C(j,1)=(((c(i+1,1)-c(i,1))/(B(j,i+1)-B(j,i)))*(A(j,1)-B(j,i))+c(i,1));

else if A(j,1)<B(j,11)
C(j,1)=100;
else if A(j,1)>B(j,1)
C(j,1)=0;
end
end
end
end
end
```

## B.2. Calculating value of n

```
clear all
close all

n=[0.2:0.05:0.9];

A=xlsread('exp25c.xlsx','Sheet1');
t=[21600,43200,64800,86700,129600,173100,216960,259200]; % 8 time steps in
seconds
O=[ ];
    %O is the distance here elevation(mm)0.4(mm)
g=0;
for p=1:1:100 %Percent Concentrations
g=g+1;
for f=1:15 % different "n"s
for j=1:8 %columns or time steps
    for i=1:112% rows in each column

        if i~=1
        if p<A(i,j) && p>A(i-1,j)
            R=(O(i)/(t(j)^n(f)));
            Q=R-(O(i-1)/(t(j)^n(f)));
            Z=(A(i,j)-A(i-1,j));
            W=A(i,j)-p;
            B(j,f,g)=R-(W*Q/Z);
        end
        end
    end
end
end
end
m=0;
for p=1:1:100
    m=m+1;
k=mean(B,1); %mean of each column 1=column , 2=row

for s=1:15
    for l=1:8
a(l,s,m)=abs(1-(B(l,s,m)./k(1,s,m))); %[(d/t^n - d/t^n(average))^2]
    end
end
end

C=squeeze(mean(a,1));
```

```

for p=1:1:100

d(p)=min(C(:,p));

if d(p)==C(1,p)
    N(p)=0.2;
else if d(p)==C(2,p)
    N(p)=0.25;
else if d(p)==C(3,p)
    N(p)=0.3;
else if d(p)==C(4,p)
    N(p)=0.35;
else if d(p)==C(5,p)
    N(p)=0.4;
else if d(p)==C(6,p)
    N(p)=0.45;
else if d(p)==C(7,p)
    N(p)=0.5;
else if d(p)==C(8,p)
    N(p)=0.55;
else if d(p)==C(9,p)
    N(p)=0.6;
else if d(p)==C(10,p)
    N(p)=0.65;
else if d(p)==C(11,p)
    N(p)=0.7;
else if d(p)==C(12,p)
    N(p)=0.75;
else if d(p)==C(13,p)
    N(p)=0.8;
else if d(p)==C(14,p)
    N(p)=0.85;
else
    N(p)=0.9;
end

```

```

        end
    end
end

g=squeeze(sum(a,1));
u=squeeze(sum(C,1));

for pp=1:1:100
    for ss=1:15

        if C(ss,pp)<1.25.*d(pp)

            h(ss,pp)=C(ss,pp);

        end
    end
end

```

### B.3. Smoothing the data

close all

```

clear all
x = []
Y=[]

%Smooth the data using the loess and rloess methods with a span of 10%:

yy1 = smooth(x,y,0.1,'loess');
yy2 = smooth(x,y,0.1,'rloess');
%Plot original data and the smoothed data.

[xx,ind] = sort(x);
subplot(2,1,1)
plot(xx,y(ind),'b.',xx,yy1(ind),'r-')
set(gca,'YLim',[0 100])
legend('Original Data','Smoothed Data Using "loess"',...
    'Location','NW')
subplot(2,1,2)
plot(xx,y(ind),'b.',xx,yy2(ind),'r-')
set(gca,'YLim',[0 60])
legend('Original Data','Smoothed Data Using "rloess"',...
    'Location','NW')

```

#### B.4. Calculating diffusion coefficient

```

clear all
close all
c=xlsread('diff40c.xlsx')/100;
Rot=848.2; %Density of toluene in that temperature T=40C Kg/m3( in T=25 862.24 &
in T=0 885.42)
Rob=1013; %Density of Bitumen in that temperature T=40C
dro=Rot-Rob;
deltax=3*10^-3; %3mm is each space step
deltat=43200; %12hours is time step
n=99; %number of elements in vertical row
y=0;
for ll=-10:1:10
    a0(1)=ll;
    for uu=-10:1:10
        a0(2)=uu;
        for nn=-10:1:10
            a0(3)=nn;
for j=2:6 % 6 time steps starting from 12 hours to 60 hours
    for i=2:98 % number of elements in vertical row-2
Ro(i,j)=Rot.*c(i,j)+Rob.*(1-c(i,j));
dcdx(i,j)=(c(i+1,j)-c(i,j))./deltax;
v(i,j)=(dcdx(i,j)).^2;
d2cd2x(i,j)=(c(i+1,j)-2*c(i,j)+c(i-1,j))./(deltax^2);
dcdt(i,j)=(c(i,j)-c(i,j-1))./deltat;
dDdc(i,j)=(a0(2)+2*a0(3)*c(i,j)).*0.5*10^-10;
D(i,j)=(a0(1)+a0(2).*c(i,j)+a0(3).*c(i,j).^2).*0.5*10^-10;
w(i,j)=c(i,j);
    end
end
f=d2cd2x./v;
b=dcdt./v;
h=(1+(w./Ro).*dro);
q=(h.*b);
m=dDdc+D.*(f+dro./Ro);
p=abs(m-q);
p(:,1)=[];
for j=1:5

for i=1:98
    if isnan(p(i,j))]==1
        p(i,j)=0;
    end
end
end
p1=1/n*sum(p,1);

```

```

y=y+1;
O(y)=p1(4);
if y>2
    if O(y)<O(y-1)
        e(y)=O(y);
        opt=a0;
    end
end

    end
end
end

```

## B.5. Boltzman-Matano Method

```

clc
clear all
close all
c=[];
x=[];
figure;hold;
plot(x,c,'-*');
grid on;
title('Concentration Profile')
xlabel('Distance(m)'); ylabel('Toluene Fraction');
%%integration
i=0;
for k=1:91
    i=i+1;
    if k==1
        C(i)=c(i)
        X(i)=x(i)
    else
        C(i)=c(i)
        X(i)=x(i)
    integral=trapz(C,X);
    int(i)=integral;
    end
end

%% derivation
dxdC = diff(x)./diff(c);
% associated time values (central difference)
CC = c(1:end-1)+diff(c)./2;

%% Final Equation
t=259200;
% for l=1:98 %to make integral array and derivative array of the same
% dimension i remove the last element
% w(l)=int(l);
% end
w=(int(:,1:90))';
D=(-0.5/t).* (dxdC).*w;

```

## B.6 fitting single file and Fickian diffusion and finding gamma

```

clc
clear all
close all

t=24*3600;
x=[];

c=[];
C1=c./100;
u=x./(t^0.25);
G=1;
H=10;
D=5*10^-10;
A=exp(-H.* (u+0.33));
C=(1+G.*A).^-1;
m=(x-1.5)./1000;
l=m./(4*t*D).^0.5;
C2=0.5+0.35*erf(l);

plot(x,C1,'o',x,C,'x',x,C2,'-')
hold
g=size(u);
for i=1:g
    for j=1:101
        r(j)=(j-1)*0.01;
    d(i,j)=r(j).*C2(i)+(1-r(j)).*C(i);
end
q(i,j)=(C1(i)-d(i,j)).^2;

a(i)=min(q(i,:));
b=a(i);
for o=1:101
    if b==q(i,o)
        m(i)=o;
    end
end
end
for i=1:g
    f(i)=m(i)./100;
CC(i)=f(i).*C2(i)+(1-(f(i))).*C(i);
end
plot(x,CC,'black')

```

## C. Experimental Data

### C.1. 273K Experiment Smoothed Data

Elevation(mm)	6 hours	12 hours	24 hours	36 hours	48 hours	60 hours	72 hours
3.9	0	0	0	0	0	0	0
4.2	0	0	0	0	0	0	0
4.5	0	0	0	0	0	0	0

4.8	0	0	0	0	0	0	0
5.1	0	0	0	0	0	0	0
5.4	0	0	0	0	0	0	0
5.7	0	0	0	0	0	0	0
6	0	0	0	0	0	0	0
6.3	0	0	0	0	0	0	0
6.6	0	0	0	0	0	0	0
6.9	0	0	0	0	0	0	0
7.2	0	0	0	0	0	0	0
7.5	0	0	0	0	0	0	0
7.8	0	0	0	0	0	0	0
8.1	0	0	0	0	0	0	0
8.4	0	0	0	0	0	0	0
8.7	0	0	0	0	0	0	0
9	0	0	0	0	0	0	0
9.3	0	0	0	0	0	0	0
9.6	0	0	0	0	0	0	0
9.9	0	0	0	0	0	0	0
10.2	0	0	0	0	0	0	0
10.5	0	0	0	0	0	0	0
10.8	0	0	0	0	0	0	0
11.1	0	0	0	0	0	0	0
11.4	0	0	0	0	0	0	0
11.7	0	0	0	0	0	0	0
12	0	0	0	0	0	0	0
12.3	0	0	0	0	0	0	0
12.6	0	0	0	0	0	0	0
12.9	0	0	0	0	0	0	0
13.2	0	0	0	0	0	0	0
13.5	0	0	0	0	0	0	0
13.8	0	0	0	0	0	0	0
14.1	0	0	0	0	0	0	0
14.4	0	0	0	0	0	0	0
14.7	0	0	0	0	0	0	0
15	0	0	0	0	0	0	0
15.3	0	0	0	0	0	0	0
15.6	0	0	0	0	0	0	0
15.9	0	0	0	0	0	0	0
16.2	0	0	0	0	0	0	3.341231 2
16.5	0	0	0	0	0	0	3.881312 3
16.8	0	0	0	0	0	0	5.991283 123

17.1	0	0	0	0	0	0	0	15.12312 322
17.4	0	0	0	0	0	0	0	17.99123 123
17.7	0	0	0	0	0	0	0.114917369	19.88123 123
18	0	0	0	0	0	0	0.84124302	23.88123 123
18.3	0	0	0	0	0	0	20.3334112	25.88123 2
18.6	0	0	0	0	0	0	22.881232	27.99123 83
18.9	0	0	0	0	0	1.24213811 2	22.99123723	28.99123 823
19.2	0	0	0	0	0	1.63721750 6	24.8812722	29.88123 2
19.5	0	0	0	0	0	10.7712346 4	26.9912823	30.99812 32
19.8	0	0	0	0	0	13.9913248 4	27.9912872	32.00912 32
20.1	0	0	0	0	0	15.9913473 5	28.99127823	33.99123 23
20.4	0	0	0	0	0	17.772353	32.53392788	34.15081 053
20.7	0	0	0	0	0	20.8823573 5	32.881232	34.25529 317
21	0	0	0	0	0	22.7723562 4	33.12222	34.68768 968
21.3	0	0	2.3424205 49	2.34242054 9	24.8823573 3	33.12344124	34.78258 218	
21.6	0	0	28.926380 14	25.992353	25.8821393 5	33.7712322	34.82229 22	
21.9	0	0	29.251651 85	27.0012349 4	27.1100234 8	33.99123	34.99483 3	
22.2	0	0	29.051851 01	28.99235	28.9923575 3	35.223213	35.01991 232	
22.5	0	0.22211659 9	29.700882 61	29.7008826 1	29.8882355 3	35.8123712	36.1	
22.8	0	1.27090257 7	30.040505 08	30.0405050 8	31.8823571 2	35.9912312	36.12232	
23.1	0	32.1741820 3	31.642315 53	31.6423155 3	32.9913583 5	36.22312	36.33121 23	
23.4	0	32.3386508 2	32.338650 82	32.3386508 2	33.8823457 3	37.07802642	37.33123 423	
23.7	1.59254754 8	33.3989781	34.455209 88	34.4552098 8	35.9913853 1	37.59956805	38.19912 3	
24	1.98706137	34.2552931	34.782582	34.7825821	36.2343422	37.92505457	38.88123	

	1	7	18	8			123
24.3	37.9250545 7	35.8341111 1	37.403825 73	37.4038257 3	36.9932483 4	37.92505457	39.19929 823
24.6	38.4452835 5	35.8341111 1	37.925054 57	37.9250545 7	37.199134	37.92505457	39.33322 41
24.9	39.4918365 1	37.9614916	42.417212 84	42.4172128 4	39.9913483 4	37.9614916	39.77128 232
25.2	40	39.9912823 1	42.100292 32	42.1001283 2	40.221314	40.11912324	40.00132 131
25.5	41.4092636 3	40.9404059 1	46.966593 66	46.9665936 6	42.1172343	41.2213414	40.12923 23
25.8	41.7476796 7	41.2722518 9	47.382949 87	47.3829498 7	43.8813741 3	42.2284384	40.22029 123
26.1	44.0493077 9	44.5122569 7	49.093959 34	49.0939593 4	44.9912384	43.44581239	40.31891 233
26.4	44.5122569 7	44.5122569 7	49.093959 34	49.0939593 4	45.8871234 1	44.65881239	40.40012 912
26.7	47.2716364 3	50	49.547404 41	49.5474044 1	46.5562348 4	45.99123834	40.81238 123
27	47.0802249 1	49.8529334 6	49.392981 68	49.3929816 8	47.1119134	46.881234	41.00123 923
27.3	52.6973828 4	58.6879231 5	49.402510 84	49.4025108 4	47.9981348 3	47.012293	42.99282 312
27.6	52.6973828 4	59.6798608 6	49.852933 46	49.8529334 6	48.1993494	47.5010112	43.09912 38
27.9	64.3738320 9	61.3637556 6	49.701102 94	49.7011029 4	48.991284	47.99901239	43.22391 23
28.2	65.0491564 4	61.0382233 4	49.551654 41	49.5516544 1	49.0881231 2	48.49912823	43.78919 231
28.5	72.5364456 7	62.0437404 4	50.039915 96	50.0399159 6	49.8812914	49.09912323	44.18812 312
28.8	72.8103820 2	62.3691665 1	50.362944 94	50.3629449 4	50.1912394	49.50991232	44.99128 123
29.1	73.6464821 1	63.1418689 7	51.326298 89	51.3262988 9	50.9912384 2	49.9988123	45.18823 23
29.4	74.4810531 1	63.1418689 7	51.326298 89	51.3262988 9	51.9912348 3	50.50199124	45.77123 912
29.7	75.5871210 6	65.5482911 1	52.611364 92	52.6113649 2	52.3342353	51.09912812	46.88123 2
30	75.8599792 9	65.8837082	53.893845 8	53.8938458	53.8713443	50.99881231	47.11829 23
30.3	78.3485179 8	68.9367884 1	55.649450 45	55.6494504 5	54.0013924	51.49881232	47.99812 32
30.6	79.1750106 2	70	56.387323 82	56.3873238 2	55.188123	52.00191232	48.09912 312
30.9	83.7613471 3	72.7472600 7	60	60	55.9898123 1	52.988123	48.88127 322

## C.2. 298K Experiment Smoothed Data

Elevation(mm)	6 hours	12 hours	24 hours	36 hours	48hours	60 hours	72 hours
2.1	0	0	0	0	0	0	0
2.4	0	0	0	0	0	0	0
2.7	0	0	0	0	0	0	0
3	0	0	0	0	0	0	0
3.3	0	0	0	0	0	0	0
3.6	0	0	0	0	0	0	0
3.9	0	0	0	0	0	0	0
4.2	0	0	0	0	0	0	0
4.5	0	0	0	0	0	0	0
4.8	0	0	0	0	0	0	0
5.1	0	0	0	0	0	0	0
5.4	0	0	0	0	0	0	0
5.7	0	0	0	0	0	0	0.003086 504
6	0	0	0	0	0	0	0.143085 392
6.3	0	0	0	0	0	0.040209412	0.042424 343
6.6	0	0	0	0	0	0.141341259	0.297595 38
6.9	0	0	0	0	0	0.449813081	0.919730 311
7.2	0	0	0	0	0.083449478	0.920308972	1.806917 473
7.5	0	0	0	0	0.382568595	1.608620652	3.067743 49
7.8	0	0	0	0	0.750696763	2.608982847	4.648453 974
8.1	0	0	0	0.1221316 49	1.241605928	3.808426124	6.203889 684
8.4	0	0	0.08445700 5	0.4528417 95	1.976867018	4.995690889	7.652186 178
8.7	0	0	0.50349754 9	0.9434101 99	3.091855689	6.230403071	8.967702 914
9	0	0	0.89088736 7	1.4561120 31	4.340768849	7.596983604	10.13946 72
9.3	0	0	1.44409129 1	2.1250416 13	5.520724499	8.972704547	11.23398 244
9.6	0	0	2.04686532 9	3.2428342 48	6.67830252	10.14093948	12.19867 536
9.9	0	0.34684779 4	2.85470889 3	4.6721859 47	7.836270061	11.15090096	12.95698 611

10.2	0	0.908843638	3.931693847	5.798306552	9.12239926	12.0816776	13.52458831
10.5	0	1.424523095	5.230405753	6.872072233	10.33924135	12.76611063	13.92847533
10.8	0	2.226229284	6.46890161	7.96768879	11.4294417	13.28080319	14.31159004
11.1	0	3.257779293	7.540154184	9.189597704	12.4115402	13.7068135	14.75187297
11.4	0	4.891337558	8.483608168	10.4504844	13.27601983	14.17624702	15.30749
11.7	0	6.729563285	9.381013913	11.46889814	13.90936106	14.66443754	15.97674902
12	0	8.030535874	10.25816548	12.43890105	14.42783188	15.21948461	16.73242463
12.3	0	9.045118759	11.10924964	13.32967156	14.9202753	15.82156536	17.40051343
12.6	0	10.0241286	11.93696585	14.13714892	15.42004251	16.46696052	17.93427309
12.9	0	11.00725878	12.74486127	14.76840588	15.94633906	17.16466388	18.28624789
13.2	0	11.94955107	13.52959555	15.36001866	16.51298185	17.91577161	18.81970517
13.5	0	12.8819447	14.11846618	15.9601046	17.12570715	18.7472317	19.57747179
13.8	0	13.76257619	14.84308559	16.56919072	17.756913	19.6744783	20.63412707
14.1	0	14.6161285	15.64517942	17.18871383	18.48011509	20.69811862	22.04069377
14.4	0	15.44794169	16.50197194	17.78628661	19.30162694	21.83938257	23.75903566
14.7	0	16.26016124	17.41099876	18.43718215	20.26342802	23.12788237	25.49499461
15	0	16.94142741	18.35897442	19.17857051	21.31337642	24.45552135	27.11634176
15.3	0	17.53097461	19.34086938	20.10517094	22.47846333	25.80226335	28.60336332
15.6	0	18.02247784	20.35488596	21.11771086	23.77055218	27.10958157	29.8353551
15.9	0	18.55204168	21.40095364	22.31376069	25.16628538	28.36291758	30.59270686
16.2	0	19.20194173	22.43348295	23.69423897	26.63928492	29.54157457	31.00440492
16.5	0	20.01383221	23.4769064	25.19589754	28.02076785	30.59937	31.63280241
16.8	0	20.9576657	24.54144833	26.69117695	29.36248706	31.5693819	32.30521233
17.1	0	22.0380546	25.6802024	28.155676	30.60115903	32.48477358	32.78811

		5	8	72			36
17.4	0	23.2946078 7	26.9460391 4	29.566212 68	31.74672507	33.35890557	33.64165 325
17.7	0	24.3744642 9	28.2530908	30.929184 69	32.82649151	34.20652021	34.81705 441
18	18.7417418 8	25.6207777 6	29.5731700 6	32.177880 69	33.84380577	35.04675266	36.12101 452
18.3	20.1378231	27.0149212 6	30.9205227 3	33.344399 81	34.7862687	35.86977363	37.42730 165
18.6	21.560604	28.4980512 2	32.3016288 3	34.448745 28	35.67156222	36.66184361	38.59555 152
18.9	23.9291082 5	30.1527433 7	33.7183162	35.514914 3	36.58556483	37.40078175	39.43913 076
19.2	31.1008751 8	31.7976692 4	35.1797223 9	36.541816 03	37.49092324	38.11705157	39.99718 363
19.5	50	33.5458109 9	36.6946319 3	37.526548 01	38.40255292	38.84301401	40.36021 368
19.8	68.8991248 2	35.3050164 2	38.2205120 8	38.530042 1	39.33264009	39.60789128	40.43271 029
20.1	76.0708917 5	37.0731636 8	39.8092901 5	39.526177 06	40.29705524	40.40601632	40.11089 822
20.4	78.439396	39.0328382	41.3652194 8	40.513170 24	41.29735937	41.24780107	40.20989 978
20.7	79.8621769	41.1239557 1	42.9493643 8	41.500644 97	42.32083276	42.09265121	40.65847 836
21	81.2582581 2	43.3108392 2	44.5486905 2	42.496158 7	43.36175832	42.9349905	41.38830 738
21.3	100	45.5927516 1	46.1582572 3	43.521417 21	44.41266968	43.77909858	42.44602 346
21.6	100	48.1523018 3	47.9158044 6	44.592809 58	45.53600225	44.61764578	43.59519 404
21.9	100	50.7895826	50.0374037 9	45.728257 08	46.71725527	45.44995083	44.58101 92
22.2	100	53.3303001 9	52.0169380 2	46.934104 34	47.9488823	46.35184232	45.50852 925
22.5	100	56.0654049 1	54.9514390 1	48.208689 9	49.22903764	47.33747308	46.44249 519
22.8	100	58.9759009 4	57.3470425 2	49.551782 26	50.55055998	48.49885144	47.10022 97
23.1	100	62.0662489 5	59.8821284 2	50.990927 94	52.3832953	49.81891878	47.49903 575
23.4	100	65.1915623 9	62.5867335 8	54.049879 52	54.08861663	51.27981438	48.61462 709
23.7	100	68.2231185 6	65.4539256 1	56.476984 54	56.3673307	52.88109535	50.07247 119
24	100	71.0851048 2	69.8441395 8	58.938013 69	58.46082582	54.62526133	51.92266 437

24.3	100	73.6211589 2	74.1803087 1	62.188236 71	60.99683051	56.59802759	54.12560 935
24.6	100	76.1834971 8	79.1725399 1	67.914001 29	64.64372131	58.80079809	56.80087 238
24.9	100	78.9638399 6	83.5199129 3	77.013317 01	70.19760944	61.09555166	59.70239 146
25.2	100	82.2068038 8	86.3982098 4	85.218371 86	77.33179198	63.63441341	62.90392 14
25.5	100	84.7380505 6	89.2287119 7	89.540524 71	83.73403318	66.74801643	66.30142 64
25.8	100	87.0186167 8	91.7437824 2	91.976728 51	88.13985647	71.04859908	69.78975 334
26.1	100	89.1287227 7	93.9650518 2	93.867114 98	90.85821656	76.83534055	73.23649 445
26.4	100	91.0880889	96.0485057 6	96.726900 93	93.21774095	83.12171736	76.78986 76
26.7	100	92.8302271 7	100	99.422176 4	95.15773602	87.94673354	80.53468 355
27	100	94.3996924 9	100	100	98.21389727	91.58498978	83.88513 666
27.3	100	95.8641509 8	100	100	100	93.713007	86.84919 455
27.6	100	96.9300833	100	100	100	95.40374229	89.53418 373
27.9	100	97.7912718 6	100	100	100	97.76798232	91.97018 85
28.2	100	98.6153534 2	100	100	100	100	94.15083 9
28.5	100	99.2792332	100	100	100	100	95.98710 331
28.8	100	99.8343678 3	100	100	100	100	97.56668 193
29.1	100	100	100	100	100	100	98.64321 286
29.4	100	100	100	100	100	100	99.53291 688
29.7	100	100	100	100	100	100	99.96218 274
30	100	100	100	100	100	100	100.1564 535
30.3	100	100	100	100	100	100	100
30.6	100	100	100	100	100	100	100
30.9	100	100	100	100	100	100	100
31.2	100	100	100	100	100	100	100
31.5	100	100	100	100	100	100	100
31.8	100	100	100	100	100	100	100

32.1	100	100	100	100	100	100	100
32.4	100	100	100	100	100	100	100
32.7	100	100	100	100	100	100	100
33	100	100	100	100	100	100	100
33.3	100	100	100	100	100	100	100
33.6	100	100	100	100	100	100	100
33.9	100	100	100	100	100	100	100
34.2	100	100	100	100	100	100	100
34.5	100	100	100	100	100	100	100
34.8	100	100	100	100	100	100	100
35.1	100	100	100	100	100	100	100
35.4	100	100	100	100	100	100	100

### C.3. 313K Experiment Smoothed Data

Elevation(mm)	6 hours	12 hours	24 hours	36 hours	48 hours	60 hours
6	0	0	0	0.001488634	0.001164402	0.006187315
6.3	0	0	0	0.001607086	0.000342195	0.005995673
6.6	0	0	0	0.000874051	0.001318201	0.005439162
6.9	0	0	0	0.0055986	-0.00165655	0.005169274
7.2	0	0	0	0.012195729	0.001317722	0.004861418
7.5	0	0	0	0.022298405	0.000635185	0.002622634
7.8	0	0	0	0.030872137	0.003965474	0.011014535
8.1	0	0	0	0.031287072	0.008325034	0.018129013
8.4	0	0	0	0.019207776	0.009759342	0.016627211
8.7	0	0	0	0.005564632	0.008325023	0.011289705
9	0	0	0	0.005617395	0.003766128	0.004270136
9.3	0	0	0	0.010726593	0.000744869	0.007431058
9.6	0	0	0	0.013613067	0.000469695	0.024624608
9.9	0	0	0	0.013909373	0.001437275	0.036775901
10.2	0	0	0	0.008211095	0.001637037	0.039397145
10.5	0	0	0	0.001222487	0.001363562	0.047968097
10.8	0	0	0	0.003753575	0.005901307	0.069145438
11.1	0	0	0	0.001450306	0.006314529	0.109068324
11.4	0	0	0	0.006453928	0.013990414	0.177933625
11.7	0	0	0	0.016866366	0.048594323	0.257880873
12	0	0	0	0.03193985	0.093194893	0.334338762
12.3	0	0	0	0.053544628	0.141936984	0.419092013
12.6	0	0	0.003966744	0.076969084	0.176387955	0.516142192
12.9	0	0	0.004230037	0.107309711	0.206163715	0.628643632
13.2	0	0	0.00790325	0.150968441	0.258891533	0.761622046
13.5	0	0	0.031111519	0.201419494	0.331624414	0.904146301

13.8	0	0	0.057238998	0.25986109	0.429133006	1.074109805
14.1	0	0	0.077269274	0.314404975	0.546702149	1.288418681
14.4	0	0	0.089825003	0.361917714	0.675346097	1.538930703
14.7	0	0	0.105877768	0.411583563	0.818332139	1.737633157
15	0	0	0.135070026	0.475906278	0.985146269	2.076604684
15.3	0	0	0.175441814	0.566189043	1.182076264	2.699205214
15.6	0	0	0.220741389	0.679515732	1.380735013	3.57544886
15.9	0	0	0.261438084	0.813432918	1.79425742	4.900286413
16.2	0	0	0.300972061	0.981621365	2.442065764	6.552423923
16.5	0	0	0.357134863	1.187889327	3.254210541	8.366279705
16.8	0	0.001813216	0.426926816	1.415430849	4.170881866	10.34961953
17.1	0	0.001005816	0.492610068	1.70338789	5.525508119	12.15860006
17.4	0	0.004383591	0.576766602	2.315711613	6.857018862	13.20355621
17.7	0	0.011678568	0.70837707	3.101873237	8.033371009	13.85479184
18	-0.00086334	0.013743331	0.863508033	4.000851364	9.232477765	14.15737805
18.3	0.000496606	0.016844853	1.040810215	5.221031082	10.58764806	14.1475129
18.6	0.00207463	0.04195653	1.411236526	6.634335606	12.0142041	14.33824343
18.9	0.005884919	0.094023526	2.217282478	7.918325457	12.66838069	14.56707113
19.2	0.009456928	0.172208311	3.164984909	9.273170346	13.38300479	14.95416507
19.5	0.007846682	0.27738063	4.679086339	11.07469234	13.9058314	15.60663901
19.8	0.014473758	0.417759802	7.444034133	12.73777983	14.72309157	16.46912111
20.1	0.034263712	1.548625598	10.49776257	13.7133685	15.43284798	17.4942191
20.4	0.065586567	2.309873392	12.39934367	14.50359291	16.0172047	18.65811408
20.7	0.110666828	3.259456754	13.61434652	15.39604558	16.66228388	19.98067237
21	0.170059232	4.768655653	14.65319865	15.96792889	17.62742419	21.40226064
21.3	0.24418921	7.103075283	15.38381535	16.33323955	18.73958899	23.00516373
21.6	0.343939807	8.919241283	15.90924859	16.8808112	20.07724068	24.84242246
21.9	1.845150836	10.47360325	16.36926097	17.61796131	21.64071929	26.61800127
22.2	2.783407178	11.90331104	16.7640701	18.53296542	23.38638114	28.29031168
22.5	3.861351582	13.5908891	17.11347202	19.66351769	25.1173599	29.77666237
22.8	5.097697856	14.59354344	17.49247035	21.00784253	26.76116783	30.96868577
23.1	6.495615255	15.79010309	18.0183964	22.5782803	28.28743066	31.93954544
23.4	8.056494034	17.01603408	18.71119067	24.36454698	29.69342585	32.72581515
23.7	9.781200535	18.23646753	19.63183847	26.23763073	30.9512267	33.39966085
24	11.67035618	19.47467066	20.7829359	27.9844396	32.07945438	34.06083479
24.3	13.72443641	20.66404922	22.16015975	29.58686756	33.07334661	34.70737536
24.6	15.94381731	21.77419593	23.85103372	31.13828389	33.96282274	35.36696824
24.9	18.328802	22.71863008	25.73801837	32.47113158	34.78737169	36.06051456
25.2	20.87963174	23.56042179	27.62721286	33.63540698	35.51199785	36.78156107
25.5	23.59648433	24.82218478	29.41265698	34.67709907	36.20331749	37.50161669
25.8	25.99895	26.01287599	31.13561756	35.62266103	36.91224591	38.18980628

26.1	26.82234	27.55727609	32.74515358	36.48485317	37.69651945	38.8592941
26.4	27.4459029	29.07286928	34.09767385	37.30669788	38.52829523	39.52850797
26.7	28.732294	30.67430313	35.4385458	38.03946104	39.36755801	40.24304631
27	29.73345	32.16274813	36.55316729	38.82515792	40.1935907	41.01883491
27.3	30.68689934	33.69947638	37.56929187	39.65160462	40.99692274	41.84763848
27.6	32.35472873	35.30577919	38.64365815	40.5284363	41.81383965	42.72693564
27.9	34.04240685	37.03192717	39.77295957	41.47954281	42.68349106	43.62675008
28.2	35.74754829	38.94081363	40.95199426	42.50407485	43.61320501	44.47848663
28.5	37.46915664	41.04840931	42.18678641	43.56682261	44.62280409	45.29515117
28.8	39.20675239	42.76478227	43.45098842	44.64228906	45.6729328	46.19445477
29.1	40.9600953	44.64003999	44.70549576	45.73265181	46.73471759	47.1882294
29.4	42.72906836	46.03673688	45.94475613	46.83159669	47.76347549	48.23137032
29.7	44.51362	47.45970176	47.16084174	47.91328422	48.69737896	49.27465122
30	46.31373272	48.77562857	48.4178906	48.95665039	49.55410304	50.14349922
30.3	48.12940522	50.05747186	49.65245041	49.93281026	50.30952096	50.8155978
30.6	49.96064225	51.3421383	50.77110852	50.85405278	50.95715763	51.38403056
30.9	51.80744881	52.62241974	51.78351323	51.6571087	51.56792915	51.92296082
31.2	53.66982695	53.88757318	52.67637833	52.36048052	52.16391785	52.46455395
31.5	55.54777418	55.13085584	53.4687879	53.00121676	52.75939674	53.00603492
31.8	57.44128269	56.3483266	54.20307025	53.61337542	53.348549	53.55196422
32.1	59.35033913	57.53773699	54.89297006	54.24575537	53.92506366	54.10295828
32.4	61.27492469	58.69789487	55.56465964	54.8876466	54.47383526	54.65104841
32.7	63.21501531	59.82831094	56.22757953	55.51996654	55.00387341	55.20257677
33	65.17058194	60.92893714	56.88802424	56.10705566	55.54641084	55.74364731
33.3	67.14159092	62.0000541	57.55116768	56.64566019	56.08245155	56.23351677
33.6	69.12800422	63.04213968	58.23045985	57.1746563	56.60550433	56.67926159
33.9	71.12977849	64.05583089	58.94472017	57.71471352	57.12008211	57.10868318
34.2	73.14686276	65.04184628	59.64321531	58.26471279	57.62431505	57.58413163
34.5	75.17920517	66.00097423	60.35366709	58.86667332	58.12501188	58.1236172
34.8	77.22675619	66.93403078	61.07640959	59.50437094	58.60973328	58.69738204
35.1	79.28947388	67.84185051	61.8073737	60.1768047	59.08011153	59.3094498
35.4	81.36732047	68.72527046	62.54770995	60.88743243	59.5379508	59.9633704

#### C.4. Calibration Curve 273K

Elevation (mm)	0.9 toluene	0.8 toluene	0.7 toluene	0.6 toluene	0.5 toluene	0.4 toluene	0.3 toluene	0.2 toluene	0.1 toluene
2.10	1420.36	676361.2	476190. 1	1457.13	1470.90	1497.78	1518.72	1562.40	1664.27
2.40	1420.79	591996.0	416666. 6	1456.68	1470.90	1497.78	1518.23	1562.40	1665.46

2.70	1420.79	526218.72	370370.37	1456.22	1470.90	1497.78	1518.72	1562.40	1666.05
3.00	1420.79	473596.85	333333.33	1455.77	1469.51	1497.78	1518.72	1562.40	1666.65
3.30	1419.50	430150.09	303030.30	1455.77	1469.51	1497.78	1519.21	1562.40	1667.24
3.60	1419.92	394423.46	277777.78	1456.21	1469.95	1498.23	1519.18	1562.88	1669.53
3.90	1420.78	364303.26	256410.26	1456.64	1470.84	1499.14	1520.59	1563.82	1672.33
4.20	1420.78	338281.60	238095.24	1456.18	1470.84	1499.14	1520.10	1563.82	1672.93
4.50	1419.49	315441.93	222222.22	1455.73	1469.45	1498.66	1520.59	1563.82	1675.33
4.80	1419.49	295726.80	208333.33	1455.73	1469.45	1498.66	1520.10	1563.82	1672.93
5.10	1419.48	278330.24	196078.43	1456.61	1470.34	1498.60	1521.51	1564.77	1673.94
5.40	1419.91	262946.80	185185.19	1457.05	1470.79	1499.05	1521.47	1565.24	1676.85
5.70	1419.48	249031.94	175438.60	1456.14	1470.79	1499.05	1521.47	1565.24	1677.45
6.00	1419.48	236580.34	166666.67	1455.69	1469.86	1499.05	1520.98	1565.24	1677.45
6.30	1419.48	225314.61	158730.16	1455.69	1469.40	1499.05	1520.98	1565.24	1678.05
6.60	1419.91	215137.94	151515.15	1456.13	1469.84	1499.03	1521.44	1565.71	1677.96
6.90	1420.77	205908.27	144927.54	1457.01	1470.73	1499.93	1522.36	1566.65	1679.57
7.20	1419.48	197149.36	138888.89	1456.55	1470.73	1499.45	1521.86	1566.65	1678.97
7.50	1419.48	189263.39	133333.33	1456.10	1470.73	1498.97	1521.86	1567.18	1681.38
7.80	1419.48	181984.03	128205.13	1455.65	1469.35	1498.97	1521.86	1566.65	1680.78
8.10	1419.90	175296.71	123456.79	1456.09	1469.79	1499.42	1522.32	1567.65	1680.68
8.40	1420.33	169087.06	119047.62	1456.53	1470.23	1499.87	1522.78	1567.60	1681.19
8.70	1420.33	163256.19	114942.53	1456.96	1470.68	1499.85	1523.24	1568.60	1682.30
9.00	1420.33	157814.32	111111.11	1456.96	1470.68	1499.85	1522.74	1568.07	1682.30
9.30	1419.90	152677.28	107526.88	1456.06	1470.68	1498.89	1523.24	1568.60	1682.90
9.60	1419.47	147861.3	104166.	1455.61	1469.75	1498.89	1522.74	1568.07	1682.30

		3	67						
9.90	1419.90	143423.88	101010.10	1456.05	1469.74	1499.34	1522.71	1569.07	1683.41
10.20	1420.75	139289.37	98039.22	1456.92	1470.62	1500.24	1523.62	1569.49	1683.82
10.50	1420.32	135268.71	95238.10	1456.92	1470.62	1500.24	1523.62	1569.49	1684.42
10.80	1420.32	131511.25	92592.59	1456.47	1470.62	1499.76	1523.62	1569.49	1684.42
11.10	1420.32	127956.89	90090.09	1456.47	1470.62	1499.28	1523.62	1569.49	1685.03
11.40	1420.32	124589.60	87719.30	1456.02	1470.62	1498.80	1523.62	1569.49	1684.42
11.70	1419.89	121358.07	85470.09	1456.01	1470.60	1499.26	1524.08	1569.96	1685.53
12.00	1420.31	118359.51	83333.33	1456.88	1471.03	1500.16	1524.50	1570.91	1685.94
12.30	1420.31	115472.69	81300.81	1456.88	1470.57	1500.16	1525.00	1570.91	1686.55
12.60	1420.31	112723.34	79365.08	1456.88	1470.57	1500.16	1524.50	1570.91	1685.34
12.90	1420.31	110101.87	77519.38	1456.88	1470.57	1500.16	1525.00	1570.91	1685.94
13.20	1420.31	107599.56	75757.58	1456.88	1470.57	1499.68	1524.50	1570.91	1685.94
13.50	1420.31	105208.45	74074.07	1456.43	1470.57	1499.68	1525.00	1570.91	1686.55
13.80	1420.31	102921.31	72463.77	1456.43	1470.57	1499.68	1524.50	1570.91	1685.34
14.10	1420.31	100731.32	70921.99	1455.96	1471.01	1499.65	1525.46	1571.38	1686.45
14.40	1420.74	98662.40	69444.44	1456.40	1471.45	1499.62	1525.42	1571.85	1686.35
14.70	1421.17	96677.93	68027.21	1456.84	1470.97	1500.07	1526.38	1572.32	1688.07
15.00	1420.74	94715.74	66666.67	1456.84	1470.51	1500.07	1525.88	1572.32	1686.86
15.30	1420.31	92830.51	65359.48	1456.84	1470.51	1500.07	1526.38	1572.32	1688.07
15.60	1420.31	91045.31	64102.56	1456.84	1470.51	1500.07	1525.88	1572.32	1687.46
15.90	1420.31	89327.47	62893.08	1456.84	1470.51	1500.07	1526.38	1572.32	1688.67
16.20	1420.31	87673.26	61728.40	1456.84	1470.51	1500.07	1525.88	1572.32	1688.67
16.50	1420.31	86079.20	60606.06	1456.39	1470.51	1500.07	1525.88	1572.32	1688.67

16.80	1420.73	84567.47	59523.8 1	1456.83	1470.95	1500.05	1526.34	1572.80	1689.18
17.10	1420.73	83083.83	58479.5 3	1456.37	1470.95	1500.05	1526.83	1572.80	1689.79
17.40	1421.16	81675.71	57471.2 6	1456.80	1471.84	1500.95	1527.26	1573.74	1690.20
17.70	1421.16	80291.38	56497.1 8	1456.80	1471.38	1500.47	1527.75	1573.74	1690.80
18.00	1421.16	78953.19	55555.5 6	1456.80	1470.92	1500.47	1527.26	1573.74	1690.80
18.30	1421.16	77658.87	54644.8 1	1456.80	1470.46	1499.99	1527.75	1573.74	1690.80
18.60	1421.16	76406.31	53763.4 4	1456.80	1470.46	1499.99	1527.26	1573.74	1690.80
18.90	1421.16	75193.51	52910.0 5	1456.80	1470.46	1499.99	1527.75	1573.74	1691.41
19.20	1421.16	74018.62	52083.3 3	1456.80	1470.46	1499.99	1527.26	1573.74	1690.80
19.50	1421.16	72879.87	51282.0 5	1456.80	1470.46	1499.99	1527.75	1573.74	1691.41
19.80	1420.73	71753.95	50505.0 5	1456.80	1470.46	1499.99	1527.75	1573.74	1691.41
20.10	1420.73	70683.00	49751.2 4	1456.80	1470.46	1499.99	1527.75	1573.74	1691.41
20.40	1420.73	69643.54	49019.6 1	1456.80	1470.46	1499.99	1527.75	1573.74	1691.41
20.70	1420.30	68613.50	48309.1 8	1456.80	1470.46	1499.99	1527.75	1573.74	1691.41
21.00	1420.30	67633.31	47619.0 5	1456.80	1470.46	1499.99	1527.75	1573.74	1691.41
21.30	1420.30	66680.72	46948.3 6	1456.35	1470.46	1499.99	1527.75	1573.74	1691.41
21.60	1420.73	65774.34	46296.3 0	1456.78	1470.90	1500.44	1528.21	1574.21	1691.92
21.90	1420.73	64873.32	45662.1 0	1456.78	1470.90	1500.44	1528.21	1574.21	1692.53
22.20	1421.58	64035.06	45045.0 5	1457.66	1471.78	1501.34	1529.13	1575.16	1692.93
22.50	1421.58	63181.26	44444.4 4	1457.66	1471.78	1501.34	1529.13	1575.16	1693.54
22.80	1421.58	62349.93	43859.6 5	1457.21	1471.78	1501.34	1529.13	1575.16	1692.93
23.10	1421.58	61540.19	43290.0 4	1456.76	1471.78	1501.34	1529.62	1575.16	1693.54
23.40	1421.15	60732.88	42735.0 4	1456.76	1471.32	1501.34	1529.13	1575.16	1692.93
23.70	1421.15	59964.11	42194.0	1456.76	1470.86	1501.34	1529.62	1576.74	1694.15

			9						
24.00	1421.15	59214.55	41666.67	1456.76	1470.86	1500.86	1529.13	1575.16	1694.15
24.30	1421.15	58483.51	41152.26	1456.76	1470.40	1500.86	1529.62	1576.74	1694.76
24.60	1421.15	57770.30	40650.41	1456.76	1470.40	1500.86	1529.13	1575.16	1694.15
24.90	1421.15	57074.27	40160.64	1456.76	1470.40	1500.86	1529.62	1576.21	1694.76
25.20	1421.15	56394.81	39682.54	1456.76	1470.40	1500.38	1529.62	1575.16	1694.15
25.50	1421.15	55731.35	39215.69	1456.76	1470.40	1500.86	1529.62	1576.21	1694.76
25.80	1421.15	55083.31	38759.69	1456.76	1470.40	1500.38	1529.62	1575.16	1694.15
26.10	1421.15	54450.16	38314.18	1456.76	1470.40	1499.91	1529.62	1576.74	1694.15
26.40	1421.15	53831.41	37878.79	1456.76	1470.40	1499.91	1529.62	1576.21	1694.15
26.70	1421.15	53226.57	37453.18	1456.76	1470.40	1499.91	1529.62	1576.74	1695.37
27.00	1421.58	52650.94	37037.04	1457.19	1470.84	1500.36	1530.08	1577.21	1695.27
27.30	1421.58	52072.36	36630.04	1456.74	1470.84	1500.36	1530.08	1577.21	1695.88
27.60	1421.58	51506.36	36231.88	1456.74	1470.84	1500.36	1530.08	1576.68	1695.88
27.90	1421.57	50952.42	35842.29	1457.18	1471.28	1500.81	1530.54	1577.68	1697.00
28.20	1422.00	50425.48	35460.99	1457.62	1471.73	1501.26	1531.00	1578.16	1696.90
28.50	1422.00	49894.69	35087.72	1457.17	1471.73	1501.26	1531.00	1578.16	1697.51
28.80	1422.00	49374.95	34722.22	1456.72	1471.73	1501.26	1531.00	1578.16	1697.51
29.10	1422.00	48865.93	34364.26	1456.72	1471.73	1501.26	1531.50	1578.16	1698.12
29.40	1421.57	48352.71	34013.61	1456.72	1471.73	1501.26	1531.50	1578.16	1697.51
29.70	1421.57	47864.30	33670.03	1456.72	1471.27	1501.26	1531.99	1578.16	1698.12
30.00	1421.57	47385.66	33333.33	1456.72	1471.27	1501.26	1531.50	1578.16	1697.51
30.30	1421.57	46916.50	33003.30	1456.72	1470.81	1501.26	1531.99	1578.16	1698.12
30.60	1421.14	46442.52	32679.74	1456.72	1470.35	1501.26	1531.50	1578.16	1698.12

30.90	1421.14	45991.62	32362.46	1456.72	1470.35	1501.26	1531.99	1579.22	1698.73
31.20	1421.14	45549.40	32051.28	1456.72	1470.35	1501.26	1531.99	1578.16	1698.73
31.50	1421.14	45115.59	31746.03	1456.72	1470.35	1501.26	1531.99	1578.16	1699.34
31.80	1421.14	44689.98	31446.54	1456.27	1470.35	1501.26	1531.99	1578.16	1699.34
32.10	1421.14	44272.31	31152.65	1456.27	1470.35	1501.26	1531.99	1578.16	1699.96
32.40	1421.57	43875.52	30864.20	1456.70	1470.79	1501.71	1532.45	1578.63	1700.47
32.70	1421.57	43473.00	30581.04	1456.25	1470.79	1501.71	1532.45	1578.63	1701.69
33.00	1422.42	43103.59	30303.03	1456.67	1471.67	1502.60	1533.37	1579.58	1702.71
33.30	1422.42	42715.27	30030.03	1456.67	1471.67	1502.60	1533.87	1579.58	1703.33
33.60	1422.42	42333.88	29761.90	1456.67	1471.67	1502.13	1533.37	1579.58	1703.33
33.90	1422.42	41959.25	29498.53	1456.67	1471.67	1502.13	1533.87	1579.58	1704.56
34.20	1421.99	41578.65	29239.77	1456.67	1471.67	1501.17	1533.87	1579.58	1704.56
34.50	1421.56	41204.68	28985.51	1456.67	1471.67	1501.17	1533.87	1579.58	1707.03
34.80	1421.13	40837.16	28735.63	1456.23	1471.21	1501.17	1533.87	1579.58	1707.03
35.10	1421.13	40488.12	28490.03	1456.23	1470.75	1501.17	1533.87	1579.58	1709.50
35.40	1421.39	40152.26	28248.59	1455.33	1470.29	1501.17	1534.37	1579.58	1709.50

### C.5. Calibration Curve 298K

Elevation (mm)	0.1 toluene	0.2 toluene	0.3 toluene	0.4 toluene	0.5 toluene	0.6 toluene	0.7 toluene	0.8 toluene	0.9 toluene
2.1	1547.18	1469.70	1437.75	1405.47	1383.11	1357.91	1342.77	1327.96	1320.12
2.4	1546.59	1470.11	1438.14	1405.86	1383.50	1358.29	1343.14	1328.33	1319.74
2.7	1546.59	1469.65	1438.14	1405.86	1383.50	1358.29	1343.14	1328.33	1319.37
3	1546.08	1469.19	1436.83	1405.86	1383.09	1358.29	1341.99	1328.33	1319.37
3.3	1545.07	1468.73	1436.83	1405.44	1382.68	1357.50	1341.99	1327.95	1318.26

3.6	1545.07	1468.73	1436.83	1404.60	1382.68	1357.11	1341.99	1327.20	1318.26
3.9	1545.07	1468.27	1435.51	1404.60	1382.27	1357.11	1340.84	1327.20	1318.26
4.2	1545.07	1468.27	1435.51	1404.60	1382.27	1357.11	1340.84	1327.20	1317.15
4.5	1544.56	1467.35	1435.51	1404.18	1382.27	1356.72	1340.84	1327.20	1317.15
4.8	1545.34	1468.57	1436.70	1405.35	1383.02	1357.46	1341.96	1327.18	1318.25
5.1	1544.83	1468.57	1435.39	1404.51	1382.61	1357.07	1341.19	1327.18	1317.14
5.4	1544.83	1468.57	1435.39	1404.51	1382.61	1357.07	1340.81	1327.18	1317.14
5.7	1544.83	1467.20	1435.39	1404.51	1382.20	1357.07	1340.81	1327.18	1317.14
6	1544.83	1467.65	1435.39	1404.51	1382.20	1357.07	1340.81	1327.18	1317.14
6.3	1544.83	1467.20	1435.39	1404.09	1382.20	1356.28	1340.43	1326.06	1316.40
6.6	1544.32	1467.20	1434.51	1404.09	1381.80	1356.28	1339.66	1326.06	1316.03
6.9	1544.32	1466.74	1434.07	1403.25	1381.80	1355.89	1339.66	1326.06	1316.03
7.2	1543.81	1466.74	1434.07	1403.25	1381.39	1355.89	1339.66	1326.06	1316.03
7.5	1544.32	1465.82	1434.07	1403.25	1380.99	1355.89	1339.66	1326.06	1316.03
7.8	1543.73	1466.23	1434.47	1403.64	1381.37	1356.27	1339.27	1325.30	1316.03
8.1	1544.59	1467.04	1433.95	1404.00	1382.14	1356.24	1339.63	1326.04	1316.02
8.4	1544.59	1467.04	1433.95	1404.00	1382.14	1355.85	1339.63	1326.04	1316.02
8.7	1544.59	1466.58	1433.95	1403.58	1381.73	1355.85	1339.63	1326.04	1316.02
9	1544.59	1466.58	1433.95	1403.16	1381.32	1355.85	1339.63	1326.04	1316.02
9.3	1544.59	1466.58	1433.95	1403.16	1381.32	1355.85	1338.87	1324.92	1316.02
9.6	1544.59	1466.58	1433.95	1403.16	1380.92	1355.85	1338.49	1324.92	1314.92
9.9	1544.59	1465.67	1432.64	1403.16	1380.92	1355.06	1338.49	1324.92	1314.92
10.2	1544.08	1465.67	1432.64	1403.16	1380.92	1355.06	1338.49	1324.92	1314.92
10.5	1544.08	1465.67	1432.64	1402.74	1380.92	1354.67	1338.49	1324.92	1314.92
10.8	1544.43	1466.48	1433.44	1403.10	1381.28	1355.42	1339.23	1325.65	1315.65
11.1	1544.35	1466.43	1433.83	1403.07	1381.25	1355.80	1338.46	1324.90	1314.91
11.4	1544.35	1466.43	1433.83	1403.07	1381.25	1355.80	1338.46	1324.90	1314.91
11.7	1544.35	1466.43	1433.83	1403.07	1380.85	1355.41	1338.46	1324.90	1314.91
12	1544.35	1466.43	1432.96	1403.07	1380.85	1355.41	1338.46	1324.90	1314.91
12.3	1544.35	1465.98	1432.52	1403.07	1380.85	1355.02	1338.46	1324.90	1314.91
12.6	1544.35	1466.43	1432.52	1403.07	1380.85	1355.02	1338.46	1324.90	1314.91
12.9	1544.35	1465.52	1432.52	1403.07	1380.85	1354.63	1338.46	1324.90	1314.91
13.2	1544.35	1465.98	1432.52	1403.07	1380.85	1354.63	1338.46	1324.90	1314.91
13.5	1543.85	1465.52	1432.52	1402.65	1380.85	1354.63	1337.32	1323.78	1314.17
13.8	1543.85	1465.52	1432.52	1402.65	1380.44	1354.63	1337.32	1323.78	1313.81
14.1	1543.85	1465.52	1432.52	1402.65	1380.44	1354.63	1337.32	1323.78	1313.81
14.4	1543.34	1465.52	1432.52	1402.23	1380.44	1354.63	1337.32	1323.78	1313.81
14.7	1543.34	1465.06	1432.52	1402.23	1380.04	1354.63	1337.32	1323.78	1313.81
15	1542.83	1465.52	1432.52	1401.82	1380.04	1354.63	1337.32	1323.78	1313.81
15.3	1542.83	1465.06	1432.52	1401.82	1380.04	1354.63	1337.32	1323.78	1313.81
15.6	1542.83	1465.06	1432.09	1401.82	1380.04	1354.24	1337.32	1323.78	1313.81

15.9	1543.69	1465.87	1432.01	1402.59	1380.80	1354.60	1338.06	1324.51	1314.53
16.2	1544.11	1466.28	1432.41	1402.98	1380.78	1354.97	1338.43	1324.88	1314.90
16.5	1544.11	1466.28	1432.41	1402.98	1380.78	1354.97	1338.43	1324.88	1314.90
16.8	1544.11	1466.28	1432.41	1402.98	1380.78	1354.58	1338.43	1324.88	1314.90
17.1	1544.11	1465.82	1432.41	1402.98	1380.78	1354.58	1338.43	1323.76	1314.90
17.4	1544.11	1466.28	1432.41	1402.98	1380.78	1354.58	1338.43	1324.13	1314.53
17.7	1544.11	1465.82	1432.41	1402.98	1380.78	1354.58	1337.29	1323.76	1314.53
18	1544.11	1466.28	1432.41	1402.98	1380.78	1354.58	1337.29	1323.76	1313.80
18.3	1544.11	1465.82	1432.41	1402.98	1380.78	1354.58	1337.29	1323.76	1313.80
18.6	1544.11	1466.28	1432.41	1402.98	1380.78	1354.58	1337.29	1323.76	1313.80
18.9	1544.11	1465.82	1432.41	1402.98	1380.78	1354.58	1337.29	1323.76	1313.80
19.2	1544.11	1466.28	1432.41	1402.98	1380.78	1354.58	1337.29	1323.76	1313.80
19.5	1544.11	1465.82	1432.41	1402.98	1380.78	1354.58	1337.29	1323.76	1313.80
19.8	1544.11	1465.82	1432.41	1402.98	1380.78	1354.58	1337.29	1323.76	1313.80
20.1	1544.11	1465.82	1432.41	1402.98	1380.78	1354.58	1337.29	1323.76	1313.80
20.4	1544.11	1465.82	1432.41	1402.98	1380.78	1354.58	1337.29	1323.76	1313.80
20.7	1544.11	1465.82	1432.41	1402.98	1380.78	1354.58	1337.29	1323.76	1313.80
21	1544.11	1465.82	1432.41	1402.98	1380.78	1354.58	1337.29	1323.76	1313.80
21.3	1544.11	1465.82	1432.41	1402.98	1380.78	1354.58	1337.29	1323.76	1313.80
21.6	1544.11	1465.82	1432.41	1402.98	1380.78	1354.58	1337.29	1323.76	1313.80
21.9	1544.11	1465.82	1432.41	1402.98	1380.78	1354.58	1337.29	1323.76	1313.80
22.2	1544.11	1465.82	1432.41	1402.98	1380.78	1354.58	1337.29	1323.76	1313.80
22.5	1543.69	1465.42	1432.01	1402.59	1380.40	1354.21	1336.92	1323.40	1313.43
22.8	1543.26	1465.47	1431.61	1402.20	1380.02	1353.84	1336.55	1323.03	1313.07
23.1	1542.83	1464.61	1431.22	1401.82	1379.64	1353.46	1336.18	1322.66	1312.71
23.4	1542.83	1465.06	1431.22	1401.82	1379.64	1353.46	1336.18	1322.66	1312.71
23.7	1542.83	1464.61	1431.22	1401.82	1379.64	1353.46	1336.18	1322.66	1312.71
24	1542.83	1464.61	1431.22	1401.82	1379.64	1353.46	1336.18	1322.66	1312.71
24.3	1542.83	1464.61	1431.22	1401.82	1379.64	1353.46	1336.18	1322.66	1312.71
24.6	1542.83	1464.61	1431.22	1402.23	1379.64	1353.46	1336.18	1322.66	1312.71
24.9	1542.83	1464.61	1431.22	1401.82	1379.64	1353.46	1336.18	1322.66	1312.71
25.2	1542.83	1464.61	1431.22	1402.23	1379.64	1353.46	1336.18	1322.66	1312.71
25.5	1542.83	1464.61	1431.22	1402.23	1379.64	1353.46	1336.18	1322.66	1312.71
25.8	1542.83	1464.61	1431.22	1402.23	1379.64	1353.46	1336.18	1322.66	1312.71
26.1	1542.83	1464.61	1431.22	1402.23	1379.64	1353.46	1336.18	1322.66	1312.71
26.4	1542.83	1465.06	1431.22	1402.65	1379.64	1353.46	1336.18	1322.66	1312.71
26.7	1542.83	1464.61	1431.22	1402.65	1379.64	1353.46	1336.18	1322.66	1312.71
27	1542.83	1464.61	1431.22	1402.65	1379.64	1353.46	1336.18	1322.66	1312.71
27.3	1542.83	1464.61	1431.22	1402.65	1380.04	1353.46	1336.18	1322.66	1312.71
27.6	1542.83	1464.61	1431.22	1402.65	1380.04	1353.46	1336.18	1322.66	1312.71
27.9	1542.83	1464.61	1431.22	1402.65	1380.04	1353.46	1336.18	1322.66	1313.07

28.2	1542.83	1465.06	1432.52	1402.65	1380.04	1353.46	1336.18	1322.66	1313.44
28.5	1542.83	1464.61	1432.52	1403.07	1380.04	1353.46	1336.18	1322.66	1313.07
28.8	1542.83	1464.61	1432.52	1403.07	1380.04	1353.46	1336.18	1322.66	1313.81
29.1	1543.34	1464.61	1432.52	1403.07	1380.04	1353.46	1336.18	1322.66	1313.81
29.4	1542.49	1463.80	1431.73	1402.29	1379.28	1352.71	1335.44	1321.93	1313.08
29.7	1542.06	1463.39	1431.33	1401.90	1378.89	1352.34	1335.07	1321.57	1312.72
30	1542.56	1463.85	1431.33	1401.90	1379.30	1352.34	1335.07	1321.57	1312.72
30.3	1542.56	1463.39	1431.33	1401.90	1379.30	1352.34	1335.07	1321.57	1312.72
30.6	1542.56	1463.85	1431.33	1401.90	1379.30	1352.34	1335.07	1321.57	1312.72
30.9	1543.07	1463.39	1431.33	1401.90	1379.30	1352.34	1335.07	1321.57	1312.72
31.2	1543.07	1463.39	1431.33	1401.90	1379.30	1352.73	1335.07	1321.57	1312.72
31.5	1543.07	1463.39	1431.33	1401.90	1379.30	1352.34	1335.07	1321.57	1312.72
31.8	1543.07	1463.39	1431.33	1401.90	1379.30	1352.73	1335.07	1321.57	1312.72
32.1	1543.07	1463.39	1431.33	1401.90	1379.30	1352.73	1335.07	1321.57	1312.72
32.4	1543.07	1463.85	1431.33	1401.90	1379.70	1353.12	1335.07	1321.57	1312.72
32.7	1543.07	1463.39	1431.33	1401.90	1379.70	1353.12	1335.07	1321.57	1312.72
33	1543.07	1463.39	1431.33	1401.90	1379.70	1353.12	1335.07	1321.57	1312.72
33.3	1543.07	1463.39	1431.33	1401.90	1379.30	1352.73	1335.07	1321.57	1312.72
33.6	1543.07	1463.39	1431.33	1401.90	1379.70	1352.73	1335.07	1321.57	1312.35
33.9	1543.07	1463.39	1431.33	1401.90	1379.70	1352.73	1335.07	1321.57	1311.98
34.2	1543.07	1463.39	1431.33	1401.90	1379.70	1353.12	1335.07	1321.57	1311.62
34.5	1543.07	1463.39	1431.33	1401.90	1379.70	1352.73	1335.07	1321.57	1311.62
34.8	1543.07	1463.39	1430.90	1401.90	1379.70	1352.73	1335.07	1321.57	1311.62
35.1	1543.07	1463.39	1430.03	1401.90	1379.70	1352.73	1335.07	1321.57	1311.62
35.4	1543.07	1463.39	1430.03	1401.90	1379.70	1352.73	1335.07	1321.57	1311.62

## C.6. Calibration Curve 313K

Elevation (mm)	0.1 toluene	0.2 toluene	0.3 toluene	0.4 toluene	0.5 toluene	0.6 toluene	0.7 toluene	0.8 toluene	0.9 toluene
2.1	1484.54	1418.70	1387.79	1350.98	1326.43	1298.76	1281.65	986.83	1251.76
2.4	1485.25	1419.83	1388.48	1350.89	1326.73	1299.07	1281.62	986.56	1251.75
2.7	1483.84	1417.68	1386.84	1350.50	1326.35	1298.35	1280.91	986.57	1250.75
3	1484.08	1418.38	1387.53	1350.79	1326.65	1298.66	1281.58	986.85	1251.74
3.3	1482.67	1417.09	1386.70	1349.62	1326.28	1298.30	1280.53	986.31	1250.74
3.6	1483.38	1418.21	1387.40	1350.69	1326.96	1298.61	1281.55	986.86	1251.73
3.9	1481.50	1416.93	1386.16	1349.92	1326.58	1298.25	1280.50	986.32	1250.73
4.2	1481.42	1417.30	1386.16	1349.88	1326.18	1297.88	1280.84	986.87	1251.06
4.5	1481.27	1416.76	1386.85	1350.60	1326.51	1298.20	1280.46	986.33	1250.72
4.8	1480.80	1416.76	1386.03	1349.43	1326.13	1297.48	1280.46	986.88	1250.72
5.1	1480.65	1416.23	1387.13	1350.15	1326.08	1298.17	1280.09	986.07	1251.05
5.4	1480.57	1416.60	1386.72	1350.11	1326.43	1298.15	1280.43	986.35	1250.71

5.7	1479.64	1415.32	1385.90	1349.34	1326.06	1297.44	1280.43	986.89	1250.71
6	1479.64	1415.32	1385.50	1349.34	1325.68	1297.44	1279.38	986.08	1249.71
6.3	1479.41	1415.59	1386.59	1350.41	1326.36	1298.11	1280.40	986.36	1250.71
6.6	1479.41	1415.59	1386.59	1349.24	1326.36	1297.39	1280.40	986.90	1250.71
6.9	1478.94	1415.16	1385.37	1349.24	1325.61	1297.39	1279.35	986.10	1249.71
7.2	1478.48	1414.31	1385.73	1349.24	1325.24	1297.03	1279.35	986.37	1249.71
7.5	1479.18	1415.00	1386.46	1349.54	1326.29	1297.34	1279.66	986.38	1250.70
7.8	1478.72	1415.00	1386.05	1349.15	1326.29	1297.34	1279.32	986.11	1250.70
8.1	1478.25	1414.15	1385.24	1349.15	1325.91	1297.34	1279.32	986.11	1249.70
8.4	1477.79	1414.15	1385.60	1349.15	1325.16	1296.98	1279.32	986.38	1249.70
8.7	1477.71	1414.10	1385.93	1348.73	1325.51	1296.61	1278.61	986.12	1250.03
9	1478.49	1414.85	1385.93	1349.05	1326.21	1297.29	1279.28	986.12	1249.69
9.3	1478.03	1413.99	1385.52	1349.05	1325.47	1296.94	1279.28	986.39	1249.69
9.6	1477.56	1413.99	1384.70	1349.05	1325.09	1296.58	1278.59	986.13	1249.69
9.9	1477.56	1413.57	1385.80	1348.67	1325.09	1296.22	1278.24	986.13	1249.69
10.2	1477.88	1414.31	1385.80	1348.60	1325.79	1296.90	1278.91	986.13	1249.35
10.5	1477.80	1414.69	1385.80	1348.96	1325.39	1296.89	1278.56	985.86	1249.68
10.8	1477.80	1414.69	1385.39	1348.96	1325.02	1296.53	1278.21	985.87	1249.68
11.1	1477.34	1413.84	1385.67	1348.57	1325.02	1296.17	1278.21	986.14	1249.02
11.4	1477.34	1413.84	1385.67	1348.57	1325.02	1296.17	1278.21	986.14	1248.69
11.7	1478.04	1414.53	1385.67	1348.87	1326.07	1297.20	1279.22	986.14	1249.67
12	1477.58	1414.53	1385.26	1348.87	1325.69	1296.84	1278.52	985.88	1249.67
12.3	1477.58	1414.53	1385.99	1348.87	1325.32	1296.13	1278.18	986.15	1249.67
12.6	1477.58	1414.53	1386.35	1348.87	1324.95	1296.13	1278.18	986.15	1248.68
12.9	1477.12	1413.68	1385.54	1348.48	1324.95	1296.13	1278.18	986.15	1248.68
13.2	1477.12	1413.68	1385.54	1348.48	1324.95	1296.13	1278.18	986.15	1248.68
13.5	1477.04	1414.05	1385.13	1348.06	1325.30	1296.47	1277.82	985.62	1249.01
13.8	1477.82	1414.80	1385.13	1348.77	1325.62	1296.79	1278.15	985.62	1249.67
14.1	1477.82	1414.37	1386.22	1348.77	1325.25	1296.08	1278.15	986.16	1249.67
14.4	1477.36	1414.37	1386.22	1348.77	1324.88	1296.08	1278.15	986.16	1248.67
14.7	1477.36	1414.37	1386.22	1348.77	1324.88	1296.08	1278.15	986.16	1248.67
15	1477.36	1414.37	1385.82	1348.39	1324.88	1296.08	1278.15	986.16	1248.67
15.3	1477.36	1413.52	1385.00	1348.39	1324.88	1296.08	1277.45	985.63	1248.67
15.6	1477.36	1413.95	1385.00	1348.00	1324.88	1296.08	1277.11	985.36	1248.67
15.9	1478.06	1414.64	1385.73	1348.68	1325.92	1296.75	1278.12	985.63	1249.66
16.2	1478.06	1414.64	1386.10	1348.68	1325.18	1296.39	1278.12	985.90	1249.33
16.5	1478.06	1414.64	1385.69	1348.68	1324.80	1296.03	1278.12	986.17	1248.67
16.8	1478.06	1414.64	1385.69	1348.68	1324.80	1296.03	1278.12	986.17	1248.67
17.1	1477.60	1414.22	1385.69	1348.68	1324.80	1296.03	1278.12	986.17	1248.67
17.4	1478.06	1414.22	1385.69	1348.29	1324.80	1296.03	1278.12	986.17	1248.67
17.7	1477.60	1414.22	1385.28	1348.29	1324.80	1296.03	1277.77	985.91	1248.67
18	1477.60	1414.22	1384.88	1348.29	1324.80	1296.03	1277.42	985.64	1248.67
18.3	1477.60	1414.22	1385.24	1348.29	1324.80	1295.68	1277.08	985.64	1248.67
18.6	1477.60	1414.22	1385.20	1347.91	1324.80	1295.68	1277.08	985.64	1248.67

18.9	1478.76	1415.33	1385.56	1348.97	1325.48	1296.70	1278.08	985.64	1249.32
19.2	1478.76	1415.33	1385.56	1348.59	1325.48	1295.99	1278.08	986.19	1248.66
19.5	1478.30	1415.33	1385.56	1348.59	1325.10	1295.99	1278.08	986.19	1248.66
19.8	1478.30	1415.33	1385.56	1348.59	1325.10	1295.99	1278.08	986.19	1248.66
20.1	1478.30	1414.48	1385.56	1348.59	1325.10	1295.99	1278.08	986.19	1248.66
20.4	1478.30	1414.91	1385.56	1348.59	1324.73	1295.99	1278.08	986.19	1248.66
20.7	1478.30	1414.48	1385.15	1348.59	1324.73	1295.99	1278.08	986.19	1248.66
21	1478.30	1414.48	1385.15	1348.59	1324.73	1295.99	1278.08	986.19	1248.66
21.3	1478.30	1414.48	1385.15	1348.20	1324.73	1295.99	1278.08	986.19	1248.66
21.6	1478.30	1414.48	1385.15	1348.20	1324.73	1295.99	1278.08	986.19	1248.66
21.9	1478.30	1414.48	1385.15	1348.20	1324.73	1295.99	1277.39	985.65	1248.66
22.2	1478.30	1414.48	1385.11	1348.20	1324.73	1295.99	1277.39	985.65	1248.66
22.5	1478.30	1414.48	1385.07	1348.20	1324.73	1295.63	1277.05	985.66	1248.66
22.8	1478.30	1414.48	1385.43	1348.20	1324.73	1295.63	1277.05	985.66	1248.66
23.1	1478.30	1414.06	1385.43	1348.20	1324.73	1295.63	1277.05	985.66	1248.66
23.4	1478.30	1414.06	1385.43	1348.20	1324.73	1295.28	1277.05	985.93	1247.67
23.7	1478.30	1414.06	1385.03	1348.20	1324.73	1294.92	1277.05	986.20	1247.67
24	1478.30	1414.06	1385.03	1348.20	1324.36	1294.92	1277.05	986.20	1247.67
24.3	1478.30	1414.06	1385.03	1348.20	1324.36	1294.92	1277.05	986.20	1247.67
24.6	1478.30	1414.06	1385.03	1347.82	1323.99	1294.92	1277.05	986.20	1247.67
24.9	1478.30	1414.06	1385.03	1347.82	1323.99	1294.92	1277.05	986.20	1247.67
25.2	1478.69	1414.43	1385.03	1347.78	1324.71	1295.26	1277.38	986.20	1248.00
25.5	1478.30	1414.06	1385.03	1347.43	1323.99	1294.92	1277.05	986.20	1247.67
25.8	1479.07	1414.80	1385.03	1348.14	1324.68	1295.60	1277.72	986.20	1248.32
26.1	1479.07	1414.80	1384.62	1348.14	1324.31	1295.60	1277.72	986.20	1248.32
26.4	1478.30	1414.06	1384.62	1347.43	1323.99	1294.92	1277.05	986.20	1247.67
26.7	1479.07	1414.38	1384.62	1348.14	1324.31	1295.60	1277.72	986.20	1248.32
27	1478.69	1414.43	1384.62	1347.78	1323.97	1295.26	1277.38	986.20	1248.00
27.3	1479.07	1414.38	1384.62	1348.14	1324.31	1295.60	1277.37	985.93	1248.32
27.6	1478.69	1414.43	1384.62	1347.78	1323.97	1295.26	1277.38	986.20	1248.00
27.9	1479.15	1413.58	1383.81	1347.40	1323.97	1295.26	1276.69	985.66	1248.00
28.2	1478.69	1413.58	1383.81	1347.40	1323.97	1295.26	1276.69	985.66	1248.00
28.5	1478.69	1413.58	1383.81	1347.40	1323.97	1295.26	1276.69	985.66	1248.00
28.8	1478.69	1413.58	1383.81	1347.40	1323.97	1295.26	1276.69	985.66	1248.00
29.1	1479.15	1413.16	1383.41	1347.40	1323.97	1295.26	1276.35	985.40	1248.00
29.4	1479.54	1413.53	1383.41	1347.75	1324.31	1295.60	1276.68	985.40	1248.32
29.7	1479.46	1413.90	1383.41	1348.11	1324.66	1295.59	1277.02	985.67	1248.65
30	1479.93	1413.90	1383.41	1348.11	1324.66	1295.59	1277.02	985.67	1248.65
30.3	1479.93	1413.90	1383.41	1348.11	1324.66	1295.59	1277.02	985.67	1248.65
30.6	1479.46	1413.90	1383.77	1348.11	1324.66	1295.59	1277.02	985.67	1248.65
30.9	1479.46	1413.90	1383.77	1348.11	1324.66	1295.59	1277.02	985.67	1248.65
31.2	1479.46	1413.90	1384.49	1348.11	1324.66	1295.23	1277.02	985.94	1248.65
31.5	1479.46	1413.90	1384.09	1348.11	1324.66	1294.88	1277.02	986.21	1248.65
31.8	1479.46	1413.90	1384.09	1348.11	1324.66	1294.88	1277.02	986.21	1248.65

32.1	1479.46	1413.48	1384.09	1348.11	1324.66	1294.88	1277.02	986.21	1248.65
32.4	1479.46	1413.48	1384.09	1348.11	1324.66	1294.88	1277.02	986.21	1248.65
32.7	1479.46	1413.06	1384.09	1348.11	1324.66	1294.88	1277.02	986.21	1248.65
33	1479.00	1412.63	1383.28	1348.11	1324.29	1294.88	1277.02	986.21	1248.65
33.3	1479.00	1412.63	1382.88	1348.11	1324.29	1294.88	1277.02	986.21	1247.99
33.6	1479.00	1412.63	1382.88	1347.72	1324.29	1294.88	1277.02	986.21	1247.66
33.9	1478.54	1412.63	1382.88	1347.34	1324.29	1294.88	1276.33	985.67	1247.66
34.2	1478.07	1412.63	1382.88	1346.95	1323.92	1294.88	1275.98	985.41	1247.66
34.5	1478.07	1412.63	1382.47	1346.95	1323.92	1294.88	1275.98	985.41	1247.66
34.8	1478.07	1412.63	1381.67	1346.95	1323.92	1294.88	1275.98	985.41	1247.66
35.1	1477.61	1411.79	1381.67	1346.95	1323.55	1294.88	1275.98	985.41	1247.66
35.4	1477.61	1411.37	1381.67	1346.95	1323.55	1294.88	1275.98	985.41	1247.66

## C.7. Fadaei et al raw data

Elevation(m)	40 s	90s	140s	190s	240s
0	0.001096379	0.001096379	0.001096379	- 0.012480149	- 0.006677214
1.9077E-06	0.001100974	0.001100974	0.001100974	-0.01237541	- 0.006318496
3.8154E-06	0.001107866	0.001107866	0.001107866	- 0.012224138	- 0.006040865
5.7231E-06	0.001080298	0.001080298	0.001080298	- 0.012119425	- 0.005821126
7.6308E-06	0.001045836	0.001045836	0.001045836	- 0.011968191	- 0.005589872
9.5385E-06	0.001015969	0.001015969	0.001015969	- 0.011747196	- 0.005451144
1.14462E-05	0.000972315	0.000972315	0.000972315	- 0.011689047	- 0.005150632
1.33539E-05	0.000926361	0.000926361	0.000926361	- 0.011584388	- 0.004919527
1.52616E-05	0.00091717	0.00091717	0.00091717	- 0.011386726	- 0.004538318

1.71693E-05	0.000926361	0.000926361	0.000926361	-	0.011061247	-	0.004226524
0.000019077	0.000963124	0.000963124	0.000963124	-	0.010573219	-	0.003764779
2.09847E-05	0.001048134	0.001048134	0.001048134	-	0.010027364	-	0.003072549
2.28924E-05	0.001137731	0.001137731	0.001137731	-	0.009319339	-	0.002277057
2.48001E-05	0.001243399	0.001243399	0.001243399	-	0.008472664	-	0.001459147
2.67078E-05	0.001406475	0.001406475	0.001406475	-	0.007580343	-	0.000331266
2.86155E-05	0.001571821	0.001571821	0.001571821	-	0.006850832	-	0.00073793
3.05232E-05	0.00172566	0.00172566	0.00172566	-	0.005902077	-	0.001863408
3.24309E-05	0.001890955	0.001890955	0.001890955	-	0.004988853	-	0.003044981
3.43386E-05	0.002056223	0.002056223	0.002056223	-	0.004168795	-	0.004293902
3.62463E-05	0.002212285	0.002212285	0.002212285	-	0.003257098	-	0.005689975
0.000038154	0.002395857	0.002395857	0.002395857	-	0.002219437	-	0.007141242
4.00617E-05	0.002561044	0.002561044	0.002561044	-	0.001182817	-	0.008738677
4.19694E-05	0.002749141	0.002749141	0.002749141	-0.00017024	0.010424676		
4.38771E-05	0.002923445	0.002923445	0.002923445	0.000990696	0.012141976		
4.57848E-05	0.003083961	0.003083961	0.003083961	0.002138847	0.013935782		
4.76925E-05	0.003239867	0.003239867	0.003239867	0.003262792	0.015975495		
4.96002E-05	0.003359073	0.003359073	0.003359073	0.004293902	0.017830323		
5.15079E-05	0.003494309	0.003494309	0.003494309	0.005426926	0.020098977		
5.34156E-05	0.003643278	0.003643278	0.003643278	0.006684372	0.022621213		
5.53233E-05	0.003796808	0.003796808	0.003796808	0.007917451	0.025327805		
0.000057231	0.003970933	0.003970933	0.003970933	0.009228816	0.028384952		
5.91387E-05	0.004135866	0.004135866	0.004135866	0.010697819	0.031722526		
6.10464E-05	0.004319094	0.004319094	0.004319094	0.012232878	0.035304327		
6.29541E-05	0.004488551	0.004488551	0.004488551	0.013674855	0.03941515		
6.48618E-05	0.00465798	0.00465798	0.00465798	0.015171432	0.043607957		
6.67695E-05	0.004813647	0.004813647	0.004813647	0.016609234	0.048177469		
6.86772E-05	0.004955558	0.004955558	0.004955558	0.017909417	0.052878319		
7.05849E-05	0.005088295	0.005088295	0.005088295	0.01903865	0.057567299		
7.24926E-05	0.005191269	0.005191269	0.005191269	0.020155346	0.062579087		
7.44003E-05	0.005326264	0.005326264	0.005326264	0.021259541	0.067693624		
0.000076308	0.0054132	0.0054132	0.0054132	0.022407519	0.072930313		
7.82157E-05	0.005536729	0.005536729	0.005536729	0.023689	0.078116886		

8.01234E-05	0.005625934	0.005625934	0.005625934	0.024991283	0.083264391
8.20311E-05	0.005667104	0.005667104	0.005667104	0.026403913	0.088352124
8.39388E-05	0.00572428	0.00572428	0.00572428	0.02780336	0.093255352
8.58465E-05	0.005758585	0.005758585	0.005758585	0.029256704	0.097955902
8.77542E-05	0.005788315	0.005788315	0.005788315	0.031053677	0.102694496
8.96619E-05	0.005850058	0.005850058	0.005850058	0.033070002	0.107254207
9.15696E-05	0.005911798	0.005911798	0.005911798	0.035304327	0.111606742
9.34773E-05	0.005971247	0.005971247	0.005971247	0.037954503	0.115907752
9.5385E-05	0.006076419	0.006076419	0.006076419	0.041006112	0.120147616
9.72927E-05	0.006197581	0.006197581	0.006197581	0.044510372	0.124417854
9.92004E-05	0.006341586	0.006341586	0.006341586	0.048341836	0.128768046
0.000101108	0.006469573	0.006469573	0.006469573	0.052583819	0.133266753
0.000103016	0.006615824	0.006615824	0.006615824	0.057219943	0.137682791
0.000104924	0.006798609	0.006798609	0.006798609	0.062114732	0.141957801
0.000106831	0.006976792	0.006976792	0.006976792	0.067006106	0.146054242
0.000108739	0.007175499	0.007175499	0.007175499	0.072342763	0.149974443
0.000110647	0.0073833	0.0073833	0.0073833	0.07785133	0.153867013
0.000112554	0.0045	0.0045	0.0045	0.083454496	0.157722441
0.000114462	0.004598152	0.004788263	0.005632199	0.089087169	0.161599079
0.00011637	0.004705738	0.005101167	0.006886364	0.094727511	0.165409838
0.000118277	0.00482113	0.00543677	0.008267953	0.100395669	0.169126692
0.000120185	0.004946995	0.005796363	0.009792066	0.105925798	0.172769813
0.000122093	0.005084123	0.006184574	0.011469933	0.111309714	0.176406511
0.000124001	0.005234653	0.00659871	0.013325178	0.116549599	0.180055637
0.000125908	0.005395562	0.007044773	0.015417317	0.121607068	0.183509716
0.000127816	0.005571861	0.007513302	0.017791526	0.126625839	0.186911755
0.000129724	0.005738648	0.008001079	0.020482893	0.131496074	0.190215576
0.000131631	0.005920683	0.008516981	0.023519306	0.136309537	0.193450164
0.000133539	0.006126076	0.009079395	0.027055891	0.140977701	0.196875653
0.000135447	0.006344609	0.009677432	0.031157476	0.145502604	0.200332705
0.000137354	0.006578949	0.010303556	0.036032536	0.149876411	0.203728939
0.000139262	0.00683129	0.011000027	0.04195898	0.154101174	0.207064998
0.000141117	0.00709643	0.01173048	0.049454429	0.158130324	0.210414372
0.000143078	0.007379854	0.012504126	0.056714332	0.162034089	0.213667939
0.000144985	0.007679641	0.013355606	0.06391993	0.165823638	0.216880961
0.000146893	0.008008902	0.014247679	0.071071565	0.169490764	0.220035828
0.000148801	0.00834871	0.015209149	0.078169577	0.173275336	0.223088333
0.000150708	0.008680534	0.016224234	0.085214305	0.177071191	0.226128835
0.000152616	0.009043421	0.01730788	0.092206087	0.180792973	0.229201824
0.000154524	0.009461779	0.018461145	0.099145258	0.184573202	0.232085441
0.000156431	0.009919138	0.019724131	0.113427737	0.188289201	0.234799381
0.000158339	0.010375401	0.021122224	0.119305315	0.191783218	0.237415729
0.000160247	0.010890806	0.02255358	0.125406584	0.195382856	0.239935426
0.000162155	0.011371914	0.024069295	0.131435988	0.198855579	0.242359373

0.000164062	0.01185331	0.025621914	0.137284969	0.202304099	0.244557784
0.00016597	0.012368757	0.027232479	0.143094908	0.205884318	0.246940822
0.000167878	0.012864541	0.028907514	0.148659881	0.209366369	0.249247029
0.000169785	0.013358503	0.030705328	0.153964588	0.212978364	0.251658288
0.000171693	0.013863173	0.032548238	0.159217053	0.216609948	0.254199326
0.000173601	0.01439619	0.034552747	0.164350349	0.220161756	0.256783066
0.000175508	0.014925229	0.036742781	0.169394971	0.223715298	0.259451684
0.000177416	0.015432386	0.039068545	0.174361644	0.227288216	0.262161656
0.000179324	0.015967115	0.041672427	0.179232442	0.23056957	0.264861602
0.000181232	0.016486604	0.044436469	0.183820435	0.233739708	0.267391114
0.000183139	0.016949213	0.047560112	0.187961449	0.236685469	0.269911819
0.000185047	0.017410612	0.051043804	0.192006919	0.239637363	0.272549528
0.000186955	0.01789656	0.055037956	0.195865305	0.242647627	0.275185941
0.000188862	0.018401083	0.059859972	0.199677567	0.245445788	0.277704459
0.00019077	0.018993722	0.065739603	0.203177691	0.248233524	0.280180924
0.000192678	0.01956594	0.072001434	0.206671634	0.25087268	0.282541301
0.000194585	0.020187598	0.07822207	0.21006823	0.253304498	0.284646561
0.000196493	0.02082281	0.08440174	0.213423028	0.255745508	0.286638696
0.000198401	0.021589718	0.090540672	0.216871929	0.258340938	0.288535027
0.000200309	0.022387173	0.096639093	0.220386579	0.260876098	0.290458942
0.000202216	0.02329341	0.102697228	0.223858533	0.263394005	0.292426491
0.000204124	0.024217954	0.108715305	0.227332773	0.265869388	0.294331586
0.000206032	0.025221899	0.120238902	0.230800247	0.268319486	0.296377398
0.000207939	0.026331563	0.126474783	0.234252068	0.270870576	0.298376766
0.000209847	0.027554499	0.132916903	0.237697087	0.2735299	0.300249454
0.000211755	0.028915266	0.139540197	0.24115275	0.276304526	0.302253707
0.000213662	0.030389855	0.14618225	0.244784238	0.27925949	0.304340268
0.00021557	0.031974519	0.15276364	0.248380871	0.282119495	0.306324607
0.000217478	0.033629104	0.159372186	0.252020596	0.285091576	0.308534173
0.000219385	0.035456323	0.166006415	0.255779831	0.288108594	0.310839756
0.000221293	0.037337113	0.172426263	0.259579738	0.29103917	0.313248234
0.000223201	0.039268858	0.178635821	0.263309083	0.293924953	0.315687532
0.000225109	0.041422466	0.184798897	0.267019432	0.296742086	0.318165102
0.000227016	0.043673985	0.190803798	0.270719278	0.299491306	0.320727376
0.000228924	0.04605519	0.196551368	0.274416943	0.302213519	0.323170746
0.000230832	0.048661355	0.202156874	0.278054013	0.305013029	0.32567501
0.000232739	0.051504834	0.207778044	0.28173055	0.307920682	0.328278067
0.000234647	0.054619366	0.213087285	0.28553631	0.310927055	0.330970968
0.000236555	0.057939586	0.218514074	0.289362549	0.314070216	0.333660504
0.000238462	0.061512528	0.224082285	0.293257558	0.317104409	0.336552787
0.00024037	0.065702747	0.229521775	0.297260423	0.320132741	0.339401824
0.000242278	0.070384208	0.234993494	0.301111436	0.323155162	0.342155092
0.000244186	0.074869282	0.240303457	0.304989013	0.326125082	0.344715716
0.000246093	0.079333108	0.24550669	0.308733239	0.329089415	0.347213572

0.000248001	0.083775771	0.250535736	0.312504425	0.332163415	0.349634352
0.000249909	0.088197356	0.255436531	0.316207401	0.335200066	0.352105545
0.000251816	0.092597948	0.260347597	0.319835224	0.338275897	0.354648749
0.000253724	0.09697763	0.265192039	0.323420042	0.341238644	0.35712258
0.000255632	0.101336488	0.269894987	0.326791866	0.344067086	0.359542502
0.000257539	0.105379453	0.274575826	0.330077133	0.346702759	0.361938403
0.000259447	0.108806692	0.279209649	0.333230922	0.349110507	0.364368943
0.000261355	0.11250747	0.283706162	0.336346621	0.351367437	0.366673515
0.000263263	0.116559783	0.288083984	0.339226978	0.353497398	0.368838948
0.00026517	0.120796557	0.292353113	0.342056693	0.355620186	0.370794347
0.000267078	0.125658634	0.296328758	0.344813708	0.357780131	0.372649811
0.000268986	0.131015273	0.300249454	0.347588909	0.359940006	0.374571513
0.000270893	0.136817296	0.304123882	0.350374481	0.362129091	0.37646567
0.000272801	0.143055381	0.307968506	0.35321481	0.364222795	0.378375349
0.000274709	0.149552826	0.311878673	0.355842441	0.366200176	0.380271889
0.000276617	0.156332222	0.315852989	0.358555007	0.368222068	0.382119895
0.000278524	0.163405314	0.319819561	0.361329278	0.370280754	0.383905624
0.000280432	0.170629858	0.323723744	0.364200869	0.37253446	0.385636653
0.00028234	0.178124087	0.327705658	0.367182859	0.374808606	0.387418949
0.000284247	0.185907656	0.331663621	0.370150479	0.377260313	0.389209942
0.000286155	0.193831494	0.335651286	0.373103793	0.379752004	0.390876667
0.000288063	0.20176107	0.339569024	0.376007023	0.3824037	0.392601462
0.00028997	0.20973105	0.343395137	0.378953498	0.385121402	0.394481106
0.000291878	0.217494908	0.347296165	0.382013434	0.387939245	0.396569489
0.000293786	0.225271554	0.35118091	0.385079033	0.390680825	0.398684948
0.000295694	0.232758197	0.35500487	0.388100865	0.393312256	0.400964625
0.000297601	0.240110701	0.358842573	0.391135358	0.395952769	0.403242228
0.000299509	0.24734015	0.362407683	0.394084792	0.39869875	0.405429047
0.000301417	0.254611958	0.365813953	0.396977969	0.401404378	0.407668743
0.000303324	0.261846861	0.369158032	0.399911988	0.404172639	0.409906493
0.000305232	0.269229821	0.372469566	0.402906639	0.406914076	0.412169214
0.00030714	0.276396272	0.375669983	0.405817705	0.409466416	0.414315531
0.000309047	0.283384158	0.378825068	0.408558109	0.411771356	0.416393531
0.000310955	0.290270878	0.382070215	0.411312463	0.413919174	0.4185439
0.000312863	0.296912209	0.385382612	0.414134182	0.415978542	0.420699355
0.000314771	0.303394079	0.388725854	0.416841645	0.417997069	0.422813471
0.000316678	0.309648192	0.39220388	0.419635968	0.419875406	0.424807567
0.000318586	0.315813598	0.395737803	0.422350243	0.42169445	0.426650028
0.000320494	0.321930669	0.399326365	0.42503821	0.423520806	0.42846019
0.000322401	0.32781399	0.402790164	0.426354331	0.42439217	0.429307483
0.000324309	0.33372185	0.406274213	0.42962382	0.426999405	0.431855882
0.000326217	0.339531028	0.409750812	0.43284154	0.429558476	0.434395736
0.000328124	0.345152794	0.413172736	0.435956502	0.432076444	0.436856128
0.000330032	0.350546307	0.416473817	0.438906012	0.434566713	0.439119243

0.00033194	0.35574614	0.419635968	0.441644638	0.436961868	0.441206648
0.000333848	0.360756303	0.422601758	0.444092719	0.439182811	0.443168108
0.000335755	0.365755634	0.425446541	0.446203401	0.441317938	0.44500494
0.000337663	0.370678645	0.428237519	0.448122684	0.443460564	0.446794345
0.000339571	0.375540855	0.431092667	0.449956415	0.44563591	0.448625084
0.000341478	0.380499643	0.433971949	0.451812046	0.447881414	0.45047783
0.000343386	0.385657819	0.436887723	0.453711171	0.450076594	0.452308456
0.000345294	0.390890653	0.439864893	0.455559888	0.452153065	0.454076565
0.000347201	0.396112208	0.442800241	0.457485867	0.454127762	0.455807635
0.000349109	0.401273861	0.445789414	0.459590161	0.456101294	0.45757953
0.000351017	0.406199289	0.448743041	0.461815193	0.458185144	0.459404157
0.000352925	0.410981561	0.451755606	0.460849404	0.460337833	0.461360974
0.000354832	0.415817819	0.454850859	0.463046403	0.462598371	0.463494435
0.00035674	0.420725914	0.458002356	0.465397535	0.464983615	0.465811456
0.000358648	0.425611106	0.461307402	0.467893032	0.467503917	0.468282146
0.000360555	0.430518907	0.464664954	0.470577579	0.470226792	0.470928367
0.000362463	0.435460879	0.467891356	0.473451091	0.473169938	0.473732244
0.000364371	0.440287954	0.470958586	0.476420532	0.476272558	0.476568506
0.000366278	0.444983345	0.473767104	0.479381461	0.479356201	0.479406722
0.000368186	0.449562341	0.476344917	0.48226292	0.482367813	0.482158028
0.000370094	0.453939806	0.478867968	0.485080731	0.485387754	0.484773709
0.000372002	0.458058128	0.481123768	0.487899978	0.488476934	0.487323022
0.000373909	0.461922843	0.483292767	0.490726245	0.491587441	0.489865049
0.000375817	0.465716215	0.485446474	0.493462501	0.494600499	0.492324503
0.000377725	0.469433334	0.487368646	0.495969289	0.497383033	0.494555545
0.000379632	0.473021289	0.489213438	0.49815859	0.499813384	0.496503797
0.00038154	0.47640471	0.490842298	0.499964839	0.501825751	0.498103927
0.000383448	0.479409099	0.492222585	0.501329566	0.503416796	0.499242336
0.000385355	0.481975945	0.49324658	0.502243629	0.504593491	0.499893767
0.000387263	0.484135355	0.493985758	0.502750796	0.505367327	0.500134266
0.000389171	0.486215067	0.494550934	0.502941804	0.505790937	0.500092672
0.000391079	0.488467013	0.495144238	0.502977215	0.506008792	0.499945639
0.000392986	0.491039721	0.495932269	0.503096301	0.506277173	0.499915429
0.000394894	0.493916507	0.4969829	0.503461837	0.50674212	0.500181554
0.000396802	0.497160651	0.498437384	0.504132522	0.507476001	0.500789044
0.000398709	0.500639378	0.500012892	0.505125361	0.50850276	0.501747962
0.000400617	0.504239996	0.501782031	0.506389191	0.509764657	0.503013726
0.000402525	0.50804346	0.503686076	0.507890936	0.511240316	0.504541556
0.000404432	0.524046378	0.5157141	0.512832861	0.520704207	0.517980009
0.00040634	0.528266551	0.518336488	0.514952659	0.522337568	0.519530064
0.000408248	0.53270297	0.521412708	0.517447523	0.52434409	0.521450827
0.000410156	0.537453702	0.524787593	0.520142083	0.526681154	0.52367803
0.000412063	0.542466326	0.528443557	0.523119528	0.529241909	0.526207152
0.000413971	0.547705236	0.532219271	0.526379574	0.532118213	0.529049148

0.000415879	0.55300383	0.536069095	0.529948003	0.535166532	0.532022454
0.000417786	0.558263283	0.540069005	0.533642306	0.538278211	0.535092557
0.000419694	0.563335	0.544079783	0.537222356	0.541436027	0.537963292
0.000421602	0.5680186	0.54780794	0.540486864	0.54418334	0.540481643
0.000423509	0.572354844	0.551198958	0.543442369	0.546517247	0.54243514
0.000425417	0.576521515	0.554295651	0.546079296	0.548587705	0.543945122
0.000427325	0.58055615	0.557134133	0.548408277	0.550347298	0.545305371
0.000429233	0.584363046	0.559794154	0.550612665	0.551855684	0.546676862
0.00043114	0.587989891	0.562114956	0.55254189	0.553237151	0.547956818
0.000433048	0.591283673	0.564190895	0.554315884	0.554568717	0.549181851
0.000434956	0.594339352	0.566084504	0.555961689	0.555860901	0.550464692
0.000436863	0.597439998	0.567920638	0.55747068	0.557194429	0.551687779
0.000438771	0.600633928	0.569812158	0.559109443	0.558633997	0.553079927
0.000440679	0.604151433	0.571957208	0.560881429	0.560198466	0.554684971
0.000442586	0.607730561	0.574231186	0.562606372	0.561816851	0.556339435
0.000444494	0.611342712	0.576483127	0.564274907	0.563364713	0.557902279
0.000446402	0.614942871	0.578617799	0.565858114	0.564783563	0.559324471
0.00044831	0.618414344	0.580712911	0.567293132	0.566148461	0.560776812
0.000450217	0.621841347	0.582792591	0.568811256	0.56751875	0.562318541
0.000452125	0.625241526	0.584946287	0.570377461	0.5690556	0.56395854
0.000454033	0.628778797	0.587336286	0.572088179	0.570776609	0.565715327
0.00045594	0.632544274	0.589944344	0.573922271	0.57258743	0.567528557
0.000457848	0.636620755	0.592747613	0.575892461	0.574549513	0.569221672
0.000459756	0.641066111	0.595883569	0.578149697	0.576665437	0.571000354
0.000461663	0.645865878	0.599171756	0.580655914	0.578818251	0.572897341
0.000463571	0.650696785	0.602387651	0.58315627	0.581012015	0.574766413
0.000465479	0.655431449	0.605461228	0.585556848	0.583071283	0.576564697
0.000467387	0.660083801	0.6085239	0.587896584	0.585035581	0.578211823
0.000469294	0.664644339	0.611474543	0.590194941	0.586981027	0.57983332
0.000471202	0.669268867	0.614420052	0.59250784	0.589047409	0.581510035
0.00047311	0.674053189	0.617533241	0.59508701	0.591214268	0.583411123
0.000475017	0.679007398	0.620831097	0.597813357	0.593636277	0.585627238
0.000476925	0.684183394	0.624321133	0.600755906	0.596230988	0.587961901
0.000478833	0.68960444	0.627921824	0.603806487	0.598949464	0.590348006
0.00048074	0.695079921	0.631641904	0.60693114	0.601667278	0.592793706
0.000482648	0.700489053	0.635262857	0.610061594	0.604330505	0.595206138
0.000484556	0.705698754	0.638799226	0.613136103	0.606988932	0.59773143
0.000486464	0.710749501	0.642317567	0.616047136	0.609629187	0.600141111
0.000488371	0.71573136	0.645809829	0.618910139	0.61218126	0.602504586
0.000490279	0.720741766	0.649307925	0.62174301	0.614681551	0.604804648
0.000492187	0.725761935	0.652830749	0.624643742	0.617195805	0.607113376
0.000494094	0.730771107	0.656384764	0.627543115	0.619628961	0.609399549
0.000496002	0.735771166	0.659818409	0.630457564	0.6219653	0.611667813
0.00049791	0.740697886	0.663222286	0.633282813	0.624295652	0.613953265

0.000499817	0.745511783	0.666555222	0.635921864	0.626489112	0.61599938
0.000501725	0.750260231	0.66980379	0.638435692	0.628526952	0.61782285
0.000503633	0.754999282	0.672921745	0.640818545	0.630453387	0.619469819
0.000505541	0.759716788	0.676048016	0.643137358	0.632324084	0.621079631
0.000507448	0.764404156	0.679138323	0.645381168	0.634065365	0.622665506
0.000509356	0.769118994	0.682218455	0.647654798	0.635814857	0.624202207
0.000511264	0.77385083	0.685345393	0.650008971	0.637580566	0.625757985
0.000513171	0.778571266	0.688524483	0.652359395	0.639284729	0.627244083
0.000515079	0.783326747	0.691680275	0.654616158	0.640928145	0.628707459
0.000516987	0.788017002	0.694840733	0.656893432	0.642572185	0.630206862
0.000518894	0.792727574	0.698063659	0.659182954	0.644265041	0.631729327
0.000520802	0.797439231	0.701316168	0.661495809	0.646085984	0.633233071
0.00052271	0.802210022	0.70461036	0.663857991	0.647973305	0.634722408
0.000524618	0.807007503	0.707951142	0.666370274	0.650016885	0.636312586
0.000526525	0.81181548	0.711366215	0.668924278	0.652123482	0.63799406
0.000528433	0.816597688	0.714823353	0.671559759	0.654327036	0.639802153
0.000530341	0.821384736	0.71830774	0.67430042	0.656621717	0.641763251
0.000532248	0.826153185	0.721881659	0.677077615	0.658936161	0.643798288
0.000534156	0.830874308	0.725434364	0.679842988	0.661170176	0.645813833
0.000536064	0.835609459	0.728947255	0.682582141	0.663427972	0.647778253
0.000537971	0.840331644	0.732485772	0.685327547	0.665697584	0.64983087
0.000539879	0.845013284	0.736054554	0.688107084	0.668001166	0.651855923
0.000541787	0.849643187	0.73957971	0.690838874	0.670244564	0.653775482
0.000543695	0.854196159	0.743071065	0.693509878	0.672358315	0.655653472
0.000545602	0.858699894	0.74656158	0.696166193	0.674403687	0.657428483
0.00054751	0.863129742	0.750039099	0.698756521	0.676381789	0.659136693
0.000549418	0.86747231	0.753500652	0.701353559	0.67832649	0.66087109
0.000551325	0.871724738	0.757008861	0.703980505	0.680296242	0.662585409
0.000553233	0.87590978	0.760463185	0.706579533	0.682229263	0.664287476
0.000555141	0.879986895	0.763889972	0.709194193	0.684183394	0.665882894
0.000557048	0.88397684	0.767336434	0.711787665	0.686047771	0.667406958
0.000558956	0.887889879	0.770801459	0.714370006	0.688011503	0.668972991
0.000560864	0.89174518	0.774283973	0.71697038	0.690044584	0.670531881
0.000562772	0.895501417	0.7777856	0.719655517	0.692180588	0.672154212
0.000564679	0.899183421	0.781318396	0.722423018	0.694410448	0.673872264
0.000566587	0.902772931	0.784886061	0.725254685	0.696732112	0.675655135
0.000568495	0.906315685	0.788394574	0.728129749	0.699061323	0.677483459
0.000570402	0.909810793	0.791909004	0.731077659	0.701418134	0.679494473
0.00057231	0.913268001	0.795418748	0.73405312	0.703865853	0.681572928
0.000574218	0.916620904	0.798844237	0.737051965	0.706365421	0.683681586
0.000576125	0.91985081	0.802281186	0.74001604	0.708835732	0.685776979
0.000578033	0.922981144	0.805682826	0.742919179	0.711184952	0.687788374
0.000579941	0.926013876	0.809033236	0.745774568	0.713477732	0.68974535
0.000581849	0.928979786	0.812345694	0.748545198	0.715737859	0.691715287

0.000583756	0.931878221	0.815682302	0.751293942	0.717949727	0.693656084
0.000585664	0.934680085	0.818953724	0.754015377	0.7201238	0.695554312
0.000587572	0.937392067	0.822246991	0.7567413	0.722388018	0.697410608
0.000589479	0.939989354	0.825472404	0.759476991	0.72456022	0.699177689
0.000591387	0.942459349	0.828679254	0.762174397	0.726657852	0.700860324
0.000593295	0.944806029	0.831838928	0.764845384	0.728713455	0.70250717
0.000595202	0.947039662	0.834941626	0.767512412	0.730727732	0.704152406
0.00059711	0.949138279	0.838045894	0.770145394	0.732673655	0.705752406
0.000599018	0.951166103	0.84117769	0.772763919	0.734708444	0.707354495
0.000600926	0.953111577	0.844265175	0.775389592	0.736781643	0.709044883
0.000602833	0.954993163	0.847364965	0.778000798	0.738907461	0.710766006
0.000604741	0.956836578	0.850436539	0.780681978	0.740991787	0.712520582
0.000606649	0.95861907	0.853499474	0.783391986	0.743142515	0.714314516
0.000608556	0.960323124	0.856543597	0.786096255	0.745307896	0.716166541
0.000610464	0.96197882	0.859577611	0.788833206	0.747434659	0.717969089
0.000612372	0.963562615	0.862569119	0.791556066	0.749526391	0.719793508
0.000614279	0.965087589	0.865527274	0.794265035	0.751699505	0.721706314
0.000616187	0.966545636	0.868468944	0.797017726	0.753831441	0.723648773
0.000618095	0.967939232	0.871402476	0.799748505	0.756019995	0.725601342
0.000620003	0.969339866	0.874318176	0.802521549	0.758221332	0.727635714
0.00062191	0.970723731	0.877261487	0.805294282	0.760488502	0.729743978
0.000623818	0.972072	0.880222001	0.808054531	0.762764081	0.731782512
0.000625726	0.973421063	0.883135671	0.810802492	0.765067145	0.733866069
0.000627633	0.974726266	0.88602458	0.813533633	0.767402438	0.735941839
0.000629541	0.975978263	0.888874057	0.81627174	0.769747256	0.737994724
0.000631449	0.977203222	0.891692456	0.818997922	0.772066038	0.73999499
0.000633356	0.9784182	0.894493469	0.821693941	0.774461357	0.742030191
0.000635264	0.979556393	0.897218004	0.824360471	0.776872644	0.744069857
0.000637172	0.98061081	0.899862072	0.827023121	0.779235906	0.746048925
0.00063908	0.981619905	0.902456513	0.829632423	0.781570492	0.748012406
0.000640987	0.982563878	0.904996761	0.832263259	0.78389777	0.750001258
0.000642895	0.983476279	0.907528895	0.834952694	0.786222957	0.751954155
0.000644803	0.984362903	0.910004505	0.837587278	0.788540855	0.753917675
0.00064671	0.985224057	0.912403158	0.84017917	0.790864248	0.755868676
0.000648618	0.98603075	0.914747404	0.842753111	0.793210596	0.757830006
0.000650526	0.986806297	0.91707679	0.84533094	0.795554195	0.759764725
0.000652433	0.987551103	0.919401888	0.84791893	0.797942288	0.761704069
0.000654341	0.988276044	0.921651352	0.850556967	0.800336713	0.763723023
0.000656249	0.988961802	0.923859171	0.853227111	0.802668618	0.765781225
0.000658157	0.98961668	0.925976128	0.85586413	0.804970936	0.767877789
0.000660064	0.990207541	0.928046275	0.858468765	0.807229748	0.769910938
0.000661972	0.990737799	0.930014253	0.861027383	0.809443523	0.771954988
0.00066388	0.991229936	0.931933881	0.863484002	0.811632194	0.773939661
0.000665787	0.9917175	0.933814152	0.865929665	0.81385297	0.775964964

0.000667695	0.992166257	0.935575455	0.868344517	0.816088686	0.778022044
0.000669603	0.992605695	0.937294175	0.870711224	0.818306337	0.780070609
0.00067151	0.993034633	0.938959246	0.873034684	0.820517825	0.782095024
0.000673418	0.993425559	0.940559825	0.875305872	0.822668048	0.784111304
0.000675326	0.993780097	0.942147381	0.877557056	0.824860976	0.786104014
0.000677234	0.994109804	0.943695931	0.879792478	0.827009511	0.788112081
0.000679141	0.994409914	0.945194569	0.882016272	0.829137036	0.790119819
0.000681049	0.99471167	0.946663194	0.88422094	0.831255127	0.792137308
0.000682957	0.99500268	0.948154949	0.886416346	0.833415094	0.794184441
0.000684864	0.995310152	0.949640628	0.888585533	0.835613878	0.796170476
0.000686772	0.995624096	0.951120143	0.890789336	0.837859453	0.798163671
0.00068868	0.995949342	0.952590246	0.892968929	0.840089831	0.80017865
0.000690587	0.996304088	0.9540603	0.895175065	0.842363742	0.802207568
0.000692495	0.996683138	0.955522301	0.897418349	0.844635139	0.804279351
0.000694403	0.997036509	0.956943602	0.899644595	0.846861347	0.806334972
0.000696311	0.997381366	0.95835859	0.901826539	0.849100525	0.808345818
0.000698218	0.997682866	0.959705812	0.903946645	0.851263883	0.810324655
0.000700126	0.997938999	0.960952601	0.906005875	0.853352844	0.812245901
0.000702034	0.998182466	0.962158028	0.908039396	0.855441647	0.81416962
0.000703941	0.998436057	0.963328605	0.910051125	0.857515798	0.816091033
0.000705849	0.998669898	0.964454184	0.912023484	0.859614649	0.817998481
0.000707757	0.998896018	0.965526315	0.913962322	0.861733661	0.819936248
0.000709664	0.99911091	0.966605185	0.915875124	0.863866366	0.821878398
0.000711572	0.999333576	0.967647611	0.917758675	0.865994329	0.823815654
0.00071348	0.999542713	0.96867758	0.919636026	0.868079463	0.825811837
0.000715388	0.999739588	0.969652608	0.921507154	0.87015846	0.827834151
0.000717295	0.999920751	0.970633228	0.923342642	0.872265172	0.829884328
0.000719203	1.000090988	0.971574201	0.925132589	0.874361604	0.831928307
0.000721111	1.000229281	0.972474532	0.926848455	0.876422411	0.833939534
0.000723018	1.000360341	0.973315965	0.928503124	0.878442327	0.835953901
0.000724926	1.000481861	0.974140773	0.930149912	0.880441427	0.837940622
0.000726834	1.000616037	0.974949094	0.931770248	0.882452857	0.839963408
0.000728741	1.000736033	0.975741065	0.933382858	0.884464879	0.841982585
0.000730649	1.000845398	0.976511162	0.934960985	0.886464094	0.844006819
0.000732557	1.000981326	0.977293411	0.936490017	0.888460184	0.846029584
0.000734465	1.001103127	0.978014634	0.937963889	0.890413492	0.84801046
0.000736372	1.001234011	0.978683914	0.939391475	0.892266375	0.84996075
0.00073828	1.001346201	0.979335224	0.940766714	0.894100755	0.851866242
0.000740188	1.001417831	0.979975655	0.94210489	0.895918734	0.853761158
0.000742095	1.001517086	0.980596999	0.94341777	0.897740901	0.855635262
0.000744003	1.001608158	0.981210437	0.944715297	0.89955425	0.857515798
0.000745911	1.001677259	0.981800938	0.945952384	0.901340516	0.859342946
0.000747818	1.001779653	0.982411047	0.947198791	0.90313292	0.861191284
0.000749726	1.00184861	0.982992892	0.948439901	0.904927693	0.863058439

0.000751634	1.001907178	0.983521008	0.949677273	0.906690375	0.864909655
0.000753542	1.002009285	0.984082358	0.950926709	0.908516795	0.866779453
0.000755449	1.002115843	0.984640218	0.952148461	0.910302051	0.868629431
0.000757357	1.002184516	0.985119544	0.953298759	0.912009216	0.870404016
0.000759265	1.002217687	0.98557455	0.95440816	0.913626867	0.872155958
0.000761172	1.002217687	0.985990792	0.955459921	0.91519325	0.873867792
0.00076308	1.002213113	0.986393837	0.956482614	0.916689587	0.875553851
0.000764988	1.002199388	0.986787756	0.957484241	0.918181576	0.877245821
0.000766895	1.002184516	0.987144877	0.95844185	0.919676198	0.878951411
0.000768803	1.002216543	0.987537934	0.959438797	0.921206409	0.880722799
0.000770711	1.002226835	0.987932458	0.960437835	0.922740519	0.88250498
0.000772619	1.00220625	0.988253778	0.961397738	0.9242284	0.884290104
0.000774526	1.0022154	0.988622645	0.962358336	0.925704904	0.886078114
0.000776434	1.002234839	0.988981341	0.963337668	0.92715642	0.887882269
0.000778342	1.002267989	0.989336434	0.964264718	0.928569556	0.889723143
0.000780249	1.00231826	0.989685348	0.965207463	0.929978633	0.891554961
0.000782157	1.002365075	0.990065578	0.966108938	0.931392071	0.893364708
0.000784065	1.002395889	0.990395712	0.967002259	0.932796279	0.89518999
0.000785972	1.002424411	0.990718534	0.967871173	0.93417956	0.896971137
0.00078788	1.002463183	0.991026405	0.968717377	0.935557104	0.898705046
0.000789788	1.002507634	0.991336043	0.969548414	0.936917266	0.900418092
0.000791696	1.002555477	0.991635954	0.970367321	0.938261828	0.902095872
0.000793603	1.002596462	0.991871518	0.971143597	0.939546406	0.903742468
0.000795511	1.002637426	0.992119301	0.97190379	0.940773279	0.905340093
0.000797419	1.002660175	0.992345021	0.972604669	0.941916878	0.906862208
0.000799326	1.002653351	0.992536156	0.973242506	0.942989459	0.908331312
0.000801234	1.002613533	0.992724446	0.973809274	0.944012822	0.909719283
0.000803142	1.002566864	0.99292377	0.974332801	0.9450036	0.911078847
0.000805049	1.002520167	0.993086248	0.974850569	0.945999179	0.912417411
0.000806957	1.002478003	0.993264829	0.975392512	0.947025191	0.913752921
0.000808865	1.002410722	0.993443124	0.975924318	0.948042812	0.915115442
0.000810773	1.002368499	0.993632407	0.976470118	0.949071232	0.916499355
0.00081268	1.002338816	0.993851368	0.977049511	0.950103913	0.917893846
0.000814588	1.002345667	0.994081119	0.97762839	0.951134407	0.919333715
0.000816496	1.002344526	0.994301672	0.97820953	0.952156357	0.920759172
0.000818403	1.002367358	0.99449817	0.978767737	0.953180802	0.922161662
0.000820311	1.002338816	0.994655853	0.979293461	0.954174737	0.923556946
0.000822219	1.002323971	0.994815782	0.979817517	0.955149362	0.92490891
0.000824126	1.002297699	0.994974233	0.980305307	0.956101716	0.926190555
0.000826034	1.002272561	0.99510527	0.980780589	0.957056782	0.927447026
0.000827942	1.00228056	0.995262053	0.981295716	0.9580052	0.928714299
0.00082985	1.002336533	0.995438306	0.981824237	0.958953132	0.929982026
0.000831757	1.002391325	0.995609343	0.982360524	0.959897453	0.931275495
0.000833665	1.002481423	0.995800961	0.982933039	0.960854926	0.932550586

0.000835573	1.00258508	0.996009369	0.983477634	0.96178123	0.933817507
0.00083748	1.002662449	0.996196572	0.983975664	0.96267817	0.935037857
0.000839388	1.002734062	0.996362684	0.984445076	0.963562615	0.936233731
0.000841296	1.002790852	0.996511464	0.984882096	0.964409088	0.937418608
0.000843203	1.002853273	0.996663672	0.985282979	0.965232928	0.93856445
0.000845111	1.002904308	0.996818078	0.985677391	0.966040299	0.939697967
0.000847019	1.002932647	0.996975883	0.986054719	0.966807532	0.940784769
0.000848927	1.002949645	0.9971407	0.986435006	0.967558713	0.94183837
0.000850834	1.002947378	0.997271386	0.986753317	0.968252608	0.942823185
0.000852742	1.00287596	0.997329413	0.987002142	0.96887207	0.943746331
0.00085465	1.002805611	0.997349956	0.987222788	0.969397164	0.94458239
0.000856557	1.002673821	0.997335456	0.987381113	0.96987989	0.945378949
0.000858465	1.002496239	0.997284687	0.987477336	0.97030737	0.946123392
0.000860373	1.002274846	0.99717944	0.987527397	0.970693082	0.946806437
0.00086228	1.002036797	0.997049842	0.987548469	0.971044542	0.947423675
0.000864188	1.001773904	0.996892156	0.987532665	0.971331374	0.948015572
0.000866096	1.001494014	0.996708682	0.987499734	0.971600356	0.948564679
0.000868004	1.001250213	0.996562632	0.987514225	0.971882028	0.949095179
0.000869911	1.001031227	0.996435882	0.987566905	0.972180679	0.949648595
0.000871819	1.000825629	0.996329728	0.987616933	0.972526598	0.950237504
0.000873727	1.000685958	0.996285769	0.987757698	0.972910865	0.950872777
0.000875634	1.000602045	0.996266226	0.98791276	0.973349084	0.951579404
0.000877542	1.000543725	0.996266226	0.988091249	0.973804965	0.952322105
0.00087945	1.000493537	0.996310193	0.988295688	0.974286962	0.953081679
0.000881357	1.000460841	0.996354141	0.988499806	0.974804858	0.953884631
0.000883265	1.000439816	0.996409049	0.988727096	0.975349785	0.954674231
0.000885173	1.000450329	0.996484651	0.988952682	0.975895919	0.955461481
0.000887081	1.000463177	0.996550451	0.989175269	0.976421985	0.956216822
0.000888988	1.000511048	0.996638118	0.989431216	0.976918255	0.956959109
0.000890896	1.000556559	0.996747592	0.989678872	0.977386369	0.957700794
0.000892804	1.000600879	0.99686666	0.989915695	0.977864453	0.958438767
0.000894711	1.000656831	0.996995287	0.990185612	0.978349605	0.959194547
0.000896619	1.000734869	0.997144332	0.990453651	0.978850122	0.959931166
0.000898527	1.00077677	0.997245989	0.990692842	0.979317128	0.960673206
0.000900434	1.000811672	0.997333039	0.990912328	0.979784205	0.961394692
0.000902342	1.000837258	0.997440534	0.991133974	0.980223649	0.962113998
0.00090425	1.000848886	0.997522585	0.991348821	0.980666043	0.962849275
0.000906158	1.000859349	0.99759372	0.991554352	0.981126488	0.963592793
0.000908065	1.000903513	0.997682866	0.991782441	0.981613043	0.964339922
0.000909973	1.00096275	0.997783958	0.992031684	0.982080301	0.965090586
0.000911881	1.0010057	0.99788975	0.99226645	0.982531141	0.965817819
0.000913788	1.001045148	0.997996624	0.992503268	0.98297385	0.966521812
0.000915696	1.001088056	0.998099782	0.992766106	0.983413906	0.967235404
0.000917604	1.001123989	0.998188455	0.993014484	0.983872947	0.967949586

0.000919511	1.001151798	0.998262685	0.993242208	0.98431843	0.968642199
0.000921419	1.001183072	0.998308151	0.993460687	0.98474105	0.969306067
0.000923327	1.001212018	0.998377505	0.99367999	0.985138309	0.969929711
0.000925235	1.001223594	0.998420527	0.993865117	0.985510403	0.970523694
0.000927142	1.001222437	0.998448002	0.994032462	0.985858849	0.971098446
0.00092905	1.001246741	0.99849696	0.994224467	0.986230366	0.971645393
0.000930958	1.001265254	0.99853754	0.99440494	0.98659956	0.972196614
0.000932865	1.001310363	0.99861507	0.994580145	0.986971725	0.97274194
0.000934773	1.001376247	0.998724694	0.994792242	0.987373201	0.973328925
0.000936681	1.001462856	0.998856784	0.995024937	0.98780371	0.973965769
0.000938588	1.001565516	0.999027862	0.995268221	0.988255088	0.974621901
0.000940496	1.001703733	0.99922468	0.99554047	0.988729706	0.975309898
0.000942404	1.001845164	0.999403343	0.995807097	0.98922468	0.976018002
0.000944312	1.002000112	0.999599344	0.996068137	0.989703481	0.976723308
0.000946219	1.002114698	0.999761959	0.996302867	0.990145614	0.977392002
0.000948127	1.002209682	0.99989842	0.996510245	0.990538579	0.978030065
0.000950035	1.002275989	1.000008846	0.996669756	0.990889243	0.978611234
0.000951942	1.002313691	1.000080431	0.996801069	0.991226099	0.979155567
0.00095385	1.002353659	1.000170709	0.996918859	0.991528839	0.979653669
0.000955758	1.002379913	1.000237478	0.99704257	0.991801535	0.980132254
0.000957665	1.002391325	1.000299516	0.997168546	0.992055817	0.980595618
0.000959573	1.002391325	1.000360341	0.997288314	0.992287999	0.981032853
0.000961481	1.002384478	1.000401256	0.997387405	0.992491881	0.981426297
0.000963389	1.002374206	1.000411774	0.997491221	0.992681508	0.981799567
0.000965296	1.002367358	1.000417617	0.997559968	0.992865775	0.98214596
0.000967204	1.002354801	1.000400087	0.99763228	0.993066109	0.982483387
0.000969112	1.002328539	1.000356833	0.997676845	0.993253519	0.982859551
0.000971019	1.002333107	1.000355663	0.997741849	0.993466959	0.98327008
0.000972927	1.002335391	1.000389568	0.997833262	0.993712535	0.983671361
0.000974835	1.002374206	1.000463177	0.997967816	0.993968801	0.984087758
0.000976742	1.002415285	1.000536723	0.998105776	0.994231941	0.984496242
0.00097865	1.002432395	1.000592717	0.998214801	0.994509352	0.984922369
0.000980558	1.002433535	1.000607875	0.998323701	0.994742666	0.985328493
0.000982466	1.002426692	1.000610207	0.998396628	0.994948254	0.985730786
0.000984373	1.002402735	1.000602045	0.998437252	0.995127506	0.986101314
0.000986281	1.002371924	1.000579888	0.998467111	0.995297821	0.98643235
0.000988189	1.002347951	1.000553059	0.998488603	0.995467858	0.986720194
0.000990096	1.002321687	1.000535557	0.998511285	0.995630242	0.987004786
0.000992004	1.002283988	1.000529722	0.99854112	0.995775187	0.987284821
0.000993912	1.002242842	1.000518051	0.99856856	0.995891732	0.987576122
0.000995819	1.002250844	1.000553059	0.998655598	0.996025289	0.987854961
0.000997727	1.002257703	1.000605543	0.99875327	0.996177011	0.988131901
0.000999635	1.002248558	1.000641681	0.998821103	0.996317519	0.988400404
0.001001543	1.002267989	1.000682463	0.998912658	0.996491964	0.988691853

0.00100345	1.002338816	1.000756986	0.999020741	0.996686788	0.989016504
0.001005358	1.002401594	1.000823303	0.999145293	0.996915219	0.98938708
0.001007266	1.002480283	1.000909323	0.999307548	0.997152808	0.989738443
0.001009173	1.0025976	1.001024266	0.999496674	0.997401898	0.990124964
0.001011081	1.002710199	1.001165699	0.999687759	0.997675641	0.99050899
0.001012989	1.002829446	1.00130805	0.999880786	0.997951007	0.990903351
0.001014896	1.002914511	1.001405127	1.000045232	0.998178873	0.991278527
0.001016804	1.002984762	1.001491706	1.000181255	0.99837631	0.991616834
0.001018712	1.003060608	1.001592026	1.000326424	0.998573331	0.991945273
0.00102062	1.003127336	1.001674957	1.000438648	0.998749699	0.992279126
0.001022527	1.0031861	1.001748603	1.000550725	0.998916223	0.992580413
0.001024435	1.003259491	1.001834824	1.000663822	0.999101422	0.992867036
0.001026343	1.003289957	1.00190603	1.000750002	0.999248364	0.993125258
0.00102825	1.003333941	1.001951937	1.000830281	0.999386793	0.993386653
0.001030158	1.003372265	1.001996672	1.000922102	0.999532091	0.993626144
0.001032066	1.003411697	1.00207232	1.00100686	0.999680689	0.993868866
0.001033973	1.00345336	1.002123858	1.001086897	0.999833745	0.994111051
0.001035881	1.00347137	1.002169642	1.001166857	0.999987711	0.994346475
0.001037789	1.003485999	1.002213113	1.001239798	1.000150785	0.994586352
0.001039697	1.003527622	1.002273704	1.001345045	1.000334612	0.994847987
0.001041604	1.003556856	1.002315976	1.001443233	1.000491202	0.995113918
0.001043512	1.003553484	1.002334249	1.001505551	1.000648674	0.995340972
0.00104542	1.003571469	1.002357084	1.001552835	1.000798877	0.995552772
0.001047327	1.003588327	1.002375348	1.00159894	1.000934879	0.9957359
0.001049235	1.003565849	1.002331965	1.001593178	1.001047468	0.995881923
0.001051143	1.003521998	1.002274846	1.001560905	1.001112399	0.99600692
0.00105305	1.003479247	1.002239412	1.001522853	1.001165699	0.996117084
0.001054958	1.003412824	1.002160487	1.001467473	1.001172648	0.996181902
0.001056866	1.003308004	1.002058571	1.001393576	1.001161065	0.996229572
0.001058774	1.00318384	1.001958821	1.001294173	1.001099649	0.996246679
0.001060681	1.003057213	1.001829078	1.001180755	1.0010057	0.996210018
0.001062589	1.002895238	1.001685317	1.001021945	1.000867486	0.996139102
0.001064497	1.002678369	1.001513626	1.000823303	1.000710417	0.996049775
0.001066404	1.002476863	1.001324237	1.00063935	1.000541391	0.995935862
0.001068312	1.002296556	1.001168015	1.000485364	1.000412943	0.995842677
0.00107022	1.002102102	1.000997576	1.000343969	1.000288985	0.995754318
0.001072127	1.001945053	1.000852374	1.000237478	1.000189456	0.995739584
0.001074035	1.001850908	1.000769788	1.000187113	1.000149613	0.995755546
0.001075943	1.001779653	1.000722062	1.000180083	1.000134374	0.99581814
0.001077851	1.001727897	1.000712746	1.000214056	1.000157818	0.995934636
0.001079758	1.0017348	1.000745346	1.000287814	1.000238649	0.996088942
0.001081666	1.001764705	1.00079306	1.000368525	1.000338121	0.996278441
0.001083574	1.001821034	1.000853536	1.000455001	1.000446825	0.996471242
0.001085481	1.001881919	1.000933717	1.000548392	1.000592717	0.996673406

0.001087389	1.001984057	1.001047468	1.000681298	1.000747674	0.996910364
0.001089297	1.002104392	1.001177281	1.000827955	1.000930233	0.997144332
0.001091204	1.00220625	1.001286077	1.00096275	1.001092693	0.997369286
0.001093112	1.002288558	1.001380868	1.001089215	1.00126294	0.997574435
0.00109502	1.002375348	1.001460548	1.001195809	1.0013878	0.997755086
0.001096928	1.002384478	1.001491706	1.001234011	1.001446696	0.997890951
0.001098835	1.002395889	1.001520546	1.001264097	1.001470935	0.997987022
0.001100743	1.002384478	1.001555141	1.001272196	1.001473244	0.998065008
0.001102651	1.002315976	1.0015217	1.001230539	1.001415521	0.998104577
0.001104558	1.002219974	1.001468627	1.001194651	1.001371625	0.998097384
0.001106466	1.002136451	1.001413211	1.00115759	1.001362381	0.998114167
0.001108374	1.0020643	1.001379713	1.001144846	1.00133233	0.998134542
0.001110281	1.002006992	1.001339266	1.001120512	1.001293016	0.998157309
0.001112189	1.00190029	1.001259469	1.001059067	1.001244427	0.998151318
0.001114097	1.001785402	1.001188862	1.000992933	1.001192336	0.998129748
0.001116005	1.001633502	1.001074142	1.000909323	1.001099649	0.99809019
0.001117912	1.001494014	1.00094417	1.000810509	1.001010342	0.998031422
0.00111982	1.0013878	1.000877947	1.000760478	1.000926748	0.99797862
0.001121728	1.001324237	1.000838421	1.000718568	1.000863999	0.997973818
0.001123635	1.001247899	1.000789569	1.000670813	1.000801203	0.997961813
0.001125543	1.001185388	1.000755822	1.000649839	1.000761642	0.9979402
0.001127451	1.001130942	1.000734869	1.000642846	1.000755822	0.997908972
0.001129358	1.001069504	1.000674308	1.000612539	1.000736033	0.997881339
0.001131266	1.000980165	1.000577555	1.000579888	1.000702265	0.997838071
0.001133174	1.000881434	1.00049237	1.000514549	1.000655666	0.997785161
0.001135082	1.000762805	1.000419954	1.000424628	1.000556559	0.997729815
0.001136989	1.000623031	1.000317066	1.000328764	1.000438648	0.997666007
0.001138897	1.000493537	1.000226939	1.000259723	1.000345138	0.997614207
0.001140805	1.000408268	1.000197657	1.000231623	1.000278452	0.997584078
0.001142712	1.000350986	1.000191799	1.000209371	1.000249187	0.997614207
0.00114462	1.000301856	1.000185942	1.0002082	1.000230452	0.997663598
0.001146528	1.00025387	1.000192971	1.000204686	1.000223426	0.99772139
0.001148435	1.0002	1.0002	1.0002	1.0002	0.997765914

### C.8. Sadighian et al, Athabasca vacuum residue + pentane raw data.

Elevation (mm)	0	4860 sec	9120 sec	15780 sec	32040 sec
170	0.011179224	0.031816471	- 0.005832701	0.013937941	0.026264943

171	0.014931897	0.041406345	0.011352393	0.029814077	0.03396921
172	0.011397119	0.046336593	0.017572667	0.031220753	0.038700146
173	0.003807968	0.039067021	- 0.000827838	0.022038095	0.041163055
174	- 0.007791484	0.015976416	- 0.014498619	0.00981241	0.027111613
175	- 0.010205339	0.00991437	- 0.005548259	0.012168816	0.024767187
176	- 0.008761951	0.019928208	0.004679402	0.017914387	0.027123113
177	0.00595648	0.030518354	0.020109371	0.030113298	0.037475466
178	0.025038658	0.032203853	0.024889825	0.042843831	0.05042289
179	0.029011547	0.03349316	0.028090012	0.048449362	0.063643247
180	0.018549916	0.023766331	0.022491115	0.037717867	0.074877752
181	0.013536311	0.024893431	0.020031065	0.030847705	0.083350014
182	0.010343796	0.034503589	0.014523168	0.028609359	0.084548526
183	0.012968342	0.036588447	0.011113672	0.030100148	0.087024278
184	0.02485151	0.033766916	0.024035339	0.042018456	0.101277057
185	0.026555244	0.026681722	0.034717714	0.061822572	0.109147784
186	0.024853657	0.026764272	0.041220636	0.070182437	0.115577731
187	0.028607856	0.021265863	0.045746454	0.063083887	0.125016731
188	0.042630341	0.027892511	0.050784028	0.070168746	0.150128729
189	0.051094274	0.036419651	0.048707087	0.071668802	0.166851375
190	0.054713225	0.037561153	0.050170853	0.075703329	0.181503762
191	0.039377478	0.021811466	0.035097664	0.079747857	0.184223673
192	0.032788263	0.020052049	0.03320311	0.096239534	0.195980514
193	0.032021741	0.025615492	0.043839593	0.114378638	0.207921054
194	0.023858174	0.02831186	0.047677534	0.115557136	0.21557721
195	0.021389516	0.031576446	0.046035407	0.12430942	0.229503598
196	0.023247538	0.036383528	0.053866078	0.147119583	0.258407315
197	0.0273318	0.037065665	0.06257897	0.165305882	0.270296075
198	0.047000407	0.057322468	0.078543811	0.179356897	0.276288801
199	0.056419017	0.078409511	0.10089803	0.200793995	0.302091018
200	0.051828296	0.078475251	0.10521551	0.218935046	0.318935683
201	0.057138728	0.08450419	0.110469712	0.224923262	0.320086337
202	0.062037457	0.100925082	0.128518944	0.232314783	0.325218907
203	0.062921231	0.108408452	0.148285151	0.236879583	0.329786961
204	0.067878853	0.115574712	0.167607256	0.24752096	0.340298714
205	0.075114214	0.127747952	0.185841257	0.264033623	0.35053606
206	0.082635254	0.144183741	0.205502082	0.289652551	0.366381779
207	0.070938896	0.149849251	0.216879172	0.302245092	0.378750504
208	0.05790199	0.162736166	0.232430417	0.312196322	0.378474475

209	0.075595792	0.179079513	0.258961585	0.334390847	0.383836041
210	0.104684016	0.194558399	0.273818401	0.351141847	0.398687549
211	0.133115995	0.218694967	0.290704263	0.374078483	0.417257426
212	0.148844202	0.241383018	0.319008387	0.390285757	0.431333011
213	0.154463223	0.267146257	0.345922414	0.401376862	0.434660879
214	0.152543095	0.287357918	0.360717205	0.41222318	0.438075933
215	0.157774794	0.314427458	0.376026484	0.428602022	0.450093175
216	0.181171498	0.339847991	0.391401254	0.432854745	0.464859691
217	0.21584766	0.358851715	0.404890092	0.44157331	0.481146584
218	0.253971826	0.378953006	0.422425953	0.470765101	0.501539889
219	0.296135582	0.402566344	0.439860574	0.498093087	0.514309733
220	0.348265596	0.428005793	0.463555413	0.510900391	0.522159487
221	0.396893648	0.454100472	0.486598344	0.522536121	0.530797233
222	0.439214378	0.477469716	0.504996765	0.534209069	0.535721886
223	0.473274519	0.484450429	0.51345477	0.535178562	0.537190741
224	0.5184459	0.501894605	0.519206997	0.542710869	0.54456117
225	0.566140534	0.538322623	0.529387001	0.56080854	0.56192927
226	0.611389084	0.563240535	0.548970859	0.575862858	0.58914727
227	0.649437438	0.577006996	0.56439229	0.581845432	0.604908391
228	0.691695601	0.591312902	0.581874774	0.589179627	0.608971927
229	0.728111976	0.599024932	0.595748403	0.607218902	0.60927811
230	0.757577273	0.608167995	0.609748965	0.624087389	0.617638412
231	0.784275564	0.626745224	0.615537409	0.625250186	0.631840745
232	0.809244331	0.6532839	0.625303111	0.632860578	0.643593791
233	0.831714952	0.680067587	0.644665082	0.650246948	0.651949852
234	0.84965837	0.703895785	0.668063759	0.668570032	0.664161489
235	0.864704578	0.726277153	0.689338583	0.685593214	0.677196188
236	0.878531983	0.74364786	0.707877151	0.699529757	0.688125112
237	0.892097164	0.760386952	0.721571401	0.706392641	0.694939404
238	0.905222242	0.778043021	0.733994277	0.710216447	0.704030918
239	0.915933253	0.789582933	0.749062775	0.722732121	0.722543029
240	0.920780203	0.798464536	0.762039193	0.737045213	0.741838891
241	0.925698014	0.810501944	0.775958205	0.749851379	0.758158441
242	0.932198789	0.829254949	0.792182373	0.763093667	0.774504153
243	0.939886145	0.846040149	0.804351528	0.775583392	0.785449476
244	0.948705404	0.86065986	0.815739157	0.788631562	0.789548223
245	0.956506622	0.872603474	0.825798325	0.79984728	0.791112949
246	0.961091006	0.882669233	0.841067177	0.818324287	0.796618491
247	0.962886025	0.893160544	0.851067484	0.834865428	0.805378266
248	0.966210718	0.906367793	0.859769648	0.839072383	0.821804427
249	0.965719286	0.913804041	0.870152914	0.841326488	0.834809306

250	0.970676522	0.91958304	0.883142663	0.853894834	0.838416071
251	0.975676847	0.924165427	0.892821124	0.868372017	0.842195392
252	0.980732004	0.92948409	0.901871177	0.878806884	0.845091257
253	0.983842939	0.936296634	0.91210013	0.889975247	0.849216445
254	0.982150963	0.941574258	0.917028571	0.896115567	0.857962762
255	0.983640334	0.943122645	0.919664814	0.901102261	0.866010153
256	0.981849514	0.940208527	0.915981049	0.904264608	0.866743359
257	0.979265497	0.934503007	0.917326465	0.906965159	0.869518857
258	0.981460859	0.937077365	0.924923671	0.914430943	0.879222395
259	0.984488746	0.947593218	0.933394463	0.925180952	0.890624196
260	0.985328494	0.95111689	0.937002181	0.935891162	0.896145468
261	0.987537955	0.952043069	0.935211137	0.936709578	0.89555861
262	0.992915719	0.954739232	0.938482086	0.936803699	0.895950602
263	0.995890626	0.957191409	0.941657395	0.938100335	0.90133777
264	0.992260315	0.957543395	0.943572322	0.937742348	0.906199166
265	0.987862329	0.952902595	0.941276848	0.94020349	0.906476333
266	0.990821584	0.956793693	0.943072318	0.948629193	0.904505915
267	0.993361996	0.967236884	0.949044305	0.954992707	0.902675386
268	0.98922826	0.971596415	0.945284749	0.953324542	0.905389605
269	0.988006558	0.973245136	0.944501939	0.952950826	0.915188203
270	0.992575574	0.977055897	0.952325204	0.952778503	0.924434485
271	0.997375628	0.978098573	0.96131962	0.953920012	0.932208144
272	1.000566573	0.977252725	0.962831705	0.954837826	0.932349808
273	1.002691643	0.977102641	0.961638617	0.957792254	0.930697377
274	0.998759253	0.979765873	0.96166346	0.955995973	0.928750326
275	0.995385855	0.982087759	0.96348453	0.956289694	0.932587342
276	0.995768774	0.97913496	0.965960059	0.959274304	0.934930748
277	0.99562482	0.977969685	0.966179448	0.959082577	0.93138701
278	0.995001841	0.981795686	0.966526199	0.962081814	0.933424937
279	0.995351133	0.983416338	0.967422076	0.965087674	0.937711488
280	0.995370315	0.981921149	0.965706186	0.965916201	0.939567165
281	0.992579388	0.978961986	0.961005235	0.963499873	0.938413019
282	0.995488602	0.976479409	0.95989721	0.964628589	0.937111732
283	0.996526318	0.972408107	0.963107951	0.961992547	0.931906916
284	0.995867726	0.971592039	0.971363527	0.963216308	0.940831205
285	0.997159529	0.977839015	0.977069195	0.969002106	0.953712752
286	0.997461144	0.982901553	0.976138382	0.972397732	0.959142054
287	1.000289191	0.98307741	0.975115388	0.976934175	0.957708099
288	1.00293793	0.985349772	0.974378061	0.978366521	0.956308744
289	1.002385849	0.985091881	0.971983624	0.973141828	0.95587773
290	0.999322002	0.987623506	0.973887295	0.973817383	0.959356226

291	0.993108603	0.988931314	0.97337396	0.974801915	0.956801154
292	0.992925247	0.988968671	0.97302389	0.972481495	0.953004619
293	0.996622073	0.987376244	0.976002753	0.971579406	0.954680002
294	0.998742994	0.98410537	0.978000461	0.973772056	0.955911799
295	0.995553548	0.983744685	0.981614451	0.974288689	0.953867774
296	0.993648391	0.983071039	0.98050789	0.970645077	0.947782506
297	0.995013971	0.983316721	0.981073678	0.972134212	0.947872206
298	0.995087429	0.985300065	0.98252653	0.978768078	0.956937851
299	0.995660724	0.987012264	0.984482455	0.986402093	0.967104883
300	0.995049887	0.984437276	0.983635895	0.986353947	0.964678826
301	0.995693613	0.984370216	0.982654291	0.98649283	0.961538086
302	0.997701771	0.986005528	0.981643899	0.990479337	0.964948412
303	0.998784226	0.991666393	0.980928631	0.989537842	0.968820119
304	0.996943785	0.992625153	0.981597795	0.987906338	0.968348278
305	0.999383557	0.989372889	0.981037813	0.98556309	0.970133978
306	1.000320525	0.986370556	0.975838089	0.978097033	0.971022885
307	0.99813853	0.982805488	0.973048988	0.978026975	0.967988553
308	0.997101913	0.982255576	0.973260946	0.980706017	0.966905548
309	0.996452874	0.985906203	0.977437425	0.984729958	0.968628
310	0.997686859	0.993653925	0.982757842	0.988120691	0.972631659
311	0.999835511	0.994880001	0.981922637	0.989988215	0.97116163
312	1.001701514	0.992914391	0.982614471	0.990698269	0.971249496
313	1.006541775	0.997017747	0.98491039	0.994609609	0.977677318
314	1.008528659	1.00067097	0.987190147	0.997087479	0.979899769
315	1.004213312	1.000537111	0.986686579	0.993923013	0.976318521
316	1.002233254	0.998862718	0.985222406	0.989460954	0.974518499
317	1.00086448	0.99440629	0.982649956	0.983609875	0.972513465
318	0.998136577	0.990524657	0.981662189	0.979073185	0.972939233
319	0.997017061	0.988303543	0.980610544	0.979796868	0.974077212
320	0.99398546	0.985997442	0.975767493	0.979339843	0.972001668
321	0.995609182	0.989066495	0.975736344	0.980317647	0.974147508
322	0.996720144	0.988947511	0.980952464	0.983984581	0.977575031
323	0.994538274	0.984040878	0.978829069	0.983455729	0.977159136
324	0.995631036	0.984616623	0.97870512	0.981925067	0.977260433
325	1.000240224	0.988995246	0.985055975	0.988197127	0.982614402
326	1.006295646	0.992798731	0.988465591	0.995197003	0.987279316
327	1.005692598	0.992800411	0.988235659	0.994735106	0.985547796
328	1.002343829	0.990718632	0.98355317	0.993681416	0.980987208
329	1.00311784	0.991421702	0.984427986	0.993059113	0.981453457
330	1.004658092	0.996201614	0.990532841	0.992305049	0.986596068
331	1.003201622	0.995051781	0.994092857	0.989443875	0.988036774

332	0.999111923	0.987824783	0.99243443	0.987874501	0.986601633
333	0.996667688	0.984143539	0.989207051	0.989321439	0.983835352
334	0.99453822	0.985134682	0.98909991	0.990921435	0.983293588
335	0.99847784	0.990332084	0.993122927	0.993038864	0.985833579
336	1.003173658	0.99498116	0.996707406	0.995548866	0.987508974
337	1.003794484	0.994971301	0.994237292	0.994899619	0.985877801
338	1.004319147	0.990904485	0.991404261	0.99420524	0.986774198
339	1.003688347	0.98876267	0.988941251	0.996446096	0.988464502
340	0.99573852	0.984209699	0.98746813	0.994337388	0.983396295
341	0.994078549	0.986013933	0.98662543	0.992775266	0.979738752
342	0.997593335	0.98964969	0.98571569	0.990870483	0.980054173
343	0.997326113	0.98808904	0.980273175	0.985991076	0.979931296
344	0.997782988	0.987611809	0.980540089	0.986431925	0.982686982
345	0.999370729	0.988649369	0.982498036	0.9920494	0.986734513
346	1.000072465	0.98868191	0.982077036	0.996809881	0.986892604
347	1.000759267	0.993969946	0.984575104	0.997169065	0.988164208
348	1.002649887	0.99857385	0.989411813	0.99632945	0.988383574
349	1.004314449	0.999401497	0.994725354	0.996432188	0.9869077
350	1.003408869	0.996940271	0.994804041	0.995222676	0.983106025
351	1.00251908	0.99560594	0.993502307	0.996449126	0.984321325
352	1.004795634	0.993688816	0.995168119	0.995450761	0.989164105
353	1.002812202	0.992315084	0.997674618	0.992064437	0.99349891
354	1.000812201	0.993082641	0.995334705	0.992431925	0.992163151
355	1.00247927	0.99497514	0.99196135	0.997154054	0.990619599
356	1.002277291	0.99136489	0.990347641	0.995233823	0.991013007
357	1.002217953	0.99203091	0.992435494	0.993717528	0.99175838
358	1.005667041	0.995819108	0.993534209	0.999111553	0.993187815
359	1.009126135	0.998217804	0.992759761	1.002340494	0.996423511
360	1.008860223	0.997145161	0.989696976	1.001182011	0.996669523
361	1.008775772	0.993495632	0.985977726	0.999706079	0.993989894
362	1.011238041	0.991380591	0.987134126	1.000140737	0.996298504
363	1.012996372	0.996018075	0.990181786	1.001366817	0.999833476
364	1.009656294	0.999936511	0.992385073	1.003470174	1.001632979
365	1.007465098	1.001305059	0.994678377	1.005893668	1.002707843
366	1.005131867	0.997132266	0.992764893	1.002625041	0.999250328
367	1.000121643	0.990834425	0.987746827	0.998922492	0.995081745
368	0.997510451	0.991078046	0.988740844	0.997835736	0.99284806
369	0.995887175	0.993248931	0.990784473	0.998764252	0.991434435
370	0.997323051	0.995008795	0.991240039	0.996180266	0.992177805
371	1.001892086	0.997328015	0.992101972	0.995558804	0.993007579
372	1.005359249	0.997062527	0.994264886	0.995700859	0.996962624

373	1.005544063	0.997910896	0.993547413	0.996169315	0.999209795
374	1.004455192	0.998366367	0.992067132	0.996055113	0.999313384
375	1.004214661	0.995533471	0.993834882	0.99752603	0.998341071
376	1.003734476	0.99476063	0.997645527	1.001379248	0.998049528
377	1.005131505	0.992017184	0.998486224	1.001529781	0.997927085
378	1.005628627	0.991857832	0.996571044	1.001162319	0.997333126
379	1.006460368	0.995691961	0.994247121	1.001596372	1.000527595
380	1.005663161	0.998637885	0.992777668	1.004231431	1.002596998
381	1.004745203	0.996579849	0.989846865	1.006916888	0.998846391
382	1.003330528	0.994722485	0.989138178	1.007294728	0.997006245
383	1.002496862	0.998355505	0.991277636	1.007245099	0.99643572
384	1.002301857	0.998191929	0.99134086	1.003042417	0.992018125
385	1.006249205	0.998954113	0.992346889	1.00193992	0.990060009
386	1.00777318	0.997717455	0.995904648	1.004435597	0.990800731
387	1.009102241	0.998853851	0.998313901	1.007669666	0.995447231
388	1.008430699	0.998454557	0.99851388	1.007653123	0.997278496
389	1.008274986	1.000787149	0.999743353	1.005809333	0.99607116
390	1.009669393	1.006145182	1.000119646	1.005752872	0.99596016
391	1.006174048	0.999759964	0.999085474	1.000837921	0.99216774
392	1.008682795	0.996607739	1.002882657	1.003704014	0.99542459
393	1.014751463	0.99963908	1.00689451	1.006689477	1.00409494
394	1.015309342	1.000907886	1.005687255	1.002910552	1.006412865
395	1.011408966	0.998125371	1.000292153	1.001986659	1.003321472
396	1.008236159	0.997915562	0.9971309	1.002509706	0.999203398
397	1.006123104	0.997256237	0.99811648	1.003166633	0.995896025
398	1.000532973	0.992158907	0.994274058	1.00188639	0.994306051
399	1.000891835	0.989523208	0.994388441	1.001042192	0.99173988
400	1.002820346	0.989008761	0.997330617	0.999011557	0.994802504
401	1.002769511	0.992320485	1.002701913	0.996977139	1.000938333
402	1.005024155	0.996612572	1.005179167	0.995670864	1.004871827
403	1.006259827	1.002220043	1.002475362	0.996447132	1.00366886
404	1.007740546	1.008319132	1.002423583	1.000708782	1.003955473
405	1.009667919	1.007717516	1.00272414	1.003711472	1.005445182
406	1.004451323	1.000920226	0.998364699	1.003143746	1.00053364
407	1.001762881	0.99862505	0.999556386	1.005045137	0.999785415
408	1.004496177	1.001249556	1.002384012	1.009080594	1.004038952
409	1.002288827	0.999734736	0.997354848	1.005561949	1.003693784
410	0.994259112	0.997197043	0.990922473	0.998430394	0.99985358
411	0.992416203	0.997961589	0.989339042	0.991506548	0.997410819
412	0.999657941	1.000591341	0.990239659	0.993559234	1.001229335
413	1.00760944	1.001359209	0.989698423	1.002529563	1.003488157

414	1.008166862	0.999193467	0.988759239	1.003352674	1.003067065
415	1.011444493	1.001839374	0.990324147	1.002935252	1.005032998
416	1.010936911	1.002126816	0.991591722	1.001506452	1.006584507
417	1.009169284	1.004322591	0.996972496	1.003552167	1.013855499
418	1.011080643	1.005993142	1.001572307	1.005148416	1.017341915
419	1.010179529	1.00667313	1.000176692	1.00795213	1.012010361
420	1.00981035	1.007943695	1.00015154	1.010976776	1.007676667
421	1.012022832	1.009434655	1.001380293	1.011620449	1.007541357
422	1.006576028	1.004769506	0.995411043	1.006504709	1.002437273
423	1.003626439	1.00110007	0.990437058	1.002480458	0.998893018
424	1.008908803	1.005004402	0.991789526	1.002136352	1.001652196
425	1.013116808	1.004493665	0.994563313	1.004859443	1.003216786
426	1.010871489	0.997800561	0.99623377	1.006401214	1.003115252
427	1.005346151	0.993951546	0.996375119	1.005670613	1.002116141
428	1.004385105	0.997363414	0.996145508	1.00879952	1.007180968
429	1.004450432	1.002910074	0.999456747	1.009831468	1.009134841
430	1.003434149	1.000214241	0.998169068	1.00624789	1.004048733
431	1.00274479	0.996896119	0.996531994	1.003348862	0.998484749
432	1.004874146	0.998368772	1.001310203	1.006161577	1.003745948
433	1.00637435	1.000025995	1.003819696	1.010110663	1.010788037
434	1.006314783	0.999166515	1.003702556	1.012251511	1.011185151
435	1.004143763	0.996155193	1.002348708	1.010860034	1.010957718
436	1.002719464	0.996043041	1.002742234	1.009159267	1.011530749
437	1.000172026	0.995572801	1.006135431	1.008067578	1.011987363
438	0.9992788	0.993738817	1.006923793	1.006474243	1.010744492
439	0.999759305	0.995921004	0.99926597	1.006500048	1.007590302
440	1.001669829	0.998234644	0.995722959	1.008616232	1.005619481
441	0.999539631	0.992774367	0.996427489	1.004765343	1.000757859
442	0.99628002	0.991087236	0.997709719	1.001394386	0.999623923
443	0.995211023	0.997194202	0.99874275	1.003468087	1.005170296
444	0.996884156	1.002896599	0.999381959	1.00354067	1.011042962
445	1.000088715	1.005643002	0.999656643	1.000485097	1.009539846
446	1.002105509	1.006754313	1.00180205	1.00484348	1.006993417
447	0.999282476	1.003086011	0.999096457	1.006923795	1.001914535
448	0.998448717	1.002388477	0.997924921	1.007967204	1.002966739
449	1.002864386	1.005250865	1.001785259	1.009210356	1.007440827
450	1.002636968	1.006474607	1.002898891	1.011136766	1.00670095

**C.9. Sadighian et al, Athabasca atmospheric residue + pentane raw data.**

Elevation (cm)	0 Sec	3420 Sec	6780 S	14820 Sec	25980 Sec
0.276	- 0.832254326	- 0.298296603	- 0.005601565	- 1.084445195	- 0.018196391
0.368	- 0.806338604	- 0.333124305	- 0.026311355	- 1.004675937	- 0.066749545
0.46	- 0.779555066	- 0.364460551	- 0.053200853	- 0.932447908	- 0.111220732
0.552	- 0.752486319	- 0.392436726	- 0.075175382	- 0.867600607	- 0.151425192
0.644	- 0.725705887	- 0.417204893	- 0.092306889	- 0.809883747	- 0.187203508
0.736	- 0.699747188	- 0.438950517	- 0.104608182	- 0.758962249	- 0.218451667
0.828	-0.67507974	-0.45789699	0.112022559	- 0.714426201	- 0.245147195
0.92	- 0.652078682	- 0.474288053	0.11441596	- 0.675817441	- 0.267380327
1.01	- 0.631419794	- 0.488069723	0.111687714	- 0.643356887	- 0.285041478
1.1	- 0.612618492	- 0.499783652	0.103663998	- 0.615845337	- 0.299038948
1.2	- 0.593561823	- 0.510426882	0.088162677	- 0.591062853	- 0.310895183
1.29	- 0.577150715	- 0.517647511	0.067999142	- 0.574588562	- 0.318770302
1.38	- 0.559659514	- 0.521863334	0.041895888	-0.56559136	- 0.324158757
1.47	- 0.538869066	- 0.521365259	0.010654977	- 0.568814863	- 0.325800598
1.56	- 0.520420892	- 0.514906999	- 0.021606682	- 0.589193212	- 0.317963258
1.66	- 0.552618814	- 0.520700147	- 0.069553448	- 0.604438394	- 0.299162091
1.75	- 0.600932497	- 0.527037459	- 0.114168271	- 0.605600435	- -0.27999589
1.84	- 0.663043337	- 0.533860524	- 0.159945253	- 0.590408471	- 0.260385277
1.93	- 0.732355192	- 0.539286079	- 0.206305354	-0.55836162	- 0.241145819
2.02	-0.80296193	-0.54162178	- 0.252796438	- 0.511511079	- -0.22300366
2.12	- 0.873899272	- 0.538905717	- 0.302407372	- 0.447473181	- 0.204233232
2.21	- -	- -	- -	- -	- -

	0.922111477	0.532010154	0.342438872	0.385556409	0.188144126	
2.3	- 0.945827226	- 0.519989645	- 0.373842547	- 0.324542351	- 0.172231253	- 0.172231253
2.39	- 0.939246734	- 0.502585737	- 0.393991369	- -0.26905008	- 0.156550298	- 0.156550298
2.48	- 0.898905421	- 0.479739588	- 0.400518333	- 0.223580419	- 0.141621732	- 0.141621732
2.58	- 0.814888475	- 0.449711998	- 0.389911497	- 0.190357841	- 0.126927831	- 0.126927831
2.67	- 0.710222303	- 0.421097202	- 0.365138542	- 0.178621589	- 0.116244383	- 0.116244383
2.76	- 0.588478091	- 0.392922451	- 0.329871496	- 0.184362045	- 0.109052138	- 0.109052138
2.85	- 0.461428655	- 0.366208299	- 0.289609577	- 0.207445024	- 0.107546336	- 0.107546336
2.94	- 0.341583021	-0.34204196	-0.24976083	- 0.247059143	- 0.114587015	- 0.114587015
3.04	-0.23094073	- 0.320231268	- 0.210922838	- 0.306799873	- 0.134978349	- 0.134978349
3.13	- 0.158785249	- 0.306210477	-0.18300381	- 0.369069597	- 0.164536171	- 0.164536171
3.22	- 0.113566131	-0.29730781	- 0.162111371	- 0.433502146	- 0.202284691	- 0.202284691
3.31	-0.09268869	- 0.292916301	- 0.147416196	- 0.496139324	- 0.245282995	- 0.245282995
3.4	- 0.091542561	- 0.292523339	- 0.137020004	- 0.553945776	- 0.289772336	- 0.289772336
3.5	-0.10504631	- 0.295993249	-0.12715212	- 0.608155331	- 0.334457223	- 0.334457223
3.59	- 0.121484041	- 0.301542012	- 0.117204176	- 0.644539956	- 0.364796571	- 0.364796571
3.68	- 0.135175906	- 0.307547387	- 0.105471401	- 0.666761909	- 0.382394999	- 0.382394999
3.77	- 0.142503983	- 0.312349038	-0.0928423	- 0.673478793	- 0.386259992	- 0.386259992
3.86	- 0.142185414	- 0.314664236	- 0.081032984	- 0.663613174	- -0.37681179	- -0.37681179
3.96	- 0.133941781	- 0.312775792	- 0.070237258	- 0.632012183	- 0.351877523	- 0.351877523
4.05	-0.12361821	- 0.305661054	- 0.062043582	- 0.585539784	- -0.31802338	- -0.31802338
4.14	- 0.116664601	- 0.291998451	- 0.053251973	- 0.525395364	- 0.274823456	- 0.274823456
4.23	- 0.119541784	-0.27044116	- 0.041348904	- 0.456426274	- 0.223015936	- 0.223015936
4.32	- 0.137865576	- 0.239726408	- 0.023642827	- 0.384297859	- 0.162758621	- 0.162758621

4.42	- 0.179845335	- 0.193612066	0.006083106	- 0.307473641	- 0.086272239
4.51	- 0.234761023	- 0.141075518	0.043836435	- 0.245937662	- 0.009616602
4.6	- 0.298355293	-0.0790115	0.091253063	- 0.194054387	0.072514126
4.69	- 0.362370712	-0.00887767	0.144894342	- 0.152896408	0.15782254
4.78	-0.41774515	0.066632067	0.199969446	- 0.122522993	0.243781227
4.88	- 0.456148975	0.151057566	0.25769493	- 0.099650521	0.336492733
4.97	- 0.459826985	0.221624919	0.303935941	- 0.085809273	0.414284134
5.06	-0.42956046	0.282269273	0.343457642	- 0.075941699	0.483771321
5.15	- 0.364792797	0.329865544	0.375152156	- 0.069109015	0.542202369
5.24	- 0.267926233	0.362319017	0.397501115	- 0.064576743	0.586555905
5.34	- 0.129469351	0.379221083	0.409836245	- 0.059643786	0.615933006
5.43	0.012193269	0.378043023	0.409159084	- 0.052449373	0.622984112
5.52	0.156308965	0.364036787	0.396968451	- 0.041353897	0.611779344
5.61	0.289218093	0.340252789	0.372609621	- 0.026720807	0.583164085
5.7	0.396824672	0.309770631	0.336309168	- 0.010121334	0.539029226
5.8	0.470287831	0.272506547	0.285273793	0.007450803	0.476457552
5.89	0.486961241	0.239987971	0.234920016	0.018860347	0.413498709
5.98	0.457615324	0.211375274	0.185347014	0.022669079	0.349464942
6.07	0.388487063	0.18784275	0.139629622	0.015600575	0.288009588
6.16	0.289624163	0.16926228	0.099950883	- 0.004726687	0.231846444
6.26	0.162086523	0.153310478	0.066422455	- 0.041782977	0.178649921
6.35	0.047809742	0.141428202	0.04903378	- 0.082687458	0.14068803
6.44	- 0.054337637	0.130460892	0.046365732	- 0.123803152	0.112594798
6.53	- 0.139272312	0.119566783	0.05946889	- 0.159906953	0.093828227
6.62	- 0.205147085	0.10821854	0.088369038	- 0.186870469	0.083666665

6.72	- 0.254544847	0.095144547	0.138673596	- 0.200626806	0.082247059
6.81	- 0.277319726	0.084013445	0.199610284	- 0.194555994	0.09024897
6.9	-0.27896479	0.074845961	0.27290414	- 0.170306004	0.107728359
6.99	- 0.258030376	0.068461889	0.354952448	-0.12969727	0.135605818
7.08	- 0.212115268	0.064869835	0.441280327	- 0.075327133	0.17530233
7.18	- 0.130143781	0.06412344	0.536345521	- 0.001895998	0.235023228
7.27	- 0.031647761	0.067540093	0.616474526	0.072556249	0.302918727
7.36	0.081083761	0.07669552	0.686785051	0.150066991	0.380910442
7.45	0.196833481	0.093233356	0.742255407	0.225352883	0.463877059
7.54	0.303653255	0.116963358	0.776766674	0.29287192	0.544791877
7.64	0.397549152	0.147897403	0.782901389	0.35174535	0.621097152
7.73	0.45048239	0.17364802	0.755796601	0.385083764	0.667619506
7.82	0.468883859	0.190478748	0.698540549	0.396614404	0.686399086
7.91	0.450828636	0.191950816	0.614024002	0.384788638	0.673895246
8	0.395598678	0.172280894	0.507754225	0.350112414	0.629501765
8.1	0.293334042	0.12178972	0.376134922	0.289250081	0.547199669
8.19	0.172829246	0.053193386	0.259105308	0.221606297	0.452819895
8.28	0.038768234	- 0.029224843	0.155642437	0.149842301	0.350936029
8.37	- 0.095152864	- 0.116222709	0.073606659	0.080403176	0.251284687
8.46	- 0.213566761	- 0.198778204	0.018286385	0.018861225	0.162528368
8.56	-0.30507406	- 0.274936776	- 0.006987459	- 0.033426129	0.088106542
8.65	-0.33500381	- 0.322695947	0.003746712	- 0.061237178	0.051850946
8.74	- 0.308470843	- 0.347140617	0.043514993	- 0.068212239	0.050452603
8.83	- 0.224082914	- 0.346123394	0.108760795	- 0.053230164	0.087592804
8.92	- 0.097319765	- 0.322688494	0.191803654	- 0.019450593	0.159584218
9.02	0.085876226	- 0.262721396	0.299041766	0.040593122	0.283721926
9.11	0.258258161	- 0.186950571	0.40118629	0.107467687	0.421835245
9.2	0.417228532	- 0.089964916	0.50126801	0.183084105	0.576562935

9.29	0.55012619	0.020869442	0.595448223	0.263404552	0.738901825
9.38	0.649514996	0.137331288	0.680515579	0.346061539	0.900744672
9.48	0.724187339	0.264118887	0.76464686	0.439072996	1.074625478
9.57	0.748135251	0.363278151	0.827149158	0.519652205	1.217649498
9.66	0.745790589	0.445587209	0.88171024	0.596507512	1.35208586
9.75	0.727915123	0.521399092	0.928824865	0.67077546	1.479864629
9.84	0.685780406	0.569359064	0.971439165	0.738465021	1.604177294
9.94	0.656790609	0.605367177	1.025706705	0.810595433	1.750241156
10.03	0.65853379	0.624687989	1.064148346	0.852458261	1.84088608
10.12	0.688388158	0.65595802	1.137448514	0.919057423	1.992273322
10.21	0.770436611	0.688620397	1.227522525	0.982106409	2.144497404
10.3	0.911221453	0.724062121	1.336509408	1.042539058	2.293868136
10.4	1.10610915	0.761934686	1.463509896	1.101360359	2.436240761
10.49	1.33284624	0.800631778	1.601659898	1.158664604	2.569836285
10.58	1.558898489	0.839453133	1.739492864	1.213536864	2.696309648
10.67	1.75768801	0.878136508	1.863549589	1.266967884	2.825247732
10.76	1.929309597	0.919221897	1.97111554	1.322765805	2.966763834
10.86	2.050545594	0.961223758	2.052211928	1.377213525	3.116664001
10.95	2.129773841	1.002354677	2.108684091	1.433794404	3.278614736
11.04	2.129773841	1.002354677	2.108684091	1.433794404	3.278614736
11.13	2.175479668	1.043313515	2.150667218	1.501415392	3.460270074
11.22	2.191756419	1.084091361	2.18543286	1.586862757	3.667709101
11.32	2.179316479	1.125553192	2.218594225	1.696636274	3.909131887
11.41	2.139911444	1.171706193	2.256716826	1.835144231	4.192292274
11.5	2.079630313	1.231299408	2.310632379	2.009361938	4.531975925
11.59	2.010975232	1.314960802	2.393490315	2.226881706	4.946435227
11.68	1.949652176	1.429185128	2.515634861	2.492803105	5.450761663
11.78	1.908199316	1.573427365	2.680745098	2.807952489	6.052178177
11.87	1.891732403	1.742218337	2.886975381	3.170525581	6.750990613
11.96	1.90035045	1.929093984	3.131201784	3.579322125	7.544869488
12.05	1.932300092	2.129256683	3.411175388	4.032873328	8.433317452
12.14	1.932300092	2.129256683	3.411175388	4.032873328	8.433317452
12.24	1.98805346	2.337750689	3.721342491	4.527876428	9.414065246
12.33	2.073148111	2.550023189	4.051934848	5.065377344	10.47715998
12.42	2.190216108	2.767599118	4.396768419	5.646884602	11.61725295
12.51	2.342383459	2.991519882	4.750605057	6.274419977	12.83492978
12.6	2.534767262	3.220433561	5.109172404	6.953457852	14.12840109
12.7	2.768254001	3.452431941	5.475437677	7.693720137	15.4895955
12.79	3.034206043	3.685060187	5.86137698	8.506794628	16.90483834
12.88	3.317632094	3.915823846	6.283770993	9.401626432	18.35956094
12.97	3.606762387	4.143954834	6.757417713	10.3816767	19.8424819

13.06	3.89794952	4.371680584	7.292411516	11.4458701	21.34615066
13.16	4.19157504	4.599370878	7.891078855	12.59090678	22.86601608
13.25	4.487711681	4.82820038	8.557942971	13.81043624	24.39020025
13.34	4.487711681	4.82820038	8.557942971	13.81043624	24.39020025
13.43	4.789208271	5.075882032	9.317880392	15.1002799	25.90006496
13.52	5.100453625	5.352813893	10.18327722	16.46269057	27.39459805
13.62	5.422023338	5.662754611	11.16470805	17.90374746	28.87853465
13.71	5.752113558	6.012498669	12.28203492	19.43092027	30.35328121
13.8	6.089575215	6.415342592	13.55750472	21.05084798	31.81919766
13.89	6.43566446	6.892816222	15.00533692	22.76275863	33.27526887
13.98	6.795224951	7.470437767	16.62142458	24.55274856	34.71761104
14.08	7.17631694	8.169344051	18.3847074	26.3976741	36.14005822
14.17	7.588049329	9.001879394	20.2692164	28.27585809	37.53783128
14.26	8.03733971	9.973821218	22.25476282	30.17430463	38.9105734
14.35	8.516455371	11.0849812	24.33099752	32.08798013	40.25945621
14.44	8.516455371	11.0849812	24.33099752	32.08798013	40.25945621
14.54	9.011766583	12.33333926	26.47119987	33.99769145	41.58044196
14.63	9.548676037	13.72787527	28.62050073	35.86486587	42.86938416
14.72	10.14614859	15.27318817	30.7620094	37.67826699	44.12591573
14.81	10.81796684	16.97719626	32.89232914	39.43576101	45.35184199
14.9	11.60233536	18.85770334	35.00173635	41.13155077	46.55063914
15	12.57169779	20.93664691	37.08496006	42.76706185	47.73187299
15.09	13.81988623	23.22708446	39.14542714	44.35577624	48.91198792
15.18	15.4250934	25.72168073	41.1917468	45.91811088	50.10754413
15.27	17.42277406	28.39679175	43.23012234	47.4709547	51.3277659
15.36	19.81185968	31.22690781	45.26239487	49.02345062	52.57474217
15.46	22.59052905	34.19758564	47.28748907	50.57825874	53.84790173
15.55	25.75207438	37.27735233	49.29797682	52.13515792	55.14251391
15.64	25.75207438	37.27735233	49.29797682	52.13515792	55.14251391
15.73	29.23703495	40.40074316	51.28590344	53.69739081	56.44998524
15.82	33.01256605	43.55193554	53.25034192	55.264478	57.76486157
15.92	37.08032336	46.73654215	55.19662032	56.84001963	59.08660806
16.01	41.42431783	49.94813325	57.13128931	58.43126445	60.41571594
16.1	45.97841676	53.16802536	59.06292217	60.04720237	61.75519703
16.19	50.61980208	56.36594341	61.00071223	61.69556056	63.1108057
16.28	55.20221265	59.50756579	62.95116026	63.37674667	64.48641608
16.38	59.60924729	62.56445018	64.91430527	65.08228504	65.88014354
16.47	63.78140689	65.51955838	66.88486482	66.80017311	67.28619019
16.56	67.70494479	68.36741659	68.85712067	68.52161894	68.69968872
16.65	71.3840978	71.11050489	70.83128951	70.24465967	70.12020453
16.74	71.3840978	71.11050489	70.83128951	70.24465967	70.12020453

16.84	74.79448752	73.73576902	72.79786313	71.95682069	71.5394744
16.93	77.88265512	76.2048701	74.72102057	73.62337723	72.93175283
17.02	80.64218064	78.50209032	76.58039498	75.22864416	74.28462591
17.11	83.07337028	80.62132406	78.36584674	76.76617349	75.59311358
17.2	85.1707551	82.55282689	80.06209211	78.22519285	76.84865467
17.3	86.95083225	84.29547222	81.6569991	79.5988453	78.04461223
17.39	88.46205908	85.86325732	83.14990402	80.88974513	79.18100463
17.48	89.76969957	87.28029208	84.55043601	82.10784659	80.26406334
17.57	90.92801465	88.56904243	85.87017689	83.26349716	81.30160835
17.66	91.96793495	89.74435605	87.11697724	84.36377653	82.29962569
17.76	92.90318728	90.81377486	88.29640184	85.41347314	83.26241482
17.85	93.75302102	91.7850886	89.40943082	86.41447281	84.19077658
17.94	93.75302102	91.7850886	89.40943082	86.41447281	84.19077658
18.03	94.54193813	92.66946756	90.44669995	87.36278443	85.07848115
18.12	95.25975923	93.46290129	91.39778081	88.25174805	85.91868656
18.22	95.89951509	94.16222184	92.25739743	89.07815134	86.70866313
18.31	96.463325	94.76873515	93.02010811	89.83864013	87.44592222
18.4	96.95376375	95.28776486	93.68227951	90.53024319	88.12853426
18.49	97.37632319	95.73136723	94.24784068	91.15391679	88.75732202
18.58	97.74102273	96.11626105	94.73000113	91.71604498	89.33656285
18.68	98.05951386	96.4576502	95.14624222	92.22641449	89.8724763
18.77	98.34043152	96.76508278	95.51109953	92.69434058	90.37068592
18.86	98.58815276	97.0433527	95.83321191	93.1265207	90.8351461
18.95	98.80494302	97.29446097	96.11669061	93.52693986	91.26807434
19.04	98.80494302	97.29446097	96.11669061	93.52693986	91.26807434
19.14	98.99658224	97.52131648	96.36958307	93.90006424	91.67240617
19.23	99.17166859	97.72865891	96.60480156	94.25148055	92.05368909
19.32	99.32837761	97.9137079	96.8217667	94.57885651	92.4120307
19.41	99.46459267	98.07439773	97.01901068	94.8801604	92.74789809
19.5	99.58071759	98.21198798	97.19811004	95.15622885	93.06388298
19.6	99.67859916	98.33049747	97.36128001	95.41001381	93.36309599
19.69	99.76270903	98.43643273	97.51189826	95.64614557	93.64837273
19.78	99.83860189	98.53601123	97.65366867	95.8688952	93.92168039
19.87	99.9099623	98.6327763	97.78928066	96.08087962	94.18432782
19.96	99.97760425	98.72775583	97.9201895	96.28355115	94.4376215
20.06	100.0420083	98.8209572	98.04785077	96.47763278	94.68286227
20.15	100.1043318	98.91295159	98.17495818	96.66384651	94.9212578
20.24	100.1043318	98.91295159	98.17495818	96.66384651	94.9212578
20.33	100.1624972	99.00462241	98.30378034	96.84345871	95.15403072
20.42	100.2125586	99.09528819	98.43273192	97.01606766	95.38051367
20.52	100.2512918	99.18478674	98.56023475	97.18217738	95.60077194

20.61	100.2744895	99.27313758	98.68526722	97.34347807	95.81555015
20.7	100.27838	99.35957888	98.80625748	97.50154217	96.02553531
20.79	100.2641798	99.44244052	98.92184096	97.6570047	96.23133762
20.88	100.2402571	99.51969034	99.03096297	97.80939706	96.43305907
20.98	100.2184474	99.58970665	99.13391257	97.9575791	96.6298731
21.07	100.2077027	99.65166054	99.23141356	98.10021512	96.820229
21.16	100.2118172	99.70553793	99.32448372	98.23611253	97.00265544
21.25	100.2339562	99.75148815	99.41425148	98.36402449	97.17610001
21.34	100.2339562	99.75148815	99.41425148	98.36402449	97.17610001
21.44	100.278315	99.78933589	99.50111039	98.48194515	97.3384347
21.53	100.3394357	99.81950287	99.58372098	98.58855564	97.48694392
21.62	100.4075419	99.84243994	99.66027283	98.68470705	97.62123677
21.71	100.4745901	99.85839103	99.72966055	98.77119121	97.74144583
21.8	100.5297972	99.86811944	99.79087662	98.84870667	97.84812961
21.9	100.5604692	99.87328361	99.84318145	98.91886397	97.94328831
21.99	100.559051	99.87580693	99.88655659	98.98367099	98.02955633
22.08	100.5283834	99.87666327	99.9218206	99.04392566	98.10897623
22.17	100.4784987	99.87564051	99.95013996	99.09893637	98.18285264
22.26	100.419495	99.87232423	99.97270166	99.14779017	98.25222746
22.36	100.3585942	99.86673061	99.99062368	99.19013165	98.31795316
22.45	100.305907	99.85869458	100.0047183	99.22581666	98.38054503
22.54	100.305907	99.85869458	100.0047183	99.22581666	98.38054503
22.63	100.2722955	99.84718123	100.0151247	99.25465571	98.43970511
22.72	100.2586281	99.83139081	100.021125	99.27626351	98.49414879
22.82	100.2653002	99.81081646	100.0217459	99.28997968	98.54258887
22.91	100.2926427	99.78504665	100.0164459	99.29503612	98.58366812
23	100.3345431	99.75370335	100.0054571	99.291383	98.61656199
23.09	100.3776686	99.71670479	99.98950461	99.28049624	98.64230444
23.18	100.4072086	99.67487856	99.97001485	99.26547584	98.66403983
23.28	100.4143907	99.63001533	99.94820057	99.24988797	98.68516429
23.37	100.3984152	99.58410915	99.92474229	99.23646028	98.70765206
23.46	100.3627157	99.53846133	99.90015662	99.22670606	98.73204334
23.55	100.3106884	99.49334891	99.87535699	99.22112354	98.75821349
23.64	100.3106884	99.49334891	99.87535699	99.22112354	98.75821349
23.74	100.2477034	99.44957776	99.85258183	99.22014595	98.78581035
23.83	100.1833229	99.4095654	99.83430976	99.2244673	98.81373814
23.92	100.1223959	99.37437936	99.82109659	99.23384116	98.8408195
24.01	100.0675691	99.34476844	99.81367778	99.24827408	98.86679488
24.1	100.0220329	99.32220145	99.81254955	99.2677616	98.89193535
24.2	99.98643042	99.30793415	99.81607181	99.2915487	98.91654368
24.29	99.95713755	99.30143867	99.82104587	99.31817461	98.94074308

24.38	99.92793867	99.29991056	99.82450135	99.34569407	98.96448466
24.47	99.89362468	99.29984575	99.8249266	99.37219632	98.98784536
24.56	99.85150748	99.29867993	99.82204536	99.39644904	99.01112728
24.66	99.798963	99.29466424	99.81624425	99.41760905	99.03461403
24.75	99.7338959	99.28579316	99.80861949	99.43495265	99.05903572
24.84	99.7338959	99.28579316	99.80861949	99.43495265	99.05903572
24.93	99.66191579	99.27136428	99.80175764	99.44928885	99.08586398
25.02	99.58996277	99.2526369	99.79748196	99.46223277	99.1161936
25.12	99.52304388	99.23079384	99.79623852	99.47485325	99.15092169
25.21	99.46771215	99.20755431	99.79815938	99.4881358	99.19029724
25.3	99.43190505	99.18571827	99.80304639	99.50318041	99.2331367
25.39	99.44232436	99.17483823	99.81269245	99.52447533	99.27523781
25.48	99.45972829	99.16620081	99.81481793	99.54530498	99.3140521
25.58	99.47730088	99.15657041	99.81263656	99.56562393	99.35123906
25.67	99.49763078	99.14615039	99.80814386	99.58599412	99.38770951
25.76	99.52282767	99.13545231	99.8019819	99.60674276	99.42371838
25.85	99.55409421	99.12487308	99.79422238	99.62802251	99.45928378
25.94	99.55409421	99.12487308	99.79422238	99.62802251	99.45928378
26.04	99.59199002	99.11465809	99.78469593	99.64987104	99.49433834
26.13	99.63659777	99.10490784	99.77313515	99.67224656	99.5287884
26.22	99.68770444	99.09561757	99.75929712	99.69507418	99.56255213
26.31	99.74491703	99.08670838	99.74300238	99.7182729	99.59557126
26.4	99.8077364	99.07804779	99.72412886	99.74176588	99.62781202
26.5	99.87561358	99.06946942	99.70260327	99.7654847	99.65926357
26.59	99.9480016	99.06079827	99.67839287	99.78937004	99.68993339

### C.10. Wen et al, Cold Lake bitumen + heptane.

Elevation	138 min	319 min	606 min	1398 min	1753 min
-0.848	0.034388715	0.052507837	0.082445141	0.135360502	0.161786834
-0.795	0.039717868	0.059216301	0.089529781	0.144420063	0.172163009
-0.742	0.043730408	0.066238245	0.097899687	0.151912226	0.182163009
-0.689	0.049435737	0.074984326	0.108181818	0.160909091	0.194357367
-0.636	0.056363636	0.083448276	0.117899687	0.172664577	0.207711599
-0.583	0.067053292	0.09354232	0.129090909	0.18645768	0.222727273
-0.53	0.078871473	0.106896552	0.143134796	0.200846395	0.240815047
-0.477	0.09169279	0.123448276	0.162288401	0.219028213	0.263667712
-0.424	0.110532915	0.143166144	0.185172414	0.239310345	0.28984326
-0.371	0.134639498	0.167272727	0.211974922	0.262758621	0.318401254
-0.318	0.161097179	0.193009404	0.243166144	0.290752351	0.346990596
-0.265	0.210031348	0.232476489	0.283730408	0.323667712	0.376739812
-0.212	0.294984326	0.304702194	0.331974922	0.357931034	0.405266458

-0.159	0.38137931	0.384702194	0.380094044	0.38984326	0.430031348
-0.106	0.442100313	0.428495298	0.421034483	0.416990596	0.451630094
-0.053	0.502068966	0.457429467	0.46	0.442978056	0.474890282
0	0.577774295	0.506332288	0.498181818	0.469655172	0.499310345
0.053	0.658369906	0.564169279	0.537492163	0.496489028	0.523291536
0.106	0.741504702	0.617492163	0.577680251	0.522695925	0.54523511
0.159	0.832476489	0.672915361	0.619090909	0.548840125	0.568056426
0.212	0.924106583	0.732727273	0.660658307	0.574890282	0.592131661
0.265	0.978831843	0.795478707	0.703458195	0.60033769	0.616846976
0.318	0.994626679	0.860637301	0.749203374	0.628241175	0.640987192
0.371	0.995164863	0.922481829	0.79658109	0.657266744	0.665502074
0.424	0.996044476	0.965770704	0.850375308	0.686267792	0.691188837
0.477	0.996545715	0.985716064	0.909348354	0.716095102	0.717806685
0.53	0.996390678	0.991038925	0.956501447	0.747534149	0.74619621
0.583	0.995183344	0.99384711	0.980142946	0.779055314	0.775046613
0.636	0.995932688	0.996802037	0.988667412	0.813928217	0.805017387
0.689	0.996247015	0.998511212	0.992866226	0.850562948	0.835364908
0.742	0.995386568	0.997337214	0.994364802	0.886583893	0.867758615
0.795	0.995171475	0.996316702	0.995388139	0.922619785	0.90222236
0.848	0.996098467	0.997553801	0.99523146	0.953553182	0.935067348
0.901	0.997211464	0.998853602	0.996343919	0.975646785	0.960836561
0.954	0.995235296	0.997122614	0.996411002	0.986015284	0.976640574
1.007	0.994741889	0.995793511	0.995020259	0.992236553	0.986421701
1.06	0.996872387	0.996717555	0.994828601	0.995355031	0.992815781
1.113	0.996533259	0.996285635	0.995264184	0.995078466	0.993499861
1.166	0.994774112	0.995763629	0.993877362	0.993815517	0.993104301
1.219	0.995327681	0.997524599	0.993966211	0.995389566	0.995296739
1.272	0.996009404	0.997432407	0.994277053	0.99579286	0.996566232
1.325	0.994930292	0.996723237	0.994281122	0.994775727	0.995641287

### C.11. Zhang et al, Athabasca bitumen + pentane raw data.

distance (cm)	210 min	330 min	630 min	1470 min	2910 min	5790 min
0.0192787 5	0.00478815 4	0.00392469 6	0.00030872 6	0.00731389	0.00848940 6	0.00277093 9
0.0578362 5	0.00477234 8	0.00380046 8	0.00107555 5	0.00745987 8	0.00652790 2	0.00143829 4
0.0963937 5	0.00353508	0.00351532	0.00035646 9	0.00544293 6	0.00461415 4	- 0.00029230 1
0.1349512 5	0.00278407 4	0.00312627 9	0.00042314 1	0.00528105 8	0.00337172 7	- 0.00126012 4
0.1735087 5	0.00544467 5	0.00488960 1	0.00178275 2	0.00677072 8	0.00328557 9	- 0.00121155 9
0.2120662 5	0.00718200 6	0.00574961 8	0.0026805	0.00656086 6	0.00363831 9	-7.63561E- 05

0.2506237 5	0.00886646 7	0.00588187 8	0.00307728	0.00711333 2	0.00370901 2	0.00064367 8
0.2891812 5	0.00777820 1	0.00671652 5	0.00396733 8	0.00674587 3	0.00354645 4	-2.98179E- 05
0.3277387 5	0.00634585 4	0.00546354 8	0.00297824 6	0.00593100 1	0.00314637 6	0.00113713 8
0.3662962 5	0.00665352 6	0.00645894 2	0.00507789 4	0.00541749 7	0.00458925 1	0.00193687 9
0.4048537 5	0.00493038 6	0.00558087 7	0.00258712 8	0.00416006 8	0.00424353 5	- 0.00039921 7
0.4434112 5	0.00440865 9	0.00522286 3	0.00159978 5	0.00248845 2	0.00309767 7	- 0.00184750 1
0.4819687 5	0.00356875 7	0.00537839 3	0.00033012 1	0.00294256 5	0.00289573 8	- 0.00123412 3
0.5205262 5	0.00504913 7	0.00551986 5	0.00168856 1	0.00412286 8	0.00391472	- 0.00051695 3
0.5590837 5	0.00422278 2	0.00502021 6	0.00195953	0.00373753 3	0.00288536 9	- 0.00127557 7
0.5976412 5	0.00421191 3	0.00352528 4	0.00232066	0.00460392 8	0.00191669 6	0.00019470 8
0.6361987 5	0.00356498 7	0.00468126 2	0.00224683 3	0.00454830 7	0.00257719 1	0.00095574 5
0.6747562 5	0.00307569 9	0.00353486 1	0.00014084 8	0.00510085	0.00332709 8	- 0.00027021 2
0.7133137 5	0.00567963 9	0.00532354	0.00119445 5	0.00698060 9	0.00507981 3	0.00242290 8
0.7518712 5	0.00597337 3	0.00529610 6	0.00200081 1	0.00775783 1	0.00636540 1	0.00104268 2
0.7904287 5	0.00613475 4	0.00610248 9	0.00239589	0.00668125 2	0.00563908	0.00054769 4
0.8289862 5	0.00386429 5	0.00623750 7	0.00092534 1	0.00584328 1	0.00463803 7	0.00089406 5
0.8675437 5	0.00403738 9	0.00448464 4	0.00019649 1	0.00365655 7	0.00427164 1	0.00076587 5
0.9061012 5	0.00353430 8	0.00445752 4	- 0.00047265 4	0.00361228 4	0.00389141 6	0.00104410 4
0.9446587 5	0.00496558 2	0.00429765 5	0.00135308 6	0.00528251 5	0.00509785 4	0.00264888 2
0.9832162 5	0.00510363 1	0.00396428 7	0.00102936 3	0.00526416	0.00378531 7	0.00066973 3
1.0217737 5	0.00794194 1	0.00444174 3	0.00172546 2	0.00500415 5	0.00435357	0.00146577 2
1.0603312 5	0.00695834 3	0.00425878 8	0.00153773 5	0.00383531 6	0.00413977 4	0.00124643 9
1.0988887 5	0.00569439 8	0.00550432 2	0.00219977 6	0.00513898 5	0.00417756 5	0.00229641
1.1374462 5	0.00285893 3	0.00453926 1	0.00137644 3	0.00413397 5	0.00300416 6	0.00093335 1

1.1760037 5	0.00162180 3	0.00454115 9	0.00110958 2	0.00339863 8	0.00292023 9	0.00057074
1.2145612 5	0.00191805 7	0.00389656 1	0.00139559 8	0.00272351 2	0.00382163 1	0.00164001 9
1.2531187 5	0.00285284 7	0.00451645 5	0.00128433 9	0.00230740 6	0.00357386 3	0.00127142 7
1.2916762 5	0.00513266 4	0.00479255 4	0.00202031 4	0.00381412	0.00365522 3	0.00197540 7
1.3302337 5	0.00528938	0.00387712 5	0.00144812 5	0.00325060 4	0.00294840 1	0.00146329 5
1.3687912 5	0.00389672 5	0.00355794 7	0.00097813 4	0.00308338 5	0.00325085 9	0.00050439 4
1.4073487 5	0.00162682 9	0.00205071 2	- 0.00017631 2	0.00225655 8	0.00181972	- 0.00056210 1
1.4459062 5	0.00252698 9	0.00310094	0.00088402 4	0.00407978 6	0.00442779 9	- 0.00029097 7
1.4844637 5	0.00284909	0.00205501 1	0.00111350 5	0.00479257 3	0.00407917 3	- 0.00073945 6
1.5230212 5	0.00254389	0.00235749 2	0.00051582 5	0.00403388 3	0.00285847	- 0.00100531 5
1.5615787 5	0.00331359 7	0.00221886 9	0.00088125 2	0.00441353	0.00325975 2	- 0.00023217 6
1.6001362 5	0.00435306	0.00371462	0.00117246 2	0.00438264 9	0.00353854 4	0.00130976 5
1.6386937 5	0.00436799 2	0.00327724 4	0.00077792	0.00384890 1	0.00363927 9	0.00193368
1.6772512 5	0.00226321 9	0.00192602 6	- 0.00087015 8	0.00265569	0.00183267 7	0.00169124 2
1.7158087 5	0.00212563	0.00283968 5	0.00040270 5	0.00455869 4	0.00376371 7	0.00322350 7
1.7543662 5	0.00167350 2	0.00358443 8	-4.30551E- 05	0.00364519 3	0.00423250 3	0.00215125 8
1.7929237 5	0.00289015 8	0.00465024 2	0.00138866 1	0.00418579 7	0.00479603 8	0.00105860 1
1.8314812 5	0.00199202 9	0.00344948 1	0.00064716 4	0.00374512 8	0.00405110 3	- 0.00014108 5
1.8700387 5	0.00200700 3	0.00361328 2	0.00191573 5	0.00366392 8	0.00306685 3	0.00014817
1.9085962 5	0.00259669 2	0.00285604 4	0.00054671	0.00258561 8	0.00366434 1	- 0.00063421 9
1.9471537 5	0.00335040 6	0.00286391 8	0.00073614 6	0.00324074	0.00311276	0.00023417 9
1.9857112 5	0.00289524 6	0.00315311 6	- 0.00016963 2	0.00247469 5	0.00173362 7	0.00116051 2
2.0242687 5	0.00380198 2	0.00287007 8	0.00033484 7	0.00208818 4	0.00090403 2	0.00221402 6

2.0628262 5	0.00481919 2	0.00403880 9	0.00061447 5	0.00341349 8	0.00102159 1	0.00231339 8
2.1013837 5	0.00378997 8	0.00360176 5	0.00124985 6	0.00375896 1	0.00122976 3	0.00347504 4
2.1399412 5	0.00465152 1	0.00446421 6	0.00211369 8	0.00340812 9	0.00314433 6	0.00538730 5
2.1784987 5	0.00304682 3	0.00566123 6	0.00157190 6	0.00333032 5	0.00398960 4	0.00552269
2.2170562 5	0.00363328 4	0.00535946 5	0.00158004 1	0.00393844 1	0.00596163 8	0.00906181 3
2.2556137 5	0.00380980 4	0.00494873 1	0.00151078 5	0.0038954 5	0.00534166 9	0.01234211 8
2.2941712 5	0.00469214 8	0.00420814 2	0.00092502 1	0.00480811 7	0.00490250 7	0.01835174
2.3327287 5	0.00486997 9	0.00290709 9	-4.87858E- 05	0.00400758 5	0.00381676 1	0.02336373
2.3712862 5	0.00411908 4	0.00289816 8	- 0.00065094 8	0.00444052	0.00530802 6	0.03086428 5
2.4098437 5	0.00325863	0.00232997	- 0.00133630 8	0.00272554 6	0.00557095 2	0.03951574 7
2.4484012 5	0.00208365 9	0.00189287 3	- 0.00175902 4	0.00215479 6	0.00424658 6	0.04819561
2.4869587 5	0.00151116 2	0.00176257 6	- 0.00095884 5	0.00207837 6	0.00343285 5	0.05653211 3
2.5255162 5	0.00195152 4	0.00220236 9	- 0.00065564 7	0.00358092 8	0.00388451 1	0.06407722 1
2.5640737 5	0.00152798 6	0.00163095	- 0.00029991 4	0.00351195	0.00459126 3	0.07280421 2
2.6026312 5	0.00299223 9	0.00132714 7	0.00057997 9	0.00528269	0.00802828	0.08075935 8
2.6411887 5	0.00492204 2	0.00163202 8	0.00076539 7	0.00488114 8	0.01112211 8	0.08914740 9
2.6797462 5	0.00562399 1	0.00249522 4	0.00131859 1	0.00495963 6	0.01644896 9	0.09559587 8
2.7183037 5	0.00519004 8	0.00323553 7	0.00223568 1	0.00514104 8	0.02240230 9	0.10232724 6
2.7568612 5	0.00370179 2	0.00234059 5	0.00146240 3	0.00509212 4	0.02925528 6	0.10896152 2
2.7954187 5	0.00414660 9	0.00337000 8	0.00133585 8	0.00556741 1	0.03889919 9	0.11711155 5
2.8339762 5	0.00340683 2	0.00277814 5	0.00147582 1	0.00554975 5	0.04862020 6	0.12019636
2.8725337 5	0.00268650 6	0.00381048 6	0.00343178	0.00663525 5	0.05878102 6	0.1274133
2.9110912 5	0.00470645 7	0.00437036 9	0.00382933 7	0.00968932 2	0.06920005 7	0.13093656 3
2.9496487 5	0.00428713 6	0.00395013 9	0.00358028 1	0.01214198	0.07888040 8	0.13759571
2.9882062	0.003696	0.00394213	0.00194603	0.01598846	0.08809110	0.14178471

5			3	3	5	8
3.0267637 5	0.00283443 8	0.00395493 2	0.00301447 3	0.02293423 1	0.09860961	0.14897733 1
3.0653212 5	0.00281578	0.00378750 9	0.00311875 8	0.03269483 5	0.10734044 7	0.15322400 4
3.1038787 5	0.00239305 6	0.00380197 5	0.00315833 2	0.04475149 4	0.11635734 6	0.16097333 5
3.1424362 5	0.00209779 9	0.00335947	0.00344282 2	0.05611468 4	0.12376302 3	0.16564594 4
3.1809937 5	0.00255805 5	0.00338620 6	0.00528739 6	0.06852778 9	0.13242501 5	0.17452506 2
3.2195512 5	0.00299639 5	0.0023678	0.00958381 4	0.08060656 4	0.13836086 2	0.18018012 4
3.2581087 5	0.00475969 2	0.00442078	0.01646193 5	0.09469038 3	0.14594841 5	0.18847716 3
3.2966662 5	0.00533385 1	0.00718268 8	0.02611989 6	0.10680997 3	0.15363664 6	0.19255562
3.3352237 5	0.00594023 9	0.01116024 4	0.03781758 5	0.11922756	0.16569817 6	0.20072396
3.3737812 5	0.00782398 9	0.01641012 8	0.05338656 8	0.13029054 6	0.17384237 1	0.20645606 6
3.4123387 5	0.01064837 4	0.02429979 5	0.07116622 1	0.14169035 1	0.18370365 8	0.21365626 7
3.4508962 5	0.01942432 2	0.03698904	0.09002502 4	0.15068255 6	0.19149633	0.21829680 5
3.4894537 5	0.03515550 3	0.05918159 1	0.11350878 4	0.16861343 7	0.20809862 5	0.22911465 1
3.5280112 5	0.05023162 7	0.08045613 3	0.13018300 4	0.18075744 2	0.21684629 2	0.23509917 1
3.5665687 5	0.07380031 3	0.10577031 8	0.15188141 3	0.19994890 6	0.22845232 2	0.24418676 3
3.6051262 5	0.09753495 6	0.12913586 9	0.16566587 3	0.21048556 2	0.23656878 6	0.24957717 2
3.6436837 5	0.12443783 1	0.15446474 6	0.18441297	0.22677412 2	0.24561942 1	0.25587035 5
3.6822412 5	0.15438609 8	0.17618441 9	0.20150684 6	0.2356778	0.25262352 1	0.26040719 9
3.7207987 5	0.18691101 9	0.20171994 8	0.22648937 4	0.25348186 8	0.26586136	0.27190285 3
3.7593562 5	0.22145539 8	0.23132027 7	0.25268012 3	0.27202666 2	0.27941364 1	0.27981334
3.7979137 5	0.25811096 4	0.26592481 6	0.28185946 7	0.29454918 8	0.29629287 5	0.29196046
3.8364712 5	0.31438128 9	0.30843391 6	0.30961694 6	0.31221013 3	0.30752324 8	0.30262092 9
3.8750287 5	0.36355342 6	0.35210377 1	0.34410337 8	0.33604997 7	0.32524589 7	0.31529448 7
3.9135862 5	0.42303246 4	0.39696583 5	0.38006413 6	0.35661474 3	0.34028923 4	0.32121578 6
3.9521437 5	0.47781634 5	0.44459612 3	0.41839605 2	0.38640093 7	0.35761771 7	0.32929600 6
3.9907012 5	0.53801433 7	0.49363806 3	0.45532653 4	0.40974337 5	0.37016288 8	0.33682990 7
4.0292587 5	0.59704386 8	0.54679964 6	0.50017443	0.44191523	0.39113431 7	0.35157182

4.0678162 5	0.65221904 5	0.59359580 8	0.53962424 6	0.46964274	0.40952631 9	0.36404217 3
4.1063737 5	0.70435318 4	0.64371510 6	0.58181479 5	0.50353708 7	0.43747126 4	0.38150223 5
4.1449312 5	0.73890176 8	0.68208306 6	0.61411847 8	0.52922223 2	0.46034011 3	0.39517392 2
4.1834887 5	0.76983464 9	0.72337490 1	0.65333184	0.56130932 3	0.48835353 7	0.41178198 7
4.2220462 5	0.78947403 9	0.74185762 3	0.67623421 1	0.57993101 6	0.50813708 7	0.42330399 7
4.2606037 5	0.81446393 9	0.76535520 4	0.70185103 6	0.60347299 1	0.53161676 7	0.44075911 7
4.2991612 5	0.82708947	0.77679288 9	0.71288206 7	0.61655094	0.54440976 9	0.45374888
4.3377187 5	0.84405812 9	0.79481418 1	0.72770274 3	0.63518390 9	0.56355130 6	0.47386043 6
4.3762762 5	0.85511665 2	0.80135464 9	0.74011379 4	0.64617584 8	0.57579993 3	0.48532087 2
4.4148337 5	0.86611212 9	0.81223117 3	0.75500806 3	0.66150587 6	0.58970109 7	0.50157068 2
4.4533912 5	0.87365151 4	0.82134306 9	0.76588315	0.67094643 1	0.60047060 2	0.51037059 6
4.4919487 5	0.88728352 3	0.83948816 1	0.77844896	0.68926512 2	0.61656524 2	0.52541430 4
4.5305062 5	0.89814298	0.85222236 2	0.79297709 3	0.70063820 1	0.62617673 2	0.53908055 1
4.5690637 5	0.90977755 4	0.86416686 3	0.80686099 2	0.71893080 7	0.64000324 8	0.55377865 5
4.6076212 5	0.91714782 6	0.87466894 4	0.81858585 2	0.73139115 1	0.64867488 1	0.56596419 6
4.6461787 5	0.92136807 6	0.87928178 2	0.82453044 4	0.73824659 2	0.65879058 7	0.57378894 3
4.6847362 5	0.92418777 4	0.88426151 8	0.82730484	0.74627776 5	0.66370414 4	0.58339301 6
4.7232937 5	0.92939763 3	0.89459686 5	0.83912519	0.75397784 7	0.67427031	0.58789330 6
4.7618512 5	0.93499925 3	0.90513374 6	0.85144078	0.76167873 8	0.68722630 9	0.59661025 7
4.8004087 5	0.94807314 1	0.91422011 1	0.85846735 2	0.77241465 9	0.70187954	0.60428373 7
4.8389662 5	0.95692662	0.91844166 4	0.86225844 5	0.78023512 9	0.71437136 3	0.61408416 7
4.8775237 5	0.96625415	0.92521774 1	0.87178076 7	0.79211866	0.72269526 4	0.62362649 8
4.9160812 5	0.96123901 2	0.92836756 1	0.87826017 5	0.79714811 2	0.72530600 2	0.62864357 9
4.9546387 5	0.96336643 4	0.92940248 7	0.88858075 9	0.80208704 2	0.72904606 7	0.63568582 7
4.9931962 5	0.95984207 2	0.93558378 3	0.89809444 1	0.81052743 8	0.73666110 6	0.64102602 5
5.0317537 5	0.95942619 4	0.93627183 9	0.90292501 8	0.81649776 5	0.74108470 4	0.64601798 9
5.0703112 5	0.96888577 2	0.94487740 2	0.90954877 4	0.82633500 2	0.74640710 2	0.65001301 7
5.1088687	0.96706301	0.94328442	0.90694765	0.82650122	0.75313161	0.65503535

5	7	4	5	3	6	
5.1474262	0.97176271	0.94884193	0.91113354	0.83240329	0.76217302	0.65974002
5	3	2	5			8
5.1859837	0.97451346	0.95313723	0.91336116	0.83973055	0.76477180	0.66570857
5	3	1	2			1
5.2245412	0.97597708	0.95818822	0.92000379	0.84787648	0.77145907	0.67080456
5	3	6	7	6	5	
5.2630987	0.97184844	0.95844695	0.92262581	0.85165696	0.77449519	0.67567941
5	2	9	6	8	1	9
5.3016562	0.9799047	0.96264961	0.93287232	0.85724841	0.78175333	0.68562359
5		9				8
5.3402137	0.98550446	0.95875643	0.93717986	0.85654820	0.79042334	0.68948263
5	1	7	3	5	3	1
5.3787712	0.99359397	0.96122808	0.94415064	0.86552141	0.79851070	0.69513624
5		5	1	2	4	3
5.4173287	0.99529448	0.96352232	0.94241024	0.87147069	0.80343982	0.69685790
5	2	4	8	8	4	1
5.4558862	0.99685495	0.97180746	0.94454560	0.88038067	0.80681441	0.70165454
5	6	2	7	3	2	5
5.4944437	1.00072404	0.97668884	0.94889750	0.88408674	0.81128898	0.70707438
5	1	6	4		4	
5.5330012	0.99134664	0.97714788	0.94973154	0.88422256	0.81080373	0.70640539
5	4	6	4	2	7	1
5.5715587	0.99353033	0.98416530	0.95289819	0.88620886	0.81765595	0.70891520
5		9	1	5	4	5
5.6101162	0.99339101	0.98560583	0.95491968	0.89253962	0.8151665	0.71069419
5	6	2	7	3		
5.6486737	0.99390778	0.98392332	0.95423571	0.89081209	0.81485664	0.71556504
5	9	3	5	3	6	9
5.6872312	0.99096421	0.97929232	0.95724923	0.89250725	0.81847833	0.71904387
5	5		2	2	9	6
5.7257887	0.9837642	0.97436624	0.95450192	0.88793946	0.82261902	0.72357986
5		3	8	5	6	5
5.7643462	0.98080639	0.97466836	0.95498573	0.89651845	0.82585580	0.72654629
5	1	8	2	2	1	8
5.8029037	0.98521008	0.97903884	0.96089851	0.90976278	0.83613136	0.73482926
5	8	8	6	3	2	7
5.8414612	0.98623002	0.98225167	0.96115259	0.90981100	0.84215771	0.73598542
5	4	1	2	7	2	9
5.8800187	0.98299764	0.97740073	0.95979801	0.90517151	0.84104700	0.73638305
5	6	8			8	7
5.9185762	0.99068158	0.97891904	0.96218531	0.90769368	0.84119643	0.73904552
5	6	7	8	2	2	2
5.9571337	0.98958275	0.97950850	0.96116284	0.91356296	0.84147347	0.74205885
5	2	2	9		6	5
5.9956912	0.99168603	0.98153291	0.97060427	0.91533973	0.84650678	0.74498853
5	8	7		1	2	7
6.0342487	0.99615706	0.98369907	0.97770293	0.91662763	0.84853757	0.75050651
5	7	6	9	9	5	5
6.0728062	1.00060034	0.98573084	0.98568731	0.91875633	0.85041332	0.75304834
5	1	3	2	6	5	9
6.1113637	0.99770131	0.98568514	0.97871538	0.92280128	0.85061036	0.75440886
5	3	3			5	4
6.1499212	0.99701394	0.98777797	0.97994763	0.92946285	0.85970704	0.75375247
5		6	5	3	2	4

6.1884787 5	0.99185960 8	0.99007573 9	0.97655886 7	0.93446342 8	0.86143796 9	0.75815707 2
6.2270362 5	0.98950103 2	0.98658103 8	0.97803548 6	0.93791676	0.86238788 7	0.75868146 1
6.2655937 5	0.98610297 9	0.98774119 2	0.97750227 3	0.93966436 2	0.86412787 9	0.75953573 6
6.3041512 5	0.98476277 2	0.98756000 2	0.97697947 1	0.93605740 1	0.86123674 3	0.76329438 1
6.3427087 5	0.98807792 8	0.98113685 9	0.97836003 6	0.94157883 8	0.86645486	0.76973696 1
6.3812662 5	0.99601165 3	0.98546372 9	0.98294581 9	0.94104128 3	0.87136818 8	0.76979845 1
6.4198237 5	0.99827899 4	0.98532965 9	0.98968475 4	0.94553606 8	0.87934897 8	0.77681849 1
6.4583812 5	0.99816125 9	0.98571465 4	0.99341554 9	0.94812278 6	0.88067756 2	0.77995691 9
6.4969387 5	1.00170022 2	0.98448583 6	0.99086577 3	0.94788149 9	0.88405472 9	0.78231214 3
6.5354962 5	1.00401511 5	0.98486193 3	0.99402416 9	0.94875862 2	0.88378851 5	0.78403949 3
6.5740537 5	1.00397682 7	0.98894250 1	0.99505938 9	0.95135845 4	0.89308399 8	0.78582258 1
6.6126112 5	1.00148993 8	0.99001683 9	0.99110912 6	0.94674979 9	0.88736601	0.78402742 8
6.6511687 5	0.99730523 8	0.98004301 2	0.98405768 6	0.94026866 5	0.88645319 6	0.78045652 4
6.6897262 5	0.99784170 8	0.97934495 8	0.98741376 8	0.94214955	0.89128072 4	0.78580705
6.7282837 5	0.99608606 6	0.97712718 6	0.99300140 3	0.94254957 2	0.89355370 8	0.79080232
6.7668412 5	0.99310119 6	0.97831901	0.99056875	0.94659587 9	0.89149729 8	0.79635829 1
6.8053987 5	1.00031433 4	0.98256162 1	0.99317214 9	0.95684139	0.89769888 1	0.80891662 9
6.8439562 5	1.00327646 9	0.98839821 2	0.99607682 6	0.96542256	0.90461184	0.83008392 9
6.8825137 5	1.00508818 7	0.99084759 3	0.99505679 5	0.96755208 6	0.90644901 6	0.86611971 1
6.9210712 5	0.99967028 2	0.99252725	0.99601025 2	0.96658601 7	0.9135051	0.94172190 5